JOURNAL OF BIOLOGICAL REGULATORS & HOMEOSTATIC AGENTS
Volume 34, No. 5 (Supplement 3), September – October, 2020

Technology in Medicine

CONTENTS

Efficacy of focal muscular vibration in the treatment of upper limb spasticity in subjects with stroke outcomes: randomized controlled trial

I. Aprile[1], C. Iacovelli[1], C. Pecchioli[2], A. Cruciani[1], L. Castelli[3] and M. Germanotta[1]

[1]IRCCS Fondazione Don Carlo Gnocchi, ONLUS, Florence, Italy; [2]IRCCS San Raffaele Pisana, Department of Neuroscience, Rome, Italy; [3]Fondazione Policlinico Universitario A. Gemelli IRCCS, UOC Neuroriabilitazione ad Alta Intensità, Rome, Italy

Focal muscular vibration (FMV) is a non-invasive technique that showed positive effects on spasticity of the upper limb in stroke subjects but different protocols have been proposed so the studies are not comparable and, to date, it is not clear which muscles should be treated, agonist, or antagonist muscles to obtain the better result on spasticity. The objective of this study is to evaluate the effects on spasticity of FMV on the upper limb flexor spastic muscles compared to the effects of FMV on the upper limb extensor muscles in subacute stroke patients. We treated 28 subacute stroke patients (mean age 64.28±13.79) randomized into two groups: Group A and Group B. Group A was treated by applying FMV to the flexor muscles of the upper limb, while Group B was treated by applying FMV to the extensor muscles of the upper limb. The effects on spasticity were assessed by Modified Ashworth Scale (primary outcome) and the upper limb motor function by instrumental robotic outcomes; moreover, muscle strength and pain were evaluated using Motricity Index and Numerical Rating Scale, respectively (secondary outcomes). Patients were subjected to FMV for three consecutive days and were evaluated three times: before treatment (T0), after a week (T1) and after a month (T2) from the end of treatment. Within group, analysis showed statistically significant changes over time of the MAS at the three joints (shoulder, elbow and wrist) in both groups, but post-hoc analysis showed that, only in Group A, MAS was significantly lower at T2, when compared with T0 at the shoulder and elbow. NRS, significantly changed over time only in the Group B. Motricity Index, did not change over time neither in the Group A, nor in the Group B. No statistically significant differences were detected in the between group analysis. Regarding the instrumental robotic outcomes, we detected a statistically significant reduction of the time required to complete the task (Duration) in both group a T2. In conclusion, this study highlighted how the same treatment protocol can determine an improvement in muscle tone and in the Duration to perform a task, regardless of the muscles treated, while the pain improves if we treat the agonist muscles.

Stroke is the major cause of permanent disability with an incidence in Italy of 293 affected persons per 100,000 inhabitants. The onset of spasticity following stroke, affecting about 20-40% of patients, is one of the most disabling conditions and has a negative influence on the patient's autonomy and quality of life. Upper limb spasticity due to a stroke is one of a common complication and it can lead to abnormal limb posture with flexion of the arm and hand. Furthermore, it can interfere with both active and passive functions, causing a reduction in quality of life (1). The development of spasticity during

Key words: focal muscular vibration, Stroke, spasticity, pain

Corresponding Author:
Dr Chiara Iacovelli,
IRCCS Fondazione Don Carlo Gnocchi,
Via di Scandicci 269,
50143 Florence Italy
Tel.: 39 (0)6 33.08.65.54
e-mail: ciacovelli@dongnocchi.it

0393-974X (2020)

the rehabilitation process of these patients is a very limiting factor for the functional recovery of the affected side (2-4).

Focal muscular vibration (FMV) is a non-invasive technique that showed positive effects on spasticity and pain with an improvement of the strength in the upper limb of stroke subjects (5, 6). Introduced by Hagbarth and Eklund at the end of the 1960s, FMV is based on the tonic vibration reflex, i.e. a reflex muscular contraction in response to a vibratory stimulus. In people without tone alterations, mechanical vibration (with a frequency of 100 cycles per second and amplitude 3 mm) produce a reflex contraction; this slowly increases until it reaches the plateau. The duration of contraction thus generated is linked to the presence of vibration, and it finishes once the stimulus is removed. Based on this mechanism, some authors (7, 8) suggest that the FMV should be applied to the antagonist muscles to obtain a significant reduction in spasticity.

However, the literature shows a reduction in spasticity through the application of FMV directly on the spastic muscle (9, 10). These effects seem to be related to the stimulation of cortical motor areas because the effects of vibration on the target muscles result from the activation of the Ia spindle afferents (11) and the Ia inputs can alter the excitability of the cortico-spinal pathway (12) modulating intracortical inhibitory, facilitating inputs to the primary motor cortex, and augmenting proprioceptive inputs to the central nervous system. These effects on the central nervous system are important for enhancing motor control and performance. Moreover, Marconi et al. (13) using transcranial magnetic stimulation showed that a repetitive focal muscle vibration therapy, combined with physiotherapy, may help to reduce abnormalities of the corticospinal excitability and of the intracortical inhibitory systems in the damaged hemisphere of post-stroke patients. Nevertheless, it remains unclear which approach is most effective in reducing spasticity: to treat the agonist or antagonist muscles? Considering the prevalence of spasticity in stroke patients and the effects on their functional recovery, it is important to identify the most effective treatment to guarantee a more suitable rehabilitation process. In addition to this, it is worth remembering that FMV is less invasive and has lower costs than botulinum toxin, the current gold standard in the treatment of spasticity.

The objective of the study is to evaluate, in subjects with subacute stroke, the effects of FMV on the upper limb flexor spastic muscles compared to the effects of FMV on the upper limb extensor muscles. Specifically, the two approaches will be compared on the effects on spasticity and upper limb motor function, assessed by clinical scales and instrumental robotic outcomes; moreover, muscle strength, and pain will be evaluated.

MATERIALS AND METHODS

This was a randomized (1:1), controlled, parallel-group clinical trial on subacute stroke subjects. The study was conducted at the Fondazione Don Carlo Gnocchi of Rome and it was registered with ClinicalTrials.gov (NCT04087928). Twenty-eight patients with subacute stroke, with mean age 64.28 years (SD 13.79), were recruited. Informed consent was obtained from each patient before starting the study. Inclusion criteria were subacute stroke (within 1 year of the event), single cortical and subcortical event, spastic paresis of upper limb (Modified Ashworth Scale Score ≥ 2 at the flexor muscles of the hand and arm). Exclusion criteria were comorbidity of the paretic upper limb (fractures, trauma, or peripheral neuropathies); treatment with focal or systemic antispastic drugs. Patients were randomized into two groups: group A was treated by applying FMV to the flexor muscles of the upper limb, while group B was treated by applying FMV to the extensor muscles of the upper limb. Homogeneity between the two groups was guaranteed by randomizing the patients on the Modified Ashworth Scale (MAS).

This work followed the ethical standards of the Helsinki Declaration of 1964 and its subsequent amendments; moreover, it was approved by the ethics committee of the Don Carlo Gnocchi Foundation (date: May 3, 2019; FDG_15/2019/CE_FdG/FC/SA). The data of patients enrolled in the study were collected in special password-protected Computerized Report Forms (CRFs). Each participant has been assigned a code not identifiable by unauthorized personnel. All participants were evaluated by an independent observer who was blinded to the intervention performed in the protocol.

Study procedures

Treatment with FMV was performed using a device capable of providing a vibratory stimulus (EVM, Endomedica, Italy), applying specific transducers to the muscles. Patients were subjected to FMV for three consecutive days. Each session consisted of three sessions of 10 minutes each, interspersed with one minute of rest. A vibration frequency of 100 Hz has been applied, according to the literature (14-16). For the group A the flexor muscles of the arm (biceps muscle and flexor muscles of the hand) were treated; for the B group, extensor muscles of the arm (triceps and extensor muscles of the hand) were treated. So, group A was the group in which agonist muscles were treated while group B was the group of patients in which antagonist muscles were treated.

Patients were evaluated three times: before treatment (T0), after a week (T1), and after a month (T2) from the end of treatment. The primary outcome was the change in spasticity assessed through MAS, a six-point ordinal scale used for grading hypertonia: a score of 0 on the scale indicates no increase in tone while a score of 4 indicates rigidity. Muscle tone is scored by passively moving the individual's limb and assessing the amount of resistance to movement felt by the examiner (17). The secondary outcomes were the changes in the Motricity Index (MI), and in the Numerical Rating Scale (NRS). The MI aims to evaluate upper limb motor impairment after stroke, considering three different movements: pinch-grip, elbow flexion, and shoulder abduction. These were each scored (0-33) according to the instructions of Collin and Wade (18) and the total upper extremity score involved adding one to the sum of the three actions (maximum possible score=100) (19).

The NRS is a quantitative one-dimensional numerical scale of pain assessment at 11 points; the scale requires the operator to ask the patient to select the number that best describes the intensity of his pain, from 0 to 10, at that precise moment (20). Other outcomes were the evaluation of reaching movements, by robot MOTORE (Mobile roboT for upper limb neurOrtho Rehabilitation, Humanware, Italy) (21), and the evaluation of tone and fingers strength, obtained by Amadeo (Tyromotion, Austria) (22).

MOTORE is a robotic device that allows passive, active, and active-assistive planar movements of the shoulder and elbow joints; is a planar end-effector device designed for application in neuro-rehabilitation protocols and it adopts specific mechanical, electrical, and control solutions to meet the requirements of neuro-rehabilitation. The device can help the patient when he/she is not able to accomplish the task, prevent movements different from the ideal trajectories, provide different weight and viscosity behaviors, maintain a proper orientation on the plane. The device generates force feedback without any intermediate link to the ground or frame, thanks to the motion of the wheels and using the information obtained from the load cell. It provides several rehabilitation exercises and an Evaluation Task, based on a center-out point-to-point reaching activity: following visual feedback, subjects are asked to move the device from the center to a peripheral target and come back to the center, making a total of 16 reaching movements. Once the test is completed, these indices are computed:

- Duration (s): time required to complete the task;
- Velocity (m/s): average velocity of the device during the test;
- Length (m): length of the path traveled by the subject toward the i-th target (i = 1:8);
- Score: mean of the ratios between the actual distance covered by the patients and the required distance to be traveled, computed for each required movement. It ranges from 0 (no movement) to 10 (the patient can fully perform the required task);
- Useful Work (J): the amount of total work directed towards the target.

Amadeo is a robotic device specifically designed for hand rehabilitation that allows passive, active, and active-assistive finger flexion and extension movements, it is an end-effector robot, with 5 degrees of freedom (DOF), it provides the motion of one or all five fingers, thanks to a passive rotational joint placed between the fingertip and an entity moving laterally. The set-up involved securing a small magnetic disc to the pulp of each finger with adhesive tape for connection with the end-effector, which would move back and forth within sliders aligned with the finger movement direction. The wrist is immobilized using a Velcro strap so that the elbow and shoulder are inhibited from moving. The robot can calibrate the full passive range of motion (pROM) for each finger before the start of a session and supply the assistive force to patients to complete the remaining range of motion during an exercise. Moreover, the maximum

flexion and extension force for each finger are recorded to calibrate the exercise when a strength control is required. It provides rehabilitation exercises and evaluation tasks. These evaluations were carried out: force assessment (Hand Flexion and Hand Extension) and muscle tone assessment (Tone).

Statistical Analysis

Within-group changes in clinical scales over time (T0 vs T1 vs T2) were assessed using Friedman's ANOVA test. When the test was significant, pairwise comparisons with Bonferroni adjustment were performed. To compare the effects of the two approaches (flexor muscles versus extensor muscles vibration) we first computed the absolute changes of the clinical scales (T1-T0; T2-T0; T2-T1), and then we compared each change in the two groups by using the Mann-Whitney U test. Concerning the instrumental outcome measure, a two-way mixed ANOVA test was carried out, with time (three levels: T0, T1, and T2) as the within-group variable, and group (2 levels: flexor versus extensor muscles) as the between-group variable. Statistical analyses were performed with built-in functions of SPSS 21 (IBM, Armonk, NY).

RESULTS

Between September 2019 and December 2019, 40 subjects were assessed for eligibility (Fig. 1).

The reasons for exclusion were the comorbidity of the paretic upper limb (4 subjects, 50%), the degree of spastic paresis of upper limb (2 subjects, 25%), and a time since stroke outside inclusion criteria range (2 subjects, 25%). According to the inclusion criteria, we recruited 28 subacute stroke

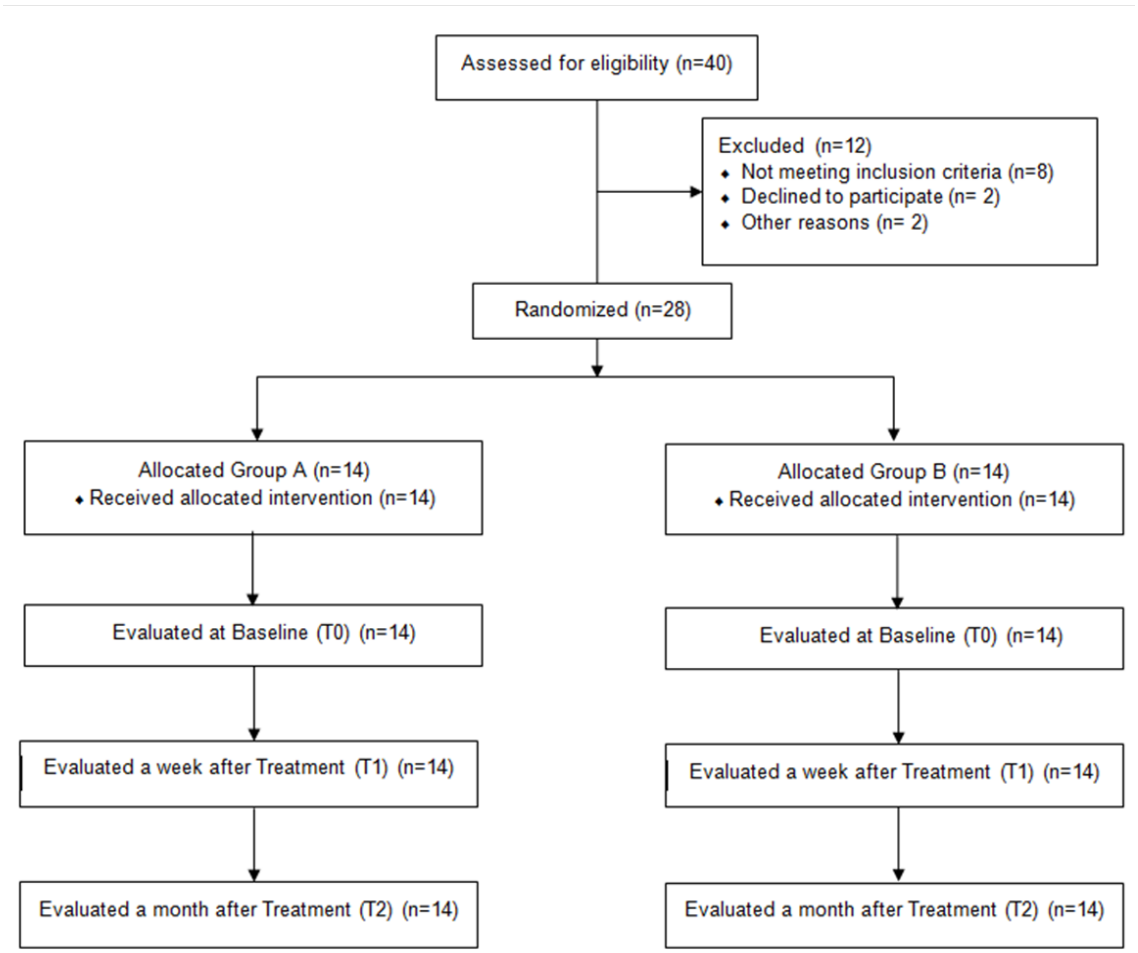

Fig.1. *CONSORT Flow Chart.*

patients comprising 19 males and 9 females, aged between 42 and 91 years (mean age 64.28±13.79 years), 18 ischemic and 10 hemorrhagic stroke; 14 with left hemiparesis and 14 with right hemiparesis. Time post the acute event ranged from 62 to 173 days (mean days 129.28±25.19).The patients were randomized in Group A or Group B and the demographic characteristics at baseline of each group are shown in Table I.

Clinical scales

As reported in Table II, the within-group analysis showed statistically significant changes over time of the MAS at the three joints (shoulder, elbow, and wrist) in both groups. Post-hoc analysis showed that, in Group A, MAS is significantly lower at T2, when compared with T0 at the shoulder and elbow. Instead, due to the Bonferroni correction, post hoc analysis did not show any significant difference between evaluation neither in the MAS at the wrist in the group A, nor in the MAS at the three joints in the Group B. Moreover, pain, as measured by the NRS, significantly changed over time in Group B only; however, the Bonferroni correction caused the lack of significant differences in the post-hoc analysis. Finally, strength, as measured by the Motricity Index, did not change over time either in Group A or in Group B. Comparing the changes (T1-T0; T2-T1 and T2-T0) in the clinical scale of muscle tone (MAS), motor function (MI) and pain (NRS) in the

Table I. *Characteristics of the sample.*

	Group A	*Group B*	*p-value*
	n (%) Mean±SD		
Subjects	14 (50.00)	14 (50.00)	
Gender. Male/Female	12 (85.71) / 2 (14.29)	7 (50.00) / 7 (50.00)	0.072
Age (years)	62.47±14.34	66.38±13.38	0.413
Time post the acute event (days)	133.40±21.57	124.53±28.97	0.339
Aetiology. Ischemic/Haemorrhagic	8 (57.14) /6 (42.86)	10 (71.42) / 4 (28.58)	0.467
Lesion Side. Left/ Right	6 (42.86) / 8 (57.14)	8 (57.14) / 6 (42.86)	0.525

Table II. *Within-group analysis of clinical scales: descriptive statistics and results of the non-parametric Friedman Anova tests.* ***T0****: baseline;* ***T1****: after a three-day treatment;* ***T2****: one month after the end of the treatment.*

		T0	**T1**	**T2**	**P**	**T0vsT1**	**T0vsT2**	**T1vsT2**
Group A (flexor muscles)	MAS_shoulder	2.4 (0.2)	0.9 (0.3)	0.7 (0.2)	**0.006**	0.142	**0.032**	1
	MAS_elbow	2.6 (0.3)	1.1 (0.2)	0.8 (0.2)	**0.001**	0.176	**0.01**	0.896
	MAS_wrist	2.3 (0.2)	1 (0.2)	0.6 (0.1)	**0.042**	1	0.142	0.771
	NRS	4.5 (0.6)	4.2 (0.5)	3.4 (0.6)	0.132	-	-	-
	MI	42.4 (5.8)	46.4 (6.1)	47.1 (5)	0.125	-	-	-
Group B (extensor muscles)	MAS_shoulder	2.4 (0.2)	0.8 (0.2)	0.9 (0.2)	**0.018**	0.718	0.233	1
	MAS_elbow	2.3 (0.2)	0.9 (0.2)	0.8 (0.2)	**0.031**	0.509	0.187	1
	MAS_wrist	2.1 (0.3)	0.6 (0.1)	0.6 (0.2)	**0.016**	0.35	0.287	1
	NRS	4.9 (0.8)	3.7 (0.8)	3.4 (0.6)	**0.005**	0.187	0.150	1
	MI	33.8 (6.9)	43.4 (4)	39.6 (4.5)	0.084	-	-	-

two groups (Group A and Group B), no statistically significant differences were detected (Table III).

Instrumental outcomes

In Table IV, the results of the statistical analysis related to the data provided by the two robotic devices are reported. The interaction factor time*group was not significant for all the investigated outcomes, meaning a similar trend over time in the two groups. The main effect Time was statistically significant for the Duration; post-hoc analysis highlighted a statistically significant reduction a T2 when compared to both T0 (p=0.007) and T1 (p=0.013), while no differences were identified between T0 and T1 (p=0.949).

Table III. *Between-group analysis of clinical scales: descriptive statistics and results of the Mann-Whitney U tests comparing the improvement between the two groups.* ***T0****: baseline;* ***T1****: after a three-day treatment;* ***T2****: one month after the end of the treatment.*

	Group A Mean (SD)	Group B Mean (SD)	P
Absolute changes (T1-T0)			
MAS_shoulder	-0.5 (0.8)	-0.6 (0.8)	0.964
MAS_elbow	-0.5 (0.6)	-0.4 (0.7)	0.751
MAS_wrist	-0.3 (0.8)	-0.5 (0.7)	0.555
NRS	-0.3 (2.3)	-1.2 (1.7)	0.413
MI	3.7 (9.9)	9.5 (16.1)	0.856
Absolute changes (T2-T0)			
MAS_shoulder	-0.7 (0.9)	-0.5 (0.9)	0.375
MAS_elbow	-0.9 (0.8)	-0.5 (0.8)	0.280
MAS_wrist	-0.6 (0.9)	-0.5 (0.5)	0.458
NRS	-1.1 (1.9)	-1.5 (2.1)	0.867
MI	4.8 (8.8)	5.8 (13.2)	>0.999
Absolute changes (T2-T1)			
MAS_shoulder	-0.2 (0.9)	0.2 (0.4)	0.169
MAS_elbow	-0.3 (0.6)	-0.2 (0.6)	0.616
MAS_wrist	-0.4 (0.7)	0.0 (0.6)	0.280
NRS	-0.8 (2.0)	-0.3 (2.3)	0.458
MI	0.8 (11.1)	-3.8 (6.5)	0.302

Table IV. *Instrumental outcome measures: descriptive statistics and results of the two-way mixed Anova tests.* ***T0****: baseline;* ***T1****: after a three-day treatment;* ***T2****: one month after the end of the treatment.* ***SE****: standard error.*

Outcome	Group	T0 Mean (SE)	T1 Mean (SE)	T2 Mean (SE)	time	time*group
Duration (s)	Group A	217 .9 (25.2)	209.9 (30.0)	184.2 (24.2)	**0.011**	0.723
	Group B	186.5 (31.6)	192.7 (37.6)	147.4 (30.3)		
Velocity (m/s)	Group A	0.068 (0 .012)	0.068 (0.011)	0.076 (0.011)	0.247	0.703
	Group B	0.057 (0.014)	0.059 (0.014)	0.061 (0.014)		
Length (m)	Group A	1.73 (0.31)	1.56 (0.27)	1.73 (0.32)	0.587	0.741
	Group B	1.81 (0.38)	1.85 (0.34)	1.97 (0.40)		
Score	Group A	7.6 (0.8)	8.1 (0.7)	8.3 (0.6)	0.105	0.523
	Group B	7.3 (1.0)	7.6 (0.9)	7.5 (0.8)		
Useful Work (J)	Group A	9.28 (2.18)	9.06 (2.02)	9.68 (2.18)	0.474	0.844
	Group B	9.10 (2.74)	8.24 ()2.53	9.72 (2.73)		
Hand Flexion (N)	Group A	31.7 (8.2)	33.1 (7.4)	28.3 (7.2)	0.427	0.407
	Group B	30.6 (9.1)	34.1 (8.2)	33.4 (8.0)		
Hand Extension (N)	Group A	5.8 (2.0)	5.9 (2.3)	7.4 (2.7)	0.195	0.458
	Group B	3.9 (2.2)	4.5 (2.5)	4.5 (3.0)		
Hand Tone (N)	Group A	-1.5 (0.5)	-3.0 (1.1)	-1.4 (0.4)	0.190	0.402
	Group B	-1.6 (0.5)	-2.2 (1.1)	-1.9 (0.4)		

DISCUSSION

Spasticity is a motor disorder characterized by a velocity-dependent increase in muscle tone or tonic stretch reflexes associated with hypertonia (23). Spasticity negatively influences the impaired and performance of the upper limb in stroke patients. In some studies, FMV has been used in patients after stroke showing a reduction of upper limb spasticity, as well as an improvement in motor performance and a reduction of pain (5, 6). Regarding the effect on spasticity of the upper limb in stroke patients, in some studies agonist muscles were treated (9, 10, 24) while in others antagonist muscles were treated (7 ,8, 25). However, it is not clear which mechanism is behind these effects.

Focal muscle vibration stimulates the muscle spindles and alpha-motoneurons, which initiate a muscle contraction caused by the tonic vibration reflex. Moreover, the vibrations are perceived by the mechanoreceptors of the skin and of the joint, which can facilitate the gamma-system and promote the activation of the motoneurons. Sensory stimuli can cause improvements in strength and decrease muscle tone in chronic stroke patients, confirming that the somatosensory stimulation may influence motor recovery, due to the stronger connections that might form between somatosensory neurons and functionally related motor output neurons in the cortex (26). To date a clear explanation about the neurophysiological mechanisms underlying the observed improvement of the upper limb spasticity in stroke patients are not available. Some studies showed neurophysiological reorganization of the cerebral cortex following muscular vibration (12, 13). Presumably, this neurophysiological effect is mediated through the activation of muscle spindles input via Ia-afferent fibers.

The afferent signals reach cortical area 3, but they also activate directly the neurons in area 4 of the motor cortex (27) and it could reduce abnormalities of the corticospinal excitability and the intracortical inhibitory systems in the damaged hemisphere of poststroke patients (13). Several authors showed positive effects of the Focal muscle vibration on spasticity but different protocols have been proposed so the studies are not comparable and, to date, it is not clear which muscles should be treated, agonist, or antagonist muscles.

In our randomized trial, we observed that a significant reduction of the upper limb spasticity was observed in all segments of the upper limb, shoulder, elbow, and wrist, and in both groups (group A and group B). This result means that we observed a significant reduction of the tone muscles either in patients underwent to the vibration of the biceps and hand flexor muscles or in the patients underwent to the vibration of the triceps and hand extensor muscles. So, the muscle target of the FVM seems not to significantly change the positive effect observed about spasticity reduction. This data sustains a possible central mechanism related somatosensory stimulation through the FMV that could influence motor recovery, due to the new connections between somatosensory neurons and motor neurons in the cortex.

It should be noted that even if the vibration treatment consists of three sessions on consecutive days, its effect is prolonged for the month following the end of the treatment, indeed when the flexor muscles were treated (group A) the post-hoc analysis showed a significant change between T2 and T0 evaluation. In the group B, because of the statistical correction, it was not possible to identify the time interval when most of this improvement happen.

Other studies previously reported an improvement of the pain after focal muscle vibration (6, 16) but using different protocols. In our study, pain significantly improved when agonist spastic muscles were treated. Constantino et al. reported a reduction of pain using an FMV but, differently from us, they treated the antagonist muscles and used a vibration frequency of 300 Hz. We hypostasized that the positive effect of FMV on pain of the upper limb in our cases is due to the positive effects of FMV on the flexor muscles spasticity, this latter is the main cause of upper limb pain in stroke patients.

Instrumental evaluation of our patients showed a reduction of the time required to complete the required reaching task, measured using a robotic device, in both groups. Therefore, this result suggests a positive effect of FVM (both on agonist, and

antagonist muscles) on motor performance. On the contrary, hand strength, as measured by the robotic device, did not improve, probably because the motor deficit in our patients was more severe distally (at the hand) then proximally (shoulder and arm).

This is the first RCT in which the same protocol of FMV was used to treat agonist or antagonist muscles of the spastic upper limb in stroke patients and it highlighted how the same treatment protocol can determine an improvement in muscle tone and in the duration of performance regardless of the muscles treated, while the pain improves if we treat the agonist muscles.

The limits of our work are the small sample size and the lack of long term follow-up after several months but despite of these limitations these preliminary data can be useful in clinical practice sustaining the use of focal muscle vibration to treat spasticity in the upper limb and suggesting the side of treatment also considering the presence of pain in the patient to be treated. Moreover, our results suggest further studies in which a combined the treatment of agonist and antagonist muscles of spastic upper limb could be experimented.

REFERENCES

1. Mayer NH, Esquenazi A. Muscle overactivity and movement dysfunction in the upper motoneuron syndrome. Phys Med Rehabil Clin N Am 2003; 14:855-83. doi:10.1016/S1047-9651(03)00093-7.
2. Bhakta BB. Management of spasticity in stroke. Br Med Bull 2000; 56:476-85. doi:10.1258/0007142001903111.
3. Sommerfeld DK, Eek EUB, Svensson AK, Holmqvist LW, Von Arbin MH. Spasticity after Stroke: Its Occurrence and Association with Motor Impairments and Activity Limitations. Stroke 2004; 35:134-9. doi:10.1161/01.STR.0000105386.05173.5E.
4. Thibaut A, Chatelle C, Ziegler E, Bruno MA, Laureys S, Gosseries O. Spasticity after stroke: Physiology, assessment and treatment. Brain Inj 2013; 27:1093-105. doi:10.3109/02699052.2013.804202.
5. Murillo N, Valls-Sole J, Vidal J, Opisso E, Medina J, Kumru H. Focal vibration in neurorehabilitation. Eur J Phys Rehabil Med 2014; 50:231-42.
6. Constantino C, Galuppo L, Romiti D. Efficacy of mechano-acoustic vibration on strength, pain, and function in poststroke rehabilitation: A pilot study. Top Stroke Rehabil 2014; 21:391-9. doi:10.1310/tsr2105-391
7. Ageranioti SA, Hayes KC. Effects of vibration on hypertonia and hyperreflexia in the wrist joint of patients with spastic hemiparesis. Physiother Canada 1990; 42:24-33.
8. Liepert J, Binder C. Vibration-induced effects in stroke patients with spastic hemiparesis - A pilot study. Restor Neurol Neurosci 2010; 28:729-35. doi:10.3233/RNN-2010-0541
9. Noma T, Matsumoto S, Shimodozono M, Etoh S, Kawahira K. Anti-spastic effects of the direct application of vibratory stimuli to the spastic muscles of hemiplegic limbs in post-stroke patients: A proof-of-principle study. J Rehabil Med 2012; 44:325-30. doi:10.2340/16501977-0946.
10. Caliandro P, Celletti C, Padua L, et al. Focal muscle vibration in the treatment of upper limb spasticity: a pilot randomized controlled trial in patients with chronic stroke. Arch Phys Med Rehabil 2012; 93:1656-61. doi:10.1016/j.apmr.2012.04.002.
11. Roll JP, Vedel JP, Ribot E. Alteration of proprioceptive messages induced by tendon vibration in man: a microneurographic study. Exp brain Res 1989; 76:213-22.
12. Steyvers M, Levin O, Van Baelen M, Swinnen SP. Corticospinal excitability changes following prolonged muscle tendon vibration. Neuroreport 2003; 14:1901-5. doi:10.1097/01.wnr.0000093296.63079.
13. Marconi B, Filippi GM, Koch G, et al. Long-term effects on cortical excitability and motor recovery induced by repeated muscle vibration in chronic stroke patients. Neurorehabil Neural Repair 2011; 25:48-60. doi:10.1177/1545968310376757.
14. Brunetti O, Filippi GM, Lorenzini M, et al. Improvement of posture stability by vibratory stimulation following anterior cruciate ligament reconstruction. Knee Surg Sports Traumatol Arthrosc 2006; 14:1180-7. doi:10.1007/s00167-006-0101-2.
15. Fattorini L, Ferraresi A, Rodio A, Azzena GB, Filippi GM. Motor performance changes induced by muscle vibration. Eur J Appl Physiol 2006; 98:79-87. doi:10.1007/s00421-006-0250-5.

16. Casale R, Damiani C, Maestri R, Fundarò C, Chimento P, Foti C. Localized 100 Hz vibration improves function and reduces upper limb spasticity: A double-blind controlled study. Eur J Phys Rehabil Med 2014; 50:495-504.
17. Bohannon RW, Smith MB. Interrater reliability of a modified Ashworth scale of muscle spasticity. Phys Ther 1987; 67:206-7.
18. Collin C, Wade D. Assessing motor impairment after stroke: A pilot reliability study. J Neurol Neurosurg Psychiatry 1990; 53:576-9. doi:10.1136/jnnp.53.7.576.
19. Bohannon RW. Motricity index scores are valid indicators of paretic upper extremity strength following stroke. J Phys Ther Sci 1999; 11:59-61. doi:10.1589/jpts.11.59.
20. Downie WW, Leatham PA, Rhind VM, Wright V, Branco JA, Anderson JA. Studies with pain rating scales. Ann Rheum Dis 1978; 37:378-81. doi:10.1136/ard.37.4.378.
21. Germanotta M, Cruciani A, Pecchioli C, et al. Reliability, validity and discriminant ability of the instrumental indices provided by a novel planar robotic device for upper limb rehabilitation. J Neuroeng Rehabil 2018; 15:39. doi:10.1186/s12984-018-0385-8.
22. Germanotta M, Gower V, Papadopoulou D, et al. Reliability, validity and discriminant ability of a robotic device for finger training in patients with subacute stroke. J Neuroeng Rehabil 2020; 17:1-10.
23. Lance JW. Disordered muscle tone and movement. Clin Exp Neurol 1981; 18:27-35.
24. Toscano M, Celletti C, Viganò A, et al. Short-term effects of focal muscle vibration on motor recovery after acute stroke: A pilot randomized sham-controlled study. Front Neurol 2019; 10: doi:10.3389/fneur.2019.00115.
25. Cody FWJ, Henley NC, Parker L, Turner G. Phasic and tonic reflexes evoked in human antagonistic wrist muscles by tendon vibration. Electroencephalogr Clin Neurophysiol - Electromyogr Mot Control 1998; 109:24-35. doi:10.1016/S0924-980X(97)00063-5.
26. Cordo P, Lutsep H, Cordo L, Wright WG, Cacciatore T, Skoss R. Assisted movement with enhanced sensation (AMES): Coupling motor and sensory to remediate motor deficits in chronic stroke patients. Neurorehabil Neural Repair 2009; 23:67-77. doi:10.1177/1545968308317437.
27. Binder C, Kaya AE, Liepert J. Vibration prolongs the cortical silent period in an antagonistic muscle. Muscle and Nerve 2009; 39:776-80. doi:10.1002/mus.21240.

JOURNAL OF BIOLOGICAL REGULATORS & HOMEOSTATIC AGENTS Vol. 34, no. 5 (S3), 11-44 (2020)

Robotic treatment of the upper limb in chronic stroke and cerebral neuroplasticity: a systematic review

F. Bressi, M. Bravi, B. Campagnola, D. Bruno, A. Marzolla, F. Santacaterina, S. Miccinilli and S. Sterzi

Physical Medicine and Rehabilitation Department, Campus Bio-Medico University of Rome, Italy

Stroke is the second cause of mortality and the third cause of long-term disability worldwide. Deficits in upper limb (UL) capacity persist at 6 months post-stroke in 30-66% of hemiplegic stroke patients with major limitations in activity of daily living (ADL), thus making the recovery of paretic UL function the main rehabilitation goal. Robotic rehabilitation plays a crucial role since it allows to perform a repetitive, intensive, and task-oriented treatment, adaptable to the patients' residual abilities, necessary to facilitate recovery and the rehabilitation of the paretic UL. It has been proposed that robot-mediated training may amplify neuroplasticity by providing a major interaction of proprioceptive and/or other sensory inputs with motor outputs, with significant modifications in functional connectivity (coherence) within the fronto-parietal networks (inter- and intra-hemispheric functional connectivity) related to processes of movement preparation and execution. However, the neurophysiological mechanisms underlying this reorganization are not entirely clear yet. Therefore, the aim of this study is to revise the literature, which assesses the effect of robotic treatment in the recovery of UL deficits measured in terms of neuroplasticity in patients affected by chronic stroke. This systematic review was conducted using PubMed, PEDro, Cinahl (EBSCOhost), Scopus and Cochrane databases. The research was carried out until February 2020 it included articles written in English language, published between 2009 and 2020, and the outcomes considered were neuroplasticity assessments. We included 23 studies over 6145 records identified from the preliminary research. The selected studies proposed different methods for neuroplasticity assessment (i.e. transcranial direct current stimulation (tDCS), EEG-Based Brain Computer Interface (BCI) and Neuroimaging (fMRI)), and different Robotic Rehabilitation treatments. These studies demonstrated a positive correlation between changes in central nervous circuits and post-treatment clinical outcomes. Our study has highlighted the effectiveness of robotic therapy in promoting mechanisms that facilitate re-learning and motor recovery in patients with post-stroke chronic disabilities. However, future studies should overcome the limitations of heterogeneity found in the current literature, by proposing a greater number of high-level RCTs, to better understand the mechanisms of robot-induced neuroplasticity, follow the clinical progress, estimate a prognosis of recovery of motor function, and plan a personalized rehabilitative programme for the patients.

Description of the condition: stroke

The current World Health Organization (WHO) definition for stroke, introduced in 1970 and still applied, is "rapidly developing clinical symptoms and/or signs of focal, and at times global, disturbance of cerebral function, lasting more than 24 hours or

Key words: stroke; robotics; rehabilitation; neuronal plasticity; upper extremity

Corresponding author:
Dr F. Bressi,
Physical and Rehabilitation Unit,
Campus Bio-Medico University, Rome, Italy,
Via Alvaro del Portillo 5,
00128, Rome, Italy
e-mail: f.bressi@unicampus.it

0393-974X (2020)

leading to death, with no apparent cause other than that of vascular origin". It is characterized by "a sudden ischemic or hemorrhagic interruption in the blood flow to the brain" (1). This acute condition determines an irreversible brain tissue damage leading to a partial or total neurological loss (2-4). According to the AHA/ASA Guidelines (1), only a low percentage of patients fully recover the upper extremity function: this leads to a loss of independence and a lower quality of life for most stroke survivors (5). Kwakkel et al. (6) have demonstrated that, at six months from acute onset, only 11.6% out of a total of 102 stroke patients have recovered function and hand dexterity, while 38% only had a partial recovery. It should also be considered that according to WHO forecasts (7), stroke events will increase by 30% between 2000 and 2025.

After-stroke rehabilitation is a life-long process: following an acute rehab phase, it takes place at different times during a chronic period, depending on the patient's needs and on the phases of the illness. Furthermore, motor recovery of the post-stroke upper limb (UL) represents a challenge for rehabilitators. Firstly, the UL has different degrees of freedom; secondly, hand and finger movements are subject to a complex and specific cortico-motoneuronal control. Thirdly, it is classically known that the upper limb has a more extensive cortical representation than the lower limb, so it is easier for the area responsible for its control to be damaged (8). Additionally, current literature shows that there is a stronger correlation between hand function and execution of normal ADLs than with the function of other limbs (9). Therefore, the strategies that favor its recovery need to be further studied and understood. The goal of post-stroke rehabilitation should be to promote the recovery of lost function, regain independence and achieve early reintegration into social and domestic life.

Description of interventions: robots/rehabilitation

Rehabilitation is an important and essential step of post-stroke recovery. It combines different techniques and therapeutic strategies, without the proof of superiority of one over the other. The current literature suggests that an effective intervention must be intensive, task-specific, repetitive, and multisensorial (3). These characteristics are the basic requirements to facilitate motor learning in order to stimulate the process of "neuroplasticity" (10, 11).

The American Heart Association's 2016 Guidelines for Adult Stroke Rehabilitation and Recovery (12) recommend that robot-assisted training promote motor function and recovery after a stroke in association with conventional therapy (Level of Evidence A). Robotic rehabilitation can have a number of advantages in terms of reduced socio-economic burden and accessibility to care for most patients, and also allows healthcare professionals to monitor and treat patients at home in the chronic phase (3,12). The robotic assistive device has the advantage of several modalities for facilitating the voluntary movement according to the motor command: passive, active-aided, active, counter-resistance adjusted for each session, unior bimanual work. In the active-aided mode, the training is ''errorless'' since the robotic devices can complement the voluntary movement for each try (13). Robotic rehabilitation is a field in ever-growing evolution, so new devices are constantly designed for rehabilitation treatments, to go beyond the historical limits of those already on the market and stimulate the best motor recovery of patients.

Neuroplasticity

Neural plasticity is the basis for an adaptation process of functional and structural characteristics of the nervous system in response to a changing environment and/or after brain damage, like stroke. It represents an intrinsic characteristic of the CNS (14), which promotes recovery and learning of new information (15). The main authors are in favor of the hypothesis that development of neuroplasticity is based on mechanisms of cortical reorganization, structural and regenerative changes, and genetic factors (16-18). In addition, it seems that phenomena of cerebral plastic remodeling involve not only the perilesional area, but also the contralateral cortex, through strengthening of connections (19) and mechanisms known as long-term potentiation (LTP) and long-term depression (LTD) (20-23) Considering the human being in its complexity, a purely routine exercise is not as compelling and

necessary as the learning of a challenging motor skill (22). In this context, robotic rehabilitation is a highly stimulating method for stroke patients, as it provides a type of haptic interaction, which varies the types of assistance, gravitational relief, intensity and impedance, and allows to associate methods of virtual reality (8, 22). In addition, robots provide feedback on the performance achieved, which motivates the patient and further strengthens the relearning process in the motor cortex (24).

Iandolo et al. (25) pointed out how robot-therapy induce changes in neural plasticity and behavioral performance, and how they can be quantified by multimodal assessments of both sensorimotor performance and brain/muscular activity pre/post or during intervention. In fact, modern neuroimaging techniques play an important role in order to characterize the neural correlates of neurorehabilitation to obtain a clear picture of the underlying complex mechanism of neuroplastic changes accompanying the recovery. Oujamaa et al. (13), also showed that techniques promoting distal motor capacities (EMG-stim, robot-aided therapy, bilateral movements) seem efficient and that the emergence of central neuromodulation can complement motor training.

Based on these last affirmations, the aim of this study is to review the current literature about the effects of upper limb robotic treatment measured in terms of neuroplasticity in patients with chronic stroke, in order to better understand the mechanisms of robot induced neuroplasticity underpinning motor improvement. This may be important to monitor clinical improvement, predict a recovery prognosis for motor function, and design potentially personalized rehabilitation methods for the patient. Moreover, the neuroplasticity reservoir comprehension in post-stroke patients can be used to implement neuromodulation strategies (26-28)

MATERIALS AND METHODS

Inclusion criteria

We have considered clinical trials in English language, published between 2009 and February 2020. All the included studies investigated the effects of upper limb robotic rehabilitation on neuroplasticity in patients affected by chronic stroke from six months on. All the studies considered have been conducted on adult subjects (>18 years) affected by chronic stroke and they evaluated neuroplasticity data.

Search strategy

We have developed our search question using the PICO framework (Population, Intervention/Exposure, Comparison, and Outcome) (Table I). Scientific research has been based on PubMed/Medline, PEDro, Cinahl (EBSCOhost), Scopus and Cochrane databases using the following MeSH terms: "upper limb AND rehabilitation AND EEG AND stroke", "Plasticity AND upper limb robot therapy AND stroke", "TMS and chronic stroke", "Neuronal Plasticity AND Stroke Rehabilitation AND robot", "Plasticity AND robot", "Plasticity AND upper limb rehabilitation", "Robotic AND upper limb rehabilitation AND stroke", "Upper Extremity AND Stroke Rehabilitation AND Robot AND Electroencephalography AND Magnetic Resonance Imaging, "Stroke Rehabilitation AND Upper Extremity AND robot AND fMRI AND Clinical Trial", "Stroke Rehabilitation AND Upper Extremity AND Magnetic Resonance Imaging

Table I. *The PICO format.*

Population	Male or Female Adults aged 18 years or older, affected by chronic stroke
Intervention/Exposure	Upper limb robotic therapy or upper limb robotic therapy associated with any intervention that provided neuroplasticity
Comparison	Healthy subjects or sham treatment or exclusively robot-assisted therapy
Outcome	Neuroplasticity documented with exams/interventions (tDCS, fMRI)

AND Electroencephalography", "Stroke Rehabilitation AND Upper Extremity AND robot* AND eeg AND Clinical Trial AND Humans", "Robotic rehabilitation AND stroke AND MEG", "Robotic rehabilitation AND stroke AND EEG", "stroke rehabilitation AND upper extremity AND robot AND EEG", "stroke rehabilitation AND upper extremity AND robot AND fMRI", "stroke rehabilitation AND functional neuroimaging AND robot", "Robotic AND upper limb rehabilitation AND chronic stroke", "Functional Neuroimaging AND Stroke Rehabilitation AND Robotics".

DATA COLLECTION AND ANALYSIS

Study selection and eligibility criteria

Two independent authors have examined all studies. Records found in databases were first verified in their titles and abstracts, rejecting all non-significant works. Subsequently, the remaining articles were analyzed and discussed in their full text, to assess if they met the following eligibility criteria:

- Participants were adults (>18) with stroke in chronic phase (≥ 6 months after the event);
- All the studies were published from January 2009;
- Studies were written in English language;
- Studies involved robot devices for upper limb (29);
- Neuroplasticity documented using data provided by exams (i.e. EEG, fMRI).

Every different opinion among the reviewers was debated to reach a common consensus for the included studies.

Data extraction and synthesis

Eligible studies were analyzed to detect the following data: population studied (age, gender, handedness), characteristics of stroke (type, time from stroke onset, affected hemisphere, type of lesion), grade of impairment, intervention (rehabilitation protocol, type of robot, number of sessions), other intervention (if present), control group treatment, outcomes and results. The acquired data were subsequently synthetized in a tabular form (Table II).

Methodological quality assessment

Two different reviewers rated methodological quality of selected studies using The PEDRO Scale (30) and Levels of Evidence by Oxford Centre for Evidence-based Medicine (31). Disagreements were argued to reach a common judgment.

Assessment of risk of bias

We used the Risk of bias Assessment Tool of the Review Manager - RevMan (version 5.3. Copenhagen: The Nordic Cochrane Centre, The Cochrane Collaboration, 2014) to determine the risk of bias for each selected study.

Measurements of treatment effect

The effects of the treatment had to be measured by clinical results and neuroplasticity to address two main aspects: motor improvements and neuroplasticity evidence.

RESULTS

Search results / Description studies

The selection process of the studies analyzed in this review was carried out by applying the PRISMA Statement. Every step is explained in Fig. 1. We identified 6145 records from a preliminary research, 2279 from PubMed/Medline, 859 from Cochrane Library, 1498 from CinaHL, 1421 from Scopus and 88 from PEDro respectively. By screening their titles and abstracts, 768 records were considered eligible, however, once duplicates across databases were removed, 81 articles remained. After abstract review, 51 of them were investigated as potentially

Table I. *The PICO format.*

Population	Male or Female Adults aged 18 years or older, affected by chronic stroke
Intervention/Exposure	Upper limb robotic therapy or upper limb robotic therapy associated with any intervention that provided neuroplasticity
Comparison	Healthy subjects or sham treatment or exclusively robot-assisted therapy
Outcome	Neuroplasticity documented with exams/interventions (tDCS, fMRI)

appropriate for manual review, of which 28 were excluded: 13 did not evaluate neuroplasticity, 3 did not include robotic treatment, 6 did not include patients in chronic phase and 6 associated brain stimulation with treatment. Ultimately, after full-text reading, 23 articles were included. Based on the type of trial, 2 records were RCTs, 18 record was a pilot study, 1 record was a proof-of-principles study, 1 record was a multidomain analysis and 1 record was a clinical study.

Study participants

A total number of 258 patients, affected by chronic stroke, was involved in the selected studies, with 6 drop out: one from Vlaar et al. (32); one (33) because of transient nausea; two (34) because they did not complete the training; one (35) because of hand fracture and one (36) did not complete the training. Patients' clinical characteristics are specified on table n. II, except for Tung et al. (37) who did not report them in the article. According to the inclusion criteria, time from stroke onset is ≥ 6 months for every selected study. Furthermore, some studies (32, 38-40) used healthy subjects as a control group matched for characteristics (e.g. age, gender) with study group. The total number of volunteers recruited is 30, of which 10 are women.

Robot devices

The devices used in the various studies can be classified according to the treated district: eleven studies (36-46) have rehabilitated the entire upper

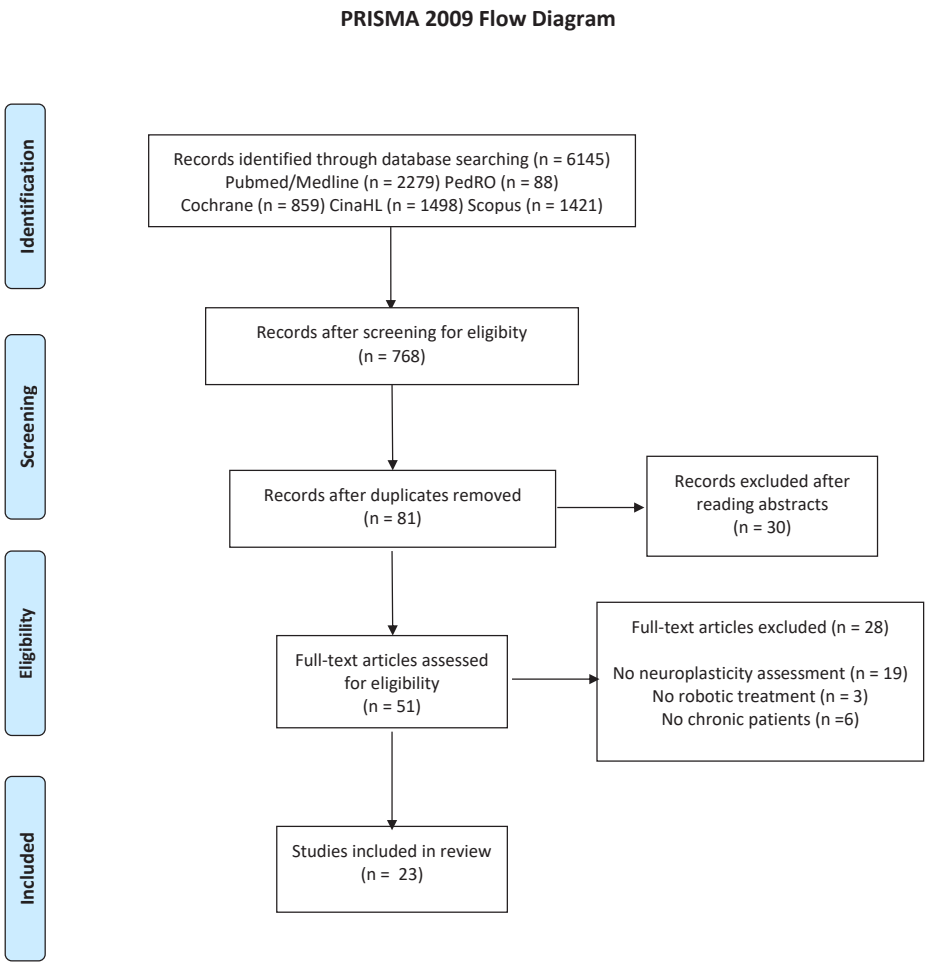

Fig. 1. *Prisma 2009 flow diagram.*

Table II. *Data extraction and synthesis.*

Author, Year, Type of study	Number and characteristics of patients, Characteristics of stroke, Impairment	Outcomes	Interventions/ Protocol	Control	Results
Ang KK et al., 2014, RCT	26 (1 drop out); Gender: 16 M + 10 F. Age: 51.4 ± 11.6 y. Handedness: 23R +3L Type of stroke: 10 ischemic + 16 hemorrhagic. Site of lesion: 8 Cortical + 18 Subcortical. Time from stroke: 297.4 ± 238.7 d. Affected Hemisphere: 11 L +15 R.	FMA; EEG data from BCI-Manus (rBSI).	BCI screening->Randomization in BCI-Manus or Manus Group -> r Rehabilitation session: 18 hours of intervention, delivered over 4 weeks (1.5 hours each, 3 times per week)	Manus Group: 12 Therapy sessions with MIT-Manus 2.	FMA at week 4 improved in both groups, with no intergroup differences (p 0.51). FMA scores at week 12 were attained in more subjects from BCI-Manus (7 of 11 [63.6%]) than Manus (5 of 14 [35.7%]). Negative correlation between rBSI and FMA score improvement (p .044)
Bae SJ et al, 2017, pilot study	9 Gender: 8 M + 1 F Age: 45.3y; Handedness: R Type of stroke: 1 Ischemic + 8 Hemorrhagic Site of lesion not known; Time from stroke: 3745.56 ± 1446,84 d; Affected Hemisphere: 9 R	fNIRS (ΔOxyHb) during experiment	Recruitment -> robot training 1 session divided in 3 cycles with different speeds (0,25Hz - 0,5 Hz-0.75 Hz) applied in random order (with each cycle consisting on rest-task-rest)	No control group	Passive wrist movements by robot caused cortical activation of the controlesional SM1, PMA and SAC (mainly observed in the SM1 and SAC $p<0,05$). Greatest activation of the SM1, PMA and SAC was observed at a speed of 0.75 Hz. No significant differences of ΔOxyHbs in each ROI
Baghat NA et al, 2014 pilot study	1 Gender: M Age: 45y Handedness not known Type of stroke: Ischemic Site of lesion: subcortical; Time from stroke not known; Affected Hemisphere: R	FMA, MAS EEG and EMG during experiment	First evaluation -> experimental protocol -> final evaluation A single session of robotic treatment with four different training mode: Passive, VelocityTriggered, Observation and Backdrive	Three healthy volonteers who underwent the same treatment	MRCPs were identified during backdrives, passive and triggered modes. There was a relatively high CA (medians around 75%) across all training modes, in particular in Triggered and Backdrive modes. Accuracies were significantly higher than chance levels (50%) for both healthy and stroke participants ($p<0.001$; α-level adjusted using Bonferroni correction multiple comparison: 0.0062).

Belardinelli P et al, 2017 pilot study	8 Gender: 7 M + 1 F Age: 57±11 y; Handedness: R Type of lesion: 3 Ischemic + 5 Hemorrhagic Site of lesion: not known; Time from stroke: 75.5±36.8m; Affected Hemisphere: R	FMA EEG data from BRI; MEG	Measure of clinical outcomes and MEG acquisition->Treatment -> Measure of clinical outomes and MEG acquisition 20-session training program (four weeks). Every session contained 15 runs, each lasting 2–3 min. A run consisted of 11 trials. (run: 2 s of rest period, 2s of preparation period, 6 s movement imagination period and a 6 s rest period).	No control group	FMA improved significantly from 16.23 ± 6.79 [6.80±28.60] to 19.52 ± 7.91 [10.85±35.25] (p 0.0015, paired t-test). For 5 patients the amplitude of muscle activity was found to be significantly increased (p 0.001). For 2 patients it was significan-tly decreased (p 0.001). For 1 patient no signifi-cant changes (p 0.08) were recorded. All patients showed significantly increased CMC in the β frequency band after the intervention by presenting a distributed, bihemisphe-ric pattern with considerable interindividual variability.
Belfatto A et al, 2018 Multidomain analysis	5 Gender: 5M Age: 61±11 y; Handedness: R Tipe of stroke: not known Site of lesion: not known; Time of stroke: more than 6 months; Affected Hemisphere: not known	FMA WMFT ROM EEG	Patients enrollment -> patient assessment -> robotic treatment with EEG recording -> patient assessment 12 sessions of robot-assisted movements (3 sessions per week), each one lasting 40 min that comprehended the execution of point-to-point reaching movements and hand-to-mouth movements.	No control group	- FMA, all patients gained at least 1 point (max pre-post Δ 9 points) (p 0.06). - WMFT scale, subjects reached at least 1 point of improvement (max Δ 5 points) (p 0.06).The EEG analysis showed that there was a desynchronization in cM1 bilaterally, in pre- and post-rehabilitation phases. The desynchronization spreads from β band to α and β frequencies and from part to the overall movement execution in both ipsi- and contralateral areas. There is not a clear trend in the α-based LC distribution pre/post-treatment since both ERDi and ERDc decrease, while LC in the beta band moves from negative (T0) to positive (T1) values (ERDc decreades while ERDi seems stable).
Brauchle D et al, 2015 pilot study	2 Gender: 2 M Age: 54±2,82y; Handedness: R Type of lesion: 1 Ischemic + 1 Hemorrhagic Site of lesion: not known; Time of stroke: 117±55,1d; Affected Hemisphere: R	BMI-EEG	Randomization -> Training and EEG evaluation One group performed BRI task, with participant's arm attached to the orthotic exoskeleton. The other one performed a BRI task identical to the first one except that their arms were not attached to the exoskeleton. Each session lasted approximately 30 min and consisted of five runs, each consisting of 10 trials.	3 healthy subjects who were not attached to the exoskeletron	All subjects enrolled were able to modulate sufficient sensorimotor ERSP in the β-band and they had very similar patterns of robot control regardless of the clinical condition (healthy/patient) or the feedback modality (pro-prioceptive/visual), but patients showed lower average performances than their healthy contro-parts with proprioceptive feedback for the full feed-back duration. A distributed cortical net-work of task-related coherent activity in the θ-band showed significant differences between healthy subjects and stroke patients as well as between early and late periods of the task

Calabrò RS et al, 2017 pilot RCT	35 Gender: 9 M + 11 F Age: 66±5y; Handedness: not known Tipe of stroke: Ischemic Site of lesion: subcortical; Time of stroke 6±1m; Affected Hemisphere: L	MAS, FMA-UE FIM SICI, HMR	Evaluation of the outcomes -> randomization -> training with (Group-A) or without (group-B) MV-> evaluation of outcomes ->evaluation after 2 months 40 daily sessions (1 hour/session, 5 sessions/week for 8 weeks). Subjects performed repetitively a group of exercises to improve arm and elbow movements.	10 patient (group B) who didn't receive MV	In group-A there was a greater reduction of MAS (p 0.007, d:0.6) and HMR (p<0.001, d:0.7), and a more evident increase of SICI (p<0.001, d:0.7) up to 4 weeks after the end of the treatment, as compared to group-B. Likewise, group-A showed a greater result in FMA-UE (p 0.007, d 0.4) up to 4 weeks after the end of the treatment. A significant correlation was found between the degree of MAS reduction and SICI increase in the agonist spastic muscles (p 0.004).
Calabrò RS et al, 2019 RCT	50 Gender: 25 M + 25 F Age: 64±0.5y; Handedness: R41 + L9 Type of lesion: Ischemic Site of lesion: subcortical; Time after stroke 10±0.6m; Affected Hemisphere: 29 R + 21 L	FMA and 9HPT EEG	Pre-T evaluation (clinical outcomes and EEG) --> randomization in AHT and CHT -> rehabilitation --> post-T evaluation (clinical outcomes and EEG) AHT group: intensive robotic training of the affected hand. CHT group: intensive conventional physio-therapy of the affected hand. 40 sessions, 45 min each, 5 times/week for 8 weeks	25 patients who underwent therapist-guided conventional hand training	The AHT group presented improvements in FMA and 9HPT greater than CHT (both p < 0.001). These results were paralleled by a larger increase in the fronto-parietal TRCoh in the AHT than in the CHT group (p < 0.001) and a greater rebalance between the SAI of both the hemispheres (p < 0.001).
Chowdury A et al, 2013 clinical study	5 (1 dropout) Gender: 2 M + 3 F Age: 61.6 ± 5.31y; Handedness: not known Tipe of stroke: Ischemic Site of lesion: not known; Time of stroke: 21.8 ± 4,5m; Affected Hemisphere: not known	ARAT, UE strength EEG data from BCI-robotic system	Patients enrollment -> patient assessment -> robotic treatment with EEG recording -> patient assessment Intervention: physical practice stage using assist-as-needed control of the exoskeleton by the participant, followed by an h-BRI mediated neurofeedback stage.	No control group	The group-mean increase in the performance of the h-BRI, basis of CA, was 19.01% (p <0.05, paired t-test). The last session the average CA increased up to 77.17±3.65. GS and ARAT also showed significant (p<0.05, paired t-test) improvements in hand functionnality (group-mean change in GS +9.83 kg and in ARAT +23.75). Results of the average ERD/ERS β-band for EEG every channel for the first and last session of intervention show significant (p<0.05, paired t-test) reduction in both ipsi- and contra-lesional β desynchronization.

Gandolfi M et al, 2018 pilot study	7 Gender: M Age:≥ 18y Handedness: R Type of stroke: 5 Ischemic + 2 Hemorrhagic Site of lesion: subcortical; Time from stroke: 66.57 ± 36.61m; Affected Hemisphere: 1 R + 6 L	FMA, MAS EEG and EMG during experiment	First evaluation -> experimental protocol -> final evaluation A single session of robotic treatment with four different training mode: Passive, Velocity Triggered, Observation and Backdrive	Eight healthy volonteers performing the same experimental motor paradigm	Changes in FMA were significant at T2 (p 0.008) and in MAS at T1 and T2 (both p0.017). After training, Desynchronization on the ipsilesional sensorimotor areas increased during passive and active movement, as compared with T0.
Nam HS et al, 2017 pilot study	1 Gender: M Age: 56y Handedness: L Type of lesion: Hemorrhagic Site of lesion: cortical; Time from stroke: 11m; Affected Hemisphere: not known	FM, MAS, JHFT, TFT fMRI	Assessed of clinical outcomes and fMRI acquisition -> training -> evaluation of outcomes and fMRI acquisition -> evaluation of clinical out-comes at 2-month follow-up 10-session robotic mirror therapy: each session consisted of 4 tasks (ball in holes, soccer game, dot tracing and moving a cup), each performed for 5 minutes. (30 min total)	No control group	At the follow-up evaluation, TFT score improved from 2 to 1 for eye level and from 3 to 1 for overhead level, other parameters revealed no difference. The fMRI during the passive motion revealed a considerable increase in brain activity at the lower part of the right superior parietal lobule.
Pellegrino G et al, 2012 pilot study	7 Gender: 5M + 2F Age: 60±18 y; Handedness: R; Type of lesion: Ischemic; Site of lesion: cortical; Time after stroke: frome 1 to 5y; Affected Hemisphere: 5 R + 2 L	FMA, Hand motor control EEG	Clinical, hand motor control and EEG evaluation -> robotic rehabilitation -> cinical, hand motor control and EEG evaluation 1 hour/day for 3 days a week. All subjects underwent 6 weeks of training with InMotion2 robot and 6 weeks with the InMotion3 robot	No control group	Improvement of FMA scores and hand motor control performance and changes of brain connectivity in high frequency rhythms (24-90 Hz). The improvement of motor performance correlated with the modulation of the interhemispheric S1 coherence in the high β band (24-33 Hz)
Rathee D et al, 2019 pilot study	5 (1 dropout) Gender: 2 M + 3 F Age: ± y; Handedness: not known Tipe of stroke: Ischemic Site of lesion: 2 subcortical + 3 cortical; Time of stroke: ± ; Affected Hemisphere: not known	ARAT, UE strenght MEG data from BCI-robotic system	Patients enrollment -> patient assessment -> robotic treatment with MEG recording -> patient assessment The intervention consisted of two stages. The first one was the PP stage of 30 min followed by a MP stage of almost 46 min including the BCI calibration time of around 16 min.	No control group	All the participants increased in ARAT score (p 0:00028). The MCID values for GS were reported as 5.0 and 6.2 kg and for ARAT as 12 and 17 points (impaired dominant and nondominant UL). Significant functional connectivity sub-networks for alpha (8-15 Hz), beta-low (15-26 Hz), beta-high (26-35 Hz) frequency bands; but these subnet-works are stable only for beta-low (15-26 Hz) band. For all the participants, the intra-hemispherical FC values in motor cortical regions involving M1, S1 and SMA ipsi- and contralesional hemi-spheres increase with UL functional recovery. The group analysis showed increase in node strengths in the motor cortex region and decrease in the node strengths in the frontal, parietal and occipital areas of the contralesional hemisphere.

Saita K et al, 2016 pilot study	7; Gender: 3 M + 4 F; Age: 60.6 ± 8.4y; Handedness: R; Type of stroke: 3 Ischemic + 4 Hemorrhagic; Site of lesion: subcortical; Time of stroke: 35.0 ± 44.0m; Affected Hemisphere: 5 R + 2 L	FMA, FMA-UE, ARAT, MAL, MAS FNIRS	Detailed clinical evaluation -> BTX-A injection -> robot rehabilitation -> home exercises (2 weeks) -> follow-up at the end of home exercises (T1) and after 1 month (T2) Rehabilitation consisted in repeated flexion and extension movement of elbow joint at least 200 times at session. Therapy lasted 60 min per session, 10 times/week, for 2 weeks	No control group	At 2 weeks follow up: FMA ($p=0.043$), ARAT scores ($p=0.026$), MAL score ($p=0.018$). At 4-months follow up: FMA ($p0.041$), FMA-UE ($p0.041$), ARAT scores ($p0.018$), MAL score ($p0.018$). MAS score was not significally at follow ups. The analysis of ΔHbO using NIRS-SP, showed an increase of activity at the baseline activation maps of the primary sensorimotor area of the controlesional hemisphere and the prefontal area of the ipsilesional hemisphere ($p<0.001$). Compared with baseline activation maps, activity increased in the primary sensorimotor area of the ipsilesional hemisphere at 2 weeks and at 4-month follow up ($p<0.001$). At 4-month follow up, activity addictionally increased in the contralesional hemisphere ($p<0.001$). HHb changes were not significant on the t-statistic map
Sale P et al, 2015, pilot study	2 Gender: 1 M + 1 F; Age: 65.5 ± 13.43y; Handedness: not known Tipe of stroke: Hemorrhagic Site of lesion: cortical; Time of stroke: not known; Affected Hemisphere: 1 R + 1 L	FMA, BBT, MAS, ROM and MI EEG	Evaluation of the outcomes -> training while EEG was recorded-> evaluation of outcomes 30 sessions lasting 45 min each, 5 days a week, for 6 weeks. Rehabilitative protocol: exercises aimed at improving both movement type and mode of execution of the movement itself, with progression from passive to free movement.	No control group	Improvements were found in FMA, BBT, ROM and MI whereas a decrease was found on the MAS. In EEG datas were observed: reduced delta rhythms (1–4 Hz) and increased alpha rhythms (8–12 Hz) during the resting state eyes-closed condition; increased alpha desynchronization to eyes opening; and decreased alpha desynchronization during the robotic rehabilitation task
Saleh S et al, 2012 pilot study	2 Gender: M Age: 58.5 ± 10.6 y; Handedness: R Type of stroke: not known Site of lesion: subcortical; Time after stroke: more than 6 months; Affected Hemisphere: 1 R + 1 L	WMFT, JTHFT and FMA fMRI	Clinical assessment and fMRI collection -> robotic training -> clinical assessment and fMRI collection NJIT-RAVR training: subjects play video games to improve subjects' hand/ arm coordination, reaching, grasping, and finger individuation. (3 hours/day, 4 days/ week, for 2 weeks.)	No control group	Both the FMA gain and FCCs were numerically higher in the MI-BCI group. Increases in FC of the supplementary motor area, the contra- and ipsilesional motor cortex, and parts of the visuo-spatial system with mostly association cortex regions and the cerebellum correlated with individual upper-extremity function improvement.

Saleh S et al, 2017 pilot study	19 Gender: 14 M + 5 F Age: 59.6±10.6y for RAVR group, 57±12,8y for RTP group; Handedness: not known Type of lesion:18 Ischemic + 1 Hemorrhagic Site of lesion: 8 cortical 11 subcortical; Time from stroke: 90±53 m; Affected Hemisphere: 8 R + 11 L	JTHFT fMRI	Measure of clinical outomes and fMRI acquisition-> randomization in RAVR and RTP group -> Treatment -> Measure of clinical outomes and fMRI acquisition 4 days a week, 3 h per day for 2 weeks. RAVR group: training programme with robotic assistance RTP group: training with repetitive task practice (RTP) reach and grasp exercises and functional tasks	9 patients who underwent repetitive task practice (RTP)	Both groups improved in the JTHFT score, with the percentage change reaching statistical significance in the RAVR (Z = −2.8, p 0.005). No significant between-group difference in the change in JTHFT scores. The activation magnitude in the cerebellum, left temporal lobe, and right precentral gyrus was significantly reduced after RAVR-based training, also a significant decrease in the extent of activity in the RAVR group after training (Z = −2.894, p 0.0038). The change in LI after training was significantly different between groups (RAVR group LI median = −0.125, RTP group LI median = 0.07, Z = −2.21, p = 0.027)
Sergi F et al, 2017 pilot study	2; Gender: F; Age: 68-77 y; Handedness: R; Type of lesion not known Site of lesion:2 mixed stroke; Time of stroke: 1.85-1.18 y; Affected Hemisphere: dx	FMA; MRC; Grip %, planar coordinates fMRI	Pre-T evaluation (motor function testing and fRMI) --> rehabilitation -> post-T evaluation (kinematic analysis and fMRI) Robot therapy (Mit Manus InMotion 2 e 3): 12-week, 3 times/ week.	2 healthy volunteer participated to 1 MRI session to determine brain regions normally active during UE movement with the MRI compatible	Patient 1, compared to patient 2, had greater gains in motor function and greater reduction in interhemispheric functional connectivity between the ipsilesional and controlesional M1 during the resting-state
Trujillo P et al, 2017 pilot study	10 Gender: 8 M + 2F Age: 55.7±16,2 y; Handedness: not known; Type of stroke: Ischemic Site of lesion: not known; Time after stroke: 5.7 ± 4.92; Affected Hemisphere: not known	FMA fMRI	Outcomes and EEG recording -> Training -> outcomes and EEG recording 12 training sessions, each one lasting 40 minutes, 3 sessions a week for 4 weeks. Each session consisted in 20 min of intensive repetition of reaching movement and hand to mouth movement	No control group	Significant negative correlation between PRIT0 and the ΔFMA (ρ −0.77, P 0.009). DART0 also showed a negative relationship with ΔFMA, not significant. A significant negative correlation between PRI(T0) and the ΔFMA% (ρ−0.69, P0.03), and a trend to a negative correlation between DART0 and ΔFMA% (ρ −0.54, P 0.11). BSIT0 did not correlate with neither the ΔFMA nor the FMA% The comparison between T0 and T1 for PRI and DAR indices did not show any significant variation.

Tung SW et al 2013 pilot study	6 Gender: not known Age: not known; Handedness: not known; Type of lesion: not known Site of lesion: not known; Time from stroke: not known; Affected Hemisphere: not known	FMA EEG data from BCI-Manus	Assessement of clinical outcome -> robotic therapy with BCI- EEG recording -> follow up after 2 weeks from the end of treatment 10-sessions of 1-hour BCI therapy for 2 weeks, 5 times/week. 160 trials of EEG per session were collected.	No control group	Significant improvement in the FMA scores was reported for five patients ($p = 0.01$). The analysis showed that the number of sessions with CI ≥ 0.5 are correlated with the change in the FMA scores (Pearson's correlation coefficient of 0.819, which is statistically significant with p 0.046).
Vahdat S et al, 2019 proof-of-principles study	10 (dropout 2) Gender: 8 M + 2F Age: 62 ± 8.84 y; Handedness: not known Type of lesion: Ischemic Site of lesion: 7 cortical + 3 subcortical; Time of stroke: 47 ± 42.1m; Affected Hemisphere: 3 L + 7 R	FMA fMRI	Initial reaching test + fMRI acquisition -> somatosensory training with robotic assistance -> active robotic reaching movements -> final evaluation and fMRI acquisition Patients underwent one session of 4 blocks of somatosensory training. After a second brain scanning session, patients returned to the robotic lab to perform a final block of 50 trials of active reaching movements.	No control group	For 8 patients training resulted in more accurate perception of right-left boundary at the body midline ($t(7)=2.71$, $p< 0.05$). For 6 patients' reaching movements following perceptual learning became straighter than before ($t(5)=4.333$, $p<0.01$). FMA scores was correlated with training-induced FC changes in a network comprising SMG, (seed) and ipsi-lesional SMG and S1. A post-hoc analysis of FC values before and after training showed that these areas became more positively correlated post training.
Vlaar MP et al, 2017 pilot study	30 (dropout 1) Gender: 18 M + 12 F Age: 64 ± 11y; Handedness: 17 R + 13 L Type of lesion: Ischemic Site of lesion: Cortical; Time of stroke: 41.07 ± 48.38 m; Affected Hemisphere: 13 R + 17 L	FMA EEG Signal-to-noise ratio and laterality index during training	evaluation of level of sensory and motor impairment -> classification in no sensory, mild and severe impairment -> experimental protocol Rehabilitation consisted in active task lasts 12.5 s. For each task 20 trials were recorded. The first two periods were discarded to reduce the influence of transient effects, resulting in a total of 160 periods for each task.	Ten unpaired age-matched volonteers who underwent the same training	Under passive conditions, wrist manipulation resulted in contralateral cortical responses in unimpaired and mild and no sensory impairment group. In severe sensory impairment group cortical responses were strongly reduced in amplitude, which related to anatomical damage. Under active conditions patients with mild sensory impairment showed reduced responses compared to the passive condition, unimpaired and participants without sensory impairment did not show this reduction.

Wang X et al, 2018 pilot study	24 Gender: 20 M + 4 F Age: 54 ± 9y; Handedness: not known Type of lesion: 14 Ischemic + 10 Hemorrhagic Site of lesion: mixed stroke; Time from stroke: 4 ± 3 y; Affected Hemisphere: 15 R + 9 L	FMA EEG fMRI (16 of 24)	Assessed of clinical outcomes -> Randomization in Robot-EEG-Text and Robot-noEEG-text -> rehabilitation programme -> evaluation immediately after and 6 months after intervention 20-session robot-assisted hand training, with an intensity of 3–5 sessions per week that was completed within 5–7 weeks. During each session, 100 repetitive hand movements were performed by each subject with intermittent rest after every 10 trials.	11 patients who underwent robot-hand training without AO and EEG guidance (Robotnon−EEG_Text, n = 11)	After the interventions, RobotEEG_AO group showed significant differrence in paretic UL motor functions across the longitudinal evaluation [X^2 (2) = 7.659, p 0.022]. Significant improvements in the paretic motor functions between pre- and post-intervention (Z = −2.135, p = 0.033) and between preintervention and 6-month follow-up (Z = −2.451, p = 0.014) in the RobotEEG_AO group. The proportion of subjects exceeding the MCID was higher in the RobotEEG_AO group (pre vs. post: 53.8%; pre vs. 6-month: 54.5%) compared with the Robotnon−EEG_Text group (pre vs. post: 36.4%; pre vs. 6-month: 36.4%).

limb; elbow rehabilitation only in Saita et al.(47); wrist rehabilitation in two studies (32, 48) and hand rehabilitation was considered in six studies (28, 35, 49-52). The remains studies combined the treatment of two different districts: Nam et al. (53) focused on wrist and elbow rehabilitation, while Ang et al. (33) and Vahdat et al. (34) on shoulder and elbow one. Regarding the technical characteristics (i.e. name, model and industry) of robot, eight trial (35, 36, 47-51, 53) didn't specify them, while two (43, 46) indicated only the name of the robot (Mitsubishi Pa10-7). InMotion2 (Massachusetts Institute of Technology, Boston, USA) was used in four studies (33, 34, 37, 45), while Sergi et al. (42) and Pellegrino et al. (41) structured their rehabilitation program combining InMotion2 and InMotion3 (Massachusetts Institute of Technology, Boston, USA). Other devices used are: Amadeo (28, 52) (Tyromotion GmbH, Graz, Austria), ArmeoPower (40, 44) (Hocoma, Volketswil, Switzerland), Bi-Manu-Track (39) (Rehastim Co, Berlin, Germany), Mahi Exo-II (38) (MAHI lab, Houston, USA) and Wristalyzer (32) (MOOG, Nieuw-Vennep, Netherlands).

Outcome assessments

Outcomes were divided into two categories: motor aspects and neuroplasticity.

Motor aspects

The outcome measures used among all the studies were different, but they met the same aim: to access UL function and sensory-motor parameters. Two studies (40,48) did not analized motor aspect. Except of them, all studies used the Fugl-Meyer Assessment (FMA). Four studies (35, 36, 39, 47) used the Action Research Arm Test (ARAT) and one study (45) utilized the Box and Block score (BBT). Modified Ashworth Scale (MAS) was used in six studies (38, 39, 44, 45, 47,53) while Motricity Index (MI) was used in two studies (39, 45) as well as Wolf Motor Function Test (WMFT) (46, 50). Four studies (35, 36, 42, 44) also used a dynamometer to assess strength upper limb and grip, one study (41) measured hand motor control, while in one study (53) Thumb Finding Test (TFT) was performed. Three studies (50, 51, 53) also performed Jebsen Taylor Hand Function Test (JTHFT). One study (42)

used the Medical Research Council (MRC) scale to measure 18 muscles of the UL. In Saita et al. study (47) Motor Activity Log (MAL) was performed and Calabrò et al. used the Nine-Hole Peg Test (9HPT) in 2019 study (28) and Functional Indipendence Measure (FIM) in 2017 study (44). Furthermore, joint kinematic and muscle activity were recorded by robot in four studies (32, 38, 44, 46).

Neuroplasticity

Each trial assessed neuroplasticity using different modalities; the most used is EEG but performed in different ways. Six studies (32, 39, 41, 45, 46) investigated cortical activity and excitability, including Trujillo et al. (43) who also quantified cortical activity. One study (38) analyzed the intention to movement during robotic therapy and another one (28) used EEG to highlight cortical activation event related and motor potential evocked. Three studies utilized the EEG-based BRI system: one study (35) extracted the correlation of bandlimited power time-courses (CBPT features); Brauchle et al (40). registered task-related network changes of cortical functional connectivity by EEG via the imaginary part of the coherence function, while Belardinelli et al.(52) utilized this system to open and close the paralyzed hand when triggered by ipsilesional oscillatory brain activity and MEG to investigate cortical activation. Furthermore, two studies examined the EEG-based MI-BCI data: Ang et al. (33) quantified EEG data using revised Brain Simmetry Index (rBSI) and Tung et al. (37) analyzed the coherences of the EEG in the lesion and contralesion side of the hemisphere from each session and the coherence index of the lesion hemisphere. Instead, Rathee et al. (36) used a BCI-MEG system to estimate the brain connectivity networks in conjunction with rehabilitative training. Seven studies used fMRI: one study (53) analyzed cortical activity related to movement; three studies (34, 42, 50) investigated connectivity and functional connectivity related to training; one study (51) used it to characterize neural reorganization while Wang et al. (49) focused on BOLD-fMRI to observe which areas of brain were found to be active during rehabilitation. Vahdat et al. (34) also analyzed structural changes in cerebral cortex. In Saita et al. (47) and Bae et al. (48) studies fNIRS (ΔOxyHb) was measured to verify cortical activity. Finally, in Calabro et al. (44) study, the neurological assessment used were MEP and SICI (short intracortical inhibition) magnitude to measure cortical excitability.

Interventions

The analysis of the studies revealed a heterogeneity of protocols and evaluations. Nevertheless, all studies described the number of sessions and the overall duration of robotic rehabilitation treatment. Table II summarize the study partecipants, oucomes and results.

The pilot study by Baghat et al. (38) focused on the elbow rehabilitation: the aim of the study was to create a neural interface using slow movement-related cortical potentials (MRCPs) for an exoskeleton (MAHI-Exo II, MAHI lab, Houston, USA). One subject with chronic stroke underwent a single session of robotic treatment with four different training mode: Passive, where no volitional movements are required from users; Active or Backdrive mode, a resistance-training mode in which the user must move their limb without any assistance from robot; Velocity Triggered or Triggered, where the user self-initiates movement, following which the robot completes the movement and Observation, wherein the subject only observed an experimenter operate the Exo in "Triggered" mode. Each mode consisted of 80 movements (elbow flexion/estension) split into four blocks of 20. The order of the modes for each subject was randomized. Breaks were given between each block and mode to minimize user fatigue.

During training, EEG was recorded to verify neural activity. Three healthy volunteers were enrolled as control group and they underwent the same stroke patients' protocol. Gandolfi et al. (39) wanted to evaluate changes in upper limb function and EEG power after a robot-assisted bilateral arm training (R-BAT). Seven chronic stroke patients with upper limb paresis received 21 sessions (3 days/week) of R-BAT: the protocol consisted of six tasks involving unilateral, bilateral, passive, and active movements of wrist flexion/extension. During each session, patients performed up to 800 repetitions:

400 in passive-passive mode and 400 in active-passive mode (200 prono/supination and 200 wrist flexion/extension respectively).

EEG assessments and clinical outcomes were carried out at baseline, after training and at 1 month follow up. Control data was collected from eight healthy volunteers who performed the same experimental motor paradigm. Bae et al. (48) attempted to investigate differences in cortical activation according to the speeds of passive wrist movements performed by a rehabilitation robot for stroke survivors. Nine stroke patients participated in this study. Passive movements of the affected wrist were performed by the rehabilitation robot at three different speeds: 0.25 Hz, slow; 0.5Hz, moderate and 0.75 Hz, fast.

The authors used functional near-infrared spectroscopy (fNIRS) to measure the brain activity during the passive movements performed by a robot. Group-average activation map and the relative changes in oxy-hemoglobin (ΔOxyHb) in primary sensory-motor cortex (SM1) and premotor area (PMA) and somatosensory association cortex (SAC) were measured. No control group was enlisted. Wang et al. (49) explored the clinical improvement and the neurological changes after 20-sessions guided or non-guided robot hand training using two measures: changes in brain discriminant ability between motor-imagery and resting states revealed from EEG signals and changes in brain network variability revealed from resting-state fMRI data collected in 24 chronic stroke subjects.

The subjects were randomly assigned to receive either combined action observation (AO) with EEG-guided robot-hand training (RobotEEG_AO, n=13), in which robot hand was activated only when significant μ suppression (8–12Hz) was detected from subjects' EEG signals in ipsilesional hemisphere or robot-hand training without AO and EEG guidance (Robotnon−EEG_Text, n=11), where robot hand was randomly activated regardless of their EEG signals. During each session, 100 repetitive hand movements were performed by each subject with intermittent rest every 10 trials. Saleh et al. (50) investigated the effect of 2 weeks of robot-aided virtual reality (RAVR) therapy for the paretic upper limb in stroke patients on changes in brain activation. Brain activation was acquired during the resting state and during visually guided hand movement.

FMRI analysis focused on characterizing functional connectivity with ipsilesional primary motor cortex (iM1) at rest and during execution of paretic hand movement. Two subjects participated and they played video games in a RAVR setup. This setup works on retraining subjects' hand/arm coordination, reaching, grasping, and finger individuation. The training was conducted for two weeks (3 hours/day, 4 days/week). In a following study, Saleh et al. (51) aimed to compare the effect of the same RAVR protocol and repetitive task practice training (RTP). They compare neural reorganization elicited in stroke patients participating in these two interventions. Ten chronic stroke subjects participated in eight 3-h sessions of RAVR therapy, while another group of nine stroke subjects participated in eight sessions of matched RTP therapy: training included repetitive reach and grasps exercises and functional tasks. FMRI datas were acquired during paretic hand movement, before and after training.

The authors compared the difference between groups and sessions (before and after training) in terms of BOLD intensity, laterality index (LI) of activation in sensorimotor areas, and the effective connectivity between ipsilesional motor cortex (iMC), contralesional motor cortex, ipsilesional primary somatosensory cortex (iS1), ipsilesional ventral premotor area (iPMv) and ipsilesional supplementary motor area. Also in Calabrò et al. (28) compared robotic and conventional treatment: 50 patients with a first-ever stroke in chronic phase, were enrolled and randomized into two groups.

The experimental group was provided with the Amadeo (Tyromotion GmbH, Graz, Austria) hand training (AHT), whereas the control group underwent occupational therapist-guided conventional hand training (CHT). Both of the groups received 40 hand training sessions (5 times a week, for 8 weeks). The aim of this study was the evaluation of the clinical and neurophysiological effects of intensive robot-assisted hand therapy compared to intensive occupational therapy in the chronic recovery phase after stroke.

For this reason, all participants underwent a clinical and electrophysiological assessment (task-related coherence, TRCoh, and short-latency afferent inhibition, SAI) at baseline and after the completion of the training.

Brauchle et al. (40) tested the feasibility of three-dimensional robotic assistance for reaching movements with a multi-joint exoskeleton during motor imagery (MI)-related during brain-states in which both the participant's effort to move and the responsiveness of the brain for peripheral input were reflected. They also registered task-related network changes of cortical functional connectivity via the imaginary part of the coherence function. Two stroke survivor and six healthy volunteers performed the first BRI task: each participant's arm was attached to the orthotic exoskeleton. Three healthy volunteers performed a second BRI task, which was identical to the first one except that their arms were not attached to the exoskeleton. Each session consisted of five runs, each composed of 10 trials. Changes in cortical physiology were recorded during therapy in both groups by electroencephalography.

In Sale et al. (45) work, the objective was to study neural underspinning of robot-aided upper limb rehabilitation in stroke patients. Two subjects underwent a program of 30 daily rehabilitation sessions: the rehabilitative protocol consisted of exercises aimed at improving both movement type and mode of execution of the movement itself, with progression from passive to free movement. EEG was recording before and after the rehabilitation program.

Trujillo et al. (43) focused on quantitative EEG (QEEG), and in particular the relationship between QEEG measures and the motor outcome in chronic stroke survivor that underwent a robot-assisted rehabilitation program. The objective of this program was to evaluate the utility of QEEG indices to predict motor recovery. Ten post-stroke patients underwent the rehabilitation protocol that consisted of 12 training sessions, each one lasting 40 minutes: 20 minutes of intensive repetition of reaching movements and 20 minutes of hand to mouth movements. Before and after training programme, resting-state EEG signals were acquired and the power ratio index (PRI), delta/alpha ratio (DAR), and brain symmetry index (BSI) were calculated.

Belardinelli et al. (52) aimed to investigate the functional relevant mechanisms of neural plasticity by evaluate cortico-muscular coherence (CMC). A brain-robot interface turned event-related beta-band desynchronization of the lesioned sensorimotor cortex during kinesthetic motor-imagery into the opening of the paralyzed hand by a robotic orthosis: training consisted in 20 sessions of 15 runs, everyone composed by 11 trials. Simultaneous MEG/EMG recordings and individual models from MRIs were used for CMC detection and source reconstruction of cortico-muscular connectivity to the affected finger extensors before and after the training program. No control group were enrolled.

Chowdhury et al. (35) also investigated CMC and if this has a role in providing meaningful neurofeedback of the therapeutic task performance leading to a faster recovery. They realized a 5-week-long clinical study on four chronic stroke patients where they used correlation of band-limited power time-courses (CBPT), a measure of corticomuscular coupling, as a feature for providing multimodal neurofeedback for hand exoskeleton-based therapy. The intervention was composed of a physical practice stage using assist-as-needed control of the exoskeleton by the 4 participants, followed by an h-BRI mediated neurofeedback stage.

In Rathee et al. (36) pilot study, the authors examined the longitudinal changes in band-limited resting-state (RS) functional connectivity (FC) networks in association with post-stroke UL functional recovery achieved by a multimodal intervention involving motor attempt (MA) based BCI and robotic hand-exoskeleton. Four adults were rehabilitated with the intervention for a period lasting up to 6 weeks. The intervention consisted of two stages. The first stage consisted of repetitive finger grasping and extension exercise provided by home-grown hand-exoskeleton device, followed by a second stage where participants were given a hybrid-BCI based multimodal contingent to the simultaneous activations in the EEG and EMG signals. Resting state MEG signals and clinical outcomes were recorded during five equispaced

sessions over the intervention period.

Belfatto et al. (46) proposed a multiparameter approach, included EEG and EMG, to evaluate post-stroke patients before and after robotic therapy: five subjects underwent 12 sessions of robotic therapy, that comprehended the execution point-to-point reaching movements and hand-to-mouth movements. The study did not enroll a control group.

Pellegrino et al. (41) aimed to assess the brain plastic reorganizations and their association with clinical progresses induced by a robot-aided rehabilitation program in chronic stroke patients. Seven patients with an upper limb motor impairment underwent a 12-weeks neurorehabilitation program: all subjects submitted six weeks of training with InMotion2 robot and six weeks with InMotion3 robot (Interactive Motion Technologies, Watertown, MA). 32-channel EEG focusing on ipsi- and contra-lesional resting state properties investigating both bipolar derivations overlying the middle cerebral artery territory characterized cerebral reorganizations and the primary somatosensory sources (S1) obtained through the Functional Source Separation (FSS) method. Power Spectral Density (PSD) and interhemispheric coherence (IHCoh) at rest were measured and correlated with clinical and hand control robot-induced improvements.

The pilot study by Sergi et al. (42) aimed to prove if robot-aided motor rehabilitation could enhance functional connectivity of the sensorimotor networks. Two patients affected by chronic stroke were firstly evaluated in motor function testing while functional connectivity was assessed by three scans of fMRI during the use of a MRI-compatible manipulandum, that was similar to the robot used during the robotic session. Later, patients undertook a 12 weeks robotic rehabilitation program, using InMotion2 shoulder-elbow robot and the InMotion3 wrist robot (Interactive Motion Technologies, Watertown, MA) (54, 55), similar to the Pellegrino et al. (41) one.

At the end of the rehabilitation, a single resting-state MRI scan was collected. Two healthy subjects were enrolled as a control group, performing a single MRI to study which brain area is normally activated during upper limb movements using the manipulandum described above. The collected data were then used as a standard for the analysis of patients' fMRI. In Tung et al. (37) pilot study the authors aimed to track the effect of the BCI technology on brain plasticity.

In this study, the EEG signals recorded during upper limb stroke rehabilitation using motor imagery BCI were analyzed to better understand the effect of BCI therapy in post-stroke rehabilitation. Six stroke patients underwent 10 sessions of 1-hour BCI with robotic feedback for 2 weeks.

A total of 160 trials of EEG per session were collected. The analysis was performed by computing the coherences of the EEG in the lesion and contralesion side of the hemisphere from each session. The coherence index of the lesion hemisphere, the rate of activation of the lesion hemisphere, was computed and its correlation with the Fugl-Meyer assessment (FMA) before and after the BCI therapy was investigated. Also, Ang et al. (33) aimed to explore the efficacy of an EEG-based Motor Imagery-Brain Computer Interface (MI-BCI) system associated with a shoulder-elbow MIT-Manus (BCI-Manus) in subjects with chronic stroke. The enrolled patients were randomized into two groups, one underwent BCI-Manus treatment and the other underwent Manus treatment alone.

As previously presented by Sergi's trial (42), patients performed point-to-point movements based on a clock-game system: the robot initiated the movement if not actively initiated by the subject after 2 seconds. In the experimental group (BCI Manus), upper limb robot-assisted treatment was guided by MI-BCI after a calibration period, that was first performed to collect the reference EEG data to train a subject-specific MI detection model that was used in the subsequent 12 therapy sessions to evaluate neuroplasticity effects in chronic stroke patients. The BCI-Manus therapy session included 4 sessions of 40 trials each with an interval break of 3 to 5 minutes. The control group session consisted of 320 trials grouped into 3 robot assisted sessions, alternating with 5 non-assisted runs of 16 trials.

Some studies focus on somatosensory system recovery: the goal of Vlaar et al. (32) pilot study was to assess the integrity of the somatosensory system in individuals with chronic hemiparetic stroke with

different levels of sensory impairment, through a combination of robotic joint manipulation and high-density EEG. A robotic wrist manipulator applied continuous periodic disturbances to the affected limb, providing somatosensory (proprioceptive and tactile) stimulation while challenging task execution. The integrity of the somatosensory system was evaluated during passive and active tasks, defined as 'relaxed wrist' and 'maintaining 20% maximum wrist flexion', respectively: 20 trials were recorded in that period. The evoked cortical responses in the EEG were quantified using the power in the averaged responses and their signal-to-noise ratio. Thirty individuals with chronic hemiparetic stroke and ten unimpaired age-matched individuals participated in this study.

Vahdat et al. (34) valued whether somatosensory training induced changes in sensory-motor connectivity in stroke patients and if these changes result in improved movement accuracy. Ten chronic stroke survivors first underwent an initial test of reaching accuracy. Afterwards, they were transferred to the brain-imaging center for structural and functional MRI scans. The next day, one session of four blocks of somatosensory training was performed: each block consisted of 50 trials, in which robot moved the arm outward on one of a set of fan shaped trajectories that deviated from the body midline. Following the sensory training, patients underwent a second brain scanning session. Finally, patients returned to the robotic lab to perform a final block of active reaching movements. Unlike Vlaar study (32), no control group were enrolled. Nam et al.(53) carried out a clinical pilot study to prove if robotic mirror therapy can provide proprioceptive stimulus to the sensory cortex and thus facilitate neuroplasticity and functional recovery on the hemiplegic arm. A stroke survivor underwent a 10-sessions robotic mirror therapy: each session consisted of four tasks (ball in holes, soccer game, dot tracing and moving a cup). Clinical outcomes and fMRI were performed before and after the intervention.

Other studies have provided the combination of rehabilitation therapies of different types compared to what has already been stated: Calabrò et al. (44) associated robotic therapy with muscle vibration (MV) to verify if could be possible to strengthen the effect of robotic rehabilitation by coupling MV. Patients were randomized into two groups of 10 individuals and underwent 40 daily sessions of Armeo-Power training (Hocoma, Volketswil, Switzerland) (1 hour/session, 5 sessions/week, for 8 weeks) with (group A) or without (group B) the application of MV on the spastic antagonist muscles (i.e., triceps brachialis, supraspinatus, and deltoid). Robot therapy consisted in a repetitively customized group of exercises to improve arm and elbow movements. Short intracortical inhibition (SICI), and Hmax/Mmax ratio (HMR) were measured before and after (immediately and 4 weeks later) the end of the treatment as well as clinical outcomes.

Saita et al. (47) investigated the combination of robot-assisted rehabilitation (RT) using a single-joint hybrid assistive limb (HAL-SJ) and botulinum toxin A (BTX-A, BOTOX®, GlaxoSmithKline, UK) as therapy for paretic arm with spasticity in post-stroke patients. BTX-A was injected into target muscle in order to the grade of spasticity in each case (dose max: 240 units, as determined by the upper limit set by health insurance in authors' country). Participants were seven patients who had spastic hemiplegia following chronic stroke. On the day following BTX-A injection, they started a two-week of RT: rehabilitation consisted in repeated flexion/extension movement of elbow joint at least 200 times at session. Cortical activity and clinical outcomes were measured via fNIRS at baseline, and two weeks and four months after following BTX-A injection.

RESULTS

Despite the heterogeneity of the proposed protocol treatments and systems/modalities to evaluate neuroplasticity, all studies have obtained good results: robotic therapy seemed to have positive effects on clinical improvements correlated with neuroplasticity changes. Table II summarizes the results obtained.

In Baghat et al. (38) study, the movement-related cortical potentials (MRCPs) were identified during three of four training modes (Backdrives or

Active, Passive and Triggered), while there was no MRCP during "Observation" mode in the healthy participants as well as in the stroke survivor. Also, there was a relatively high classification accuracy (medians around 75%) across all training modes. Particularly, it appears that classification was more successful in Triggered and Backdrive modes across all subjects. Accuracies were significantly higher than chance levels (50%) for both healthy and stroke participants ($p<0.001$; α-level adjusted using Bonferroni correction for multiple comparisons: 0.0062).

Gandolfi et al. (39) highlighted that significant improvement in all outcomes were measured during the study. Changes in FMA were significant at T2 (p 0.008) and in MAS at T1 and T2 (both p 0.017). Before training, passive movement of the affected hand resulted in bilateral or contralesional alpha and beta desynchronization of the primary sensorimotor cortex in most patients, as quantified by laterality index (LI). After training, desynchronization shifted from bilateral to ipsilesional sensorimotor areas, and active movement of the affected hand shifted from contralesional to ipsilesional sensorimotor areas, as compared with pretreatment assessment. No significant correlation was observed between LI or ERD/ERS and clinical scales, but a marked trend was detected over time: associated to a good recovery, changes in clinical scales are paralleled with changes in LI values, which evidence of ERD modifications from contralesional to ipsilesional side.

Bae et al. (48) results showed passive wrist movements by robot caused cortical activation of the controlesional sensory-motor cortex (SM1), primary motor cortex (PMA) and somatosensory association cortex (SAC) (mainly observed in the SM1 and SAC, $p<0,05$): greatest activation of these areas was observed at a speed of 0.75 Hz. The authors also highlighted that there are no significant differences of ΔOxyHb among three speeds in each region of interest and they gave two possible explanations: first, neural activities caused by passive robot movement in moderated speed could produce a decrease in cerebral blood flow; second, there is possibility that sufficient oxygen is not supplied to the area where the neuronal activity increases due to transient ischemia in the moderated speed condition. In Wang et al. (49) study, only RobotEEG_AO group showed significant difference in paretic upper-limb motor functions across the longitudinal evaluation [X^2 (2) = 7.659, p = 0.022], after the interventions: significant improvements in the paretic motor functions between pre- and post-intervention ($Z = -2.135$, $p = 0.033$) and between preintervention and 6-month follow-up ($Z = -2.451$, $p = 0.014$). The proportion of stroke subjects exceeding the minimal clinically important difference (MCID, that was 4 for FMA-UE) was higher in the RobotEEG_AO group (pre *vs* post: 53.8%; pre *vs* 6-month: 54.5%) compared with the Robotnon−EEG_Text group (pre *vs* post: 36.4%; pre *vs* 6-month: 36.4%). For brain network variability, the whole brain was first divided into six functional subnetworks, and significant increase in the temporal variability was found in four out of the six subnetworks (sensory-motor areas, attention network, auditory network, and default mode network) after intervention. These results revealed the differences in the long-term training effect and the neuroplasticity changes following the two interventional strategies: with and without neural guidance.

Sale et al. (45) wanted to evaluate whether a specific robot-aided rehabilitation can induce beneficial cortical plasticity in stroke patients. Clinical outcomes showed a decrease in motor impairment in the paretic upper limb after the robot-aided treatment in both patients enrolled. In particular, improvements after the rehabilitative treatment were found on the FMA, BBT, ROM and MI whereas a decrease was found on the MAS. In EEG datas were observed a reduced delta rhythms (1–4 Hz) and increased alpha rhythms (8–12 Hz) during the resting state eyes-closed condition; increased alpha desynchronization during eyes opening; and a decreased alpha desynchronization during the robotic rehabilitation task. For this reason, the authors speculated that a specific robot-aided rehabilitation can modulate cortical activity during resting state and a motor task in stroke patients.

Pellegrino et al. (41) aimed to assess the brain plastic reorganizations and their association with clinical progresses induced by a robot-

aided rehabilitation program in chronic stroke patients. In fact, after the robotic rehabilitation there were improvements in FMAS scores and hand motor control performance and changes of brain connectivity in high frequency rhythms (24–90 Hz). In particular, the improvement of motor performance correlated with the modulation of the interhemispheric S1 coherence in the high beta band (24–33 Hz).

The study confirmed that an upper limb robot-based rehabilitation improved motor performance in stroke patients and demonstrated that a robot-aided rehabilitation program induced brain reorganizations. Specifically, interhemispheric connectivity between primary somatosensory areas got closer to a 'physiological level' in parallel with the acquisition of more accurate hand control.

Sergi et al. (42) investigated the neural correlates of motor recovery promoted by robot-mediated therapy in chronic stroke. Before initiation of the rehabilitation program, the resting-state scan showed strong functional connectivity between the seed region in the ipsilesional M1 and many regions of the SMN, including the target-of-interest in the contralesional M1. After training, Patient 1 showed greater reduction in functional connectivity between the seed and target regions as a result of the point-to-point movements compared to Patient 2. Motor function testing showed that Patient 1 made greater gains in the FMA, MRC and grip strength compared to Patient 2. Therefore, the efficacy of the robot-aided rehabilitation as well as the magnitude of change in functional connectivity between the right and left M1 in response to the bout of the rehabilitation was greater in Patient 1 compared to Patient 2.

Trujillo et al. (43) wanted to evaluate the utility of QEEG indices to predict motor recovery. Their results showed that there is a significant negative correlation between QEEG indices at T0 and motor outcome (PRI and the ΔFMA ($\rho = -0.77$, $P = 0.009$). DAR also showed a negative relationship with ΔFMA but was not statistically significant. Similarly, there was a significant negative correlation between PRI(T0) and the ΔFMA% ($\rho = -0.69$, $P = 0.03$), and a trend to a negative correlation between DAR(T0) and ΔFMA% ($\rho = -0.54$, $P = 0.11$). As regards to the brain symmetry index at T0 (BSI(T0)), it did not correlate with neither the ΔFMA nor the ΔFMA%. FMAT0 was not correlated with PRI(T0), DAR(T0), nor BSI(T0). Analogously, FMAT1 was not correlated with the same QEEG indices at T1. There was also no statistical correlation between FMAT0 and ΔFMA, nor between FMAT0 and ΔFMA%, suggesting that motor improvements were not related to initial condition. In addition, the ΔFMA and ΔFMA% were not correlated with neither the age of the patients nor the time since injury.

Regarding the tests to verify whether the relative powers in each frequency band was correlated with the ΔFMA, there was a negative correlation between the ΔFMA and the relative power of the delta ($\rho = -0.62$, $P = 0.06$) and theta ($\rho = -0.68$, $P = 0.03$) bands, and a positive correlation between ΔFMA and the relative power of the alpha band ($\rho = 0.61$, $P = 0.06$). When comparing the relative band powers between T0 and T1, no significant changes were found. Consequently, the comparison between T0 and T1 for PRI and DAR indices did not show any significant variation.

Belardinelli et al. (52) investigated cortico-muscular coherence (CMC) and if it could be used to detected neural plasticity. The FMA- UE improved significantly from 16.23 ± 6.79 (6.80±28.60) to 19.52 ± 7.91 (10.85±35.25) ($p = 0.0015$, paired t-test). For five patients the amplitude of muscle activity was found to be significantly increased (p 0.001), for two patients it was significantly decreased (p 0.001) and for one patient no significant changes (p 0.08) were recorded. All patients showed significantly increased CMC in the beta frequency band after the robotic intervention. Furthermore, group analysis of the cortical overlap showed that all patients had significantly increased ipsilesional premotor CMC after the intervention. This extended from the superior to the middle and inferior frontal gyrus, together with a confined area of increased CMC in the contralesional premotor cortex. Decreased CMC occurred in bilateral parietal areas and in the contralesional motor/premotor cortex. Premotor beta-band CMC may serve as a biomarker and therapeutic target for novel treatment approaches in this patient group.

In Saleh et al. (50) work, clinical outcomes (WMFT and JTHFT) improved after training in both subjects enrolled. The resting state functional connectivity (rsFC) maps and task-related functional connectivity (trFC) with iM1 showed different magnitudes of activation, however, the general directionality of the pattern (increases versus decreases) was similar. Specifically, both the rsFC and the trFC between iM1 and contralesional primary motor cortex (cM1) decreased after the therapy for the first subject and increased for the second subject. These results were confirmed in the 2017 study (51): results showed that both groups improved in the Jebsen Taylor Hand Function Test (JTHFT) score, with the percentage change reaching statistical significance in the RAVR (robot-assisted virtual reality) group ($Z = -2.8$, $p = 0.005$).

No significant between-group difference in the change in JTHFT scores. The activation magnitude in the cerebellum, left temporal lobe, and right precentral gyrus was significantly reduced after RAVR-based training, also a significant decrease in the extent of activity in the RAVR group after training (Mann–Whitney U test, $Z = -2.894$, $p = 0.0038$). The change in laterality index (LI) after training was significantly different between groups (RAVR group LI median = −0.125, RTP group LI median = 0.07, $Z = -2.21$, $p = 0.027$). In addition, BOLD signal in multiple regions of interest was reduced and re-lateralized to the ipsilesional side and these changes correlated with improvement in JTHFT scores. These findings suggest that RAVR training may lead to different neurophysiological changes when compared with traditional therapy.

Calabrò et al. pointed out different results from their studies. In 2019 (28) the objective was the evaluation of the clinical and neurophysiological effects of intensive robot-assisted hand therapy (AHT) compared to intensive occupational therapy (CHT) in the chronic recovery phase after stroke. Results showed that the AHT group presented improvements in both primary outcomes (FMA-UE and the 9-Hole Peg Test) greater than CHT (both $p < 0.001$). These results were paralleled by a larger increase in the frontoparietal TRCoh in the AHT than in the CHT group ($p < 0.001$) and a greater rebalance between the SAI of both the hemispheres ($p < 0.001$). These data suggest a wider remodelling of sensorimotor plasticity and interhemispheric inhibition between sensorimotor cortices in the AHT compared to the CHT group and provide neurophysiological support for the therapeutic impact of intensive robot-assisted treatment on hand function recovery in individuals with chronic stroke. In 2017 (44), their focus was to improve upper limb spasticity and function by combining muscle vibration (MV) and robotic therapy. After training, all patients of group-A (experimental group) showed a greater reduction of MAS ($p = 0.007$, $d = 0.6$) and Hmax/Mmax ratio (HMR, $p<0.001$, $d = 0.7$), and a more evident increase of short intracortical inhibition (SICI, $p<0.001$, $d = 0.7$) up to 4 weeks after the end of the treatment, as compared to group-B. Likewise, group-A showed a greater functional outcome of upper limb (FIM $p = 0.1$, $d = 0.7$; FMA-UE $p = 0.007$, $d = 0.4$) up to 4 weeks after the end of the treatment. A significant correlation was found between the degree of MAS reduction and SICI increase in the agonist spastic muscles ($p = 0.004$). Also, Saita et al. (47) investigated the combination of robot-assisted rehabilitation (RT) using a single-joint hybrid assistive limb (HAL-SJ) and botulinum toxin A (BTX-A). After therapy, FMA, Motor Activity Log (MAL), and Disability Assessment Scale (DAS) scores significantly improved at two weeks and four months (p 0.05), except DAS scores at four months (p 0.068). The fNIRS study showed that cortical activation increased in the ipsilesional primary sensorimotor area at two weeks and at the four months follow-up.

Belfatto et al. (46) results showed: in FMA, all patients gained at least 1 point (max pre-post diff of 9 points) ($p = 0.06$), while in Wolf Motor Function Test (WMFT) scale, every subject reached at least 1 point of improvement (max Δ 5 points) ($p = 0.06$). The EEG analysis showed that a desynchronization was recognizable in primary motor cortex bilaterally, in pre- and post-rehabilitation phases. The desynchronization spreads from beta band to all frequencies (alpha and beta) and from part of the movement execution to the overall movement execution in both ipsilateral and contralateral areas.

After training, ERD occurs even in the PRE-MOV window. Despite this result, a decreasing trend is evident in the alpha band for the ipsilateral and contralateral hemispheres, meaning that ERDi(T1) < ERDi(T0) and ERDc(T1) < ERDc(T0), while an average ERD intensification occurred for the contralateral side only in the beta band. There is not a clear trend in the alpha-based laterality coefficient (LC) distribution pre/post-treatment since both ERDi and ERDc decrease, while LC in the beta band moves from negative (T0) to positive (T1) values (ERDc decreades while ERDi seems stable). this study, some of the EEG findings suggested that neuroplastic processes are taking place at the cortical level. In particular, the enhancement of the ERD in the contralateral side, in the alpha band, and the increase of the LC, in the beta band, suggest the possible partial reorganization of the cortical lesioned areas, that are reflected, at a lower hierarchical level, by a modified proximal kinematics and, consequently, by slightly altered motor module recruitment patterns.

In Brauchle et al. (40) tested the feasibility of three-dimensional robotic assistance for reaching movements with a multi-joint exoskeleton during motor imagery (MI)-related desynchronization of sensorimotor oscillations in the β-band. All participants had very similar patterns of robot control regardless of the clinical condition (healthy/patient) or the feedback modality (proprioceptive/visual), but patients showed lower average performances than their healthy counterparts with proprioceptive feedback for the full feedback duration, A distributed cortical network of task-related coherent activity in the θ-band showed significant differences between healthy subjects and stroke patients as well as between early and late periods of the task. Also Chowdury et al. (35) have used a BRI system: the group-mean increase in the performance of the h-BRI, basis of its classification accuracy (CA), was 19.01% (p value<0.05, paired t-test). The last session the average CA increased up to 77.17±3.65% shows that correlation of band-limited power time-courses (CBPT) based h-BRI have a positive impact on the control of a robotic device in stroke patients.

Grip Strength (GS) and ARAT also showed significant (p value<0.05, paired t-test) improvements in hand functionality (group-mean change in GS +9.83 kg and in ARAT score was +23.75). Results of the average beta band ERD/ERS for every EEG channel in the first and last session of treatment showed significant (p value<0.05, paired t-test) reduction in both the ipsi- and contra-lesional beta desynchronization for all the participants.

Instead Rathee et al. (36) used a BCI system driven robot-assisted to verify neurophysiological patterns associated with this system. Results showed an increase in the ARAT score was observed for all the participants (p = 0:00028). The minimal clinically important difference (MCID) values for grip strength were reported as 5.0 and 6.2 kg and for ARAT as 12 and 17 points (impaired dominant and nondominant UL). MEG connectivity analysis provided significant functional connectivity sub-networks for alpha (8-15 Hz), beta-low (15-26 Hz), beta-high (26-35 Hz) frequency bands; however, these sub-networks were stable only for beta-low (15-26 Hz) band. For all the participants, the intra-hemispherical FC values in motor cortical regions involving M1, S1 and SMA ipsilesional and contralesional hemispheres increased with UL functional recovery. Thus, the group analysis showed increase in node strengths in the motor cortex region and decrease in the node strengths in the frontal, parietal and occipital areas of the contralesional hemisphere.

These findings were consistent with the theory of bilateral motor cortical association with UL recovery and predict novel FC patterns that could be important for higher level cognitive functions. BCI system was also used in Ang et al. (33) and Tung et al. (37) studies. In the first one (33) the purpose was to investigate the efficacy of an EEG-based MI BCI system coupled with MIT-Manus shoulder-elbow robotic feedback for subjects with chronic stroke with upper-limb hemiparesis to detect inter-hemispheric asymmetry (56).

Results pointed out that mean total FMA scores at weeks 0, 2, 4, and 12 weeks improved for both groups (Manus with or without BCI): 26.3 ± 10.3, 27.4 ± 12.0, 30.8 ± 13.8, and 31.5 ± 13.5 for BCI-Manus and 26.6 ± 18.9, 29.9 ± 20.6, 32.9 ± 21.4, and 33.9 ± 20.2 for Manus, with no intergroup differences (P = .51). More subjects attained further gains in FMA scores

Table III. *Quality assessment.*

PEDRO Criterion	*Ang et al. 2014*	*Bae et al. 2017*	*Baghat et al. 2014*	*Belardinelli et al 2017*	*Belfatto et al. 2018*	*Brauchle et al 2015*
Eligibility criteria	1	0	1	1	1	0
Random allocation	0	0	0	0	0	0
Concealed allocation	0	0	0	0	0	0
Baseline comparability	0	0	0	0	0	0
Blind subjects	0	0	0	0	0	0
Blind therapists	0	0	0	0	0	0
Blind assessors	1	1	1	1	1	1
Adequate follow up	1	1	1	1	1	1
Intention-to-treat analysis	1	1	1	1	1	1
Between-group comparison	1	0	1	0	0	0
Point estimates and variability	1	1	1	1	1	1
Total	6/10	4/10	6/10	5/10	5/10	4/10
Percentage score	60%	40%	60%	50%	50%	40%

PEDRO Criterion	*Calabrò et al. 2017*	*Calabrò et al. 2019*	*Chowdury et al. 2013*	*Gandolfi et al. 2018*	*Nam et al. 2017*	*Pellegrino et al 2012*
Eligibility criteria	1	1	0	1	1	1
Random allocation	1	1	0	0	0	0
Concealed allocation	0	1	0	0	0	0
Baseline comparability	1	1	0	0	0	0
Blind subjects	1	0	0	0	0	0
Blind therapists	0	0	0	0	0	0
Blind assessors	1	1	1	1	1	1
Adequate follow up	1	1	1	1	1	1
Intention-to-treat analysis	0	1	1	1	1	1
Between-group comparison	1	1	0	0	0	0
Point estimates and variability	1	1	1	1	1	1
Total	8/10	8/10	4/10	5/10	5/10	5/10
Percentage score	80%	80%	40%	50%	50%	50%

PEDRO Criterion	*Rathee et al 2019*	*Saita et al. 2016*	*Sale et al. 2015*	*Saleh et al. 2012*	*Saleh et al. 2017*	*Sergi et al. 2011*
Eligibility criteria	0	0	0	0	1	1
Random allocation	0	0	0	0	1	0
Concealed allocation	0	0	0	0	1	0
Baseline comparability	0	0	0	0	1	0
Blind subjects	0	0	0	0	0	0
Blind therapists	0	0	0	0	0	0
Blind assessors	1	1	1	1	1	1
Adequate follow up	1	1	1	1	1	1
Intention-to-treat analysis	1	1	1	1	1	1
Between-group comparison	0	0	0	0	1	0
Point estimates and variability	1	1	1	1	1	1
Total	4/10	4/10	4/10	4/10	8/10	5/10
Percentage score	40%	40%	40%	40%	80%	50%

PEDRO Criterion	*Trujillo et al. 2017*	*Tung et al. 2013*	*Vahdat et al. 2019*	*Vlaar et al. 2017*	*Wang et al 2018*
Eligibility criteria	0	0	0	1	1
Random allocation	0	0	0	0	0
Concealed allocation	0	0	0	0	0
Baseline comparability	0	0	0	0	0
Blind subjects	0	0	0	0	0
Blind therapists	0	0	0	0	0
Blind assessors	1	1	1	1	1
Adequate follow up	1	1	1	1	1
Intention-to-treat analysis	1	1	1	1	1
Between-group comparison	0	0	0	0	0
Point estimates and variability	1	1	1	1	1
Total	4/10	4/10	4/10	5/10	5/10
Percentage score	40%	40%	40%	50%	50%

at week 12 in BCI-Manus (7 of 11 [63.6%]) versus Manus (5 of 14 [35.7%]). A negative correlation was found between the rBSI and FMA score improvement (P = .044). The rBSI captures the asymmetry in spectral power between the two cerebral hemispheres and is normalized between 0 for perfect symmetry and 1 for maximal asymmetry: the results showed that patients with higher asymmetry on EEG tend to gain less motor improvement. In Tung et al. study (37), the EEG signals recorded during the course of upper limb stroke rehabilitation using motor imagery BCI were analyzed to better understand the effect of BCI therapy for post-stroke rehabilitation. Significant improvement in the FMA scores was reported for five of the six patients (p =0.01). The analysis showed that the number of sessions with cortical index (CI) $\geq$ 0.5 correlated with the change in the FMA scores (Pearson's correlation coefficient of 0.819, which is statistically significant with p = 0.046). Improvement in motor recovery was associated generally with increasing activation in the lesion hemisphere during the BCI therapy.

Table IV. *Levels of evidence by Oxford Centre for Evidence-based Medicine.*

Author and year of pubblication	Levels of Evidence
Ang KK et al. 2014	1b
Bae SJ et al. 2017	3
Baghat NA et al. 2014	3
Belardinelli P et al. 2017	3
Belfatto A et al. 2018	3
Brauchle D et al. 2015	2b
Calabrò RS et al.2017	2b
Calabrò RS et al.2019	1b
Chowdury A et al.2013	3
Gandolfi M et al.2018	2b
Nam HS et al.2017	3
Pellegrino G et al.2012	3
Rathee D et al.2019	3
Saita K et al.2016	3
Sale P et al.2015	3
Saleh S et al.2012	2b
Saleh S et al.2017	3
Sergi et al..2011	3
Trujillo P et al.2017	3
Tung SW et al 2013	3
Vahdat S et al.2019	3
Vlaar MP et al.2017	2b
Wang X et al.2018	2b

Regarding the studies that investigated the somatosensory system, Vlaar et al. (32) showed that, under passive conditions, wrist manipulation resulted in contralateral cortical responses in unimpaired and chronic stroke participants with mild and no sensory impairment. In participants with severe sensory impairment the cortical responses were strongly reduced in amplitude, which related to anatomical damage. Under active conditions, participants with mild sensory impairment showed reduced responses compared to the passive condition, whereas unimpaired and chronic stroke participants without sensory impairment did not show this reduction. Vahdat et al. (34) investigated if proprioceptive training modulates functional connectivity of sensory-motor networks and improves reaching accuracy in chronic stroke. Two networks showing training-associated functional connectivity (FC) change were identified. Network C1 was present in all patients and network C2 only in patients with FM scores > 7. Relatively larger C1 volume in the ipsilesional hemisphere was associated with less impairment (r=0.83 for NSA, r=0.73 for FMA). This association was driven by specific regions in the contralesional hemisphere and their functional connections (supramarginal gyrus with FM scores r=0.82, S1 with NSA scores r=0.70 and cerebellum with NSA score r=−0.82). Also Nam et al.(53) evaluated recovery of proprioception, but using mirror therapy: at the follow-up evaluation, thumb finding test (TFT) score improved from 2 to 1 for eye level and from 3 to 1 for overhead level, other parameters revealed no difference before and after treatment. The fMRI during the passive motion revealed a considerable increase in brain activity at the lower part of the right superior parietal lobule, suggesting the possibility of proprioception enhancement.

Methodological quality assessment

Methodological quality assessment was rated using The PEDRO Scale (30) and Levels of Evidence by Oxford Centre for Evidence-based Medicine (31). As regards the PEDro score percentage, it ranged from 40% to 80% (Table III), while Level of Evidence varied between 1b and 3 (Table IV).

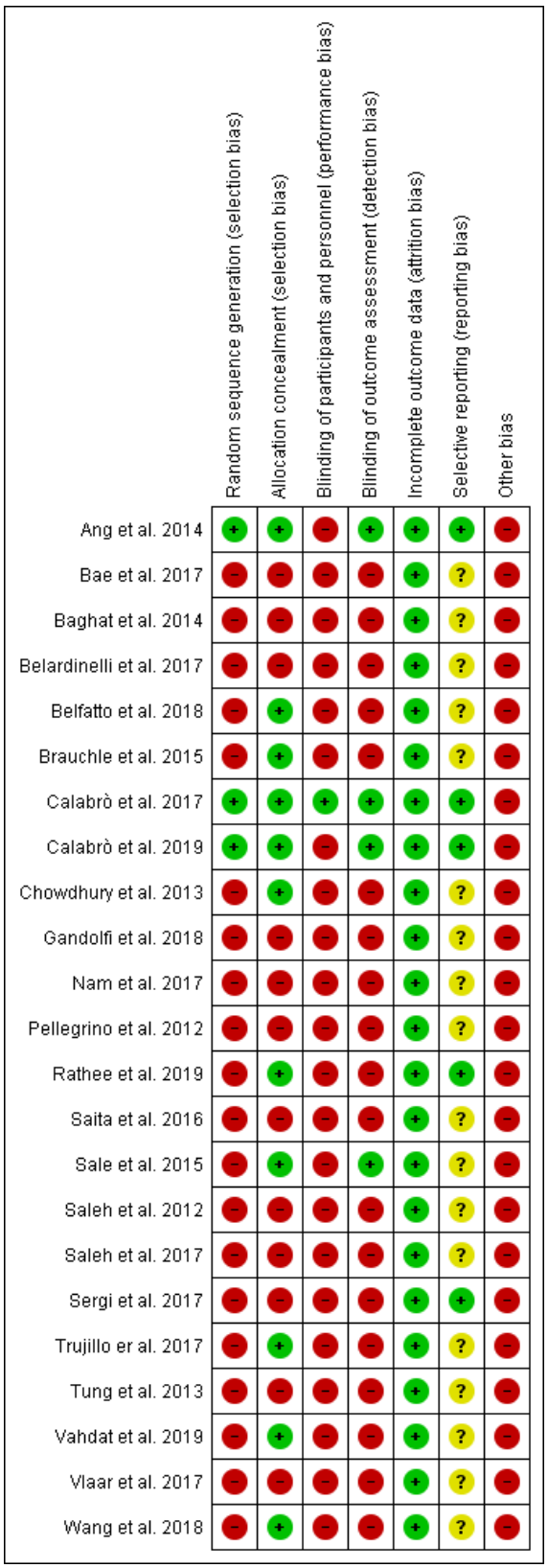

Fig. 2. *Risk of bias Assessment Tool of the Review Manager – RevMan.*

Risk of bias in included studies

The Risk of bias Assessment Tool of the Review Manager - RevMan (version 5.3. Copenhagen: The Nordic Cochrane Centre, The Cochrane Collaboration, 2014) has been used by the reviewers to classify the risk of bias for each selected study (Fig. 2). All the included studies show a low risk of attrition bias thus pointing out a comprehensive description of outcome measures and a complete data analysis (no missing data were reported) and a high risk of other bias. Conversely, a clear discrepancy exists among studies about other bias: mostly presented a high risk of selection bias ad allocation bias due to the lack of randomization sequence generation and allocation concealment. Moreover, in many studies it has not been specified whether the evaluator of the outcomes was blind. It is important to highlight that reporting bias were considered unclear for nineteen studies out of 24. This is because most of the studies are pilot, so often a control group has not been randomized. This is because it was not possible to carry out a check of the outcomes evaluated in the various studies due to the lack of a registered clinical protocol and the lack of studies to compare them given the novelty of the subject matter.

DISCUSSION

Stroke is the second most common cause of death and the third most common cause of disability worldwide. It often results into impairment of upper limbs' function (57). This leads to a loss of independence in ADLs, a reduction in patients' QoL, and, considering the geriatric population growth in future, it will bring to a high healthcare burden. The recovery of the motor function of the paretic limb has always been a challenge for rehabilitation. In this field, robotic rehabilitation constitutes a valid therapeutic response. Several studies report the effectiveness of robotic treatment in recovery after stroke outcomes and these effects would be due to its role in stimulating neuroplasticity. However, the precise mechanisms underlying this reorganization remain to be explained. Therefore, the purpose of this study was to review the current literature that, through clinical studies, investigates the effect of robotic treatment of the upper limb on neuroplasticity

development in patients affected by chronic stroke.

In past years, the chronic stage of stroke was not considered as a phase of possible recovery: it was thought that patients could recover lost abilities only in the acute/subacute phase (< 6 months). The patients reached a "plateaux", a maximum level of recovery beyond which they could not recover. With the advent of new technologies (i.e. robots) it was seen how this obstacle could be overcome: patients are stimulated in a different way than traditional therapy, with repetitive movements and intense training, that activate and promote motor recovery and brain reorganization (25). Calabrò et al. (28) highlight this aspect, stating that robotic hand training stimulated a more evident reshaping of movement-related brain oscillations and connectivity, a stronger rebalance of the mechanisms of sensorimotor integration and plasticity of corticospinal excitability between the affected and unaffected hemispheres.

These mechanisms suggest that, after training, there is a more efficient interhemispheric information transfer in robotic rehabilitation group. Also, Pellegrino et al. (41) highlight changes in inter-hemispheric functional connectivity: in their study robotic treatment improved hand motor control ability in patients and modulated the inter-hemispheric connectivity in resting state. In this way, patients can reach a better motor performance and, in this case, improve their fine hand control.

Like Pellegrino, Sergi et al. (42) speculate that the observed reduction in functional connectivity between the M1s during the resting state may underlie gains in motor function after the robot-aided rehabilitation program: as suggested by previous studies (58), motor recovery after stroke is promoted by a reduction in the inhibitory influence of the contralesional M1 on the ipsilesional M1. This statement is shared by the results of the above article, confirming a possible neuronal reorganization even in chronic stroke. Furthermore, these results agree with several neuroimaging studies that have proposed that the effectiveness of motor rehabilitation could be predicted by changes in SMN activity (59, 60). Trujillo et al. (43) evaluate changes in EEG, in particular the utility of QEEG indices to predict motor recovery.

High PRI and DAR values are associated to poorer outcomes in patients that underwent robot-assisted therapy. This study pointed out that there is a tendency of better outcomes for patients that have low DAR and PRI values and that reduced delta and theta activity seemed to be associated with favorable outcomes: these results suggest that better clinical outcomes come from higher frequency bands in brain activity. Therefore, it is possible that QEEG indices may be useful to predict motor outcomes, offering valuable information for clinical decision-making.

Since the robot is a machine, it can be used in different modalities: generally, the most used are the passive, in which it is the robot that carries out the movement, and the active, in which the patient has to carry out the movement (13). There is converging evidence that training protocols consisting of both active and passive movements (with or without visual feedback) tend to be more beneficial than passive movement alone in functional and neurophysiological outcomes (61, 62). However, there is initial evidence suggesting that passive training may induce cortical reorganization, providing evidence for the notion that proprioceptive training could improve motor function. Robots might increase the sensorimotor experience by providing novel patient-environment interactions through passive and passive-mirrored repetitive training. This is provided by Gandolfi et al. (39): passive robot-assisted bilateral arm training (R-BAT) may sustain improvement in upper limb functioning in chronically impaired stroke patients and induce specific changes in the sensorimotor network. This process may be facilitated by two mechanisms: one consists of the simultaneous activation of both hemispheres, which is thought to facilitate activation of the damaged hemisphere by reducing transcallosal inhibition from the unaffected hemisphere; the second mechanism involves facilitation of the controlesional uncrossed spinal tract and spared indirect corticospinal pathways. For these reasons, R-BAT programme could be considered as an adjuvant in physical therapy. Instead Bae et al. (48) focused on the optimal condition of speed for passive wrist movement performed by a robot in chronic stroke: this was identified in 0.75 Hz, because it was the speed associated to the greatest activation of the

SM1, PMA and SAC as demonstrated from the luck of significant differences of ΔOxyHb.

When the patients are unable to perform the tasks in the training, some robots present the assisted mode, in which the same robot starts or completes the movements when the patient cannot make them. In this way, the patient still manages to make the experience of movement and, consequently, to receive and process information that, without the help of the robot, would not have (13).

Baghat et al. (38) use four different training modalities: Active or Backdrive, Passive, Velocity Triggered and Observation. In this study the author aimed to investigate MRCP, movement-related cortical potentials, in order to differentiate movement intention in participants compared to rest with relatively high accuracy. MRCP were identify in three of four modalities (Backdrive, Passive & Triggered): this provides initial evidence for the potential applicability of MRCP as a neural control signal for a brain-machine interface to robotic systems in stroke survivors and encourages combining neural-robotic intervention to increase active patient engagement during rehabilitation. This result is shared with Wang et al. (49) study: their findings might imply that the neuroplasticity could be promoted more profoundly by the intervention with neurofeedback and might be shaped to achieve better motor skills acquisition. In fact, the group who received combined action observation with EEG guidance obtained significant improvements in the paretic motor functions and significant increase in the temporal variability in the analyzed subnetworks respect the one without it. Feedback can make robotic treatment more effective: virtual reality, somatosensory stimulation and integration with peripheral and central interfaces could help to improve recovery results.

Interfaces

Several interfaces are used in robotic rehabilitation in chronic stroke: most common are brain computer interface (BCI) and brain robot interface (BRI). BCI was used in three studies: Ang et al. (33), Rathee et al. (36) and Tung et al. (37). The last one (37) suggested that improvement in motor recovery most likely comes from increasing activation in the lesion hemisphere during BCI therapy and the result agrees with existing multimodal studies.

Results obtained suggest that aside from the natural recovery of the subjects, the 2 weeks BCI therapy is generally effective for post-stroke rehabilitation. It seems possible to track the effect of BCI technology on brain plasticity directly using EEG signals. According with these findings, Ang et al. (33) showed a negative correlation between rBSI and FMA score: patients with higher asymmetry on EEG had lower motor improvements. ERD is an index of neuronal desynchronization: considering that anodal tDCS increases cortical excitation of the ipsilesional M1 (63) tDCS may contribute to increased activity in desynchronized neurons during MI.

The increased excitability of the affected hemisphere could contribute to the rebalancing of interhemispheric inhibitory competition, which as previously mentioned, is altered after a stroke. In addition, the online accuracy readings of MI-BCI were greater in subjects who had performed tDCS. These results confirm the existence of a facilitatory effect of tDCS on MI-BCI with robotic feedback in post-stroke rehabilitation. In this case, the movement initially imagined by the patient through the MI and subsequently reproduced by the MIT-Manus passively, providing visual and motor feedback, closed the proprioceptive loop. These results are in accordance with the discovery of an activity-dependent competition between injured and non-injured corticospinal systems, resulting in persistent asymmetry and associated poor healing (64).

The discovery of a correlation between rBSI on the EEG and motor disability reduction suggests the potential use of rBSI as a prognostic measure for BCI-based stroke rehabilitation. BCI could potentially be used as an objective measurement and feedback tool for an accurate assessment of the effects in terms of functional recovery of the MI and could be a viable alternative for subjects unable to attend intensive robotic training. Rathee et al. (36) estimate the brain connectivity networks using resting-state (RS) MEG signals at five different sessions in conjunction with a multi-modal rehabilitative therapy.

The authors observe a lateralized reorganization of a

fronto-parietal network wherein the ipsilesional and the contralesional hemispheres showed enhanced and reduced connectivity strengths, respectively. Fronto-parietal connectivity is known to be involved in top-down attentional control and visuospatial processing. These findings are consistent with the theory of bilateral motor cortical association with UL recovery and predict novel FC patterns that can be important for higher level of cognitive functions.

Three study (35, 40, 52) based their rehabilitation programme on BRI. Brauchle at al. (40) illustrated that BRIs may successfully link three-dimensional robotic training to the participant's effort and allow for task-oriented practice of activities of daily living with a physiologically controlled multi-joint exoskeleton. Changes of cortical physiology during the task might also help to make subject-specific adjustments of task difficulty and guide adjunct interventions to facilitate motor learning for functional restoration, a proposal that warrants further investigation in a larger cohort of stroke patients.

Chowdhury et al. (35) affirmed that the neurophysiological changes, measured by beta band-power change, supported the motor recovery outcome, which further reinforces the feasibility of the CBPT based h-BRI system for hand functional recovery. CBPT, correlation of band-limited power time-courses, is a measure of cortico-muscular coupling and it is used as a feature for providing multimodal neurofeedback for hand exoskeleton based therapy: the fact that, in last session, classification accuracy increases significally shows that CBPT based h-BRI have a positive impact on the controllability of a robot device by stroke patients. This leads to a higher motivation level for the patients that helps them engage more with the task, follow by a higher motor recovery and confirmed by a reduction in both ipsi- and contra-lesional desynchronization. Like previous study, Belardinelli et al. (52) investigated and confirmed the role of cortico-muscular coherence using a BRI: results show that non-primary motor cortex and contralesional sources of CMC are dynamically modulated by therapeutic interventions despite severe and persistent motor impairments in the chronic stage after stroke.

The results of these studies demonstrate the importance of an integrated rehabilitation approach: BCI, MI-BCI, BRI and Robot. These systems propose that the assistance follows the user's motor intention, with the consequence being that stronger cortical changes are induced. These evidences pave the way for new combined and personalized interventions, where closed loop decoding of brain activity plays a key role for maximizing the sensorimotor recovery (27). Therefore, we can see that cortico-muscular coherence was analyzed in two BRI studies: CMC could be considered a biomarker and therapeutic target for supporting recovered function with novel treatment approaches in severely impaired stroke patients, however more research are necessary to confirm this results.

Virtual reality

In the two studies (50,51) carried out by Saleh et al., visuomotor feedback received by the subjects in the RAVR (robot-assisted virtual reality) group may have facilitated a re-activation of the lesioned hemisphere that is not present in the control group. The patterns of brain reorganization suggest that an adaptive compensatory process in the contralesional hemisphere might have driven clinical improvement in the control group. Instead, improvement in the RAVR group may have been attributed more to reinstatement of activity of ipsilesional sensorimotor networks, which results in a diminished overactivation of the unaffected hemisphere required to compensate the lost function of injured areas. This effect may be attributed to the influence that augmented visual and haptic feedback during RAVR training exerts over higher-order somatosensory and visuomotor areas. These results show that virtual reality combined with robotic assisted training were identified as viable means of providing therapy to reinstate desirable changes in the brain.

Somatosensory system

Somatosensory system was analyzed in three study (32,34,53). In two studies (34,53), patients improved in proprioception, however there are mixed results regarding motor recovery. Vahdat et al. (34) demonstrated that even a single session of

robt controlled proprioceptive training can induce connectivity changes in respective networks, which are associated with residual motor and sensory function, and translates into improved motor function in most individuals. Instead, Nam et al. (53) suggested the possibilities of enhancing proprioceptive function by using the robotic mirror system, but the capacity for recovery of motor power have been too small. To date, it is impossible to say which of the two theories is superior to the other: if Vahdat got results both at the motor and proprioceptive level, his claims are due to a single session of treatment. On the other hand, Nam et al. have enlisted only one patient, so it is not possible to generalize the results obtained. Further studies are necessary to verify the role of proprioception on recovery of motor function in stroke patients. Instead Vlaar et al. (32) quantitatively assessed the integrity of the somatosensory system using EEG and a robotic manipulator that applies periodic disturbance to wrist joint: this system allows quantitative assessment of evoked cortical activity reflecting proprioceptive and tactile information during meaningful upper limb control tasks executed under both passive and active conditions.

Combined therapy

Robotic therapy is associated with other therapies, which often amplify the result. Two articles combine different therapies with robotic therapy: Calabrò et al (44), associates muscle vibration (MV) and Saita et al. (47) injections of botulinum toxin. Both have obtained positive results. Calabrò et al. (44), MV induced a MAS decrease, paralleled by an HMR decrease and a SICI strengthening in all the patients of group-A who underwent MV-robot rehabilitation (ArmeoPower, Hocoma, Volketswil, Switzerland). The stronger effect of the combined approach on spasticity and upper limb functions may depend on a sort of associative plasticity between the two coupled trainings, which could have reshaped corticospinal plasticity with a consequent reduction of segmental excitability at the spinal level and an entrainment of recovery processes at the cortical level. Saita et al. (47) work demonstrates clinical efficacy of combining robot therapy with BTX-A injection. Robotic therapy motivates patients and facilitated use-dependent neuroplasticity: the present study showed increased cortical activation of the ipsilesional hemisphere following 2 weeks of training and of both hemispheres at the 4-month follow-up, associated with changed motor-related cortical activity, even 4 months after BTX-A injection.

Both combined approach led to a greater improvement in mood, anxiety, and upper limb motor function (FMA-UE increase in both studies, DAS score improve statistically in Saita study), moreover the recovery of motor-related cortical activity and the improvement of spasticity may have stimulated patients motivating them to continue using their affected limb, even after the end of robotic rehabilitation (as confirmed by results obtained in MAL scores in Saita et al. study).

Implications for practice

This review confirms that robotic therapy can be used in clinical practice and in particular in association with other rehabilitative strategies for the recovery of upper limb impairment in chronic stroke patients, because of its effectiveness in promoting motor control and stimulating neuronal plasticity. Moreover, robotic therapy has also proved to be safe and well tolerated. In addition, the use of feedback and biofeedback (e.g. proprioception, virtual reality and BRI/BCI) can be of support to improve the rehabilitative result.

Implications for research

The present systematic review opens the way to further research in the field of robot assisted post-stroke therapies of the upper limb. Firstly, the present review emphasises the lack of a clear definition and a common classification of robotic rehabilitation devices. As regards treatment protocols, future studies should be more detailed in the description of the type of robot used, dosage, start times and duration of treatment and in the stratification of the population being treated. To achieve a reduced risk of bias, future trials should include a population of patients with similar characteristics. In the near future, scientists should increase the number and quality of RCTs; they should also include kinematics parameters (mostly measured by the robot itself) as an

additional measure to better monitor the improvements due to robotic therapy in post-stroke patients.

Future robotic treatments should improve upper limb capacity in ADL/IADL in addition to motor, muscle and tone gains. A longer-term follow-up is required to analyze the permanence of the robotic treatment over time. A systematic safe procedure for robot uses similar to that of drugs should be considered. Finally, in order to describe and understand the precise mechanism of neuroplasticity and the recovery of the disability of the upper limb on the basis of robotic therapy, future studies should use internationally shared neuroimaging and neurophysiological measures.

Limitations of this study

Even if this review can have important implications for future research, there are some limitations. Firstly, the low number of articles included link to the fact that few researchers investigates the effect of robotic treatment of the upper limb on neuroplasticity development in patients affected by chronic stroke. Other important limitations are correlated with the enrollment: the small sample size, the absent of a control group, the lack of follow up and the different characteristics of subjects (e.g. type of stroke and time of stroke) do not allow having sharable results. Even the heterogeneity of robots and rehabilitation protocols could be a limitation as there are no shareable results: most of the studies only perform one session of robotic rehabilitation, so it is not possible to say with certainty that results obtained are linked to this kind of therapy. In addition, the outcome measures used to assess the effectiveness of robotic therapy are not always the same as well as neural imaging.

The data emerging from our review show the effectiveness of robotic therapy in promoting mechanisms that facilitate re-learning and motor recovery in patients with chronic post-stroke disabilities, especially when combined with other methods (i.e. VR, BRI and BCI) in an integrated rehabilitation approach. However, the precise mechanisms underlying neural reorganization and neuroplasticity require further study. The understanding of the processes of neuroplasticity induced by robots may have useful clinical implications, allowing us to follow the progress of patients, estimate a prognosis of recovery of motor function, and plan more personalized rehabilitation methods.

REFERENCES

1. Sacco RL, Kasner SE, Broderick JP et al. An updated definition of stroke for the 21st century: A statement for healthcare professionals from the American heart association/American stroke association. Stroke. 2013; 44(7):2064-89.
2. Norouzi-Gheidari N, Archambault PS, Fung J. Effects of robot-assisted therapy on stroke rehabilitation in upper limbs: Systematic review and meta-analysis of the literature. J Rehabil Res Dev. 2012; 49(4):479-96.
3. Poli P, Morone G, Rosati G et al. Robotic technologies and rehabilitation: new tools for stroke patients' therapy. Biomed Res Int. 2013; 2013 :153872.
4. Masiero S, Poli P, Rosati G, et al. The value of robotic systems in stroke rehabilitation. Expert Review of Medical Devices. 2014; 11(2):187-98.
5. Kwakkel G, Kollen BJ, Van der Grond JV et al. Probability of regaining dexterity in the flaccid upper limb: Impact of severity of paresis and time since onset in acute stroke. Stroke. 2003; 34(9):2181-6.
6. WHO. World Health Statistics 2008. WHO Libr. 2008.
7. Gassert R, Dietz V. Rehabilitation robots for the treatment of sensorimotor deficits: A neurophysiological perspective. J Neuroeng Rehabil 2018 5; 15(1):46.
8. Yue Z, Zhang X, Wang J. Review Article Hand Rehabilitation Robotics on Poststroke Motor Recovery. Behav Neurol. 2017; 2017.
9. Weber LM, Stein J. The use of robots in stroke rehabilitation: A narrative review. Vol. 43, NeuroRehabilitation. NeuroRehabilitation. 2018; 43(1):99-110.
10. Nudo RJ. Postinfarct cortical plasticity and behavioral recovery. Stroke. 2007; 38(2S):840-5.
11. Winstein CJ, Stein J, Arena R et al. AHA/ASA Guideline Guidelines for Adult Stroke Rehabilitation and Recovery. Stroke. 2016; 47(6):98-169.
12. Kahn LE, Lum PS, Rymer WZ et al. Robot-assisted movement training for the stroke-impaired arm: Does it matter what the robot does? J Rehabil Res Dev. 2006; 43(5):619-29.
13. Oujamaaa L, Relavea I, Froger J et al. Rehabilitation

of arm function after stroke. Literature review. Ann Phys Rehabil Med.2009 52(3):269-93
14. Lucca LF, Pignolo L, Mazzoleni S. La robotica in neuroriabilitazione. Piccin; 2016; 244
15. Duffau H. Brain Plasticity and Reorganization Before, During, and After Glioma Resection. Glioblastoma. Elsevier 2016; 225-36.
16. Kleim JA, Chan S, Pringle E et al. BDNF val66met polymorphism is associated with modified experience-dependent plasticity in human motor cortex. Nat Neurosci. 2006; 9(6):735-7.
17. Coleman ER, Moudgal R, Lang K et al. Early Rehabilitation After Stroke: a Narrative Review. Curr Atheroscler Rep. 2017; 7:19(12):59.
18. Slavin S, Laurence DS. Another look at vicariation. Brain Inj Recover. 1988; 165-79.
19. Sinke MRT, Otte WM, van Meer MPA et al. Modified structural network backbone in the contralesional hemisphere chronically after stroke in rat brain. J Cereb Blood Flow Metab. 2018; 38(9):1642-53.
20. Bliss TVP, Gardner-Medwin AR. Long-lasting potentiation of synaptic transmission in the dentate area of the unanaesthetized rabbit following stimulation of the perforant path. J Physiol. 1973; 232(2):357-74.
21. Kandel ER, Schwartz JH, Jessell TM et al. Principles of Neural Science. 2007th ed. Casa Editrice Ambrosiana, editor. 2003.
22. Turner DL, Ramos-Murguialday A, Birbaumer N et al. Neurophysiology of robot-mediated training and therapy: A perspective for future use in clinical populations. Frontiers in Neurology. 2013; 13:4:184.
23. Nudo RJ, Wise BM, SiFuentes F et al. Neural substrates for the effect of rehabilitative training on motor recovery after ischaemic stroke. Science 1996 21; 272(5269):1791-4.
24. Stefan K, Kunesch E, Cohen LG et al. Induction of plasticity in the human motor cortex by paired associative stimulation. Brain. 2000; 123(3):572-84.
25. Iandolo R, Marini F, Semprini M et al. Perspectives and Challenges in Robotic Neurorehabilitation. Appl. Sci. 2019; 9(15):3183.
26. Alia C, Spalletti C, Lai S et al. Neuroplastic Changes Following Brain Ischemia and their Contribution to Stroke Recovery: Novel Approaches in Neurorehabilitation. Front Cell Neurosci. 2017; 16;11-76.
27. Takeuchi N, Izumi SI. Combinations of stroke neurorehabilitation to facilitate motor recovery: perspectives on Hebbian plasticity and homeostatic metaplasticity. Front Hum Neurosci. 2015; 23(9):349.
28. Calabrò R, Accorinti M, Porcari B et al. Does hand robotic rehabilitation improve motor function by rebalancing interhemispheric connectivity after chronic stroke? Encouraging data from a randomised-clinical-trial. Clin Neurophysiol. 2019; 130(5):767-80.
29. Van der Loos HFM, Reinkensmeyer DJ, Guglielmelli E. Rehabilitation and Health Care Robotics. Springer Handbook of Robotics. 2015; 1223-51.
30. PEDro Scale. Physiotherapy evidence database.
31. Oxford Centre for Evidence-based Medicine – Levels of Evidence 2009.
32. Vlaar MP, Solis-Escalante T, Dewald JPA et al., Quantification of task dependent cortical activation evoked by robotic continuous wrist joint manipulation in chronic hemiparetic stroke. J Neuroeng Rehabil. 2017; 14(1):30.
33. Ang KK, Chua KSG, Phua KS, et al. A Randomized Controlled Trial of EEG-Based Motor Imagery Brain-Computer Interface Robotic Rehabilitation for Stroke. Clin EEG Neurosci. 2014; 46(4):310-20.
34. Vahdat S, Darainy M, Thiel A et al. A Single Session of Robot-Controlled Proprioceptive Training Modulates Functional Connectivity of Sensory Motor Networks and Improves Reaching Accuracy in Chronic Stroke. Neurorehabil Neural Repair. 2019; 33(1):70-81
35. Chowdhury A, Dutta A, and Prasad G. Can Corticomuscular Coupling be Useful in Designing Hybrid-Brain Robot Interfaces Towards Hand Functional Recovery? IEEE International Conference on Systems, Man and Cybernetics (SMC). 2019.
36. Rathee D, Chowdhury A, Meena YK et al. Brain-Machine Interface Driven Post-Stroke Upper-limb Functional Recovery Correlates with Beta-band Mediated Cortical Networks. IEEE Transactions on Neural Systems and Rehabilitation Engineering. 2019; 27(5): 1020-31.
37. Tung SW, Guan C, Ang KK et al., Motor imagery BCI for upper limb stroke rehabilitation: An evaluation of the EEG recordings using coherence analysis. Conf Proc IEEE Eng Med Biol Soc. 2013; 2013:261-4.

38. Bhagat NA, French J, Venkatakrishnan A et al. Detecting Movement Intent from Scalp EEG in a Novel Upper Limb Robotic Rehabilitation System for Stroke. Conf Proc IEEE Eng Med Biol Soc. 2014; 2014:4127-4130.
39. Gandolfi M, Formaggio E, Geroin C et al. Electroencephalographic Changes of Brain Oscillatory Activity After Upper Limb Somatic Sensation Training in a Patient With Somatosensory Deficit After Stroke. Clin EEG Neurosci. 2015; 46(4):347-52.
40. Brauchle D, Vukelić M, Bauer R et al. Brain state-dependent robotic reaching movement with a multi-joint arm exoskeleton: combining brain-machine interfacing and robotic rehabilitation. Front Hum Neurosci. 2015; 9:564.
41. Pellegrino G, Tomasevic L, Tombini M, et al. Inter-hemispheric coupling changes associate with motor improvements after robotic stroke rehabilitation. Restor Neurol Neurosci. 2012; 30(6):497-510.
42. Sergi F, Krebs HI, Groissier B, et al. Predicting efficacy of robot-aided rehabilitation in chronic stroke patients using an MRI-compatible robotic device. Proceedings of the Annual International Conference of the IEEE Engineering in Medicine and Biology Society, EMBS. 2011; 7470-3.
43. Trujillo P, Mastropietro A, Scano A et al. Quantitative EEG for Predicting Upper Limb Motor Recovery in Chronic Stroke Robot-Assisted Rehabilitation. IEEE Trans Neural Syst Rehabil Eng. 2017; 25(7):1058-67.
44. Calabrò RS, Naro A, Russo M et al. Is two better than one? Muscle vibration plus robotic rehabilitation to improve upper limb spasticity and function: A pilot randomized controlled trial. PLoS One. 2017; 12(10):e0185936.
45. Sale P, Infarinato F, Del Percio C et al. Electroencephalographic markers of robot-aided therapy in stroke patients for the evaluation of upper limb rehabilitation. Int J Rehabil Res. 2015; 38(4):294-305.
46. Belfatto A, Scano A, Chiavenna A et al. A Multiparameter Approach to Evaluate Post-Stroke Patients: An Application on Robotic Rehabilitation. Appl. Sci. 2018; 8:2248.
47. Saita K, Morishita T, Hyakutake K, et al. Combined therapy using botulinum toxin A and single-joint hybrid assistive limb for upper-limb disability due to spastic hemiplegia. J Neurol Sci. 2017; 373:182-7.
48. Bae SJ, Jang SH, Seo JP, et al. A pilot study on the optimal speeds for passive wrist movements by a rehabilitation robot of stroke patients: A functional NIRS study. IEEE Int Conf Rehabil Robot. 2017; 2017:7-12
49. Wang X, Wong WW, Sun R et al. Differentiated Effects of Robot Hand Training With and Without Neural Guidance on Neuroplasticity Patterns in Chronic Stroke. Front Neurol. 2018; 9: 810.
50. Saleh S, Adamovich SV, Tunik E. Resting state functional connectivity and task-related effective connectivity changes after upper extremity rehabilitation: a pilot study. Conf Proc IEEE Eng Med Biol Soc. 2012; 2012:4559-62.
51. Saleh S, Fluet G, Qiu Q et al. Neural Patterns of Reorganization after Intensive Robot-Assisted Virtual Reality Therapy and Repetitive Task Practice in Patients with Chronic Stroke. Front Neurol. 2017; 8:452.
52. Belardinelli P, Laer L, Ortiz E et al. Plasticity of premotor cortico-muscular coherence in severely impaired stroke patients with hand paralysis. Neuroimage Clin. 2017; 14:726-33.
53. Nam HS, Koh S, Beom J et al., Recovery of Proprioception in the Upper Extremity by Robotic Mirror Therapy: a Clinical Pilot Study for Proof of Concept. J Korean Med Sci. 2017 Oct;32(10):1568-1575.
54. Krebs HI, Hogan N, Aisen ML et al. Robot aided neurorehabilitation. IEEE Trans Rehabil Eng. 1998; 6(1):75-87.
55. Krebs HI, Volpe BT, Williams D et al. Robot-aided neurorehabilitation: A robot for wrist rehabilitation. IEEE Trans Neural Syst Rehabil Eng. 2007; 15(3):327-35.
56. Van Putten MJAM. The revised brain symmetry index. Clin Neurophysiol. 2007; 118(11):2362-7.
57. AIAC, AIFI, AIMEF, AINR, AMD, ANCE, et al. SPREAD VIII ed - Ictus cerebrale: linee guida italiane di prevenzione e trattamento. 2016.
58. Ward NS, Cohen LG. Mechanisms Underlying Recovery of Motor Function After Stroke. Arch Neurol. 2004; 61(12):1844-8.
59. Dong Y, Dobkin BH, Cen SY, et al. Motor cortex activation during treatment may predict therapeutic gains in paretic hand function after stroke. Stroke. 2006; 37(6):1552-5.
60. Cramer SC, Parrish TB, Levy RM et al. Predicting functional gains in a stroke trial. Stroke. 2007;

38(7):2108-14.
61. Aman JE, Elangovan N, Yeh IL, et al. The effectiveness of proprioceptive training for improving motor function: a systematic review. Front Hum Neurosci. 2015; 28(8):1075.
62. 62. Beets IAM, Macé M, Meesen RLJ et al. Active versus passive training of a complex bimanual task: is prescriptive proprioceptive information sufficient for inducing motor learning? PLoS One 2012; 7(5):e37687.
63. Nitsche MA PW. Excitability changes induced in the human motor cortex by weak transcranial direct current stimulation. J Physiol. 2000; 15(527)3:633–9.
64. Graziadio S, Tomasevic L, Assenza G, et al. The myth of the 'unaffected' side after unilateral stroke: is reorganisation of the non-infarcted corticospinal system to re-establish balance the price for recovery? Exp Neurol. 2012; 238(2):168-75.

Hand motion analysis during robot-aided rehabilitation in chronic stroke

F. Cordella[1], F. Scotto Di Luzio[1], M. Bravi[2], F. Santacaterina[2], F. Bressi[2] and L. Zollo[1]

[1]Research Unit of Advanced Robotics and Human-Centred Technologies, Università Campus Bio-Medico di Roma, Rome, Italy; [2]Research Unit of Physical Medicine and Rehabilitation, Università Campus Bio-Medico di Roma, Rome, Italy

A high percentage of post-stroke patients reports spasticity and no functional use of the upper limb. To adapt the therapy in the most patient-specific manner, it is of paramount importance to objectively assess motor improvement during rehabilitation therapy. In this paper, a quantitative evaluation of the results obtained by using a commercial exoskeletal glove for hand rehabilitation (i.e. Gloreha Sinfonia®) is performed. A camera-based calibration procedure for the bending sensors embedded in the Gloreha Sinfonia robotic glove for hand rehabilitation is introduced to retrieve the range of motion (i.e. the flexion angle excursion of the finger metacarpophalangeal joints) of the patients' hand. Once calibrated, the sensors embedded in the glove have been used to objectively assess the motor performance of chronic post-stroke patients that underwent a robotic treatment with the Gloreha Sinfonia glove. The preliminary results obtained on ten post-stroke patients demonstrated i) that the camera-based procedure permits to retrieve joints' angular values from bending sensors embedded in the glove ii) an improvement in motor performance.

Stroke can significantly affect people quality of life, representing one of the leading causes of long-term disability (1). In 2016, the Global Burden of Diseases, Injuries, and Risk Factors Study (GBD) found that worldwide there were 80 million of stroke cases (2). Among 60% of survivors report very limited or no functional use of the upper-limb contralateral to the affected cerebral part. The hand is characterized by a diminution of the Range of Motion (ROM), expressed also in terms of spasticity, which severely affects the level of autonomy of these subjects (3). This highlights the importance of restoring basic hand functions such as opening, closing, grasping and releasing movements (4).

Over the years, it has been demonstrated that repetitive exercises are suitable for recovering some degree of hand motion after stroke. In this perspective, robot-aided rehabilitation represents a valid aid to conventional rehabilitation guaranteeing not only an intensive motor tasks-based training, but also providing a quantitative measure of motor improvements (5). In the conventional rehabilitative therapy, patients' functional improvements are monitored only by clinical scales and by therapists, which make patient evaluation strongly subjective and error prone. A quantitative evaluation lets the therapist to assess the ROM of each single hand finger, that could be affected by different degrees of impairments, and consequently to intervene on the deficit in a more precise manner.

End-effector machines/robots and exoskeletons have been proposed in the literature to rehabilitate the hand district of post stroke patients (6) and different measures have been introduced to assess

Key words: Hand motion analysis, robot-aided rehabilitation, objective evaluation, Gloreha Sinfonia

Corresponding author:
Dr Francesca Cordella,
Research Unit of Advanced Robotics and Human-Centred Technologies, Università Campus Bio-Medico di Roma,
Via Alvaro del Portillo 21, 00128 Roma, Italy
Tel.: 39 06 22541 9610 - Fax: 39 06 22541 9609
e-mail: f.cordella@unicampus.it

0393-974X (2020)

patient motor state (7, 8). It is therefore fundamental to reconstruct the hand kinematics correctly and accurately during treatment to extract performance measures such as ROM, motion velocity, smoothness, and inter-joint coordination (9). A variety of sensors, such as accelerometers and extensometers, have been embedded into robotic devices to extract kinematic parameters and evaluate the effectiveness of clinical treatments (6). Nevertheless, only a few studies have been performed to clinically validate the rehabilitation devices by also providing quantitative measures of the motor performance. Frequently, commercial devices do not provide kinematic data to the users and it is therefore necessary to find an alternative solution to acquire this information.

This work is focused on the quantitative evaluation of the results obtained by using Gloreha Sinfonia® (Idrogenet, Italy) (10), a commercial exoskeletal glove for hand rehabilitation. A few studies have been performed to investigate the efficacy of this device mainly on subacute patients (11). However, these studies do not provide quantitative measures of patients' motor improvements.

Therefore, the objective of this study is to retrieve hand joint angles from the angular sensors embedded in the Gloreha Sinfonia to objectively evaluate motor performance of chronic post-stroke patients that underwent a robotic treatment with the Gloreha Sinfonia. To this purpose, a specific calibration procedure that associates voltage from glove bending sensors to angles obtained from an optoelectronic motion capture system has been developed. It has been used for acquiring hand joint angles during therapy. Motor improvements of the subjects' hands have been measured by comparing patients' ROM at the beginning and at the end of the treatment. Clinical scales have been also submitted to patients.

The paper is organized as follows: in Section 3 the experimental setup and protocol are described so as the calibration procedure of the bending sensors embedded in the glove. Section 4 is focused on the preliminary experimental results obtained during the therapy with post-stroke patients. The discussion is provided in Section 5 and Conclusions and future directions are in Section 6.

MATERIALS AND METHODS

Gloreha Sinfonia

Gloreha Sinfonia® is a robotic exoskeleton for robot-aided neurorehabilitation (Fig. 1). It is composed of three independent modules:

- A motorized glove for hand mobilization driven by five permanent magnetic actuators (LA12 Actuator, TECHLINE). Each actuator commands the tension of a cable connected to the corresponding finger. This glove is controlled by a motor unit placed distant from patient, to maximize patient safety and ergonomics of the glove. The motor unit is connected to the computer by means of USB protocol.
- An instrumented glove in which five Bend-Sensors (Flexpoint Inc.) are positioned. The sensors are placed on the glove fingers in proper positions. Sensors are connected to an electronic board, that decodes signals and send them to the computer by means of USB protocol.
- A software for acquiring sensors data and controlling motors, installed on a touchscreen computer. It integrates virtual reality environments to replicate activities of daily living (ADLs) in a simulated scenario. This software implements different kinds of tasks, as grasping and moving objects. The motorized glove can be used as an independent module for passive mobilization of the hand or in combination with the instrumented glove to perform one-handed or bimanual tasks. Gloreha Sinfonia is equipped with two passive arm-weight supports fixed to an ergonomic table, to provide relief of limb weight force during the execution of the tasks. Moreover, the software of the Gloreha Sinfonia can record success rate of different tasks to allow monitoring patient improvements.

Fig. 1. *The Gloreha Sinfonia®.*

Calibration procedure

To perform an objective evaluation of hand motion improvements, a calibration of the bend sensors embedded in the Gloreha Sinfonia has been performed. In fact, the sensors return a voltage value corresponding to the different joint angles, but this correspondence is not directly provided by the manufacturer, therefore, in order to measure the joint angles, and consequently the ROM (i.e. the difference between the maximum and minimum flexion angles of the hand fingers), of each finger during therapy, the need for a procedure that associates voltage to angles is evident.

Fig. 2. *Experimental Setup for the Gloreha Sinfonia glove calibration.*

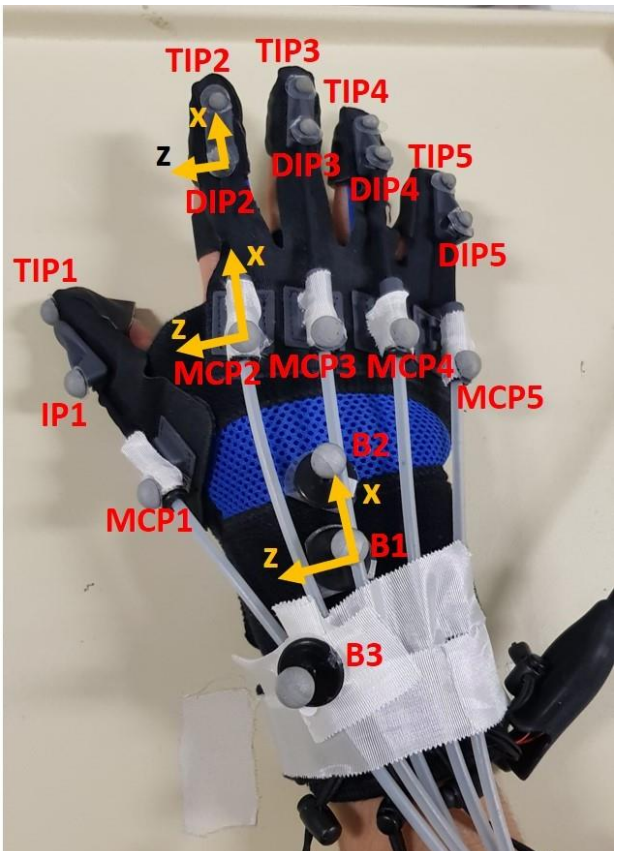

Fig. 3. *Protocol for marker placement. Marker names are outlined in red and the reference frames are shown in yellow.*

The BTS Smart D optoelectronic system has been adopted to acquire the 3D coordinates of retroreflective markers positioned on the glove (Fig. 2). The BTS is made of 8 optoelectronic cameras with an acquisition rate of 60 Hz and ≤0.2mm accuracy. A modified version of the protocol presented in (12) has been implemented for retroreflective marker positioning and angle reconstruction. Due to the mechanical structure of the Gloreha Sinfonia, only the flexion/extension (F/E) angles of the MetaCarpoPhalangeal (MCP) joints have been reconstructed. In fact, the underactuated mechanisms guarantee that when MCP joints flex, also the other hand joints flex. Furthermore, the cables present on the glove make the reconstruction of the other joint angles not reliable.

Eighteen markers have been positioned on the glove as shown in Fig. 3. The markers B1, B2 and B3 have been positioned on the hand dorsum and constitute the reference frame of the system. Three markers have been positioned on each finger in correspondence of the MCP and Distal Inter-Phalangeal (DIP) joints, and of the fingertips (TIP). The reference frames of each joint are outlined in yellow.

The F/E angles of the MCP joints are retrieved by means of a sequence of three elementary rotations (with respect to X, Y and Z axes) expressed by a set of Euler angles. The Gloreha Sinfonia is characterized by gloves of different sizes (i.e. XS, S, M, L, XL) to be adopted with hands of different dimensions. Five people whose hands fit the glove size have been involved in the calibration procedure. The sensors of both left and right glove of each size have been calibrated. After wearing the glove, the subject hand has been actively moved by the motorized glove to reach the maximum closure configuration.

Once the maximum flexion angle was reached with all the five fingers, the glove has been opened till to its maximum aperture. This action has been repeated 8 times and each time both the voltage from the glove bending sensors and the marker 3D coordinates have been synchronously acquired. A second order polynomial function has been used to fit voltage and angles. The obtained polynomial coefficients have been used to retrieve joint angles of each hand from the bending sensor voltage during therapy.

Experimental protocol

Ten chronic stroke patients have been involved in this study. All enrolled subjects referred to the Department of from October 2017 to December 2017 and were examined by a Physical and Rehabilitation Medicine specialist. All the subjects enrolled met the following inclusion criteria: ischemic or hemorrhagic chronic stroke (>6 months) confirmed at brain imaging; absence of cognitive impairment (MMSE>24), Modified Ashworth Scale <3. The exclusion criteria were chronic arm deformity; muscle-skeletal or peripheral nerve disorders, complex regional pain syndrome; severe neglect. The characteristics of the subjects and the type of treatment they underwent are listed in Table I.

Subjects were divided into two groups of treatment according to their ability of actively extend the wrist of 20 degrees (group A) or not (group B): group A received active robotic Gloreha Sinfonia treatment (i.e. the robotic glove assists patient motion only when needed), group B received passive robotic Gloreha Sinfonia treatment (i.e. the robotic glove moves the patients' hand, and he/she is completely passive). All participants underwent the following clinical evaluations at T0 (before starting the treatment) and at T1 (end of the treatment): Modified Ashworth Scale (MAS), Fugl-Meyer Assessment Upper Extremity (FMA-UE). The former is adopted to measure the increase of muscle tone, and therefore, the level of spasticity, the latter is used to assess sensorimotor impairments in post-stroke patients. For the FMA-UE only the section related to the wrist/hand is considered, and for the MSA only the section about the fingers is considered.

Group A (5 patients of 57±14.5 years old) underwent 20 consecutive daily sessions of treatment lasting 40 minutes each (from Monday to Friday). Each session consisted of 8 minutes of object grasping; 8 minutes of water pouring; 8 minutes of cubes stacking; 8 minutes of tridigital grip; 8 minutes of opening and closing of the hand. During active treatment, sensors installed on each glove finger recognized active movements, returning assistance only in case of need.

Group B (5 patients of 64.4±12 years old) underwent 20 consecutive daily sessions of treatment lasting 40 minutes each (from Monday to Friday). Each session

Table I. *Data of the involved patients.*

subject no.	gender	age	time from event	lesion	affected side	treatment
1	F	54	8y	hemorrhagic	left	active
2	F	77	6y	ischemic	left	passive
3	F	57	6y	ischemic	right	passive
4	M	61	4y	hemorrhagic	left	active
5	F	57	26y	ischemic	left	passive
6	M	50	7y	ischemic	left	active
7	F	53	10y	ischemic	left	passive
8	F	79	1y	ischemic	left	active
9	M	40	6y	ischemic	left	active
10	M	78	17y	ischemic	right	passive

consisted of: 7 minutes passive flexion and extension of each single finger; 7 minutes of passive counting (from 1 to 5); 7 minutes of passive opposition of the thumb to the other fingers (from the second to the fifth); 7 minutes of opening and closing the hand with a wave movement; 7 minutes of opening and closing the hand; 5 minutes of random flexion and extension of each finger.

Furthermore, two evaluation sessions were performed: each patient, at T0 and T1, was required to wear the instrumented glove (see Sect. 3.1) on the injured limb and, therefore, to open and close the hand five times in order to evaluate the maximum extension capacity of the limb. The study was conducted under Ethical Committee approval (Ethical Approval N. 41/17 OSS Com Et CBM) and in accordance with the Declaration of Helsinki. All patients gave their written informed consent.

RESULTS

Voltage and angles have been fit by means of a second order polynomial function with a R^2=0.97, demonstrating the goodness of the fitting. In order to measure motion improvements due to the therapy by means of Gloreha Sinfonia, the ROM of the patients' hand joints has been measured during the two evaluation sessions, i.e. at the beginning (T0) and at the end (T1) of the treatment. In Fig. 4, mean value and standard deviation of the ROM of all the fingers measured for each patient at $T0$ and $T1$ are shown. The ROM mean value (± standard deviation) computed on all the involved subjects at T0 is equal to 35.7±9.8 degrees and the one computed at T1 is equal to 44.8±1 degree.

Due to the spasticity, the hand starting position (in which the finger joint angles should be equal to 0) is different for each subject. The increase of the final ROM value should be therefore considered as an increase of the patient capacity to vary the hand aperture.

The FMA-UE value for the hand/wrist district and the MAS for the fingers at T0 and T1, measured for all the subjects, are reported in Table II. Mean and standard deviation computed on all the involved subjects is also reported.

To understand if the FMA-UE values are correlated with the increase of the ROM and to verify if the rehabilitation treatment with the Gloreha Sinfonia improves patients' motor performance, a statistical analysis has been carried out. Since data are not normally distributed, the correlation has been measured through the Spearman's rank correlation coefficient ρ, and the statistical analysis has been

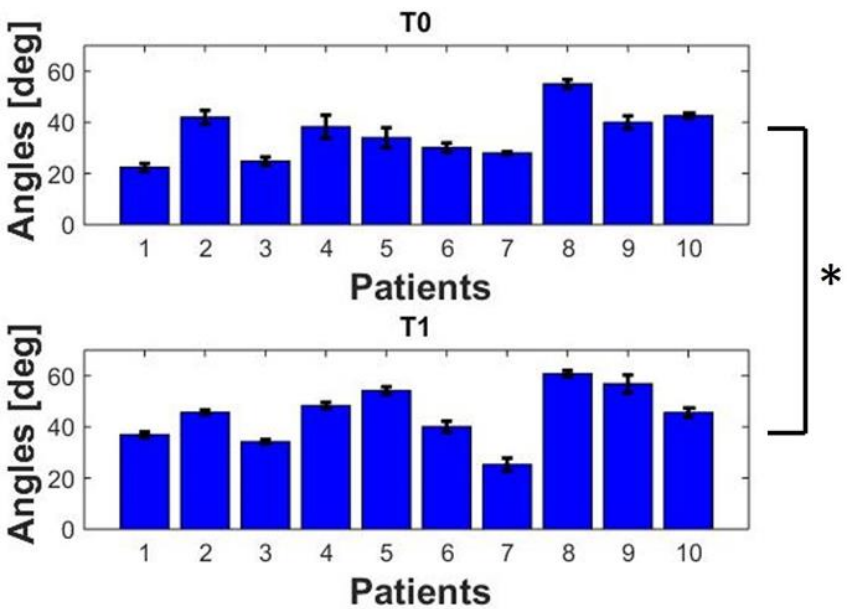

Fig. 4. *Mean value and standard deviation of the ROM of all the fingers measured for each patient at T 0 (up) and T 1 (bottom). Statistical significance between ROM computed at T0 and at T1 is indicated with *.*

Table II. *FMA-UE value for the hand/wrist district and MAS for the fingers at T0 and T1, measured for all the subjects.*

subject no.	FMA-UE at T0	FMA-UE at T1	MAS at T0	MAS at T1
1	37	48	2	1
2	25	27	1	1
3	23	25	2	1
4	34	37	3	2
5	21	38	2	1
6	39	45	2	1
7	14	17	2	1
8	45	51	1	1
9	36	48	2	1
10	13	24	2	1
mean ± sdv	28.7 ± 11*	36 ± 12*	2 ± 0.47	1.2 ± 0.42

Statistical significance between FMA-UE computed at T0 and at T1 is indicated with.*

performed by using the Wilcoxon signed-rank test. The correlation between the array with the mean values of the ROM computed on all the fingers for each subject at T1 and the array with the FMA-UE values at T1 is $\rho = 0.63$, meaning that there is a strong correlation between the two values. The Wilcoxon signed-rank test applied to the ROM and to the FMA-UE values computed at T0 and at T1 demonstrated that there is a statistically significant difference in the ROM and in the FMA-UE (p-value = 0.003 for the ROM and p-value=0.002 for the FMA-UE) before and after the therapy.

DISCUSSION

Although this paper reports preliminary results, given the small number of involved post-stroke patients, it is possible to make some interesting observations. As evident from the data reported in Table II and from the ROM values shown in Fig. 4, for the subjects with a higher improvement in the FMA-UE score an increment of the ROM is correspondingly found. It also corresponds to a decrease in the spasticity level meaning that a better clinical evaluation is reflected in an increase of the patients' capacity to actively reach higher closure/aperture hand configurations. This is confirmed by the presence of a correlation between the ROM and the FMA-UE values.

Another interesting aspect is to study if the value of the FMA-UE at T0 can be used as a predictor of the motor improvements the patient could reach with the therapy. This information could be also useful to identify the most appropriate rehabilitation

treatment for each patient. Four of the five patients (i.e. patients number 2, 3, 7, 10) with a pre-treatment FMA-UE value at T0 less than 30 showed a ROM increment between T0 and T1 less than 10 degrees (mean value is equal to 4.7±3.1), whereas four of the five patients (i.e. patients number 1, 4, 6, 9) with FMA-UE value at T0 higher than 30 showed a ROM increment between T0 and T1 higher than 10 degrees (mean value equal to 12.8±3.3). This preliminary analysis confirms the possibility of using the value of FMA-UE measured before the treatment as an indicator of the motor improvements the patient could reach after the therapy.

For all the involved subjects a statistically significant difference in the ROM measured at T0 and at T1 has been found. It means that, independently from the initial patient state, the therapy with the Gloreha Sinfonia has positive effects on motion performance. It is confirmed by the fact that a statistically significant difference has been found also in the FMA-UE measured at T0 and at T1.

In this paper, a camera-based calibration procedure to retrieve hand joint angles from data obtained from bending sensors embedded in the Gloreha Sinfonia robotic glove is presented. The adopted procedure has been used to assess the variation of the MCP joints ROM of 10 chronic post-stroke patients due to a rehabilitation treatment with the Gloreha Sinfonia glove and allowed us to objectively evaluate patients' motor improvements during the robotic treatment. These values have been measured during two evaluation sessions, i.e. at the beginning (T0) and at the end (T1) of the treatment. FMA-UE and MSA related to the hand district have been also submitted to the patients during the evaluation sessions. The obtained results demonstrated a statistically significant improvement in the ROM and in the FMA-UE and a correlation between the ROM and the FMA-UE. Future work will be devoted to better validating the performed analysis on a higher number of patients.

ACKNOWLEDGEMENTS

This work was supported partly by the Campus Bio-Medico University Strategic Projects (Call 2018) with the SAFE-MOVER project and partly by the Italian Institute for Labour Accidents (INAIL) with the 3D-aid project (CUP: E59E19001460005).

REFERENCES

1. Donnan GA, Fisher M, Macleod M, Davis SM. Stroke, Lancet 2008; 371:1612-23.
2. Global, regional, and national burden of stroke, 1990–2016: a systematic analysis for the Global Burden of Disease Study 2016.
3. Lawrence ES, Coshall C, Dundas R, Stewart J, Rudd AG, Howard R, Wolfe CDA, Estimates of the prevalence of acute stroke impairments and disability in a multiethnic population. Stroke 2001; 32:1279-84.
4. Aggogeri F, Mikolajczyk T, O'Kane J, Robotics for rehabilitation of hand movement in stroke survivors. Advances in Mechanical Engineering 2019; 11(4)1-14. DOI:10.1177/1687814019841921.
5. Micera S, Carrozza MC, Guglielmelli E, et al. A Simple Robotic System for Neurorehabilitation, Autonomous Robots 2005; 19:271. DOI: 10.1007/s10514-005-4749-0.
6. Balasubramanian S, Klein J, Burdet E, Robot-assisted rehabilitation of hand function, Current Opinion in Neurology 2010; 23:6:661-70. DOI:10.1097/WCO.0b013e32833e99a4.
7. Giang C, Pirondini E, Kinany N, et al. Motor improvement estimation and task adaptation for personalized robot-aided therapy: a feasibility study, BioMedical Engineering OnLine, 2020; 19:33. DOI: 10.1186/s12938-020-00779-y.
8. Crea S, Nann M, Trigili E, et al. Feasibility and safety of shared EEG/EOG and vision-guided autonomous whole-arm exoskeleton control to perform activities of daily living, Scientific Reports 2018; 8,10823. DOI: 10.1038/s41598-018-29091-52018.
9. Krebs HI, Palazzolo JJ, Dipietro L, Ferraro M, Krol J, Rannekleiv K, Volpe BT, Hogan N. Rehabilitation robotics: performance-based progressive robot-assisted therapy, Autonomous Robots 2003; 15:7-20.
10. Borboni A, Mor M, Faglia R. Gloreha hand robotic rehabilitation: Design, mechanical model, and experiments. Journal of Dynamic Systems, Measurement, and Control 2016; 138:11.

11. Bernocchi P, Mul' C, Vanoglio F, Taveggia G, Luisa A, Scalvini S. Home-based hand rehabilitation with a robotic glove in hemiplegic patients after stroke: a pilot feasibility study, Topics in Stroke Rehabilitation 2018; 25, 114-9.

12. Cordella F, Zollo L, Guglielmelli E, Siciliano B. Human hand motion analysis and synthesis of optimal power grasps for a robotic hand, International Journal of Advanced Robotic Systems, 2014; 11:3. DOI: 10.5772/57554.

Sensorized assessment of bilateral hand movements in patients with stroke driven by rhythmic auditory or visual-auditory stimulation

S. Ghanbari Ghooshchy[1,2], M. Iosa[1,2], I. Ciancarelli[3], A. Cereatti[4], P. Zoccolotti[1,2], U. Della Croce[5], S. Paolucci[2] and G. Morone[2]

[1]Department of Psychology, Sapienza University of Rome, Italy; [2]IRCCS Fondazione Santa Lucia, Rome, Italy; [3]Department of Life, Health and Environmental Sciences, University of L'Aquila, Italy; [4]PoliToBIOMed Lab, Department of Electronics and Telecommunications, Politecnico of Turin, Italy; [5]Department of Biomedical Sciences, University of Sassari, Italy

There is a growing body of literature about the efficacy in neurorehabilitation of the devices providing rhythmic auditory stimulations or visual-auditory stimulations, such as videogames, for guiding the patients' movements. Despite being presented as tools able to motivate patients, their efficacy was not been proven yet, probably due to the limited knowledge about the factors influencing the capability of patients to move the upper limbs following an external stimulus. In this study, we used a marker less system based on two infrared sensors to assess the kinematics of up and down in-phase and anti-phase bilateral hand oscillations synchronized or not with an external stimulus. A group of stroke survivors, one of age-matched healthy subjects and one of young healthy subjects were tested in three conditions: no stimulus, auditory stimulus, and video-auditory stimulus. Our results showed significant negative effects of visual-auditory stimulus in the frequency of movements ($p = 0.001$), and of auditory stimulus in their fluidity ($p = 0.013$). These results are conceivably related to the attentional overload required during the execution of bilateral movements driven by an external stimulus. However, a positive effect of external stimulus was found in increasing the range of movements of the less functional hand in all subjects ($p = 0.023$). These findings highlight as the type of stimulus may play a crucial role in the patient's performance with respect to movements that are not-externally driven.

In recent years, neurorehabilitation has been supported more and more by technological devices. The movements previously asked of the patients by the physiotherapist to the patients, and manually assisted as needed, often became guided by an external stimulus, such as in training based on rhythmic auditory stimuli (1, 2) or in video-game based therapy (3, 4). These approaches provide auditory or visual-auditory stimuli with the idea that these stimuli act as facilitators in neurorehabilitation. Some studies reported motor but also cognitive improvements following video-game based therapy especially in stroke survivors (4, 5), even though conclusive evidence is still needed (3). Some studies were related to a single hand approach, with the task involving only the paretic side (6, 7). Other studies had a bilateral approach with the non-paretic hand useful for helping and guiding the movements of the paretic one (8). However, the role of the non-paretic hand could more so, be related to neural networks. Kinaesthetic afferences from one limb can influence the motor pathways to the other one (9-12).

Key words: rhythmic auditory stimulation, visual-auditory stimulation, video-game based therapy, neurorehabilitation

Corresponding Author:
Dr G. Morone,
IRCCS Fondazione Santa Lucia,
Via Ardeatina 306/354,
00179 Roma RM, Italy
e-mail: g.morone@hsantalucia.it

0393-974X (2020)

The orchestration of simultaneous reaching movements could be controlled by one single motor program, because of the isomorphic movements of two limbs (13). Furthermore, coupled bimanual training, in stroke survivors, has proven as a therapeutic intervention more effective than the unilateral training of the impaired hand (14-15). Some other studies reported a positive training effect of the non-affected hand on the affected hand thanks to the so-called bilateral transfer, id test, the ability to transfer the skill acquired with a hand to the other one (16).

The type of bilateral movement is also crucial. Some studies have shown as in-phase bilateral movements are easier to perform than anti-phase movements (17-19). A recent study showed as similar parameters between single hand movements and in-phase coupled movements, whereas anti-phase coupled movements resulted less ample, less sinusoidal but more frequent with respect to single hand movements (20). These features were particularly evident for stroke survivors who in general showed reduced similarity of bilateral movements in all conditions, but especially for anti-phase movements performed under visual control (20). Visuomotor integration in patients who suffered a stroke could be less effective than in healthy subjects, probably because of the attentional overload required by the two limbs moving in an alternating fashion (20). The capacity of such patients to interact with external stimuli (visual or visual-auditory), such as during video-game based therapy may therefore be questioned. Furthermore, also age could play a role for its influence on the visuo-motor integration: older adults typically use visual information less effectively than younger adults to reduce force control error in bimanual pinch tasks (21).

The aim of this study was to investigate the performance of manual and bimanual movements when stroke survivors were asked to follow either a rhythmic auditory or visual-auditory stimulation.

MATERIALS AND METHODS

Participants

Seventy-six participants (40 females: 53%) were enrolled in this study: 48 young healthy adults (YG, mean age: 27±5), 10 stroke survivors (PG, mean age: 63±11, time from stroke: 105±82 days), and 18 healthy adults age-matched with patients (AG, mean age: 58±11, p=0.278). Inclusion criteria for the healthy subjects were the age (YG: 18-39; AG: 40-80), the absence of any motor or cognitive pathology, and normal vision or corrected for normal with glasses. The inclusion criteria for the patients were a positive clinical diagnosis of stroke confirmed by neuroimaging, age between 40 and 80 years old, a time from acute event lower than 9 months, the presence of residual movement of paretic hand allowing to perform the task. Exclusion criteria were comorbidities such as parkinsonisms or orthopaedic pathologies of upper limb, moderate to severe cognitive deficits (highlighted by a Mini-Mental State test score <24), and presence of unilateral spatial neglect. The study was approved by the Independent Local Ethical Committee and all the participants provided the signed informed consent.

Experimental tasks

The experimental set-up was the same as one used in a previous study on bilateral coordination with and without visual control (20). Participants sat in front of a table on which the sensor platform was placed and were asked not to move their trunk from the back of the chair. Each participant was asked to oscillate up and down his/her hands over two sensors, up until a maximum height shown by a horizontal sign on a vertical bar placed in proximity to the sensors was reached. Subjects were required to perform bilateral movements with the hands kept horizontal and the palms downward, under different conditions. Three stimulation responses were instructed: 1) no stimulus to follow (NS), just spontaneous movements at self-selected comfortable speed, 2) to follow the rhythm of an auditory stimulus (AS), the frequency of which was set as the same of the NS condition, 3) to follow the rhythm of a visual-auditory stimulation (VAS), the frequency of which was set as the same of NS. From a motor point of view, two possible conditions were required: to perform the bilateral movement in-phase or in anti-phase between the two hands. The order of AS and VAS or of the in-phase and anti-phase conditions was randomized among subjects. The Researcher showed how to perform the task to participants, the simplicity of which allowed them to start the test without any training. Hence, six different conditions were possible. The less functional hand was considered that clinically assessed as paretic for patients

who suffered a stroke and the non-dominant hand for healthy subjects as evaluated by means of the Edinburgh Handedness Inventory (22).

Instrumental apparatus

We used a Distance-Multi-Sensing platform, integrating a magnetic and inertial measurement unit with a couple of Infrared Time-of-Flight (IR-ToF) proximity sensors. The IR-ToF provides an estimate of the distance between the sensor and the target (the hand) based on the time that an electromagnetic wave takes to travel that distance estimated by measuring the phase shift between the emitted and the reflected signals (23). It allowed it to avoid the use of sensors placed on the hands, that could alter the ecological performance of subjects. The accuracy of these marker less systems has already been validated in human movement analysis (24-25). The two IR-ToF sensors were used to evaluate the distances of both hands from the table on which the platform was placed. According to a previous study (20), the sampling frequency of the IR-ToF proximity sensors was set at 25Hz.

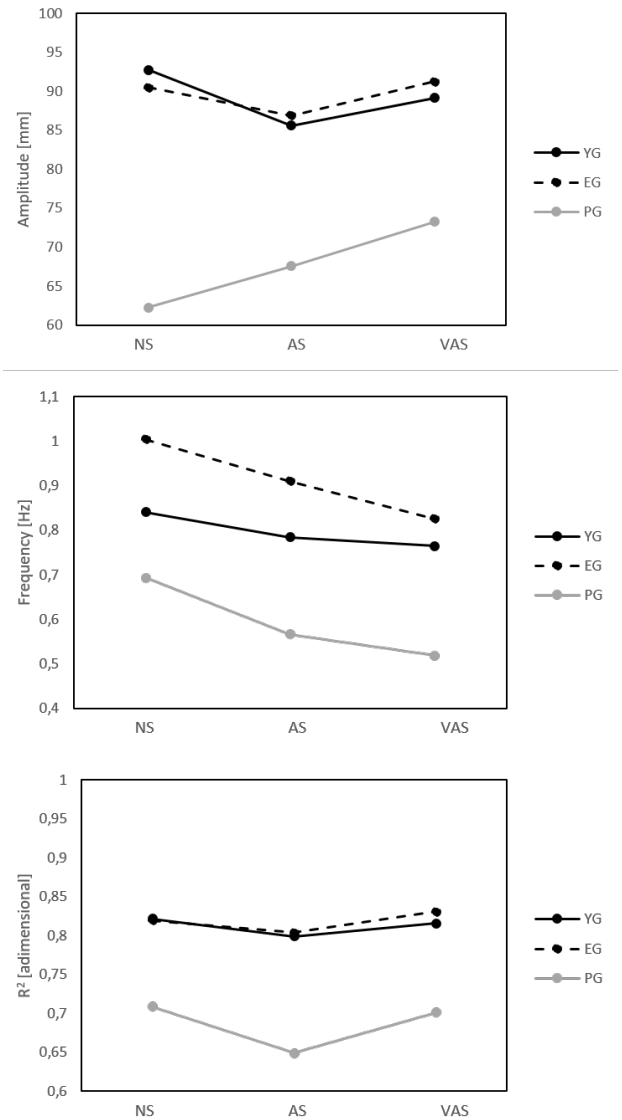

Fig. 1. *Mean data for amplitude (**above**), frequency (**middle**), and R^2 (**below**) for the young (**YG, solid black lines**), elderly (**EG, dotted black lines**), and patient group (**PG, grey lines**) in the three conditions: No Stimulus (**NS**), Auditory Stimulus (**AS**) and Visual-Auditory Stimulus (**VAS**).*

The duration of each trial was of 30s, but the first and last part of the trial were not analyzed to avoid including accelerating and decelerating portions of the signal: for each trial, at least 15s of the steady state of the signal in the middle part of the trial were analyzed. Then, the recorded data were low pass filtered at 5 Hz using a fourth order Butterworth filter. Both hands were recorded and the filtered signal obtained by each hand was fitted with a sinusoidal curve recording the amplitude and frequency of the fitting curve, with the relevant R^2 used as an indicator of how much the movement was represented by its first sinusoidal harmonic. Two commercial apps were used on a 10-inch screen tablet (with a 10 inches-screen) to provide the rhythmic auditory stimulation (with an app simulating the sound of a metronome) and visual-auditory stimulation (with an app showing a bouncing balls together with a sounds, similar to that of a metronome, for each bounce).

Statistical analysis

Data were reported in terms of mean and standard deviation. A mixed Analysis of Variance (Anova) was used for assessing the effects of the group as between-subjects factor and of motor and visual conditions as within subjects' factors. Effect size (ES) was also evaluated as partial eta squared, representing the proportion of variance attributed to one effect. For all these analyses the alpha level of significance was set at 5%.

RESULTS

In Fig. 1 the computed parameters with respect to the main effects of the factor group and type of stimulus are shown. Some other parameters are not reported in the figure but were analysed. As expected, the performances of patients were generally lower,

but the group factor not always lead to a statistically significant difference. For example, despite the amplitude of movements was numerically lower in patients, the effect of the group main factor was not statistically significant. In fact, Anova showed that the Amplitude of movements factor was only close to the statistically significant threshold among the three groups (F=2.618, p=0.080, ES=0.067). Furthermore, no significant differences were found between the two hands (side effect: F=0.750, p=0.389, ES=0.010), among the three conditions (F=0.225, p=0.109, ES=0.030), or between the in-phase and the anti-phase movements (F=1.044, p=0.310, ES=0.014). Neither the second level nor the third level interactions showed statistically significant results (p>0.05), but the side per phase interaction did (F=5.414, p=0.023, ES=0.069); note that this interaction is neither related to the group nor to the stimulus condition factors. The side per condition interaction was related to a difference in VAS condition between higher amplitudes of the more functional hand versus lower functional hand, independently of group.

Conversely, frequency of movements resulted significantly different among the three conditions (F=7.347, p=0.001, ES=0.091), with the visual feedback associated to a lower frequency (Fig. 1). No significant differences were found for the other factors such as side (F=0.252, p=0.618, ES=0.003), phase (F=0.242 p=0.625, ES=0.003), group (F=2.337, p=0.104, ES=0.060), or their interactions (p>0.05 for all of them).

Condition also significantly influenced the sinusoidal waveform of movements (R^2: F=4.448, p=0.013, ES=0.057), that resulted also significantly different among the three groups (F=10.687, p<0.001, ES=0.226) and between in-phase vs. anti-phase movements (F=11.080, p=0.001, ES=0.132). R^2 did not result significantly affected by side (F=0.009, p=.925, ES=0.001) or by the interactions among the above variables (p>0.05).

DISCUSSION

The several conditions presented in this work and the relevant analysis require a thorough discussion. The main interest of this study was to investigate the different effects of different types of stimulus. The VAS condition showed a frequency of movements significantly reduced and wider movements for patients (even though it was not statistically significant). Then, the sinusoidal waveform was reduced only in the AS condition. Anti-phase movements resulted even less sinusoidal, in accordance with a vast amount of literature (17-20). This effect was explained with the simultaneous and symmetrical recruitment of muscle groups occurring during in-phase movements that may lead to more accurate and effortless movements than anti-phase ones, in which homologous muscle groups are activated in an alternating fashion (17-19). As expected, the performance was lower in patients. However, the main effect of group was statistically significant only for R^2 revealing that the waveform of hand movements was less sinusoidal in patients than in the two enrolled healthy groups.

These results can be summarized in a significant negative effect of external stimulus for guiding bilateral movements, of the VAS condition on the frequency of movements and of AS on the fluidity of movements. However, despite only close to statistical significance, a positive effect of VAS was observed on the movement amplitude, especially in patients. This effect was significant only for least functional hand independent on the group (paretic hand in patients and non-dominant hand in healthy subjects).

Despite complex because of the many factors involved, our findings may provide interesting insights on movements synchronized with external stimuli. Video-game based therapy has been often reported as highly motivating patients who suffered a stroke (26), but a higher efficacy of interactive video-gaming and virtual reality with respect to conventional therapy has not been convincingly proven (3). Indeed, external stimuli might require an attentional workload that shifts the patient cognitive attention from the execution of the movement to the recording of the stimulus.

Our study supported the idea that visual-auditory stimuli, such as those of videogames, may improve some kinematic parameters, such as movement

amplitude, and possibly increase the range of motion, but less for enhancing speed. This may confirm the idea that the external stimulus should be simple and slow. It is also in line with the recent results of a similar study showing that visual feedback has a positive effect on increasing amplitude of movements without changing their sinusoidal regularity (20). Furthermore, visual control plays a fundamental role for managing bimanual tasks (21).

Another aspect to take into account by designers, involved in the development of bilateral devices for neurorehabilitation having auditory or visual-auditory stimuli, is that anti-phase movements are often more difficult and require training to be accurately performed (27). Furthermore, during fast anti-phase movements, people unintentionally tend to change into in-phase movements (28).

Our study has some limitations suggesting caution in data interpretation. First, the sample size was small especially for PG, making impossible to differentiate among different types and severity of stroke. Another limitation was that the visual control during VAS condition was not taken into account; by contrast, it could be very interesting, in further studies, to investigate as to whether the attention of subjects was only on the video monitor or also shifted on hands.

In conclusion, our study confirmed previous results showing that in-phase coupled movements were more synchronized than anti-phase movements in all subjects and added that external stimuli not always act as facilitators, despite being very simple. Video-game programmers involved in the development of neurorehabilitation devices should carefully take into account the findings of our study for understanding how the type of the stimuli and the relevant attentional overload may improve or worsen the performance of patients who suffered a stroke.

ACKNOWLEDGEMENTS

This work was supported by the Italian National Institute for Insurance against Accidents at Work (INAIL), in the framework of BRIC project: "PROGETTO STAR: Innovative strategies, and approaches for the motor and functional rehabilitation of subjects with neurovascular adverse event outcomes for reintegration into work".

REFERENCES

1. Malcolm MP, Massie C, Thaut M. Rhythmic auditory-motor entrainment improves hemiparetic arm kinematics during reaching movements: a pilot study. Top Stroke Rehabil 2009; 16(1):69-79.
2. Tian R, Zhang B, Zhu Y. Rhythmic Auditory Stimulation as an Adjuvant Therapy Improved Post-Stroke Motor Functions of the Upper Extremity: A Randomized Controlled Pilot Study. Front Neurosci 2020; 14:649.
3. Laver KE, George S, Thomas S, Deutsch JE, Crotty M Virtual reality for stroke rehabilitation. Cochrane Database Syst Rev 2011; (9):CD008349.
4. Costa MTS, Vieira LP, Barbosa EO, et al. Virtual Reality-Based Exercise with Exergames as Medicine in Different Contexts: A Short Review. Clin Pract Epidemiol Ment Health 2019; 15:15-20.
5. Rozental-Iluz C, Zeilig G, Weingarden H, Rand D. Improving executive function deficits by playing interactive videogames: secondary analysis of a randomized controlled trial for individuals with chronic stroke. Eur J Phys Rehabil Med 2016; 52:508-15.
6. Iosa M, Morone G, Fusco A, et al. Leap motion-controlled videogame-based therapy for rehabilitation of elderly patients with subacute stroke: a feasibility pilot study. Top Stroke Rehabil 2015; 22:306-316.
7. Martino Cinnera A, Pucello A, Lupo A, et al. Upper limb motor improvement in chronic stroke after combining botulinum toxin A injection and multi-joints robot-assisted therapy: a case report. Oxf Med Case Reports 2019; 2019(10):omz097.
8. Henrique PPB, Colussi EL, De Marchi. ACB Effects of Exergame on Patients' Balance and Upper Limb Motor Function after Stroke: A Randomized Controlled Trial. J Stroke Cerebrovasc Dis 2019; 28:2351-7.
9. Baldissera F, Cavallari P, Leocani L. Cyclic modulation of the Hreflex in a wrist flexor during rhythmic flexion-extension movements of the ipsilateral foot. Exp Brain Res 1998; 118:427-30.
10. Baldissera F, Borroni P, Cavallari P, Cerri G.

Excitability changes in human corticospinal projections to forearm muscles during voluntary movement of ipsilateral foot. J Physiol 2002; 539:903-911.
11. Cerri G, Borroni P, Baldissera F: Cyclic H-reflex modulation in resting forearm related to contractions of foot movers, not to foot movement. J Neurophysiol 2003; 90(1):81-8.
12. Borroni P, Cerri G, Baldissera F: Excitability changes in resting forearm muscles during voluntary foot movements depend on hand position: a neural substrate for hand-foot isodirectional coupling. Brain Res 2004; 1022(1-2):117-125.
13. Schmidt RA, Zelaznik H, Hawkins B, Frank JS, Quinn JTJ. Motor-output variability: a theory for the accuracy of rapid motor acts. Psychol Rev 1979; 86:415-51.
14. Rose DK, Winstein CJ. Bimanual training after stroke: are two hands better than one? Top Stroke Rehabil 2004; 11:20-30.
15. Hung CS, Lin KC, Chang WY, et al. Unilateral vs Bilateral Hybrid Approaches for Upper Limb Rehabilitation in Chronic Stroke: A Randomized Controlled Trial. Arch Phys Med Rehabil 2019; 100:2225-32.
16. Iosa M, Morone G, Ragaglini MR, Fusco A, Paolucci S. Motor strategies and bilateral transfer in sensorimotor learning of patients with subacute stroke and healthy subjects. A randomized controlled trial. Eur J Phys Rehabil Med 2013; 49:291-9.
17. Serrien DJ, Brown P. The functional role of interhemispheric synchronization in the control of bimanual timing tasks. Exp. Brain Res 2002; 147:268-72.
18. Wuyts IJ, Summers JJ, Carson RG, Byblow WD, Semjen A. Attention as a mediating variable in the dynamics of bimanual coordination. Hum Mov Sci 1996; 15:877-97.
19. Pollok B, Butz M, Gross J, Schnitzler A. Intercerebellar Coupling Contributes to Bimanual Coordination. J. Cogn. Neurosci. 2007; 19:704-19.
20. Iosa M, Ghanbari Ghooshchy S, Morone G, et al. Visuomotor Integration for Coupled Hand Movements in Healthy Subjects and Patients with Stroke. Front Bioeng Biotechnol. 2020; 30:8:591.
21. Critchley K, Kokubu M, Iemitsu M, Fujita S, Isaka T. Age-related differences in the availability of visual feedback during bimanual pinch. Eur J Appl Physiol 2014; 114:1925-32.
22. Oldfield, RC. The assessment and analysis of handedness: The Edinburgh inventory. Neuropsychologia, 1971; 9:97-113.
23. Hansard M, Lee S, Choi O, Horaud R. Time of flight cameras: principles, methods, and applications. In Time of Flight Cameras: principles, methods and applications; Springer: Berlin, Germany 2012.
24. Bertuletti S, Cereatti A, Comotti D, Caldara M, Della Croce U. Static and Dynamic Accuracy of an Innovative Miniaturized Wearable Platform for Short Range Distance Measurements for Human Movement Applications. Sensors (Basel) 2017; 17(7):1492.
25. Bertuletti S, Salis F, Cereatti A, et al. Inter-leg Distance Measurement as a Tool for Accurate Step Counting in Patients with Multiple Sclerosis. Conf Proc IEEE Eng Med Biol Soc 2019; 2019:6413-7.
26. Swanson LR, Whittinghill DM. Intrinsic or Extrinsic? Using Videogames to Motivate Stroke Survivors: A Systematic Review. Games Health J 2015; 4(3):253-8.
27. Lee TD, Swinnen SP, Verschueren S. Relative Phase Alterations During Bimanual Skill Acquisition. J. Mot. Behav 1995; 27:263-74.
28. Franz EA, Zelaznik HN, McCabe G. Spatial topological constraints in a bimanual task. Acta Psychol. (Amst) 1991; 77:137-51.

Antimicrobial efficacy of photodynamic therapy (PDT) in periodontitis and peri-implantitis: A systematic review.

M.A. Lopez[1], P.C. Passarelli[2], M. Marra[2], A. Lopez[3], A. Moffa[1], M. Casale[1] and A. D'Addona[2]

[1]Unit of Otolaryngology, UOS ORL TI, Campus Bio-Medico University, Rome, Italy; [2]Department of Head and Neck, Division of Oral Surgery and Implantology, Institute of Clinical Dentistry, Università Cattolica del Sacro Cuore, Fondazione Policlinico Universitario Gemelli, Rome, Italy; [3]Universidad Europea de Madrid, Madrid, Spain

To systematically review the literature regarding the antimicrobial effects of photodynamic therapy (PDT) on multi-bacterial species in periodontitis and peri-implantitis disease. The addressed focused question was: "Does PDT show antimicrobial efficacy against multi-bacterial species colonization in periodontal pockets and on the surface of dental implants?" Electronic databases including MEDLINE and EMBASE up to and including December 2018 were searched. Of the ninety studied analyzed, seven were included, four for the study of PDT in peri-implantitis disease and three for periodontal disease. All studies reported the multibacterial species outcomes after the application of antimicrobial PDT. All studies showed a significant reduction in the bacterial load, both in studies based on periodontal and peri-implantary disease, with an average reduction of the total amount of bacterial load of 99.3%. Moreover, the change in clinical parameters is equally important, with an average reduction of PPD of 1.01 mm (from 4.92 to 3.49 ± SD with a percentage reduction of 29%); of BoP of 50%; of RCAL of 1.19 mm (from 9.93 to 8.74, with an average percentage reduction of 12%); of PI of 0.3 (from 1 to 0.7 with a percentage reduction of 30%) and of GI of 1.2 (from 1.8 to 0.6 with a percentage reduction of 66.6%). This review demonstrated significant reduction in the bacterial load in periodontal pocket and dental implant surface with the use of PDT. The results of this review should be considered preliminary and further studies with standardized laser parameters are needed to obtain strong conclusions.

Periodontitis and peri-implantitis are inflammatory problems related to periodontal or peri-implant bone support tissue. The clinics and scientists are still exploring the clinical, immunological, and microbiological parameters around those diseases. However, although there are certain local and systemic risk factors such as tobacco smoking, diabetes mellitus and surgical operations that may can contribute to the onset of these pathologies (1-7), the primary hallmark is the dental plaque and the quality of bacterial species present in patient's oral cavity (8-12). Such bacterial microflora causes inflammation of the soft structures that may lead to erythema and bleeding, and if left for longer period of time can cause loss of clinical attachment level (RCAL) and consequently the loss of the tooth or the prosthetic restoration (13, 14).

Non-surgical manual debridement, which is not only the contemporary treatment choice, but regarded as a gold standard therapy in the treatment of those diseases (15-18). Together with a pharmacological

Key words: photodinamic therapy, PDT, periodontal disease, peri-implantitis, laser, non-surgical treatment

Corresponding Author:
Dr Pier Carmine Passarelli,
Department of Head and Neck,
Division of Oral Surgery and Implantology,
Institute of Clinical Dentistry,
Università Cattolica del Sacro Cuore,
Fondazione Policlinico Universitario Gemelli, Rome, Italy
Tel.:39 0630155278 - Fax:39 0630154751
email: piercarmine.passarelli@unicatt.it

0393-974X (2020)

therapy that can include chlorhexidine, antimicrobials, hydrogen peroxide, etc. (19) and which is not particularly effective and not exempt from same problems (20, 21). In modern dentistry, certain adjunctive therapies are being extensively explored that may add additional benefits for reducing bacterial niche (22) and Photodynamic therapy (PDT) comes as a possible support or replacement therapy for the treatment of periodontitis and peri-implantitis. Several clinical studies have investigated the efficency of the application of PDT using various laser lights and photosensitizers against various kinds of bacteria (23), including the one who has been demostrated causing periodontitis and peri-implantitis (24-28).

The use of PDT involves a laser light of specific wavelength with photosensitizer application which further stimulates photosensitizer dye molecules. This causes changes from ground singlet state to excited triplet state in the dye molecule which oxidizes to form highly reactive and cytotoxic singlet oxygen resulting bacterial cell death (29). Since the detoxification of periodontal pockets and dental implants may require different methods and no universally acknowledged treatment guidelines have been established (30), this gray area remains an area of further exploration. The current systematic review systematically reviewed the literature regarding the effect of antimicrobial PDT on the multi-bacterial species known to be the main cause of periodontitis and peri-implantitis.

MATERIALS AND METHODS

Focused question

A general protocol using the 'Preferred Reporting Items for Systematic Review and Meta-Analysis' (PRISMA) guidelines was followed (31). A focused question was devised which adhered to the general selection criteria: "Does PDT show antimicrobial efficacy against multi-bacterial species colonization responsible for periodontitis and peri-implantitis?"

Selection criteria

Independent screening of the titles for potential articles was assessed. The studies were included based on the following eligibility criteria;

- Population: Study sample consisting of patients affected by periodontitis and peri-implantitis;
- Interventions: Treatment with antimicrobial PDT;
- Comparisons: Patients' registered outcomes after therapy were confronted with results obtained with non-surgical SRP-therapy, chemical detoxification, no treatment or the microbiological registrations obtained by an investigation made at base line before starting the therapy;
- Outcomes: bacterial load and clinical index;
- Study design: The review only contained studies published in the English language. Animal studies, letters to the editor, review articles and unpublished abstracts were excluded.

Search strategy

Electronic databases including MEDLINE and EMBASE up to and including December 2018 were searched. The literature search was conducted using the combinations of the following Medical Subject Heading (MeSH) and text words: (Photochemotherapy OR photosensitizing agents OR photodynamic therapy) AND (bacteria OR infection) AND (periodontits OR peri-implantitis OR dental implants OR surface). Manual searching of the Photodiagn Photodyn Ther, Plos One, Int J Oral Maxillofac Implants, Clin Oral Implants Res and Lasers Med Sci was performed.

Screening methods and data abstraction

Titles and abstracts of studies that fulfill the inclusion criteria were screened and assessed. Data were extracted from the included studies as per following parameters: author/country, study sample and groups, types of bacterial species assessed, laboratory analysis, study outcome and laser parameters.

RESULTS

Study selection

Based on titles and abstracts search, initially 90 studies were identified. After removing duplicates (n=9) and screening of abstracts, a total of 57 articles were not relevant to the objective of the review, hence excluded. Twenty-four full-text studies were selected for screening of which, 17 studies were

eliminated because they did not match the inclusion criteria. The final selection resulted in the inclusion of 7 studies (32-38). All included studies (32-38) were conducted at either health care centers or university hospitals. Flow diagram of study selection process and results of the literature search according to PRISMA guidelines is shown in Fig. 1 (31).

General characteristics of included studies

All included studies originated from Croatia (32), Iran (33), Italy (34), Brazil (35, 36), Korea (37) and United States (38). Two studies used a total of 110 titanium dental implants (33, 35), while 1 study included a total of 72 zirconia dental implants (32). One study investigated the antimicrobial PDT effects on titanium discs (34). Three studies investigated the antimicrobial PDT effects in periodontal pockets (36-38). All studies employed antimicrobial PDT as test groups while control groups among the studies included the use of chlorhexidine (33, 35), photosensitizer alone (32), laser treatments (32-35), curettes (38), saline solution (33). A variety of bacterial species were assessed that includes Staphylococcus aureus, Streptococcus sanguinis, Streptococcus mitis, Prevotella intermedia, Aggregatibacter actinomycetemcomitans, Fusobacterium nucleatum and Porphyromonas gingivalis. Out of 7, in 5 studies there have been microbiological analysis, in particular 2 studies (32, 34) employed scanning electron microscopy, 3 studies evaluated microbial culture analysis in colony forming units (CFU) (33-35), while 1 study evaluated the outcomes using fluorescence analysis, LPS inactivation (34), 1 viable cell count (37), and 2 studies there have been clinical registration of attachment of epithelial cells and clinical index (BoP, REC, RCAL, PPD, PI)(36, 38) (Table I). No meta-analysis could be performed due to the methodological heterogeneity in the included studies, for example, study groups, laser/photosensitizer parameters and a variation in the outcomes. Therefore, the outcomes are reported as a narrative review.

Photochemotherapy related parameters

All studies used diode laser (32-38). Two studies used separate photochemotherapy protocols (32, 33), while 1 study (33) used LED lamp in addition to the diode laser. The wavelengths of diode lasers used in the included PDT studies ranged from 625 nm to 690 nm. Energy fluence was reported in 6 studies (32,

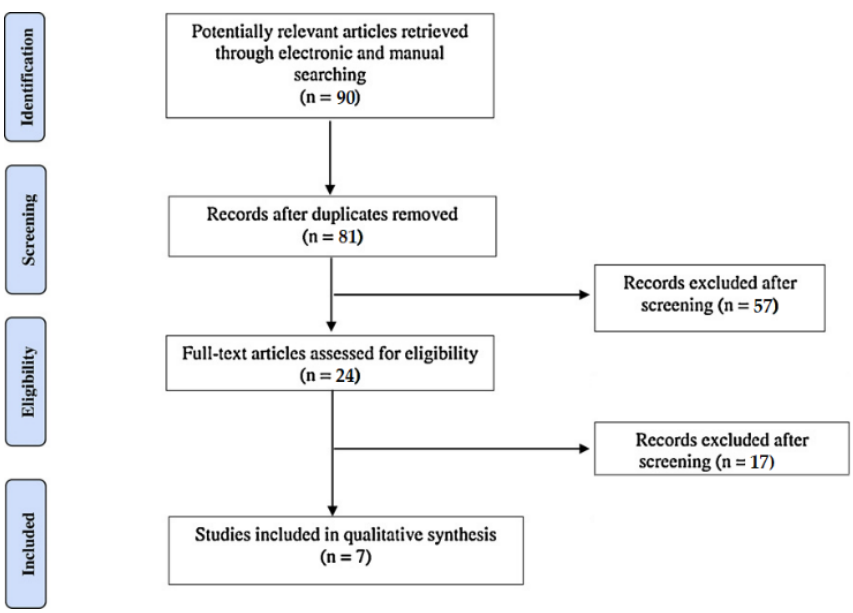

Fig. 1. *Study selection process and results of the literature search (PRISMA flow diagram).*

Table I. *General description of the included studies.*

Investigators	Country	Sample size, tipe of pathology analyed	Groups	Bacterial species or clinical index analyzed	Laboratory analysis	Main outcomes
Azizi et al. [32]	Croatia	72 zirconia dental implants; peri - implantitis	• PDT 1 • PDT 2 • LT • Toluidine blue • Positive control • No treatment	Prevotella intermedia, Aggregatibacter actinomycetemcomitans and Porphyromonas gingivalis	Scanning electron microscopy	PDT showed a significant reduction in the bacterial load without causing damage to the surface microstructures compared with other groups
Saffarpour et al. [33]	Iran	50 titanium dental implants; peri - implantitis	• PDT 1 • PDT 2 • LT • CHX • Saline solution	Aggregatibacter actinomycetemcomitans	Number of CFU per implant	PDT showed a significant reduction in the bacterial load as compared to control groups
Giannelli et al. [34]	Italy	Titanium discs; peri - implantitis	• PDT • LED	Staphylococcus aureus	Viable cell count, Scanning electron microscopy, fluorescence analysis, LPS inactivation	Comparable reduction in the bacterial load without causing damage to the surface microstructures were seen in both groups
Marotti et al. [35]	Brazil	60 titanium dental implants; peri - implantitis	• PDT • LT • CHX • No decontamination	NA	Number of CFU per implant	PDT showed a significant reduction in the bacterial load as compared to other groups
de Oliveira et al. [36]	Brazil	10 patiences and a total of 20 tooths affected by aggressive periodontitis; periodontitis	• PDT	RCAL; PPD; PI; GI; BoP; GR	NA	PDT shows similar results in the treatment of periodontitis as SRP
Park et al. [37]	Korea	Bacterial cultures; periodontitis	• Culture 1 • Culture 2 • Culture 3 • Culture 4 • Culture 5	*Streptococcus sanguinis; Streptococcus mitis; Porphyromonas gingivalis; Fusobacterium nucleatum* and *Aggregatibacter actinomycetemcomitans*	Viable cell count	TBO-mediated aPDT with LED irradiation shows effective antimicrobial activity without damaging adjacent normal tissues or resident flora.
Andersen et al. [38]	United States	33 patiences affected by aggressive periodontitis; periodontitis	• PDT • SRP • SRP + PDT	PD; BoP and CAL	NA	PDT combined with SRP leads to significant improvements of the investigated parameters over the use of SRP alone.

33, 35-38). Power outputs registered were 100mW, 100mW, 30mW, 60mW, 90mW and 150mW cm^2, respectively. The duration of irradiation was reported in all studies which ranged from 10 to 300 s (32–38). Only 4 PDT protocols reported optic fiber diameter (32, 33, 35, 36). Different photosensitizers were reported by different studies. Methylene blue were used in 3 studies (34, 35, 38) whereas toluidine blue (TBO) was used in 3 studies (32, 33, 37) and phenothiazine chloride (PTC) was used in 2 studies (32,36). Only 1 study reported the use of indocyanin green (33). In all included studies (32–38), photosensitizer was applied with the time duration that ranged between 1- and 5-min. Concentration of photosensitizer was reported only in 3 studies (32, 35, 37, 38). None of the included studies reported about the number of laser sessions fired (Table II).

Main outcomes of the studies

All studies reported the multi-bacterial species outcomes after the application of antimicrobial PDT (32-38). All studies showed a significant reduction in the bacterial load, both in studies based on periodontal and peri-implantary disease, with an average reduction of the total amount of bacterial load of 99.3%. Moreover, the change in clinical parameters is equally important, with an average reduction of PPD of 1.01 mm (from 4.92 to 3.49 ± SD with a percentage reduction of 29%); of BoP of 50%; of RCAL of 1.19 mm (from 9.93 to 8.74, with an average percentage reduction of 12%); of PI of 0.3 (from 1 to 0.7 with a percentage reduction of 30%) and of GI of 1.2 (from 1.8 to 0.6 with a percentage reduction of 66.6%).

DISCUSSION

This systematic review investigated the antimicrobial effects of PDT in the reduction of multi-bacterial species in periodontitis and peri-implantitis disease. Overall, all studies showed a significant reduction in the bacterial load. While there have been no secondary effect in the use of PDT in patients with periodontal disease (36-38), the improvement in the inflammatory response around dental implants through the use of PDT (32, 34) one can speculate being caused by its mechanism of action against the bacterial load. The accumulation of microbial plaque bacteria in the peri-implant sulcular area is succeeded by the onset of immune inflammatory

cells, like macrophages, lymphocytes, neutrophils and other cells of the immunitary system. If not cleaned, is responsible for an exalted response by which these immune cells along with local peri-implant tissues direct various inflammatory proteins that can be responsible for tissue degradation and bone resorption.

Thus, it may be assumed that the increased bleeding on probing and peri-implant plaque index recorded could be a direct impact of the reduction in perio-pathogenic microbes in peri-implant lesions following the application of PDT. Exept for one study (36), all the considered studies were missing information about laser, matherials specifics or photosensitier parameters included, and the methodological was significantly heterogen in all the procedures performed (32-38). Previous studies indicated the impact frequency of laser application on the overall effect of laser treatment.

In the present review, none of the studies regarding the use of PDT in peri-implantitis described the number of laser applications, while in the studies regarding periodontal disease (36-38), just one application on each site has been performed. It might be hypothesized that a single application of laser in PDT alone might be difficult to maintain anti-bacterial effect for a short follow-up period so it would be interesting to include a study that performs a new session of PDT after a period of time. Other factors, like fiber diameter could influence power density and energy output in the application of laser during PDT and alter a certain amount of energy released during the process, and consequently affecting the anti-bacterial and anti-inflammatory effect of photodynamic therapy.

In this review, all included studies for PDT showed a significant reduction in the number of bacteria. Therefore, it appears that PDT could play a present role in reducing bacterial load in periodontal pockets and around dental implants. Literature suggests that the gram-negative bacteria are more resistant to PDT compared with gram positive bacteria because of the presence of outer membrane in gram-negative bacteria, which hampers the uptake of the photosensitizer (39). However, because of the cationic charge of TBO, it binds to the outer membrane of the gram-negative bacteria and interacts with the lipopolysaccharide (40). It is noted that 3 studies of those whose has been considered, used TBO in their therapy (32, 33, 37) and showed significantly more substantial results than others. It may be also hypothesized that TBO is a suitable photosensitizer for destroying the bacteria causing periodontal disease and peri-implantitis, particularly the black pigmented bacteria (41). The main limitation of the present study was the number of included studies in the systematic review, the use of a non-standardized source of light for the activation of the photosensibilizer and no statistical analysis of the data in the form of meta-analysis. Due to significant heterogeneity in the outcomes of data presented, the author was unable to perform the meta-analysis. However, based on the results of included studies, it is suggested that the role of PDT in reducing bacterial load inside periodontal pockets and around dental implants, is beneficial. Additionally, further *in-vitro* and *in vivo* studies should be undertaken to appreciate the treatment outcome.

Therefore, studies with standardized control and experimental (PDT and LT) groups are suggested to validate the conclusive effect of PDT and lasers in the reduction of bacterial load in both in vitro and in vivo conditions. This systematic review demonstrated significant reduction in the bacterial load with the application of PDT in periodontal and peri-implant disease. The results of this review should be considered preliminary and further *in-vitro* and *in vivo* studies with standardized laser parameters are needed to obtain strong conclusions.

REFERENCES

1. Al Sowygh ZH, Ghani SM, Sergis K, Vohra F, Akram Z, Peri-implant conditions and levels of advanced glycation end products among patients with different glycemic control, Clin Implant Dent Relat Res 2018; (20)345-51.
2. Akram Z, Vohra F, Bukhari IA, Sheikh SA, Javed F. Clinical and radiographic peri implant parameters and proinflammatory cytokine levels among cigarette smokers, smokeless tobacco users, and nontobacco

users, Clin Implant Dent Relat Res 2018; (20):76-81.
3. AlQahtani MA, Alayad AS, Alshihri A, Correa FO, Akram Z, Clinical peri-implant parameters and inflammatory cytokine profile among smokers of cigarette, e-cigarette, and waterpipe, Clin. Implant Dent. Relat. Res 2018; 20:1016-21.
4. Al-Sowygh ZH, Aldamkh MK, Binmahfooz AM, Al-Aali KA, Akram Z, Qutub OA, et al. Assessment of matrix metalloproteinase-8 and-9 levels in the peri-implant sulcular fluid among waterpipe (narghile) smokers and never-smokers with peri-implantitis, Inhal. Toxicol 2018; 30:72-7.
5. BinShabaib MS, Mehmood A, Akram Z, ALHarthi SS. Peri-implant clinical and radiographic status and whole salivary cotinine levels among cigarette and waterpipe smokers and never-smokers, J. Oral Sci 2018; 60:247-52.
6. Abduljabbar T, Akram Z, Vohra F, Warnakulasuriya S, Javed F, Assessment of interleukin-1β, interleukin-6, and tumor necrosis factor-a levels in the peri-implant sulcular fluid among waterpipe (narghile) smokers and never-smokers with peri-implantitis, Clin. Implant Dent. Relat. Res 2018; 20:144-50.
7. Passarelli PC, Lajolo C, Pasquantonio G, D'Amato G, Docimo R, Verdugo F, D'Addona A. Influence of mandibular third molar surgical extraction on the periodontal status of adjacent second molars. J Periodontol 2019; 90(8):847-55.
8. Tenenbaum H, Bogen O, Séverac F, Elkaim R, Davideau JL, Huck O. Long-term prospective cohort study on dental implants: clinical and microbiological parameters, Clin. Oral Implants Res 2017; 28:86-94.
9. Scapoli L, Girardi A, Palmieri A, Testori T, Zuffetti F, Monguzzi R, Lauritano D, Carinci F. Microflora and periodontal disease. Dent Res J (Isfahan). 2012; 9(S2):S202-6. doi: 10.4103/1735-3327.109755.
10. Rutar A, Lang NP, Buser D, Bürgin W, Mombelli A. Retrospective assessment of clinical and microbiological factors affecting periimplant tissue conditions. Clin Oral Implants Res 2001; 12(3):189-95.
11. Tanner ACR, Sokransky SS, Goodson JM. Microbiota of periodontal pockets losing crestal alveolar bone J. periodontal res 1984; 19:279-91.
12. Boom-Van Noorlos AA, Van der Meer JW, Van der Jevel JS, Schepens E, Van Steenbergen TJ, Burger EH. Bacterioides Gingivalis stimulates bone resorption via Interleukin-1 production by mononuclear cells. J clin periodontal 1990; 17:409-13.
13. Berglundh T, Armitage G, Araujo MG, Avila-Ortiz G, Blanco J, Camargo PM. et al. Peri-implant diseases and conditions: consensus report of workgroup 4 of the 2017 world workshop on the classification of periodontal and peri-implant diseases and conditions, J. Clin. Periodontol 2018; 45:S286-91.
14. Renvert S, Lindahl C, Persson GR. Occurrence of cases with peri-implant mucositis or peri-implantitis in a 21–26 years follow-up study, J. Clin. Periodontol. 2018; 45:233-40.
15. Lupi SM, Granati M, Butera A, Collesano V, Rodriguez Y, Baena R, Air-abrasive debridement with glycine powder versus manual debridement and chlorhexidine administration for the maintenance of peri-implant health status: a six-month randomized clinical trial, Int. J. Dent. Hygiene 2017; 15:287-94.
16. Del Amo FS, Yu SH, Wang HL. Non-surgical therapy for peri-Implant diseases: a systematic review, J. Oral Maxillofac. Res 2016; 7(3):e13.
17. Bollen CM, Quirynen M. Microbiological response to mechanical treatment in combination with adjunctive therapy. A review of the literature. J Periodontol 1996; 67; 1143-58.
18. Slots J. Selection of antimicrobial agents in periodontal therapy. J Periodontal Res 2002; 37:389-98.
19. Mellado-Valero A, Buitrago-Vera P, Solá-Ruiz MF, Ferrer-García JC. Decontamination of dental implant surface in peri-implantitis treatment: a literature review, Med. Oral Patol. Oral Cir. Bucal 2013; 18(6). https://doi.org/10.4317/medoral.19420.
20. Sigusch B, Beier M, Klinger G, Pfister W, Glockmann E. A 2-step non-surgical procedure and systemic antibiotics in the treatment of rapidly progressive periodontitis. J Periodontol 2001; 72:275-83.
21. Pallasch TJ. Antibiotic resistance. Dent Clin North Am 2003; 47:623-39.
22. Akram Z, Al-Shareef SA, Daood U, Asiri FY, Shah AH, AlQahtani MA, et al. Bactericidal efficacy of photodynamic therapy against periodontal pathogens in periodontal disease: a systematic review, Photomed. Laser Surg 2016; 34:137-49.
23. Raab O. The effect of fluorescent agent on infusoria (in German) Z biol 1900; 39:524-6.
24. Wilson M. Bactericidal effect of laser light and

its potential use in the treatment of plaque-related diseases. Int Dent J 1994; 44:181-9.

25. Wilson M. Photolysis of oral bacteria and its potential use in the treatment of caries and periodontal disease. J appl bacteriol 1993; 75:299-306.
26. Wilson M, Dobson J, Harwey W. Sensitization of oral bacteria to killing by low-power laser radiation. Curr microbiol 1992;25;77-81.
27. Martinetto P, Gariglio M, Lombard GF, Fiscella B, Boggio F. Bactericidal effect induced by laser irradiation and haematophoryrin against gram-positive and gram-negative microorganism. Drugs Exp Clin Res 1986; (12):335-42.
28. DeSimone NA, Christiansen C, Dore D. Bactericidal effect of 0.95-mW helium-neon and 5-mW indium-gallium-aluminium-phosphate laser irradiation at exposure time of 30, 60 and 120 seconds on photo-sensitized Staphylococcus Aureus and Pseudomonas Aeruginosa in vitro. Phys ther 1999; (79):839-46.
29. Cieplik F, Deng D, Crielaard W, Buchalla W, Hellwig E, Al-Ahmad A, et al. Antimicrobial photodynamic therapy–what we know and what we do not, Crit. Rev. Microbiol 2018; (44):571-89.
30. Carvalho LH, D'Avila GB, Leao A, Haffajee AD, Socransky SS, Feres M. Scaling and root planing, systemic metronidazole and professional plaque removal in the treatment of cronic periodontitis in a brazilian popolation: clinical results. J Clin Periodontol 2004; 31:1070-6.
31. Moher D, Liberati A, Tetzlaff J, Altman DG. Preferred reporting items for systematic reviews and meta-analyses: the PRISMA statement, Ann. Internal Med 2009; (151):264-9.
32. Azizi B, Budimir A, Bago I, Mehmeti B, Jakovljević S, Kelmendi J, et al. Antimicrobial efficacy of photodynamic therapy and light-activated disinfection on contaminated zirconia implants: an in vitro study, Photodiagn. Photodyn. Ther 2018; (21):328-33.
33. Saffarpour A, Fekrazad R, Heibati .N, Bahador A, Saffarpour A, Rokn AR, et al. Bactericidal effect of erbium-doped yttrium aluminum garnet laser and photodynamic therapy on Aggregatibacter actinomycetemcomitans biofilm on implant surface, Int. J. Oral Maxillofac. Implants 2016; (31):71-8.
34. Giannelli M, Landini G, Materassi F. Chellini F, Antonelli A, Tani A, et al. Effects of photodynamic laser and violet-blue led irradiation on Staphylococcus aureus biofilm and Escherichia coli lipopolysaccharide attached to moderately rough titanium surface: in vitro study, Lasers Med. Sci. 2017; (32):857-64.
35. Marotti J, Tortamano P, Cai S, Ribeiro M.S, Franco J.E, de Campos T.T. Decontamination of dental implant surfaces by means of photodynamic therapy, Lasers Med. Sci. 2013; (28):303-9.
36. Rafael R. de Oliveira, Humberto O. Schwartz-Filho, Arthur B. Novaes Jr, Taba Jr.M, Antimicrobial Photodynamic Therapy in the Non-Surgical Treatment of Aggressive Periodontitis: A Preliminary Randomized Controlled Clinical Study; J periodontol 2007; 78(6):965-73.
37. Park D, Kim M, Woo Choi J, Baek JH, Lee SH, Baek K. Antimicrobial photodynamic therapy efficacy specific against periodontitis pathogen bacterial species. Photodiagnosis Photodyn Ther. 2020; 101688. doi: 10.1016/j.pdpdt.2020.101688
38. Andersen R, Loebel N, Hammond D. Treatment of Periodontal Disease by Photodisinfection Compared to Scaling and Root Planing. J Clin Dent. 2007; 18(2):34-8.
39. Rovaldi CR, Pievsky A, Sole NA, et al. Photoactive porphyrin derivative with broad-spectrum activity against oral pathogens in vitro, Antimicrob. Agents Chemother 2000; (44):3364-7.
40. Takasaki AA, Aoki A, Mizutani K, et al. Application of antimicrobial photodynamic therapy in periodontal and peri-implant diseases, Periodontol 2000 2009; (51):109-40.
41. Usacheva MN, Teichert MC, Sievert CE. Biel MA, Effect of Ca+ on the photobactericidal efficacy of methylene blue and toluidine blue against gram-negative bacteria and the dye affinity for lipopolysaccharides, Lasers Surg. Med 2006; 38 946-54.

Photodynamic therapy (PDT) in non-surgical treatment of periodontitis

M.A. Lopez[1], P.C. Passarelli[2], M. Marra[2], A. Lopez[3], A. D'Angelo[2], A. Moffa[1], S. Martinez[2], M. Casale[1] and A. D'Addona[2]

[1]Unit of Otolaryngology, UOS ORL TI, Campus-Biomedico University, Rome, Italy; [2]Department of Head and Neck, Division of Oral Surgery and Implantology, Institute of Clinical Dentistry, Università Cattolica del Sacro Cuore, Fondazione Policlinico Universitario Gemelli, Rome, Italy; [3]Dental Unit UEM, Madrid, Spain

Periodontitis represents a major problem for patients, since it is not possible to eliminate the bacteria that are responsible for this pathology with a pharmacological treatment. The present study included forty-four patients with periodontitis, who had undergone disinfection via photodynamic therapy (PDT) using a laser source having a 635 nm wavelength associated with a photoactivable substance (methylene blue). Clinical assessment of plaque index (PI), bleeding on probing (BOP), probing depth (PD), calculus index (CI), gingival recession (REC) and clinical attachment level (CAL) were recorded at base line, 1 month (4 weeks) after treatment and again 3 months (12 weeks) after treatment, while site radiography (RX) and microbiological test (MT) were recorded at base line and 3 months (12 weeks) after treatment. The outcomes show a good efficacy of the PDT in the elimination of the periodontal pathogenic microflora and in the improvement of the clinical parameters considered: from the base line to the final check after 12 weeks it has been observed a reduction in REC of about 16.9%, a reduction of CAL of about 17.85%, a reduction of the BoP of about 93.3%, a reduction of the PD of about 17%, a reduction of the CI of about 66.3%, a reduction of PI of about 44%, and microbiologically a reduction of the total amount of bacteria with proven parodontopathic properties (red complex bacteria) of about 58.74%. Within the limits of the present study, PDT can be reasonably considered as a good carrier that leads to significant improvements in the parameters (clinical and microbiological) considered.

Periodontitis is an inflammatory reaction of the bone support tissue of the tooth root. Resulting from the extension of gingival inflammation, known as gingivitis, periodontitis differs from it because of the irreversible loss of support tissue that it entails, which can evolve into loss of attachment, formation of intraosseous defects and loss of elements, as well as increased fragility of the periodontal support structure. From the point of view of general health, several studies (1-3) have proved the correlation between periodontitis and increased risk of systemic problems, with particular involvement of the cardiovascular (4) and respiratory districts. Although several contributing risk factors, both systemic (5-7) and local (8, 9), are known for the development of this disease, the responsibility of some specific bacteria in the etiology of periodontitis has been demonstrated (10, 11). The suppression of the bacteria (12, 13) has being demonstrated to be the state of the art in the prevention and treatment of this pathology. This is not easy, and it represents a particularly difficult challenge for the operator, due

Key words: periodontal disease, biomaterial, oral rehabilitation, periodontitis, photodinamic therapy, PDT, laser, non-surgical treatment

Corresponding Author:
Pier Carmine Passarelli,
Department of Head and Neck,
Division of Oral Surgery and Implantology,
Institute of Clinical Dentistry, Università Cattolica del Sacro Cuore,
Tel.: +39 0630155278 - Fax: +39 0630154751
e-mail: piercarmine.passarelli@unicatt.it

0393-974X (2020)

to the complexity of the bacterial aggregates that compose the biofilm and the location in which it is necessary to operate. The non-surgical mechanical therapy scaling and root-planing (SRP) represents the most used method, along with the surgical therapy accompanied by a pharmacological supportive therapy (14, 15), which is not particularly effective if considered individually (16).

In fact, it has important contraindications which can include gastrointestinal problems or disorders and being subject to patient compliance (17), in addition to the evident problem related to the drug resistance of the biofilm which is continuously increasing (17). Also, there is the difficulty of defining which bacteria are sensitive to which antibiotic (18, 19), in what dose and how long it must be exposed. For these reasons, alternative therapies that allow the elimination of the bacteria responsible for periodontitis are been sought.

Photodynamic therapy (PDT) comes as a possible supportive or substitutive therapy for the treatment of periodontitis. PDT is based on the principle of photoactivation, which exploits the ability of a photosensitive agent to modify its electrical state through exposition to a light source with a specific wavelength (20). In the past few years, extensive investigations into the antimicrobial action of photosensitizing agents and light have been carried out. When these molecules absorb light, they undergo an electronic transition to the excited state (electron spins paired). The excited state can return to the ground state through a triplet (electron spins unpaired) and this triplet state transfers energy directly to molecular oxygen (biological molecule naturally present in a triplet ground state). The triplet energy exchange causes oxygen electronic transition to its singlet state, which is highly reactive and causes microbial cell death by several mechanisms, including lipid peroxidation, enzyme system inhibition, protein agglutination and by reacting with other biological systems. (Fig. 1)

Several authors (21, 22) have choosen Methylene blue (a tricyclic phenothiazine) as a highly suitable antimicrobial photosensitizer. It presents physical and chemical properties which make it ideal for this purpose, such as selective binding properties to bacteria, the minimal coloring of the mucosal surface, high quantum yield of free radicals. It has a long history of safe use, low toxicity profile (23), and proven efficacy against target pathogens (24).

This process was initially studied by Raab (25) who highlighted the efficacy of PDT on protozoa. Subsequently Wilson (26-28) and other contemporary studies (29, 30) highlighted the

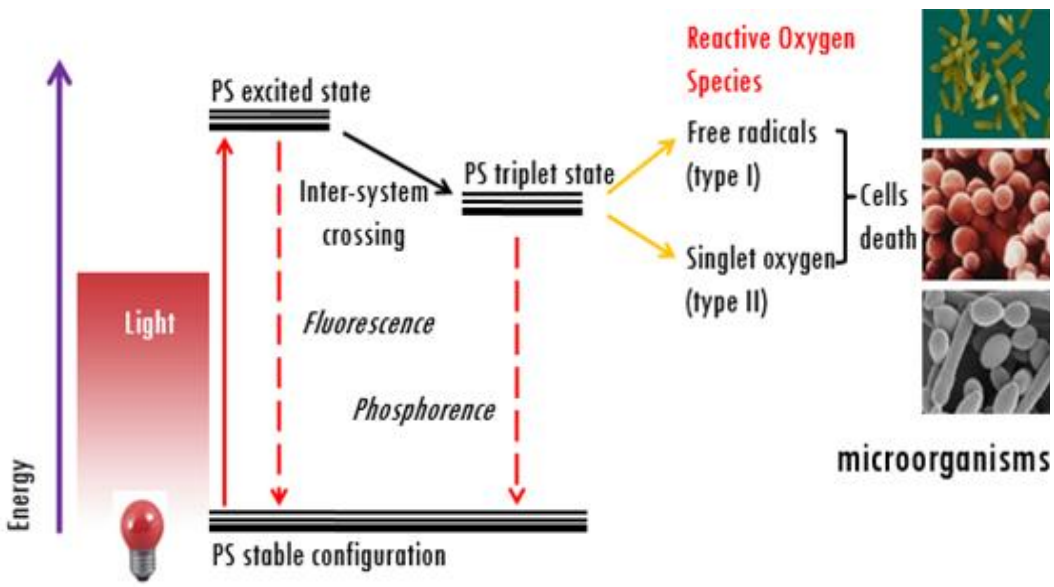

Fig. 1. *Principle of photoactivation.*

efficacy of PDT on periodontal interest bacteria in vitro and on rats, also revealing a decrease in bone loss (31). The use of PDT in the treatment of periodontal disease could overcome some present problems in current therapies, such as the decrease of the possibility to reduce plaque with the deepening of the periodontal pocket for manual SRP (32, 33) and the increase in drug resistance of the bacteria, that has been observed more and more frequently (17, 34). The aim of the present study is to verify the microbicide capacity of PDT against periodontal bacteria from a microbiological point of view. To do that, measurements of the level of proven periodontal bacteria present in the analyzed patients' sites suffering from stage III - IV periodontitis has been taken at base line and at a 12-week follow up. Also, from a clinical point of view, measurements of the diagnostic indices of the patients have been taken, before and after the therapy, with a 4 and 12-week follow-up.

MATERIALS AND METHODS

Patient selection

The present retrospective study included a population of forty-four subjects (16 females and 28 males) with periodontal disease, aged from 35 to 82 years (presenting an average age of 50.4 years), who had undergone an SRP session performed by the same operator who, immediately after performed the PDT procedure at the Oral Surgery Unit of Policlinico Universitario Agostino Gemelli (Rome, Italy) between March and April 2019. We retrospectively analyzed the clinical diagnostic indexes as well as microbiological and radiographic data recorded (Fig. 2).

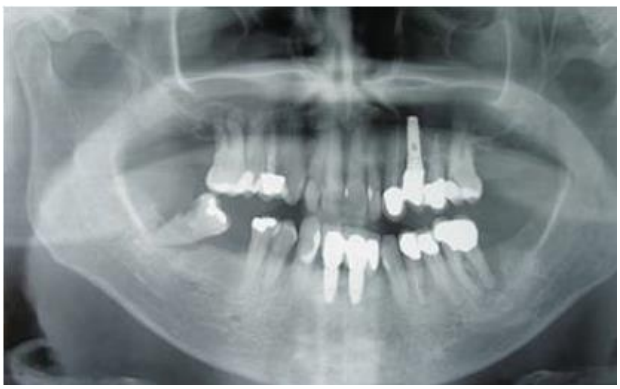

Fig. 2. *Sample of radiological investigation.*

Due to the retrospective nature of the present study, it was granted an exemption in writing by the institutional review board of the Catholic University of Sacred Heart of Rome. We have read the Declaration of Helsinki and followed its guidelines in the present investigation. The selection of the study population was based on the following criteria:

- Subjects had to be over the age of 18, in good general health conditions and with no allergy to methylene blue;
- Subjects had to have at least 10 teeth, of which at least 2 molars;
- Subjects had to present bleeding on probing and pockets of at least 5 mm;
- Pregnant or lactating women were excluded;
- Subjects with uncontrolled diabetes were excluded;
- HIV / AIDS positive subjects were excluded;
- Subjects who have had any periodontal instrumentation or antibiotic therapy in the previous six months were excluded;
- Subjects had to sign an Informed Consent to join the study.

Preoperative measurements and treatment

At the baseline visit patient's personal, medical and dental informations were collected, along with clinical diagnostic indexes:

- REC (Gingival Recession): detected on 2 sites (vestibular and lingual)
- PPD (Probing Pocket Depth): detected on 6 sites (Disto-Vestibular, Vestibular, Mesio-Vestibular, Mesio-Lingual, Lingual, Disto-Lingual)
- CAL (REC + PPD)
- BoP (Bleeding on Probing) (57): detected on 6 sites (Disto-Vestibular, Vestibular, Mesio-Vestibular, Mesio-Lingual, Lingual, Disto-Lingual) and measured by a dichotomous index, positive/negative presence of bleeding)
- CI (Calculus index) (58): detected on 6 sites (Disto-Vestibular, Vestibular, Mesio-Vestibular, Mesio-Lingual, Lingual, Disto-Lingual)
- PI (Plaque index) (59): detected on 6 sites (Disto-Vestibular, Vestibular, Mesio-Vestibular, Mesio-Lingual, Lingual, Disto-Lingual). Six sites per tooth were analyzed (Disto-Vestibular, Vestibular, Mesio-

Table I. ***(A)****: Clinical diagnostic indexes recorded on the selected patients at base line; (B): and at 12-weeks follow-up.*

Patient number	Sex	Age at baseline	Sites of interest decected	Average REC (mm) refered to the sites of interest	Average PPD (mm) refered to the sites of interest	Average CAL (mm) refered to the sites of interest	Sites presenting BOP (total)	Average CI refered to the sites of interest	Average PI refered to the sites of interest
1	M	67	23	A: 3 B: 2	A: 8 B: 5.5	A: 11 B: 7.5	A: 66 B: 0	A: 1.4 B: 0.4	A: 1.6 B: 0.5
2	M	46	22	A: 4.5 B: 3.5	A: 6 B: 5	A: 10.5 B: 8.5	A: 48 B: 1	A: 0.9 B: 0.3	A: 1.16 B: 0.4
3	F	53	19	A: 3 B: 2.5	A: 7 B: 5	A: 10 B: 7.5	A: 55 B: 0	A: 0.8 B: 0	A: 1 B: 0.3
4	F	51	19	A: 4 B: 3	A: 5 B: 4	A: 9 B: 7	A: 63 B: 0	A: 0.6 B: 0	A: 1 B: 0.4
5	M	42	17	A: 3.5 B: 2.5	A: 5 B:4.5	A: 8.5 B: 7	A: 49 B: 1	A: 0.34 B: 0	A: 0.6 B: 0.3
6	F	48	17	A: 3.5 B: 3	A: 5 B:4.5	A: 8.5 B: 7.5	A: 43 B: 2	A: 0.9 B: 0.3	A: 1 B: 0.6
7	M	40	15	A: 3 B: 2	A: 5 B: 4	A: 8 B: 6	A: 57 B: 0	A: 0.66 B: 0.2	A: 0.8 B: 0.7
8	M	44	21	A: 3.5 B: 3	A: 6 B: 4.5	A: 9.5 B: 7.5	A: 57 B: 2	A: 0.5 B: 0.2	A: 0.7 B: 0.6
9	M	55	19	A: 4 B: 3	A: 5 B: 4	A: 9 B: 7	A: 46 B: 0	A: 1 B: 0.4	A: 1.3 B: 0.8
10	M	47	19	A: 3 B: 2.5	A: 6 B: 5	A: 9 B: 7.5	A: 53 B: 0	A: 0.5 B: 0	A: 1 B: 0.3
11	M	42	12	A: 2.5 B: 2	A: 5.5 B: 4.5	A: 8 B: 6.5	A: 39 B: 0	A: 0 B: 0	A: 0.5 B: 0.4
12	M	41	13	A: 3 B: 2.5	A: 6 B: 5	A: 9 B: 7.5	A: 41 B: 0	A: 0.66 B: 0	A: 1 B: 0.5
13	M	37	11	A: 3 B: 2.5	A: 5 B: 4.5	A: 8 B: 7	A: 37 B: 0	A: 0.5 B: 0.2	A: 1.16 B: 0.7
14	M	54	19	A: 3.5 B: 2.5	A: 6 B: 5	A: 9.5 B: 7.5	A: 55 B: 0	A: 0.9 B: 0.4	A: 1.6 B: 0.66
15	M	41	14	A: 4 B: 3	A: 5 B: 4	A: 9 B: 7	A: 42 B: 0	A: 1.16 B: 0.5	A: 1 B: 0.8
16	F	68	21	A: 4 B: 3.5	A: 6 B: 5	A: 10 B: 8.5	A: 68 B: 1	A: 1.86 B: 0.66	A: 2 B: 0.9
17	M	39	10	A: 2.5 B: 2	A: 5 B: 4.5	A: 7.5 B: 6.5	A: 35 B: 0	A: 0.33 B: 0	A: 0.66 B: 0.3
18	F	48	17	A: 3 B: 2	A: 5.5 B: 4	A: 8.5 B: 6	A: 54 B: 0	A: 0.7 B: 0.33	A: 1.16 B: 0.6
19	F	61	15	A: 1 B: 2	A: 12 B: 9	A: 13 B: 11	A: 42 B: 8	A: 2 B: 2	A: 2.16 B: 2.2
20	M	47	17	A: 2 B: 2	A: 7 B: 5.5	A: 9 B: 7.5	A: 58 B: 1	A: 1 B: 0	A: 1.66 B: 0.66
21	M	52	16	A: 3 B: 3	A: 5 B: 4.5	A: 8 B: 7.5	A: 39 B: 9	A: 0.8 B: 1.3	A: 1 B: 1.8

22	F	77	23	A: 3 B: 2.5	A: 5 B: 5	A: 8 B: 7.5	A: 63 B: 8	A: 0.5 B: 1.1	A: 0.8 B: 1.66
23	M	42	16	A: 2.5 B: 2	A: 5.5 B: 5	A: 8 B: 7	A: 54 B: 0	A: 0 B: 0	A: 0.6 B: 0.3
24	M	81	15	A: 3 B: 2.5	A: 6 B: 5	A: 9 B: 7.5	A: 43 B: 0	A: 0.33 B: 0	A: 0.7 B: 0.2
25	F	41	14	A: 3 B: 2.5	A: 5 B: 4	A: 8 B: 6.5	A: 38 B: 0	A: 0.5 B: 0	A: 0.8 B: 0.1
26	F	56	20	A: 1.5 B: 0.5	A: 8 B: 5.5	A: 9.5 B: 6	A: 53 B: 0	A: 1 B: 0.33	A: 1.66 B: 0.5
27	F	43	19	A: 3 B: 2.5	A: 6.5 B: 5.5	A: 9.5 B: 8	A: 58 B: 0	A: 0.9 B: 0.5	A: 1.3 B: 0.8
28	F	68	18	A: 2.5 B: 2	A: 7 B: 5	A: 9.5 B: 7	A: 48 B: 0	A: 1 B: 0	A: 1.1 B: 0.3
29	M	43	18	A: 2.5 B: 2.5	A: 6.5 B: 5.5	A: 9 B: 8	A: 43 B: 1	A: 1.8 B: 0.5	A: 1.6 B: 0.9
30	M	64	16	A: 2 B: 2	A: 7 B: 5.5	A: 9 B: 7.5	A: 44 B: 0	A: 0.36 B: 0	A: 0.66 B: 0.36
	F	82	22	A: 4 B: 5.5	A: 6 B: 6	A: 10 B: 11.5	A: 53 B: 8	A: 0.5 B: 1.2	A: 0.66 B: 1.6
32	M	39	17	A: 3.5 B: 3	A: 5 B: 4.5	A: 8.5 B: 7.5	A: 39 B: 0	A: 1 B: 0	A: 1 B: 0.26
33	M	48	19	A: 3.5 B: 2	A: 6.5 B: 5	A: 10 B: 7	A: 49 B: 0	A: 1.6 B: 0	A: 1.6 B: 0.3
34	M	35	14	A: 4 B: 3	A: 5 B: 4	A: 9 B: 7	A: 37 B: 0	A: 2 B: 0	A: 1.63 B: 0.4
35	F	71	15	A: 2 B: 3	A: 7.5 B: 5.5	A: 9.5 B: 8.5	A: 37 B: 1	A: 1.66 B: 0.66	A: 1.16 B: 0.8
36	F	40	13	A: 3.5 B: 2	A: 5 B: 4.5	A: 8.5 B: 6.5	A: 41 B: 0	A: 1 B: 0	A: 1 B: 0.2
37	M	43	18	A: 3 B: 2.5	A: 6 B: 5	A: 9 B: 7.5	A: 43 B: 0	A: 1.16 B: 0.33	A: 1.4 B: 0.66
38	M	56	17	A: 2.5 B: 2	A: 5.5 B: 5	A: 8 B: 7	A: 47 B: 0	A: 0.63 B: 0	A: 0.96 B: 0.2
39	M	41	16	A: 2 B: 2	A: 5.5 B: 5	A: 7.5 B: 7	A: 48 B: 6	A: 0 B: 1	A: 0.6 B: 1.8
40	F	48	18	A: 2.5 B: 2	A: 6 B: 5	A: 8.5 B: 7	A: 53 B: 0	A: 1 B: 0	A: 1.3 B: 0.36
41	M	52	15	A: 1.5 B: 1.5	A: 6 B:5	A: 7.5 B: 6.5	A: 43 B: 0	A: 0.6 B: 0	A: 1.66 B: 0.5
42	M	40	17	A: 3.5 B: 2.5	A: 7.5 B: 5.5	A: 11 B: 8	A: 39 B: 1	A: 1.8 B: 0	A: 2.06 B: 0.4
43	F	38	14	A: 2 B: 1.5	A: 6 B: 5	A: 8 B: 6.5	A: 40 B: 0	A: 0.7 B: 0.2	A: 1 B: 0.7
44	M	46	18	A: 3.5 B: 3	A: 6.5 B: 5.5	A: 10 B: 8.5	A: 39 B: 1	A: 1.7 B: 0.2	A: 1.83 B: 0.8

Vestibular, Mesio-Lingual, Lingual, Disto-Lingual) and the sites of interest for the study were identified (positive BoP, PPD> 5 mm, IP > 0.5) (Tab. I).

The subjects underwent a microbiological and radiographic data collection, after which they underwent the SRP and PDT procedures as mentioned above. A first follow-up was performed at 4 weeks. The follow up ended at 12 weeks with a new microbiological and radiographic investigation, that has been compared to the ones made at base line. To maintain the same quality standard when performing SRP and PDT, all patients were treated by the same operator. Microbiological investigations were performed using salivary swab taken from the site of interest and then submitted to PCR to identify bacterial DNA (60).

Operative protocol

The photosensitizer chosen for PDT is a high viscosity methylene blue 0.005% (w/v), suspended in a solution of water and hydroxy-propyl-methylcellulose in addition to a sodium phosphate tampon. The pre-dosed syringes containing 1.2 mg of photosensitive gel were mixed for 90 seconds and then the solution was applied using a special tip which presented ended side-port irrigating, possible through two micro-holes placed laterally (Fig. 3) in order to allow the gel to fill the pockets and overflow slightly, to be delicately affixed and coat the mineralized surface of the tooth, where the biofilm is formed.

A light from a LED presenting a wavelength at 635 nm and a maximum power of 750 W was channeled inside an optical tip, configured similarly to a periodontal probe, which presented a minimum diameter of 1 mm in his thinner extremity and a total length of 9 mm, feature that allowed full access to the periodontal pocket. A uniform light was emitted from the LED and channeled through the optical tip. This allowed the complete and correct distribution of the light throughout the periodontal pocket and on the gel containing the photosensitizer, which has been irradiated for 60 seconds in each site, with an average energy density of 10-20 J/cm² per site, depending on the size of the periodontal pocket (Fig. 4) (Table II). The tip was gently slipped inside the pocket and around the tooth during the lighting cycle.

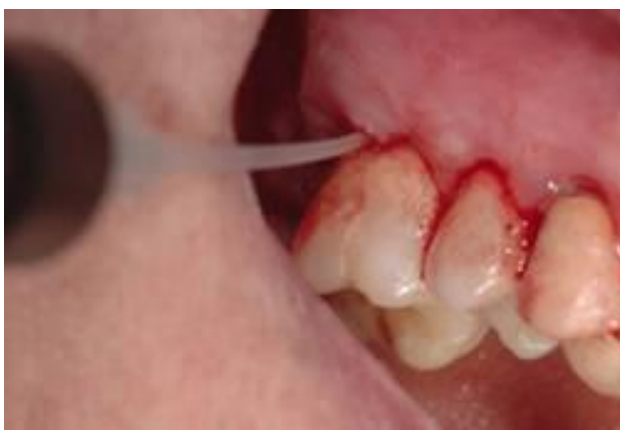

Fig. 3. *Photosensitizer being irrigated into periodontal pocket.*

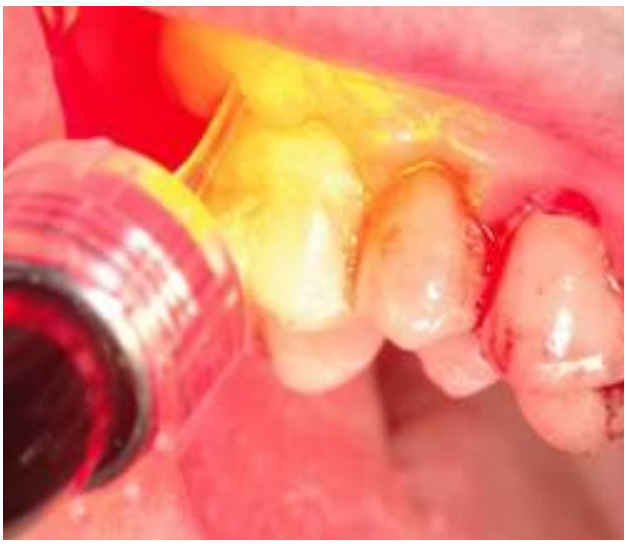

Fig. 4. *Illumination of periodontal pocket with light diffusing tip.*

Within the limit of this study, results suggest that PDT is a valid non-surgical approach for the control of periodontal problems with bacterial origin, since the reduction of REC, CAL, PDD, CI, PI and BoP is clinically evidenced, while an overall decrease of periodontogenic bacteria of 58.74% is shown microbiologically. PDT can be used in association with SRP procedure or singularly, depending on the cases. The results are encouraging and justify further studies that could include a larger number of subjects, to confirm on large-scale, the results obtained.

RESULTS

The total number of sites analyzed was 5814, with the identification of 748 sites with periodontal

Table II. *General parameters of the light source used.*

Parameters of the light source used	
Manufacturer	Laser
Light source	LED*
Wavelenght (nm)	635
Max Power (output) (mW)	750
Pulse mode (CW or Hz)*	CW
Tipe of lamp used	2 (IEC 62471)
Esposure duration (sec)	60
Minimum diameter of the optical tip (mm)	1
Length of the optical tip (mm)	9
Radiand exposure (J/cm^2)	10/20
Total number of sessions performed	One session

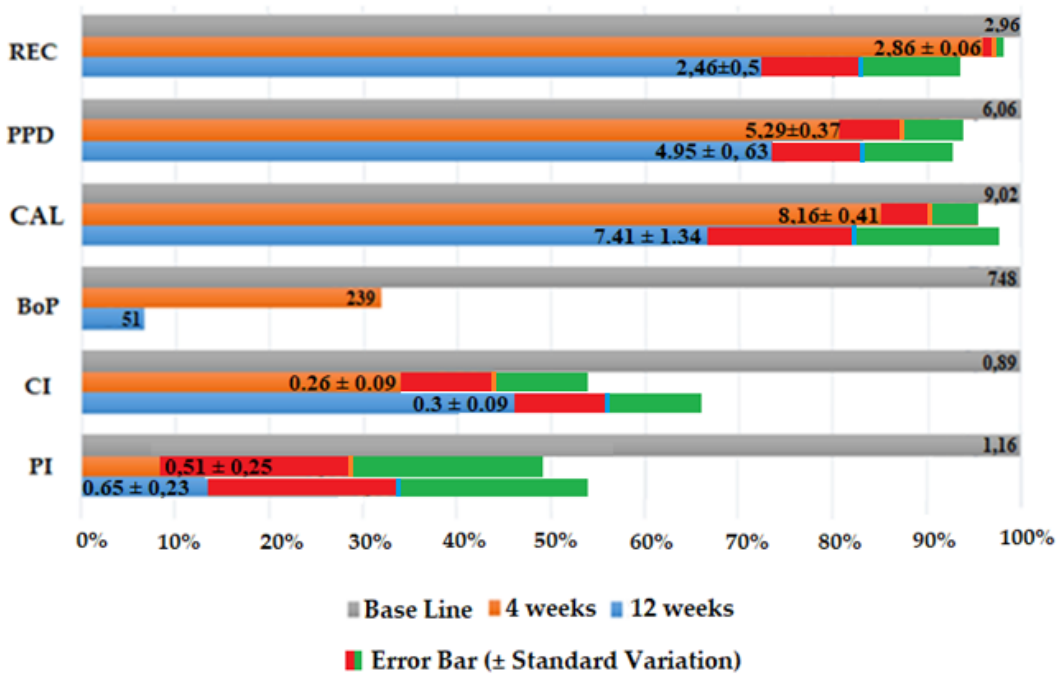

Fig. 5. *Variation (numeric and percentage) of the average value of the mean clinical scores at baseline, after 4 weeks and after 12 weeks. Numeric variations are reported inside the bars; percentage variations can be read referring to the percentage scale at the bottom of the graphic.*

involvement. No treatment-related adverse events were reported during or after the study. Clinically, it was possible to observe a decrease of REC by 0.1±0.06 mm after 4 weeks and 0.5±0.3 mm at the last control at 12 weeks, bringing its value from 2.96 to 2.46±0.5 mm with an average percentage reduction of 16.9%.

The average PPD decreased by 0.77±0.37 mm after 4 weeks and 1.11±0.53 mm after 12 weeks bringing its value from 6.06 to 4.95±0.63 mm with an average percentage reduction of 17%. The average CAL decreased by 0.86 ± 0,41 mm in the first control at 4 weeks and 1.61±1.34 mm in the last control after 12 weeks, bringing its value from 9.02 to 7.41 ± 1.34 mm with an average percentage reduction of 17.85%. The BoP decreased by 68% after 4 weeks (from 748 sites affected to 239) and by 93.3% after 12 weeks (down to 51). Average **CI** decreased by 71% after 4 weeks and by 66.3% after 12 weeks, bringing its value from 0.89 to 0.3±0.09. Average PI decreased by 56% after 4 weeks and 44% after 12 weeks from 1.16 to 0.65±0.23. (Fig. 5)

The new microbiological inspections conducted after 12 weeks, evidence a decrease in the total microflora of bacteria belonging to the red complex (Porphyromonas Gingivalis (PG), Tannerella Forsythia (TF), Treponema Denticola (TD) of 58.74%, passing from an average numeric value of 363020 to 149717±52382. More specifically, the decrease observed in the number of PG was 73.14% (the average numeric value went from 192225 to 51638±28956), of TF was 26.73% (from 52690 to 38587±4849) and of TD was 49.62% (from 118106 to 59492±18577) (Fig. 6).

DISCUSSION

In this study we have investigated the antimicrobial action of PDT in patients with evidenced presence of periodontopathogenic bacteria (belonging to the red

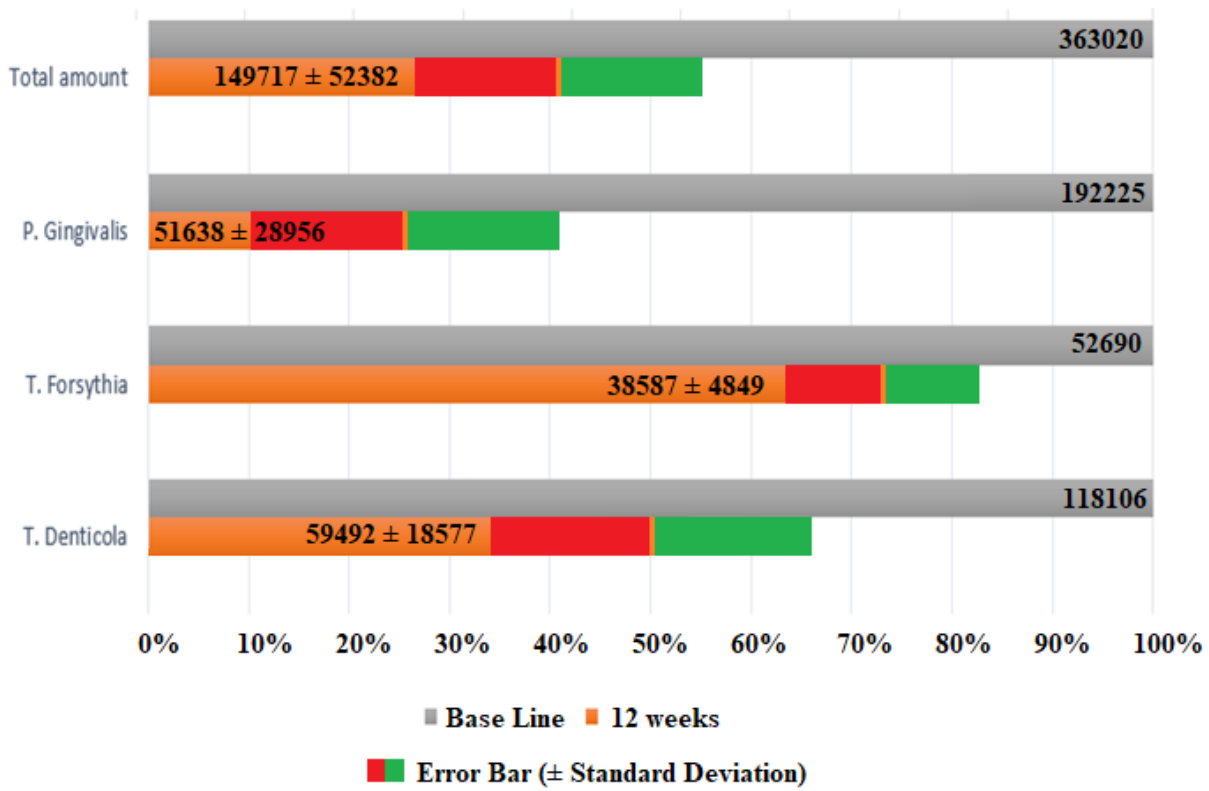

Fig. 6. *Variation (numeric and percentage) of the average value of the microbiological measurement at baseline and after 12 weeks. Numeric variations are reported inside the bars; percentage variations can be read referring to the percentage scale at the bottom of the graphic.*

complex) outside and inside the periodontal pockets. On the mineralized surface of the tooth, these pathogenic bacteria assemble to form a complex structure defined biofilm (35) that can penetrate the soft tissue of the periodontium (36). While it is rather difficult to disrupt the bacterial biofilm through SRP procedure, several studies on dogs and rats (31, 37, 38) have shown that PDT is a valid alternative in the elimination of periodontopathogenic components from the bacterial biofilm without any reported collateral effect. The same results have been highlighted in this study, confirming the fact that PDT could be excellently used to eliminate pathogenic component from the biofilm.

Furthermore, it has been shown that the periodontal disease has a fundamental infectious component (10, 11, 39, 40), so it could be reasonable to consider reducing the microbial load, that is the main cause of the disease (12, 13), as a first measure against periodontitis. Although mechanical non-surgical therapy SRP is considered one of the basic prerequisites for a long-term success of the treatment (41-43), it should also be considered that several problems related to this practice have been highlighted. In particular, the study by Flemmig et al. (44) shows how, without an adequate root-polishing support performed subsequently and separately from primary therapy, the SRP does not guarantee satisfactory microbiological and clinical results, even if supported by systemic antibiotic therapy. Furthermore, more recently, a study by Sigusch et al. (16) demonstrates that the only administration of antibiotics in cases of generalized periodontitis does not lead to a therapeutic long-term success, even if preceded by a supra and subgingival mechanical removal of plaque and calculus, since over time patient will present an increasing of PPD, increasing of CAL and recolonization of periodontogenic microflora. In addition, the success of SRP therapy is closely linked to the depth of the pocket on which action is taken (32, 33, 45) and to the skill of the operator.

For these reasons, although there is agreement that SRP therapy has an active role to reduce the bacterial count and is responsible for the switch to a type of flora more compatible with a health condition (46, 47), there are doubts about the possibility for this therapy to totally eradicate pathogenic bacteria from treated sites. Particularly, Tannarella forsythensis and Actinobacillus Actinomycetemcomitans, whose presence has been shown by several studies (48, 49) in sites previously treated with SRP therapy after a very short period, therefore, it is essential to include the patient into a program of periodontal support (SPT) (50) and the use of PDT could be implemented and find a pratical application in this context. Nonetheless, it should be noticed that in this study a small percentage of patients (5 out of 44, 11.36%) did not respond positively to the therapy, showing an amount of periodogenic bacterial load during the follow-up higher than the one before the therapy. However, these same patients were the only ones who also presented an increased CI and that have maintained a high index of BoP during the follow-up. It seems likely to attribute the failure of the therapy to a poor domiciliary compliance of the patients, despite personalized indications of oral hygiene had been given to all subjects.

It would be interesting to study the effects of PDT in subjects with peri-implant problems, considering that in implant-supported rehabilitation a characteristic assessment of the clinical parameters has been observed (51) requiring different and innovative approaches (52). In fact, in cases of perimplantitis the histological composition of the tissues presents a greater collagenase content, less blood supply (53) and less fibroblastic cellularity (5% *vs* 16%), insufficient to limit the action of inflammatory effects (54). In addition to the ease of application and to the impossibility for the bacteria to develop resistance to this therapy, the PDT has also other advantages, such as: the fact of being an atraumatic therapy and therefore helping avoid the appearance or increasing of gingival recessions; minimum treatment time (60 seconds); effective removal of the bacterial microflora and decreased correlation between operator's ability and efficacy of the therapy (compared to SRP therapy).

Finally, the possibility of using various substances as photosensitizers makes it possible to overcome the problems related to a possible allergy to methylene blue. For example, excellent results using toluidine blue as photosensitizer performing PDT have been obtained

and no side-effects have been recorded, even exposing the patients to a maximum concentration of toluidine blue solution and maximum power of the light to which the photosensitive agent reacts (31, 55, 56).

REFERENCES

1. Azzolino D, Passarelli PC, De Angelis P, Piccirillo GB, D'Addona A, Cesari M. Poor Oral Health as a Determinant of Malnutrition and Sarcopenia. Nutrients 2019; 11(12). pii: E2898. doi: 10.3390/nu11122898. Review.
2. Limebach H. Implications of oral infections on systemic disease in the institutionalized elderly with a special focus on pneumonia. Ann Periodontol 1998; 3(1):262-75.
3. Lauritano D, Boccalari E, Di Stasio D, Della Vella F, Carinci F, Lucchese A, Petruzzi M. Prevalence of Oral Lesions and Correlation with Intestinal Symptoms of Inflammatory Bowel Disease: A Systematic Review. Diagnostics (Basel) 2019; 9(3). pii: E77. doi: 10.3390/diagnostics9030077. Review.
4. De Stefano et al. Dental disease and risk of coronary heart disease and mortality. BMJ. 1993; 306(6879):688-91.
5. Maboudi A, Akha O, Heidari M, Mohammadpour RA, Gheblenama P, Shiva A. Relation between Periodontitis and Prediabetic Condition. J Dent (Shiraz) 2019; 20(2):83-
6. Freitag-Wolf S, Munz M, Wiehe R, et al. Smoking Modifies the Genetic Risk for Early-Onset Periodontitis. J Dent Res 2019; 98(12):1332-9.
7. Bollero P, Passarelli PC, D'Addona A, Pasquantonio G, Mancini M, Condò R, Cerroni L. Oral management of adult patients undergoing hematopoietic stem cell transplantation. Eur Rev Med Pharmacol Sci 2018; 22(4):876-87.
8. Passarelli PC, Lajolo C, Pasquantonio G, D'Amato G, Docimo R, Verdugo F, D'Addona A. Influence of mandibular third molar surgical extraction on the periodontal status of adjacent second molars. J Periodontol. 2019; 90(8):847-55.
9. Helmi M, AlOsaimy S, Goodson JM, Hasturk H, Natto ZS. Annual alveolar bone loss in older adults taking oral bisphosphonate: a retrospective cohort study. BMC Oral Health. 2019; 19(1):260.
10. Scapoli L, Girardi A, Palmieri A, et al. Microflora and periodontal disease. Dent Res J (Isfahan) 2012; 9(S2):S202-6. doi: 10.4103/1735-3327.109755.
11. Rutar A, Lang NP, Buser D, Bürgin W, Mombelli A. Retrospective assessment of clinical and microbiological factors affecting periimplant tissue conditions. Clin Oral Implants Res 2001; 12(3):189-95.
12. Tanner ACR, Sokransky SS, Goodson JM. Microbiota of periodontal pockets losing crestal alveolar bone J. periodontal res 1984; 19:279-91.
13. Boom-Van Noorlos AA, van der Meer JW, van derJevel JS, Schepens E, van Steenbergen TJ, Burger EH. Bacterioides Gingivalis stimulates bone resorption via Interleukin-1 production by mononuclear cells. J clin periodontal 1990; 17:409-13.
14. Bollen CM, Quirynen M. Microbiological response to mechanical treatment in combination with adjunctive therapy. A review of the literature. J Periodontol 1996; 67: 1143-58. 15. Slots J. Selection of antimicrobial agents in periodontal therapy. J Periodontal Res 2002; 37:389-98.
15. Sigusch B, Beier M, Klinger G, Pfister W, Glockmann E. A 2-step non-surgical procedure and systemic antibiotics in the treatment of rapidly progressive periodontitis. J Periodontol 2001; 72: 275-83.
16. Pallasch TJ. Antibiotic resistance. Dent Clin North Am 2003; 47:623-39. Carvalho LH, D'Avila GB, Leao A, Haffajee AD, Socransky SS, Feres M. Scaling and root planing, systemic metronidazole and professional plaque removal in the treatment of cronic periodontitis in a brazilian popolation: clinical results. J Clin Periodontol 2004; 31:1070-6.
17. Feres M, Haffajee AD, Allard K, Som S, Socransky SS. Change in subgingival microbial profiles in adult administered amoxicillin or metronidazole. J Clin Periodontol 2001; 28:597-609.
18. Wainwright M. Photodynamic antimicrobial chemotherapy (PACT). J Antimicrob Chemother 1998; 42:3-28.
19. Wilson M, Dobson J, Harvey W Sensitization of oral bacteria to killing bylow-power laser radiation. Curr Microbiol 1992; 25:77-81.
20. Wainwright M, Crossley KB. Methylene blue-A therapeutic dye for all seasons? J Chemother 2002; 14:431-43.

21. Wainwright M. Methylene blue derivatives-Suitable photo antimicrobials for blood product disinfection? Int J Antimicrob Agents 2000; 16:381-94,
22. Meisel P, Kocher T. Photodynamic therapy for periodontal diseases: State of the art. J Photochem Photobiol B 79:159-70, 2005.
23. Raab O. The effect of fluorescent agent on infusoria (in German) Z biol, 1900; 39:524-6.
24. Wilson M. Bactericidal effect of laser light and its potential use in the treatment of plaque-related diseases. Int Dent J 1994; 44:181-9.
25. Wilson M. Photolysis of oral bacteria and it's potential use in the treatment of caries and periodontal disease. J appl bacteriol, 1993; 75: 299-306.
26. Wilson M, Dobson J, Harwey W. Sensitization of oral bacteria to killing by low-power laser radiation. Curr microbiol 1992; 25:77-81.
27. Martinetto P, Gariglio M, Lombard GF, Fiscella B, Boggio F. Bactericidal effect induced by laser irradiation and haematophoryrin against gram-positive and gram-negative microorganism. Drugs Exp Clin Res 1986; 12:335-42.
28. DeSimone NA, Christiansen C, Dore D. Bactericidal effect of 0.95-mW helium-neon and 5-mW indium-gallium-aluminium-phosphate laser irradiation at exposure time of 30, 60 and 120 seconds on photo-sensitized Staphylococcus Aureus and Pseudomonas Aeruginosa in vitro. Phys ther 1999; 79;839-46.
29. Komerik N, Nakanishi H, MacRobert AJ, Henderson B, Speight P, Wilson M. In vivo killing of Porphyromonas gingivalis by toluidine blue-mediated photosensitization in an animal model. Antimicrob Agents Chemother 2003; 47:932-40.
30. Caffesse RG, Sweeney PL, Smith BA. Scaling and root planing with and without periodontal flap surgery. J Clin Periodontol 1986; 13:205-10.
31. Rabbani GM, Ash MM, Jr, Caffesse RG. The effectiveness of subgingival scaling and root planing in calculus removal. J Periodontol 1981; 52:119-23.
32. Walker CB. The acquisition of antibiotic resistance in the periodontal micro - flora. Periodontol 2000 1996; 10:79-88.
33. Kolenbrander PE. Oral microbial communities: Biofilms; interactions and genetic systems. Annu Rev Microbiol 2000; 54:413-37.
34. Page RC, Offenbacher S, Schroeder HE, Seymour GJ, Kornman KS. Advances in the pathogenesis of periodontitis: summary of developments, clinical implications and future directions. Periodontol 2000 1997; 14:216-48.
35. Sigusch BW, Pfitzner A, Albrecht V, Glockmann E. Efficacy of photodynamic therapy on inflammatory signs and two selected periodontopathogenic species in a beagle dog model. J Periodontol 2005; 76: 1100-15.
36. Soukos NS, Mulholland SE, Socransky SS, Doukas AG. Photodestruction of human dental plaque bacteria: Enhancement of the photodynamic effect by photomechanical waves in an oral biofilm model. Lasers Surg Med 2003; 33: 161-8.
37. Haffajee AD. Sokransky SS. Microbical etiological agents of destructive periodontal desease. Periodontol 2000 1995; 5: 78-111.
38. Slots J, Jenco RJ. Black-pigmented bacterioides species, capnocytophaga species and actinobacillus actinomycetemcomitans in human periodontal disease: virulence factor in colonization, survival and tissue destruction J dent res; 1984; 63: 412-21.
39. Greenstein G. Periodontal response to mechanical non-surgical therapy: a review. J Periodontol 1992; 63: 118-30.
40. Moore J, Wilson M, Kieser JB. The distribution of bacterial lopopolysaccharide (endotoxin) in relation to periodontally involved root surfaces. J Clin Periodontol 1986; 13: 748-51.
41. Badersten A, Nilveus R, Egelberg J. 4-year observations of basic periodontal therapy. J Clin Periodontol 1987; 14:438-44.
42. Flemmig TF, Miliàn E, Karch H, Klaiber B. Differential clinical treatment outcome after sysyrmic metronidazole and amoxicillin in patients harboring Actinobacillus actinomycetemcomitans and/or porphyromonas gingivalis. J Clin Periodontol 1998; 25:380-7.
43. Ramfjord SP, Caffesse RG, Morrison EC, et al. Four Modalities of periodontal treatment compared over 5 years. J Clin Periodontol 1987; 14:445-52.
44. Mousques T, Listgarten M, Philips R. Effect of scaling and root planning on the composition of the human subgingival microbial flora. J Periodontal Res 1980; 15:144-51.
45. Haffajee Ad, Cugini MA, Dibart S, Smith C, Kent RL, Socransky SS. The effect of SRP on the clinical and

microbiological parameters of periodontal diseases. J Clin Periodontol 1997; 24; 324-334.
46. Renvert S, Wikstrom M, Dahlen G, Slots J, Egelberg J. Effect of root debridement on the elimination of Actinobacillus Actinomycetemcomitans and Bacterioides gingivalis from periodontal pockets. J Clin Periodontol 1990; 17; 345-350.
47. Takamatsu N, Yano K, He T, Umeda M, Ishikawa I. Effect of initial periodontal therapy on the frequency of detecting Bacteroides Forsythus, Porphyromonas gingivalis and Actinobacillus Actinomycetemcomitans. J Periodontol 1999; 70:574-80.
48. Petersilka GJ, Ehmke B, Flemmig TF. Antimicrobial effects of mechanical debride. Periodontol 2000 2002; 28:56-71.
49. Manicone PF, Passarelli PC, Bigagnoli S, Pastorino R, Manni A, Pasquantonio G, D'Addona A. Clinical and radiographic assessment of implant-supported rehabilitation of partial and complete edentulism: a 2 to 8 years clinical follow-up. Eur Rev Med Pharmacol Sci 2018; 22(13):4045-52.
50. Lopez MA, Manzulli N, D'Angelo A, Lauritano D, Papalia R, Candotto V. The use of hyaluronic acid as an adjuvant in the management of peri-implantitis. J Biol Regul Homeost Agents 2017; 31(4S2):123-7.
51. Berglundh T, Lindhe J, Jonsson K, Ericsson I. The topography of the vascular systems in the periodontal and peri-implant tissues in the dog. J Clin Periodontol 1994; 21(3):189-93.
52. Berglundh T, Lindhe J. Dimension of the periimplant mucosa. Biological width revisited. J Clin Periodontol 1996; 23(10):971-3.
53. Reza P, Atabak K, Nasrin R, Zohreh B, Anil K, Howard C T, Amir A. Effects of Photodynamic Therapy on Clinical and Gingival Crevicular Fluid Inflammatory Biomarkers in Chronic Periodontitis: A Split-Mouth Randomized Clinical Trial J Periodontol 2014; 85(9):1222-9. doi:10.1902/jop.2014.130464.
54. Nastri L, Donnarumma G, Porzio C, et al. Effects of Toluidine Blue-Mediated Photodynamic Therapy on Periopathogens and Periodontal Biofilm: In Vitro Evaluation Int J Immunopathol Pharmacol 2010; 23(4):1125-32. doi: 10.1177/039463201002300416.
55. Mea AW, Hana H. Bleeding on Probing: What Does It Mean? Gen Dent 2012; 60(4):271-6.
56. Aliye Akcalı, Niklaus P Lang Dental Calculus: The Calcified Biofilm and Its Role in Disease Development Periodontol 2000 2018; 76(1):109-115. doi: 10.1111/prd.12151. Epub 2017.
57. Laird WR, Grant AA. Dental Bacterial Plaque Int J Biochem 1983; 15(9):1095-102. doi: 10.1016/0020-711x(83)90223-9.
58. Ramesh R, Munshi A, Panda SK. Polymerase Chain Reaction. Natl Med J India 1992; 5(3):115-9.

Robotic hand treatment of patients affected by chronic stroke: a monocentric longitudinal pilot study

S. Miccinilli[1], M. Bravi[1], C. Foti[2], M. Morrone[1], M. Maselli[1] F. Santacaterina[1], F. Scotto Di Luzio[3], L. Zollo[3], S. Sterzi[1] and F. Bressi[1]

[1]Physical and Rehabilitation Medicine Department, Campus Bio-Medico University, Rome, Italy;
[2] Clinical Sciences and Translational Medicine Department. Tor Vergata University, Rome, Italy;
[3] Biomedical Robotics Laboratory and Bio-microsystems, Biomedical Engineering Laboratory, Campus Bio-Medico University, Rome, Italy

Few studies investigated the effects of a robotic treatment in hand motor recovery after stroke. Aim of the present study was to evaluate the efficacy of treatment by means of Gloreha Sinfonia® robotic glove in hand motor recovery of a chronic stroke sample of patients with different impairment severity. Thirteen chronic stroke subjects were assigned to either active-assisted robotic treatment or passive robotic treatment according to their ability to actively extend wrist for at least 20 degrees. All subjects underwent 20 sessions of treatment with Gloreha Sinfonia® and were evaluated before (T0), after treatment (T1) and after one month (T2) with clinical scales testing motor performance [Motor Power (MP); Fugl Meyer Upper-Extremity (FMUE)] and spasticity [Modified Ashworth Scale (MAS)]. Both groups showed significant motor recovery and spasticity reduction. Further randomized controlled trials with larger samples are needed to confirm our results.

Robotic hand treatment in stroke

Stroke is the second cause of death and the third cause of disability worldwide (1, 2). The incidence of this pathology in Italy varies between 175/100.000 and 360/100.000 per year in men and between 130/100.000 and 273/100.000 in women, consisting in 80% of cases of new episodes and in 20% of cases of relapses (3). Stroke can result in severe disability in 35% of cases, with frequent involvement of the hand (4). As shown in previous studies, there is a strong relationship between upper limb functioning and quality of life (5). For this reason when stroke involves the hand, patients experience reduction of autonomy in Activities of Daily Living (ADLs) and Instrumental ADLs (IADL) with significant consequences in everyday life (6). Spasticity, reduction of articular range of movement, functional impairment, vascular and skin disorders are the main post-stroke disorders of the hand (7). Hand recovery after stroke is still a challenging objective during rehabilitation since the hand is a very complex system with more than 20 degrees of freedom, allowing a wide variety of movements and with a correspondent large cortical representation area (8-10). For these reasons, rehabilitative therapists often encounter difficulty in reproducing such a variety of movements and of hand postures and in teaching the patient how to control individual joints (8).

Intensive, repetitive and task oriented rehabilitative treatment of the upper limb was proved particularly effective in stroke patients, as shown in literature (11, 12). Robotic treatment incorporates

Key words: exoskeleton, hand, rehabilitation, robotics, stroke

Corresponding Author:
Dr Sandra Miccinilli,
Via Alvaro Del Portillo 5,
Rome 00128 Italy
Tel.: 39 06 22 541 638
e-mail: s.miccinilli@unicampus.it

0393-974X (2020)

these features promoting recovery of motor function (13). The application of robotics in the rehabilitation of a target population of moderately to severely upper limb-impaired chronic stroke subjects, in fact, proved more effective than usual rehabilitation treatment and equally effective as intensive conventional rehabilitative treatment in recovering motor function (13). Rehabilitative robots are also capable to guide movements along an accurate pathway in order to avoid the activation of wrong uncontrolled patterns and can quantify with different accuracy motor performances, returning useful information about the trend of the rehabilitation treatment (14, 15)cerebral vascular disorders, stroke, paresis, hemiplegia, upper extremity, arm, and robot.

In the last three decades an important development of robotics in the rehabilitation field was witnessed, however there are still no equal advancements in hand robotics, because of the extreme complexity of projecting a system able to fully replicate all possible hand movements (16). Gloreha® (Idrogenet, Brescia, Italy) is a commercial device for the robotic rehabilitation of the hand, conceived at the University of Brescia (Italy) and prototyped by Polibrixia, Brescia, Italy. To date, few studies from 2014 on investigated the efficacy of a robotic hand treatment delivered by means of Gloreha® in impaired stroke subjects. Examined subjects were mainly subacute post-stroke patients (<6 months from stroke accident), receiving Gloreha® treatment in passive modality together with other treatments (traditional rehabilitation, passive hand mobilization and occupational therapy) (17-21).

Only two studies investigated the effects of Gloreha in a sample of chronic subjects, proving improvements in spasticity and attention disorders (22, 23). Studies overall concluded that in subacute patients Gloreha ® robot is safe and feasible (17), reduces pain (18), improves forearm perfusion (20) and edema (19), whereas in chronic patients Gloreha® decreases spasticity, heaviness and stiffness of the impaired arm (22) and improves visuospatial exploration and attention (23). The efficacy of Gloreha® in recovering fine manual dexterity and strength and in reducing arm disability was proved only in one study considering a population of subacute patients (21). These are, to date, the only available data about the effects of Gloreha® in improving motor performance. Subacute stroke patients, however, could have improved in manual dexterity and strength, due to spontaneous recovery or to concomitant traditional treatments, rather than to robotic therapy, given the temporal proximity to the acute ischemic event.

Therefore, so far, there is insufficient data to conclude on the efficacy of Gloreha® robot in improving motor performance in stroke-impaired subjects. Since there is an urgent and compelling need for a robot for the rehabilitative treatment of the hand, aim of the present study is to evaluate the efficacy of a robotic treatment by means of Gloreha Sinfonia® in motor hand recovery of a chronic stroke sample of patients with different impairment severity. Our hypothesis is that Gloreha® treatment can improve motor performance of the hand in chronic stroke patients with different impairment severity.

MATERIALS AND METHODS

This longitudinal monocentric pilot study, carried out at the Department of Physical and Rehabilitation Medicine of Campus Bio-Medico University of Rome, was performed to test our hypothesis. All enrolled subjects referred to the Department from October 2017 to December 2017 and were examined by a Physical and Rehabilitation Medicine specialist, as explained in Fig. 3. Inclusion criteria were ischemic or hemorrhagic chronic stroke (>6 months) confirmed at brain imaging; absence of cognitive impairment (MMSE>24), Modified Ashworth Scale < 3; signed informed consent. Exclusion criteria were chronic arm deformity; muscle-skeletal or peripheral nerve disorders, complex regional pain syndrome; severe neglect.

The study was conducted under Ethical Committee approval (Ethical Approval N. 41/17 OSS Com Et CBM) and in accordance with the Declaration of Helsinki. All patients gave their written informed consent. Subjects were not randomized, conversely they were assigned to two groups of treatment according to their ability of actively extend wrist of 20 degrees of freedom, in order to adjust hand treatment to impairment severity, as already done by Borboni A. in 2016 (19).

Group A (able to extend wrist of at least 20 degrees) received active-assisted robotic Gloreha Sinfonia® treatment; group B (unable to extend wrist of at least 20 degrees) received passive robotic Gloreha Sinfonia® treatment. A trained physiotherapist delivered treatment individually. All participants underwent the following clinical evaluations at T0 (before starting treatment), at T1 (end of treatment) and at T2 (one month later): Modified Ashworth Scale (MAS); Fugl-Meyer Assessment Upper Extremity (FMA-UE); Motricity Index (MI); wrist and hand section of Motor Power (MP) Scale. Clinical scales scores were outcome measures considered. Compliance of patients to treatment and evaluations was verified by presence registration. No patient failed to accomplish treatment.

Gloreha Sinfonia

Gloreha Sinfonia® is a robotic glove for robot-aided neurorehabilitation. It is composed of independent modules:

- A motorized glove for hand mobilization driven by five permanent magnetic actuators (LA12 Actuator, TECHLINE). Each actuator controls tension of a cable connected to the corresponding finger. The actuators and control electronics are placed distant from patient, in order to maximize patient safety and ergonomics of the glove (Fig. 1);
- Inserire Fig. 1
- A sensorized glove embedding five Bend-Sensors (Flexpoint Inc.) monitoring fingers flexion (Fig. 2);
- Inserire Fig. 2
- A software for acquiring sensors data and controlling motors, running on a touchscreen computer. It includes virtual reality environments to replicate several tasks and activities of daily living (ADLs) in a simulated scenario;
- Two passive arm-weight supports fixed to an ergonomic table, facilitating treatment also for wheelchair users (Fig. 1).

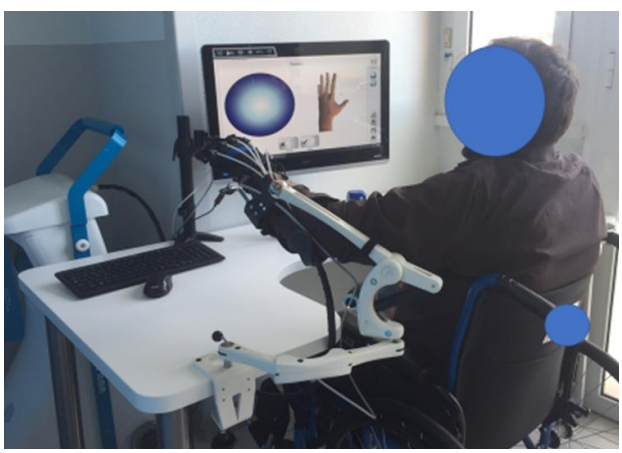

Fig. 1. *Gloreha Sinfonia® system.*

Fig. 2. *Gloreha Sinfonia® Glove.*

The software of Gloreha Sinfonia is modular and can work according to three main modalities: passive treatment (the device moves fingers); active assisted treatment (the patient starts moving fingers as much as he/she can and then the robot completes the task); bilateral treatment (patients wear the sensorized glove on the healthy hand which drives the passive mobilization of the motorized glove on the impaired hand). The system records both pre-treatments set up data and treatment results, returning a graph output, allowing real time monitoring of motor performance.

Treatment protocol

Group A underwent 20 consecutive daily sessions of treatment lasting 40 minutes each (from Monday to Friday). Each session consisted in the following exercises: 8 minutes of object grasping; 8 minutes of water pouring; 8 minutes of cubes stacking; 8 minutes of tridigital grip; 8 minutes of opening and closing of the hand. During active treatment, sensors installed on each glove finger recognized active movements, returning assistance only in case of need. Group B underwent 20 consecutive daily sessions of treatment lasting 40 minutes each (from Monday to Friday). Each session consisted in the following exercises: 7 minutes passive flexion and extension of each single finger; 7 minutes of passive counting (from 1 to 5); 7 minutes of passive opposition of the thumb to the other fingers (from the second to the fifth); 7 minutes of opening

and closing the hand with a wave movement; 7 minutes of opening and closing the hand; 5 minutes of random flexion and extension of each finger.

Statistical analysis

Since not all parameters passed the normality test (Shapiro-Wilk test $\alpha \geq 0.05$) and due to the small sample size, nonparametric methods were applied. The differences between baseline (T0), end of hand rehabilitation program (T1) and follow-up (T2) were analyzed by a Friedman's Analysis of Variance performed on within-subject factors at T0, T1 and T2. In case of significance, post hoc comparisons were done using the Wilcoxon signed ranks test. The level of significance was set at $p < 0.05$.

RESULTS

Thirteen chronic stroke subjects satisfied eligibility criteria and were enrolled. Flow chart enrollment is provided in Fig. 3. Sample demographic and anthropometric characteristics are described in Table I. According to their ability to actively extend wrist of 20 degrees, 6 subjects were assigned to group A, the other 7 subjects to group B. Baseline features of the two groups are described in Table II and Table III.

Response to treatment

Outcome measures for Group A at T1 showed statistically significant improvements in: FMA-UE shoulder/elbow section (p=0.03); MP scale total score (p=0.03); MP hand closure (p=0.02); MP wrist dorsiflexion (p=0.014); MI pinch grip (p=0.02); MAS total score (p=0.04) (Table II). Outcome measures for Group A at T2 showed statistically significant improvements in: MP total score (p=0.03); MP wrist dorsiflexion (P=0.03); MP palmar flexion (p=0.05); MI pinch grip (p=0.04) (Table II). Outcome measures for Group B at T1 showed statistically significant improvements in: FMA-UE total score (P=0.01); FMA-UE shoulder/elbow (p=0.02); FMA-UE wrist (p=0.01); MP scale total score (p=0.01); MP hand

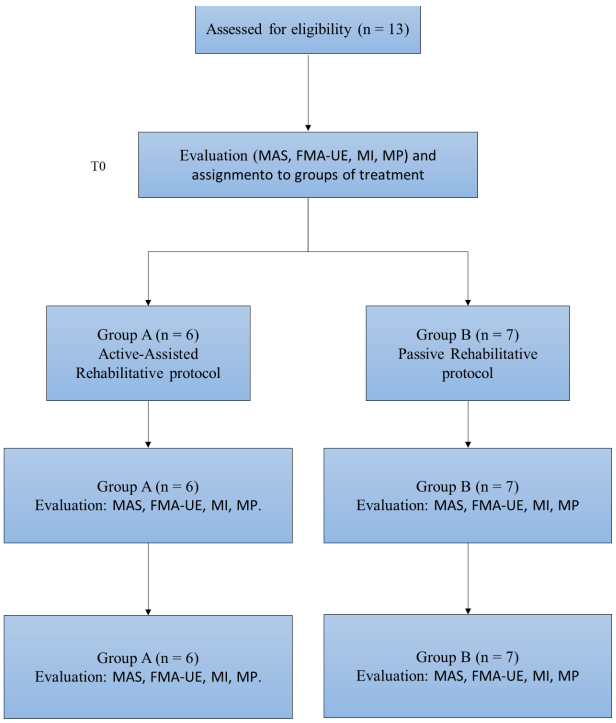

Fig. 3. *Participant flow diagram.*

Table I. *Descriptive data.*

	Active assistive group (n = 6)	Passive Group (n = 7)
Participants		
Gender, n males (%)	4 (67)	2 (29)
Age *(yr)*, mean ± SD	55.00 ± 13.15	60.00 ± 11.45
Type of stroke, n ischemic (%)	4 (67)	7 (100)
Side Affected, n right (%)	1 (17)	2 (29)
Months from stroke, mean ± SD	44.83 ± 31.51	110.00 ± 102.82

Table II. *Within active assisted group results.*

Outcomes	Pre-Treatment (T0)	Post-Treatment (T1)	1 Month Follow Up (T2)	Friedmann test (p)
Fugl-Meyer Assessment Upper Extremity (FMA-UE)				
Total, score ± SD	41.17 ± 5.15	47.33 ± 5.50	43.00 ± 8.53	0.61
Shoulder/Elbow section, score ± SD	27.50 ± 1.22	31.67 ± 1.63*	28.67 ± 3.61	**0.01**
Wrist section, score ± SD	13.67 ± 4.84	15.67 ± 4.37	14.33 ± 6.15	0.43
Motor Power (MP)				
Total, score ± SD	9.00 ± 4.94	13.00 ± 4.15*	12.33 ± 5.13*	**0.00**
Hand opening, score ± SD	2.00 ± 1.55	3.00 ± 1.41	2.83 ± 1.47	**0.04**
Hand closure, score ± SD	2.83 ± 1.17	4.00 ± 0.89*	3.67 ± 1.21	**0.01**
Wrist dorsiflexion score ± SD	1.83 ± 0.98	2.83 ± 0.98*	2.83 ± 1.47*	**0.01**
Wrist palmar flexion, score ± SD	2.33 ± 1.51	3.17 ± 1.17	3.00 ± 1.26*	**0.04**
Modified Ashworth Scale (MAS)				
Total, score ± SD	7.67 ± 1.75	5.17 ± 6.67*	6.67 ± 3.08	**0.03**
Shoulder, score ± SD	1.17 ± 0.75	1.17 ± 0.98	1.33 ± 0.82	1.00
Elbow, score ± SD	1.17 ± 0.41	0.83 ± 0.41	1.17 ± 0.75	0.44
Wrist, score ± SD	1.67 ± 0.82	0.83 ± 0.75	1.33 ± 0.82	0.07
Fingers, score ± SD	1.83 ± 0.75	1.17 ± 0.41	1.50 ± 0.55	0.07
Forearm supination, score ± SD	1.83 ± 0.75	1.17 ± 0.75	1.33 ± 1.03	0.19
Motricity Index (MI)				
Pinch grip, score ± SD	21.17 ± 2.79	27.17 ± 2.86*	25.33 ± 4.72*	**0.00**
Elbow flexion, score ± SD	24.00 ± 2.45	26.33 ± 3.27	25.00 ± 0.00	0.67
Shoulder abduction, score ± SD	24.00 ± 2.45	24.00 ± 2.45	24.00 ± 2.45	1.00
Total arm, score ± SD	71.50 ± 4.81	77.50 ± 3.21	74.33 ± 3.14	0.07

**Wilcoxon test for paired samples compared to pre-treatment results: p<0.05.*

Table III. *Within passive group results.*

Outcomes	Pre-Treatment (T0)	Post-Treatment (T1)	1 Month Follow Up (T2)	Friedmann test (p)
Fugl-Meyer Assessment Upper Extremity (FMA-UE)				
Total, score ± SD	16.57 ± 6.70	22.00 ± 9.70*	22.14 ± 7.10*	**0.00**
Shoulder/Elbow section, score ± SD	15.14 ± 5.37	18.71 ± 8.32*	19.29 ± 6.65*	**0.00**
Wrist section, score ± SD	1.43 ± 2.15	3.29 ± 2.21*	2.86 ± 1.46*	**0.00**
Motor Power (MP)				
Total, score ± SD	3.29 ± 5.25	6.14 ± 5.46*	6.00 ± 5.42*	**0.00**
Hand opening, score ± SD	0.29 ± 0.76	1.43 ± 0.79*	1.43 ± 0.79*	**0.00**
Hand closure, score ± SD	1.43 ± 1.13	2.86 ± 1.46*	2.71 ± 1.38*	**0.00**
Wrist dorsiflexion score ± SD	0.86 ± 1.86	1.00 ± 1.83	1.00 ± 1.83	1.00
Wrist palmar flexion, score ± SD	0.71 ± 1.89	0.86 ± 1.86	0.86 ± 1.86	1.00
Modified Ashworth Scale (MAS)				
Total, score ± SD	9.14 ± 1.57	5.43 ± 1.72*	6.86 ± 2.67	**0.01**
Shoulder, score ± SD	1.57 ± 0.53	1.14 ± 0.38	1.29 ± 0.49	0.22
Elbow, score ± SD	1.86 ± 0.69	1.14 ± 0.69*	1.43 ± 0.79	**0.03**
Wrist, score ± SD	1.86 ± 0.69	1.29 ± 0.76	1.43 ± 0.98	0.30
Fingers, score ± SD	2.00 ± 0.58	1.14 ± 0.38*	1.43 ± 0.53	**0.02**
Forearm supination, score ± SD	1.86 ± 0.38	0.86 ± 0.38*	1.29 ± 0.76*	**0.00**
Motricity Index (MI)				
Total arm, score ± SD	33.14 ± 16.56	41.43 ± 23.09	34.14 ± 17.63	0.40
Pinch grip, score ± SD	3.14 ± 5.37	9.00 ± 9.31	3.14 ± 5.37	0.22
Elbow flexion, score ± SD	15.86 ± 8.55	15.86 ± 8.55	16.00 ± 9.63	1.00
Shoulder abduction, score ± SD	13.43 ± 6.37	15.86 ± 8.55	15.00 ± 7.75	0.33

**Wilcoxon test for paired samples compared to pre-treatment results: p<0.05.*

opening (p=0.01); MP hand closure (p=0.01); MAS total score (p=0.01); MAS elbow (p=0.03); MAS fingers (p=0.01); MAS supination (p=0.01) (Table III).

Outcome measures for Group B at T2 showed statistically significant improvements in: FMA-UE total score (p=0.02); FMA-UE shoulder/elbow (p=0.02); FMA-UE wrist (p=0.02); MP scale total score (p=0.02); MP hand opening (p=0.01); MP hand closure (p=0.02); MAS supination (p=0.05) (Table III).

DISCUSSION

Previous studies conducted on chronic stroke subjects with hand impairment, treated by means of Gloreha®, highlighted improvements in local muscle perfusion, spasticity, heaviness and stiffness of the hand (22, 23). No study investigated the efficacy of Gloreha® in motor recovery in chronic stroke patients and, at the time of the studies, Gloreha® Sinfonia was not yet commercialized, therefore passive treatment was the only possible treatment strategy. Other authors already observed that a rehabilitative treatment delivered by a robotic device, even if intensive, should not offer less treatment options than a traditional one delivered by a physiotherapist and that robotic devices should, on the contrary, be equally or more effective (21).

Zan Yue et al. in a recent review about hand rehabilitation robotic devices in post-stroke motor recovery highlighted the importance of assessing the basal conditions of treated subjects before deciding the treatment strategy and the device to be used (16). Muscular condition (atonia/spasticity), distance from stroke (acute/subacute/chronic) and stroke level (mild/severe) are relevant conditions to be considered when using a robot (16). For these reasons, we decided to assess baseline spasticity to exclude unsuitable subjects for Gloreha glove and adopted a clinical criterion to assign patients to different groups of treatment according to baseline impairment severity. Gloreha Sinfonia ®, on the other hand, overcomes the previous limitation of the exclusively passive treatment, since both passive and active assisted treatment are now available, and treatment can be adapted according to hand impairment severity. As expected, results of our study show that, in both severely impaired and moderately impaired subjects, Gloreha Sinfonia® improves spasticity, as already observed in studies conducted on chronic stroke subjects (22).

Results derived from clinical examination quantified by means of FMA-UE, MI and MP showed consistent and significant motor performance improvements in both groups. We suppose that, as already hypothesized by Gobbo M. in 2017 (20), reduction in spasticity due to robotic treatment favors active motion recovery. For these reasons more severely impaired subjects (Group B), presenting with higher MAS score at baseline, benefited from Gloreha® passive treatment, presenting motor function improvement likely due to the reduction of spasticity. We believe that the passive modality of treatment delivered by Gloreha® could normalize muscle tone, releasing the hand and opening the way to muscle recovery and motor learning.

Less severely impaired subjects also benefited from Gloreha Sinfonia® treatment and showed improvements in motor recovery. We believe that in this group of patients the association of an intensive, repetitive, task-oriented, assisted-as-much-as-needed treatment with visual feedback, in accordance with the action-observation-therapy principles, resulted particularly effective. Gloreha Sinfonia® infact, offers a complex modality of human-robot interaction, containing several different patterns of motor induction, which can be resumed in a “task-specific induction” with real-life objects (for example grasping a bottle and picking up blocks), a “mirroring-induction”, since the patient observes an avatar of his hand performing the same tasks on the screen. Explicit visual and auditory cues (for example counting during finger flexion) could also contribute to attention capture.

Kwakkel et. al in review of literature about the effects of robot-assisted therapy on upper limb motor recovery in 2008 emphasized that to date there is no certainty about the efficacy of robots in improving ability of performing ADLs (17). We cannot assert that Gloreha Sinfonia® can improve ability in ADLs performance, however it offers some exercises based on daily life scenarios. Extending Gloreha Sinfonia

® software with other more complex exercises could be a useful solution also for patients with mild severity hand impairment.

As already observed in previous studies, also in our study Gloreha Sinfonia® device confirmed feasibility and safety, since patients well tolerated therapy, no adverse events were registered and all subjects completed treatment (17). Treatment was easy to deliver and not demanding, nor time-consuming for physiotherapists, which suggests a possible future employment of this robot in clinical daily routine. However, a randomized clinical trial, comparing treatment delivered by means of Gloreha Sinfonia® robot with a standardized and fully replicable protocol of exercises, should be performed in order to assess if this robotic treatment is equally or more effective than traditional treatment in a population of chronic stroke patients, which should be stratified according to impairment severity. Future studies should also concentrate on the effects of this robotic therapy with kinematic analysis to distinguish between therapy-induced recovery and apparent recovery due to compensation strategies.

Gloreha Sinfonia® is a possible answer to the request for a suitable robot for hand rehabilitative treatment of chronic stroke subjects and our results show that it favors motor recovery. Further randomized controlled trials with larger samples and a longer-term follow up are needed to confirm our results.

REFERENCES

1. Warlow CP, Dennis MS, Van Gijn J. et al. Stroke: A Practical Guide to Management. Arch Neurol 2002; 59(3):485-6.
2. Sacco S, Stracci F, Cerone D. et al. Epidemiology of stroke in Italy. Vol. 6, International Journal of Stroke. SAGE PublicationsSage UK: London, England 2011; 6(3):219-27 doi:10.1111/j.1747-4949.2011.00594.x.
3. Gensini GF. Stroke prevention and educational awareness diffusion. Ictus cerebrale: linee guida italiane di prevenzione e trattamento 2005.
4. Desrosiers J, Malouin F, Bourbonnais D et. al Arm and leg impairments and disabilities after stroke rehabilitation: Relation to handicap. Clin Rehabil. 2003; 17(6):666-73
5. Franceschini M, La Porta F, Agosti M et al. Is health-related-quality of life of stroke patients influenced by neurological impairments at one year after stroke? Eur J Phys Rehabil Med 2010; 46(3):389-99.
6. Nichols-Larsen DS, Clark PC, Zeringue A et al. Factors Influencing Stroke Survivors' Quality of Life During Subacute Recovery. Stroke 2005; 36(7):1480-4.
7. Raghavan P. Upper Limb Motor Impairment After Stroke. Phys Med Rehabil Clin N Am 2015; 26(4):599-610.
8. Gustus A, Stillfried G, Visser J et al. Human hand modelling: kinematics, dynamics, applications. Biol Cybern 2012; (106):741-55.
9. Santello M, Flanders M, Soechting JF. Postural Hand Synergies for Tool Use. J Neurosci 1998; 18(23):10105-15 doi:10.1523/JNEUROSCI.18-23-10105.1998.
10. Schieber MH. Muscular Production of lndividuated Extrinsic Finger Muscles Finger Movements. J Neurosci 1995; 15(1):284-97
11. Feys H, De Weerdt W, Verbeke G et al. Early and Repetitive Stimulation of the Arm Can Substantially Improve the Long-Term Outcome after Stroke: A 5-Year Follow-up Study of a Randomized Trial. Stroke. 2004; 35(4):924-9.
12. Klamroth-Marganska V, Blanco J, Campen K et al. Three-dimensional, task-specific robot therapy of the arm after stroke: a multicentre, parallel-group randomised trial. Lancet Neurol 2014; 13(2):159-66.
13. Lo AC, Guarino PD, Richards LG et al. Robot-assisted therapy for long-term upper-limb impairment after stroke. N Engl J Med. 2010; 362(19):1772-83.
14. Kwakkel G, Kollen BJ, Krebs HI. Effects of robot-assisted therapy on upper limb recovery after stroke: a systematic review. Neurorehabil Neural Repair. 2008; 22(2):111-21
15. Scotto di Luzio F, Simonetti D, Cordella F et al. Bio-Cooperative Approach for the Human-in-the-Loop Control of an End-Effector Rehabilitation Robot. Front Neurorobot 2018; 12:67.
16. Yue Z, Zhang X, Wang J. Hand Rehabilitation Robotics on Poststroke Motor Recovery. Vol. 2017, Behavioural Neurology 2017; 1-20.
17. Bernocchi P, Mulè C, Vanoglio F et al. Home-based

hand rehabilitation with a robotic glove in hemiplegic patients after stroke: a pilot feasibility study. Top Stroke Rehabil. 2018; 25(2):114-9
18. Villafañe JH, Taveggia G, Galeri S et al. Efficacy of Short-Term Robot-Assisted Rehabilitation in Patients With Hand Paralysis After Stroke: A Randomized Clinical Trial. Hand (N Y) 2018; 13(1):95-102
19. Borboni A, Villafañe JH, Mullè C et al. Robot-Assisted Rehabilitation of Hand Paralysis After Stroke Reduces Wrist Edema and Pain: A Prospective Clinical Trial. J Manipulative Physiol Ther 2017; 40:21-30.
20. Gobbo M, Gaffurini P, Vacchi L et al. Hand Passive Mobilization Performed with Robotic Assistance: Acute Effects on Upper Limb Perfusion and Spasticity in Stroke Survivors. Biomed Res Int 2017; 2017:1-6
21. Vanoglio F, Bernocchi P, Mulè C et al. Feasibility and efficacy of a robotic device for hand rehabilitation in hemiplegic stroke patients: a randomized pilot controlled study. Clin Rehabil 2017; 31(3):351-60
22. Bissolotti L, Villafañe JH, Gaffurini P et al. Changes in skeletal muscle perfusion and spasticity in patients with poststroke hemiparesis treated by robotic assistance (Gloreha) of the hand. J Phys Ther Sci 2016; 28(3):769-73
23. Varalta V, Picelli A, Fonte C et al. Effects of contralesional robot-assisted hand training in patients with unilateral spatial neglect following stroke: A case series study. J Neuroeng Rehabil 2014; 11(1):160.

Use of wearable systems for the detection of chest-abdominal wall movement aimed at respiratory monitoring in sport: a scoping review on available data

S. Miccinilli[1,2], E. Schena[3], C. Massaroni[3], M. Bravi[1], F. Campiglia[1], F. Santacaterina[1], C. Foti[4], F. Bressi[1] and S. Sterzi[1]

[1]Physical Medicine and Rehabilitation Department, Campus Bio-Medico University of Rome, Italy; [2]PhD Student in Research Doctorate in Tissue Engineering and Remodeling Biotechnologies For Body Function, Tor Vergata University, Rome, Italy; [3]Unit of Measurements and Biomedical Instrumentation, Department of Engineering, Campus Bio-Medico University, Rome, Italy; [4]Clinical Sciences and Translational Medicine Department; Research Doctorate in Tissue Engineering And Remodeling Biotechnologies For Body Function, Tor Vergata University, Rome, Italy

There is a significant request for wearable systems for vital signs and athletic performance monitoring during sport practice, both in professional and non-professional fields. Respiratory rate is a rather neglected parameter in this field, but several studies show that it is a strong marker of physical exertion. The aim of the present scoping review is to evaluate the number and kind of existing studies on wearable technologies for the analysis of the chest wall movement for respiratory monitoring in sport and fitness. The review included studies investigating the use of contact-based wearable techniques for the detection of chest wall movement for respiratory monitoring during professional or amateur sport, during fitness and physical activity. The search was conducted on PubMed/Medline, Scopus and Google Scholar electronic databases using keywords. Data extracted were entered into a Microsoft Excel spreadsheet by the leading author and then double-checked by the second author. A total of 25 descriptive studies met the inclusion criteria. Few studies on small number of athletes were found, technologies were often evaluated without a reference system, data on participants are sometimes missing. To date, we are not able to draw conclusions on which is the best and most reliable device to use during sport practice.

Over the last few decades, a significant development of wearable systems for monitoring of vital signs and physiological functions was witnessed in sports field (1, 2). Athletes and professional sporting teams require, in fact, an assessment and monitoring of physiological parameters for proper planning of intensity and volume of training and are constantly looking for tools to improve athletic performance and to obtain a competitive advantage (3). Despite the current technological effort, literature shows that the simultaneous measurement, integration and analysis of time-motion, biomechanics and physiological variables is still a fairly unexplored field, which only recently, thanks to the development of wearable and miniaturized intelligent sensors, received the due attention. Smart wearable devices consist of sensors inserted into clothing or of accessories that can be worn (4). Wearability is particularly important in sports field since by means of wearable systems is possible the continuous, personalized, and real time monitoring of patients' parameters under physiological conditions and in any environment (5-6).

Key words: sport; wearable systems, respiratory monitoring, chest wall movement detection

Corresponding Author:
Dr Sandra Miccinilli,
Università Campus Bio-Medico,
Via Alvaro del Portillo 21,
Rome, Italy
Fax: 39 0622541602
e-mail: s.miccinilli@unicampus.it

0393-974X (2020)

The importance of respiratory monitoring in sport and fitness

Commonly, vital signs and functions evaluated during sport performance include heart rate, respiratory rate, blood pressure, body temperature, calories burned, steps count, sleep pattern, and so on. Among these, respiratory rate (RR) can be considered, according to literature, a rather neglected parameter (7). There is, in fact, a wide range of wearable sensors that can measure RR (8); however, this is not a commonly monitored parameter during training. RR is usually monitored to estimate the ventilation threshold during incremental exercise (9). However, further information can be obtained from RR. In fact, there is a strong association between RR and variables that can influence physical performance, such as muscle fatigue, hypoxia, and glycogen depletion (10-12). This suggests that RR is a strong marker of physical exertion (7).

Respiratory monitoring technologies classification

RR can be assessed in different ways. Technologies for breathing monitoring and RR measurement are classified in contact-based and contactless (8, 13). Contact-based measurement techniques, where the sensor is in direct contact with body surface, can be classified depending on the characteristics of the sensor, the body positioning and the physical quantity measured by the sensor (8). Contact less techniques include those that can detect air flows, respiratory sounds, air temperature, air humidity, air components, cardiac activity modulation and chest wall movements. Chest wall movements sensors can be furtherly classified according to the kind of sensor, into deformation sensors, impedance sensors and motion sensors (13).

Traditional techniques and gold standards for breathing monitoring through chest wall movements

Currently, optoelectronic plethysmography (OEP) represents the gold standard for the detection of respiratory parameters through chest wall movements (14). This method can accurately and non-invasively measure chest-abdominal wall's volume and consequently evaluate patient's ventilation. The system was developed at the Bioengineering Department of the Politecnico di Milano University (15, 16). It is based on the motion analysis of reflective markers placed in precise landmarks on the patient's trunk. The three-dimensional position of each marker is measured by an automatic optoelectronic motion analyzer using infrared video cameras. The enclosed volume is then calculated by connecting the points to form triangles.

OEP can be used to study chest wall movements both in healthy subjects during exercise and in patients with chronic obstructive pulmonary disease, neuromuscular disorders and in intensive care units. The limitation of the method, however, is that it requires a structured and dedicated environment, such as a motion analysis laboratory, in which it is not always possible, to study the mechanics of breathing in dynamic conditions, such as during sports performance. Hence the need to use wearable systems.

Why is it important to do this review?

Since there is a growing interest for vital and functional parameters monitoring during sport and since the importance of RR was already demonstrated, a review on wearable systems for the detection of chest-abdominal wall movement described in literature is needed. To date, in fact, there are no clear indications for the use of respiratory monitoring systems in sport activities.

Objectives

The main purpose of this paper is to provide a scoping review to evaluate the number and kind of existing studies on wearable technologies for the analysis of the chest wall movement for respiratory monitoring in sport and fitness.

Search strategy (search methods for identification of studies/ electronic searches)

A search of scientific studies concerning wearable technologies for respiratory monitoring in sport and fitness was performed in PubMed/Medline, Scopus and Google Scholar electronic databases. The following keywords were used: "Hexoskin; Lifeshirt; Zephyr BioHarness; Learn Inspire Free Entertain (L.I.F.E.); Equivital LifeMonitor EQ02; Wearable AND Respiratory AND Sport; Sensor

AND Respiratory AND Sport; Wearable Resistive Sensor AND Respiratory; Wearable Capacitive Sensor AND Respiratory; Wearable Inductive Sensor AND Respiratory; Wearable Fiber Optic Sensor AND Respiratory; Wearable Impedance Sensor AND Respiratory; Wearable Accelerometer Sensor AND Respiratory; Wearable Gyroscope Sensor AND Respiratory; Wearable Magnetometer Sensor AND Respiratory".

Data collection and analysis - eligibility criteria

All included studies investigated the use of contact-based wearable techniques for the detection of chest wall movement for respiratory monitoring during professional or amateur sport, during fitness and physical activity. Exclusion criteria were studies about the use of wearable contact-based techniques not assessing respiratory parameters; studies about the use of wearable contact-based techniques for respiratory monitoring not detecting chest wall movement; studies about contactless techniques for respiratory monitoring. No language restriction was applied, however, articles not in English were not examined due to linguistic barriers. No limits neither for time, nor for status of publication, nor for length of follow up were applied to the search, since a limited number of studies was expected to be found.

Information sources

The last search was conducted on the 30th of June 2020.

Study selection (selection of studies)

Two authors independently analyzed the titles, the abstracts and the full-text articles respectively emerged from the literature search, to determine eligibility for their inclusion. Inclusion criteria were applied to relevant studies. A consensus method based on discussion was used to solve differences in opinions concerning inclusion of studies. Studies not meeting inclusion criteria were excluded since potentially biased.

Data extraction and synthesis - data charting

After reading the full text article of each included study, data extracted were entered into a Microsoft Excel spread sheet by the leading author. Data collection included: first author and publication year, title, study typology, technology used, kind of sensor used, presence of a reference system, number and kind of participants, male and female participants, objective of the study, analyzed parameters and kind of sport activity during measurements, technology results in terms of reliability and of accuracy, any limit in the study. These extracted data were arranged in a tabular form and then double-checked by the second author. All authors discussed together the relevance of findings and results.

Evidence synthesis - search results

The four consulted databases yielded 670 records, 25 of which met the selection criteria. The study selection process is outlined in Fig. 1.

The search conducted on techniques based on strain measurement methods, produced 20 results. Six of the 20 studies were related to techniques using capacitive sensors and all of them regarded the use of the technology "Zephir Bio-Harness" (17-22). Eleven of the 20 studies were related to techniques using inductive sensors. Seven of the studies about inductive sensors were about the technology "Hexoskin" (23-29), one was about the technology "Equivital Lifemonitor EQ02" (30) one was about the technology "Lifeshirt" (31), and one about the technology "New Respiratory Inductive Plethysmography" (32). One of the 20 studies was related to the use of a smart garment with fiber optic sensors (33) and 3 to the use of smart garments using piezoresistive sensors (34-36).

The search conducted on techniques based on movement measurements produced 5 results. One of these was related to the use of accelerometers (37), two for the use of a combination accelerometers and gyroscopes (38, 39), one for the combination of accelerometers and ECG signals (40) and 1 to the use of magnetometers (41). The search did not produce any study about the use of Transtoracic Impedance Sensors. Respiratory parameters registered in included studies were: RR, average RR, maximal RR, Tidal Volume (TV), minute ventilation, respiratory volume, ventilation, median RR, minute TV, inspiratory time and expiratory time.

All studies investigated RR, with exception for

Mc Cool 2002 (41). Minute ventilation was measured by Hexoskin (24, 28, 29) and Lifeshirt (31), TV was measured by Hexoskin (26), New Respiratory Inductive Plethysmograhy (32) and magnetometers (41); inspiratory and expiratory time were measured by New Respiratory Inductive Plethysmograhy (32) and magnetometers (41), expiratory time was also measured by Lifeshirt (31). Only 18 out of the 25 studies compared wearable systems to reference ones. Table I describes reported results.

A total number of 484 subjects were analyzed throughout all the included studies, 429 of which were healthy subjects, 55 of which were athletes. Seven studies (19, 22, 26, 28, 30, 38, 41) did not report the sex of enrolled subjects, therefore, as far as we know, 152 male healthy subjects and 11 male athletes were enrolled, whereas 104 female healthy subjects and 22 female athletes were enrolled (Table II).

Respiratory parameters were evaluated during different physical activities, described, and reported in Table III. Only 7 out of the 25 descriptive studies analyzed subjects in a competition context, in real training programs and during sport practice (19-23, 33, 34).

Table I. *Results*

	SENSOR	TECHNOLOGY	NUMBER OF STUDIES	STUDYES VS REFERENCE SYSTEM	MEASURED PARAMETERS	FINAL AUTHORS' JUDJMENT ON TECHNOLOGY
STRAIN MEASUREMENTS	Capacitive	Zephir Bio-Harness	6	2	RR	No significant differences between ZBH and reference systems for the FR, both under laboratory and in real life conditions.
	Inductive	Hexoskin	7	5	average RR, maximal RR, TV, minute ventilation, respiratory volume	Poor reliability of Hexoskin for respiratory data monitoring in real-life setting, especially during maximal exercise.
		Equivital Lifemonitor Eq02	1	1	RR	The system can provide a complete physiological monitoring under laboratory conditions.
		Lifeshirt	1	–	ventilation, RR, expiratory time	Good reliability and validity of LIfeshirt compared to the reference system under laboratory conditions.
		New Respiratory Inductive Plethysmograhy	1	1	Median one minute TV, inspiratory time, expiratory time	The study showed good concordance between NRIP and the reference system at rest and during mild to moderate physical activity under laboratory conditions.
	Fiber Optic	Smart Garment	1	1	RR	Good performance in measuring respiratory frequency and heart rate compared to the reference system, both under laboratory and in real life conditions.
	Resistive	Smart Garment/ sensors in contact with the chest and abdomen	3	3	RR, TV	Good accuracy of RR measurement at rest and during physical exercise, under laboratory conditions, but less accuracy of tidal volume measurement. One study also in real environment.
MOVEMENT MEASUREMENTS	Accelerometers	sensors in contact with the chest and abdomen	1	1	RR	Good accuracy of RR measurement during various body activities under laboratory conditions.
	Gyroscopes+ Accelerometers	sensors in contact with the chest and abdomen	2	2	RR	Good accuracy of RR measurement during aerobic exercise under laboratory conditions.
	Accelerometers+Ecg	Smart garment	1	1	RR	Good accuracy of RR measurement during various activities under laboratory conditions.
	Magnetometers	sensors in contact with the chest and abdomen	1	1	TV, inspiratory time, expiratory time	Good accuracy under laboratory conditions.
IMPEDANCE MEASUREMENT	Transtoracic Impedance Sensor		0	-	-	

Table II. *Population*

Healthy Subjects= 429 subjects		**Elite Athletes**=55 subjects	
Male	**Female**	**Male**	**Female**
152	104	11	22
Total unknown sex=173		Total unknown sex=22	
Total number=486 subjects			

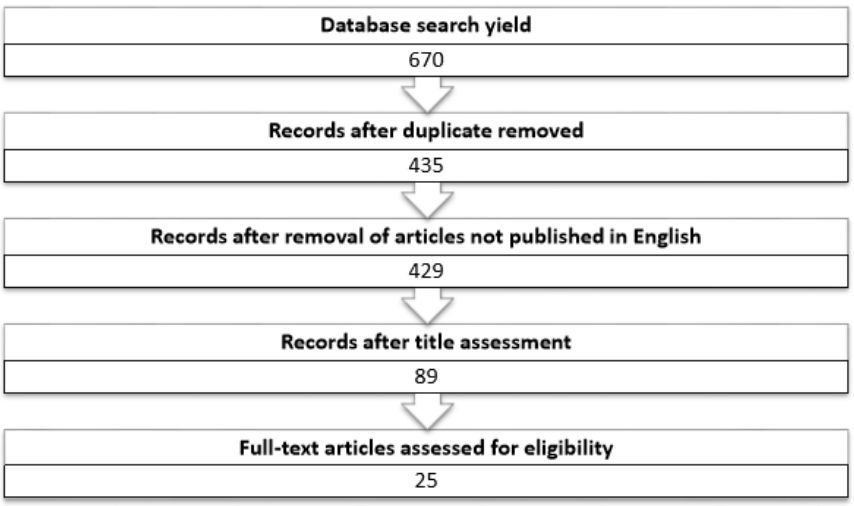

Fig. 1. *The study selection process.*

Authors reached different final judgments about used devices. Studies investigating Zephir Bio-Harness showed no significant differences between the system and the reference system for the RR, both under laboratory conditions and in real world conditions (17-22). Studies investigating Hexoskin showed less reliability of the device for respiratory data monitoring in real-life setting, especially during maximal exercise and heat (23-29). A single study investigating Equivital Lifemonitor Eq02 concluded that the device can provide a complete physiological monitoring under laboratory conditions (30).

A single study investigating Lifeshirt demonstrated good reliability and validity of Lifeshirt in measuring respiratory parameters compared to the reference system under laboratory conditions (31). A single study investigating New Respiratory Inductive Plethysmograhy showed good concordance between the reference system at rest and during mild to moderate physical activity under laboratory conditions (32). A single study investigating a fiber optic smart garment showed good performance compared to the reference system, both under laboratory and in real life conditions (33).

Studies conducted with resistive smart garments or sensors showed good accuracy of RR measurement at rest and during physical exercise under laboratory conditions, but less accuracy of tidal volume measurement (34-36). A single study investigating the use of accelerometers showed good accuracy of RR measurement during various body activities under laboratory conditions (37). Studies investigating the combined use of accelerometers and gyroscopes demonstrated a good accuracy of RR measurement during aerobic exercise under laboratory conditions (38, 39). A single study on magnetometers showed good accuracy of RR measurement during various activities under laboratory conditions (41). Results are resumed in Table I.

DISCUSSION

This study aimed at gaining information from literature about the use in sports and fitness of technologies for the detection of respiratory parameters. Given the vastness of the topic and the countless types of existing technologies and sensors, our research focused on contact-based technologies and, in the context of these, in particular on systems based on the detection of chest wall and abdomen movements. Confirming what previously stated by Nicolò in 2017 (7) and by other authors even before (42-43), there are not many studies focusing on the detection of the RR in sports. Reviews on wearable technologies used in sport found in literature, in fact, do not address this topic or only marginally deal with it, reflecting the poor interest in the study of respiratory performance during sport practice (3, 44).

Moreover, the spread of easily accessible wearable technologies, led to great expenditure and investments in the field of pedometers and technologies for calculation of energy consumption (3, 44). Market reasons have often prevailed over the need to develop accurate and targeted technologies that could be reliable and useful to monitor athletic performance. In addition to the poor interest for RR, reasons for

Table III. *Main physical activities described in studies.*

Activity	ZBH	HSK	LS	RIP	EQV	FO	RES	ACC	GYROS
Mild physical exercise			+		+		+		
Incremental exercise test at cycloergometer		+					+	++	
Parabolic flight and parachute jumps							+		
Walking and running activities on a treadmill	+	++					++	+++	+
Graded exercise up to VO2 max and sustained exercise (also in a hot environment)	+	+							
Taekwondoo fights	+								
mCAFT test	+								
Incremental treadmill test	+	+	+					+	
Constant work rate test			+						
Training programs in soccer female players	++								
Aerial skills, basketball crossfit, fitness, tennis, Zumba, middle distance running	+								
Running	++							+	
Intense running	+								
bounding	+								
jumps	+								
Trail hiking		+							
Maximal aerobic cycle ergometer test in elite cyclists		+							
Walking on the spot				+					
Trail run		+							
High intensity functional training		+							
Shooting sessions in archery						+			
Aerobic exercise								+	+

the poor development of this kind of technologies can also be found in the difficulty in carrying out an accurate analysis of the respiratory system in dynamic conditions, such as during sport practice.

The common gold standard systems, such as spirometry, pneumotacography and optoelectronic plethysmography are not suitable in sport context since they need structured environments and devoted laboratories. These technologies often require mouthpieces or bulky instruments that cannot be used during a real performance, but only under test conditions. To this end, bio-medical research is focusing on the development of wearable technologies that can be used in real contexts and during athletic performances. Our search in literature resulted difficult and probably produced only a part of the existing results. Study titles, in fact, often do not recall in the text the name or the kind of technology or sensor used or the word "sport". For this reason, keywords used for this search, necessarily included commercial names of some known technologies (7). A study included in our search discuss the technological characteristics of the system, the development of mathematical algorithms for the extrapolation of data, but little attention is often reserved to the validation of the techniques compared to gold standard reference systems on a sufficiently large number of subjects. Studies on real professional athletes are few, on very small samples and, in most cases, concern already commercialized technologies. In most cases, devices are tested in a laboratory setting, not during real sport performance. Many variables, such as heat and sweat, which influence adherence of sensors and smart garments to the skin during athletic performance, during test conditions, are therefore neglected in the general judgment of the technique. Many studies do not accurately describe the study population and differentiate between female and male subjects.

In our opinion this information is essential because wearability and, therefore, reliability of the devices are influenced by anatomical characteristics of subjects, which are different between male and females. Capacitive and inductive systems are, to date, the most widespread and tested devices. Commercial devices based on these technologies are already existing and used in sports field. Capacitive systems, such as Zephir Bio-Harness can measure RR, whereas inductive systems, can also measure other parameters such as TV, minute ventilation, respiratory volume, inspiratory and expiratory time. However, among inductive systems, commercial devices, such as Hexoskin, suffer from poor reliability in respiratory data monitoring and recording in real-life situations, especially during maximal exercise. Smart garments integrating fiber optic or resistive sensors, accelerometers, magnetometers, and gyroscopes are generally described by authors as reliable. However, studies regarding these kinds of smart garments are very few.

Accelerometers are used to derive breathing rate by measuring movements of the chest wall, however, they suffer from motion artefacts and their use in dynamic conditions can result difficult. For this reason, accelerometers are often coupled with gyroscopes or magnetometers to gain better results. According to what we found in literature, we are not able, at the moment, to draw conclusions about which is the best and most reliable device to use during sport practice and to express preference on which kind of technology to use during different kind of sports.

REFERENCES

1. Khan Y, Ostfeld A E, Lochner C, et al. Monitoring of vital signs with flexible and wearable medical devices. Adv Mater 2016; 28(22):4373-95.
2. Dias D, Cunha J P S. Wearable health devices-vital sign monitoring, systems and technologies. Sensors (Basel) 2018; 18(8):2414.
3. Aroganam G, Manivannan N, Harrison D. Review on wearable technology sensors used in consumer sport applications. Sensors (Basel) 2019; 19(9):1983.
4. Naghmeh N, Waidah B I, Abbas M, et al. A comprehensive overview of smart wearables: The state of the art literature, recent advances, and future challenges. Eng Appl Artif Intel 2020; 90:103529.
5. Peake JM, Kerr G, Sullivan JP. A Critical Review of Consumer Wearables, Mobile Applications, and Equipment for Providing Biofeedback, Monitoring

Stress, and Sleep in Physically Active Populations. Front Physiol 2018; 9:743.
6. Aliverti A. Wearable technology: role in respiratory health and disease. Breathe (Sheff) 2017; 13(2):e27-e36.
7. Nicolò A, Massaroni C, Louis Passfield L. Respiratory Frequency during Exercise: The Neglected Physiological Measure. Front Physiol 2017; 8:922.
8. Massaroni C, Nicolò A, Lo Presti D, et al. Contact-Based Methods for Measuring Respiratory Rate. Sensors (Basel) 2019; 19(4):908.
9. Carey D G, Hughes J, Raymond R, et al. The respiratory rate as a marker for the ventilatory threshold: Comparison to other ventilatory parameters. J Exerc Physiol Online 2005; 8(2):30-38.
10. Davies R C, Rowlands A V, Poole D C, et al. Eccentric exercise-induced muscle damage dissociates the lactate and gas exchange thresholds. J Sports Sci 2011; 29(2):181-9.
11. Busse M W, Maassen N, Konrad H. Relation between plasma K+ and ventilation during incremental exercise after glycogen depletion and repletion in man. J Physiol 1991; 443:469-76.
12. Voduc N, Webb K A, D'Arsigny C, et al. McArdle's disease presenting as unexplained dyspnea in a young woman. Can Respir J 2004; 11(2):163-7.
13. Massaroni C, Lo Presti D, Formica D, et al. Non-Contact Monitoring of Breathing Pattern and Respiratory Rate via RGB Signal Measurement. Sensors (Basel) 2019; 19(12):2758.
14. Romagnoli I, Lanini B, Binazzi B, et al. Optoelectronic plethysmography has improved our knowledge of respiratory physiology and pathophysiology. Sensors (Basel) 2008; 8(12):7951-72.
15. Cala SJ, Kenyon CM, Ferrigno G, et al. Chest wall and lung volume estimation by optical reflectance motion analysis. J Appl Physiol 1996; 81(6):2680-9.
16. Aliverti A, Dellacà R, Pedotti A. Optoelectronic plethysmography: a new tool in respiratory medicine. Recenti Prog Med 2001; 92(11):644-7.
17. Kim J-H, Roberge R, Powell J B, et al. Measurement Accuracy of Heart Rate and Respiratory Rate during Graded Exercise and Sustained Exercise in the Heat Using the Zephyr BioHarnessTM. Int J Sports Med 2013; 34(6):497-501.
18. Janowski M, Zieliński J, Kusy K. Exercise Response to Real Combat in Elite Taekwondo Athletes Before and After Competition Rule Changes. J Strength Cond Res 2019; 1.
19. Hailstone J, Kilding A.E. Reliability and Validity of the Zephyr™ BioHarnessTM to Measure Respiratory Responses to Exercise. Meas Phys Educ Exerc Sci 2011; 15(4):293-300.
20. Ravindranathan S, Ardakani HD, Pimental A, et al. Performance monitoring of soccer players using physiological signals and predictive analytics. MFPT 2017.
21. Sbrollini A, Morettini M, Maranesi E, et al. Sport Database: Cardiorespiratory Data Acquired through Wearable Sensors While Practicing Sports. Data Brief 2019; 27:104793.
22. Zadeh A, Taylor D, Bertsos M et al. Predicting Sports Injuries with Wearable Technology and Data Analysis. Inf Syst Front 2020.
23. Montes J, Stone TM, Manning JW, et al. Using Hexoskin Wearable Technology to Obtain Body Metrics in a Trail Hiking. Int J Exerc Sci 2015; 8(4):425-30.
24. Montes J, Young JC, Tandy R, et al. Reliability and Validation of the Hexoskin Wearable Bio-Collection Device During Walking Conditions. Int J Exerc Sci 2018; 11(7):806-16.
25. Elliot CA, Hamlin MJ, Lizamore CA. Validity and Reliability of the Hexoskin Wearable Biometric Vest During Maximal Aerobic Power Testing in Elite Cyclists. J Strength Cond Res 2019; 33(5):1437-44.
26. Smith CM, Chillrud SN, Jack DW, et al. Laboratory Validation of Hexoskin Biometric Shirt at Rest, Submaximal Exercise, and Maximal Exercise While Riding a Stationary Bicycle. J Occup Environ Med 2019; 61(4):104-11.
27. Feito Y, Moriarty TA, Mangine G, et al. The use of a smart-textile garment during high-intensity functional training: a pilot study. J Sports Med Phys Fitness 2019; 59(6):947-54.
28. Tanner E A, Montes J, Manning J W, et al. Validation of Hexoskin Biometric Shirt to COSMED K4 B2 Metabolic Unit in Adults during Trail Running. Sports Technology 2015; 8(3-4):118-23.
29. Villar R, Beltrame T, Hughson RL. Validation of the Hexoskin Wearable Vest during Lying, Sitting,

Standing, and Walking Activities.Appl Physiol Nutr Metab 2015; 40(10):1019-24.
30. Liu G-Z, Guo Y-W, Zhu Q-S, Huang B-Y, et al. Estimation of Respiration Rate from Three-Dimensional Acceleration Data Based on Body Sensor Network. Telemed J E Health 2011; 17(9):705-11.
31. Kent L, O'Neill B, Davison G, et al. Validity and Reliability of Cardiorespiratory Measurements Recorded by the LifeShirt during Exercise Tests. Respir Physiol Neurobiol 2009; 167(2):162-67.
32. Retory Y, Niedzialkowski P, de Picciotto C et al. New Respiratory Inductive Plethysmography (RIP) Method for Evaluating Ventilatory Adaptation during Mild Physical Activities. PLoS One 2016; 11(3):e0151983.
33. Lo Presti D, Romano C, Massaroni C, et al. Cardio-Respiratory Monitoring in Archery Using a Smart Textile Based on Flexible Fiber Bragg Grating Sensors. Sensors (Basel) 2019; 19(16):3581.
34. Di Rienzo M, Rizzo F, Meriggi P, et al. Applications of a Textile-Based Wearable System for Vital Signs Monitoring. Conf Proc IEEE Eng Med Biol Soc. 2006; 2006:2223-6.
35. Massaroni C, Di Tocco J, Bravi M, et al. Respiratory Monitoring During Physical Activities with a Multi-Sensor Smart Garment and Related Algorithms. IEEE SENS J 2020; 20(4):2173-80.
36. Chu M, Nguyen T, Pandey V, et al. Respiration Rate and Volume Measurements Using Wearable Strain Sensors. NPJ Digit Med 2019; 2(1):8.
37. Liu Y, Zhu SH, Wang GH, et al. Validity and Reliability of Multiparameter Physiological Measurements Recorded by the Equivital Lifemonitor During Activities of Various Intensities. J Occup Environ Hyg 2013; 10(2):78-85.
38. Yoon J-W, Noh Y-S, Kwon Y-S, et al. Improvement of Dynamic Respiration Monitoring Through Sensor Fusion of Accelerometer and Gyro-Sensor. J Electr Eng Technol 2014; 9(1):334-43.
39. Karacocuk G, Höflinger F; Zhang R, et al. Inertial Sensor-Based Respiration Analysis. IEEE Trans Instrum Meas 2019; 68(11):4268-75.
40. Lepine NN, Tajima T, Ogasawara T, et al. Robust respiration rate estimation using adaptive Kalman filtering with textile ECG sensor and accelerometer. Conf Proc IEEE Eng Med Biol Soc 2016; 2016:3797-800.
41. McCool FD, Wang J, Ebi KL. Tidal Volume and Respiratory Timing Derived from a Portable Ventilation Monitor. Chest 2002; 122(2):684-91.
42. Cheng A C, Black J F, Buising, K L. Respiratory rate: the neglected vital sign. Med J Aust 2008; 189(9):531.
43. Cretikos MA, Bellomo R, Hillman K, et al. Respiratory rate: the neglected vital sign. Med J Aust. 2008; 188(11):657-9.
44. Peake J M, Kerr G, Sullivan J P. A Critical Review of Consumer Wearables, Mobile Applications, and Equipment for Providing Biofeedback, Monitoring Stress, and Sleep in Physically Active Populations. Front Physiol. 2018; 9:743.

Non-implantable bone conduction device for hearing loss: a systematic review

A. Moffa[1,2], L. Giorgi[3], M. Cassano[2], V. Rinaldi[1], A. Natalizia[1], F. Bressi[4], E. Guglielmelli[3] and M. Casale[1]

[1]Unit of Integrated Therapies in Otolaryngology, Campus Bio-Medico University, Rome, Italy; [2]Unit of Otolaryngology, University of Foggia, Foggia, Italy; [3]Research Unit of Advanced Robotics and Human-Centered Technologies, Campus Bio-Medico University of Rome, Italy; [4]Unit of Physical Medicine and Rehabilitation, Campus Bio-Medico University of Rome, Italy

There are different treatment options that employ a bone conduction transmission of the sound, for different types of hearing loss, as well as hearing aids, medical intervention via prostheses and surgically implanted medical devices. A middle ear disease causes a decline in the conductive mechanism of hearing. The current possibilities of compensating Conductive Hearing Loss (CHL) solutions include both surgical and no surgical Bone Conduction Devices (BCDs). Due to the invasiveness of the implantable devices and their specific requirements in terms of the temporal bone anatomy, non-implantable BCDs are in some cases preferred in the clinical routine. The goal of this review is to investigate the beneficial effects and safety of non-implantable BC devices, analysing the different type of solutions found so far. A systematic review was performed to identify all the clinical studies evaluating the use of non-invasive BCDs. A qualitative analysis based on data extracted was conducted. From 37 articles, 11 prospective studies and 1 retrospective study were selected for a full analysis, for a total of 173 patients from 4- to 77-years-old. Eight of these studies included adult patients, while the other four are paediatric studies. All the studies analyse non-implantable BCDs commonly used in case of CHL, sensorineural HL and single side deafness. Three of them analyse an adhesive device, six compare the adhesive device with a sound processor mounted on a support fitted on the head, one compare it also with an implant, one analyse the sound processor mounted on different type of support, and one compare different type of sound processor. All the studies showed advantages from the use of non-invasive BCDs, both on adults and children. The non-invasive BCDs analysed in this review show good results both from the audiological and subjective point of view and could be considered a safe and effective solution for patients suffering from conductive hearing loss, sensorineural hearing loss or single-side deafness. More studies are required to confirm these promising results.

The WHO reported that around 466 million people worldwide (34 million children) suffer from disabling Hearing Loss (HL), defined as HL greater than 40 dB in the better hearing ear in adults and 30 dB in the better hearing ear in children. Advances in medicine and technology have led to many new treatment options for all different types as well as severities of hearing aids, medical intervention via prostheses and surgically implanted medical devices such as cochlear, middle ear, or as currently reviewed, bone conduction implants (1). While most patients with moderate

Key words: BC, hearing aid, hearing loss, eyeglasses hearing aid, adhesive hearing aid

Corresponding Author:
Dr Antonio Moffa,
Integrated Therapies in Otolaryngology,
Campus Bio-Medico University,
Via Álvaro del Portillo 21, 00128 Roma, Italy
Tel.: 39 06.22.54.11
e-mail address: a.moffa@unicampus.it

0393-974X (2020)

to severe HL can be supplied with conventional hearing aids, some patients either do not benefit enough from hearing aids or cannot wear them due to anatomical or skin-related issues. When a middle ear disease is present, it initially causes a decline in the conductive mechanism of hearing, as shown by the presence of a mild-to-moderate air-bone gap in pure tone audiometry. Although this type of HL is less disabling than purely sensorineural hearing loss, a conductive loss that affects both ears can also compromise communication skills and quality of life. The most frequent permanent causes of Conductive HL (CHL) are related to Chronic Otitis Media (COM) with or without cholesteatoma, ear malformations, otosclerosis and adhesive process. Current possibilities of compensating CHL solutions include both surgical and no surgical Bone Conduction Devices (BCDs). Surgically implanted direct-drive BCDs, either percutaneous or active transcutaneous, provide the best hearing rehabilitation, because they are directly fixed to the skull (2). Moreover, because of the size of the transducer, these implants have more specific requirements in terms of the temporal bone anatomy, which reduces the number of potential users.

Non-implantable BCDs transmit the sound to the inner ear with direct conduction through the bone, bypassing external and middle ear. Typically, non-implantable BCD allows a more natural perception of the sound with less distortion and whistle when compared to traditional air conduction hearing aids. This device guarantees a better speech comprehension and sound localization in noisy environment. These hearing aids are located outside the ear, leaving the hearing channel free for a better comfort, and helping to reduce problems due to chronic ear infections or allergies that can limit its use (3, 4, 5). The indications for this system are patients with unified or bilateral CHL or Single Sided Deafness (SSD), without any age limitations. Thereafter, considering technological innovations in sound processors, the initial indications have been extended to mild/moderate forms of mixed HL, with bone conduction threshold levels of 35 dB or better.

MATERIALS AND METHODS

For the first time, a review was conducted on the only non-implantable BCDs described in the literature for the HL treatment. This work helps to provide a clearer picture of the effects of the interventions, as well as assisting clinicians in forming their opinions and giving recommendations. The study was performed according to the Preferred Reporting Items for Systematic Reviews and
Meta-Analyses (PRISMA) guidelines (6).

Data source and study searching

An electronic search was performed on PubMed/MEDLINE and Google Scholar. An example of a search strategy is the one used for PubMed/MEDLINE: “bone conduction”, “hearing aid”, “bone conduction device”, “eyeglasses”, “adhesive device”, “not implantable”, “softband”, “headband”, “hearing loss”, “single side deafness”, “contralateral routing of sound system”, “speech perception in noise”, “sound localization”, “quality of life”. The other searches were adjusted to fit the specific requirements for each database. Then, a cross-reference search of the included studies was performed to minimize the risk of missing relevant data. The last research was run in April 2020.

Inclusion/exclusion criteria

The selection of the studies was based on clinical studies of non-implantable BC devices, made both on adult and paediatric patients affected by different types of hearing loss, for example different type of CHL, SHL and SSD. Exclusions criteria were studies not in English, reviews, conference abstracts, letters and studies with unclear and/or incomplete data. Moreover, clinical studies on the use of implantable devices, except if compared to non-implantable ones, were excluded from this review.

Data extraction and data analysis

All articles were initially screened by title and abstract, then the full-text version of each publication was assessed and those whose content was judged not to be strictly related to the subject of this review, were excluded. Data extraction of the studies included the population demographics and baseline characteristics, details on intervention and control conditions, study

designs, outcomes, and time of measurement as well as risk estimates.

Statistical analysis and summary of findings

It was not possible to perform the intended statistical analysis and summary of findings as described in our protocol, due to heterogenic reporting style and lack of data in individual studies included in this review. Thus, the effect on individual outcomes and overall quality assessment were solely narratively described. Available data in the retrospective studies were used. Authors of the included studies were not contacted for further information.

RESULTS

Search criteria returned 37 articles, which were reduced to 20 after the removal of irrelevant articles and duplicates. These were screened and further 8 were excluded, resulting in 12 articles fulfilling criteria for inclusion in this review. The flow diagram shown in Fig. 1 (PRISMA Flow Diagram) depicts the selection process. All the original articles included were prospective studies, except for one retrospective case-control study. Eight of these studies included adult patients, while the other four are paediatric studies. The population in the included studies consisted of 173 patients aged 4 to 77 years. The baseline characteristics of these studies are reported in Table I, while a further description of the studies conducted in the reports can be found in Table II.

Primary outcomes

Dahm V. et al evaluated the hearing benefit, advantages, and disadvantages in twelve patients suffered from CHL for at least 3 months, using ADHEAR, an adhesive device. Results of the Freiburg monosyllables word test and the mean speech recognition threshold (SRT) in quiet, show a statistically significant difference between the unaided and aided condition. Contrary, for the masking-noise situation, OlSa revealed a not statistically significant improvement of the SRT

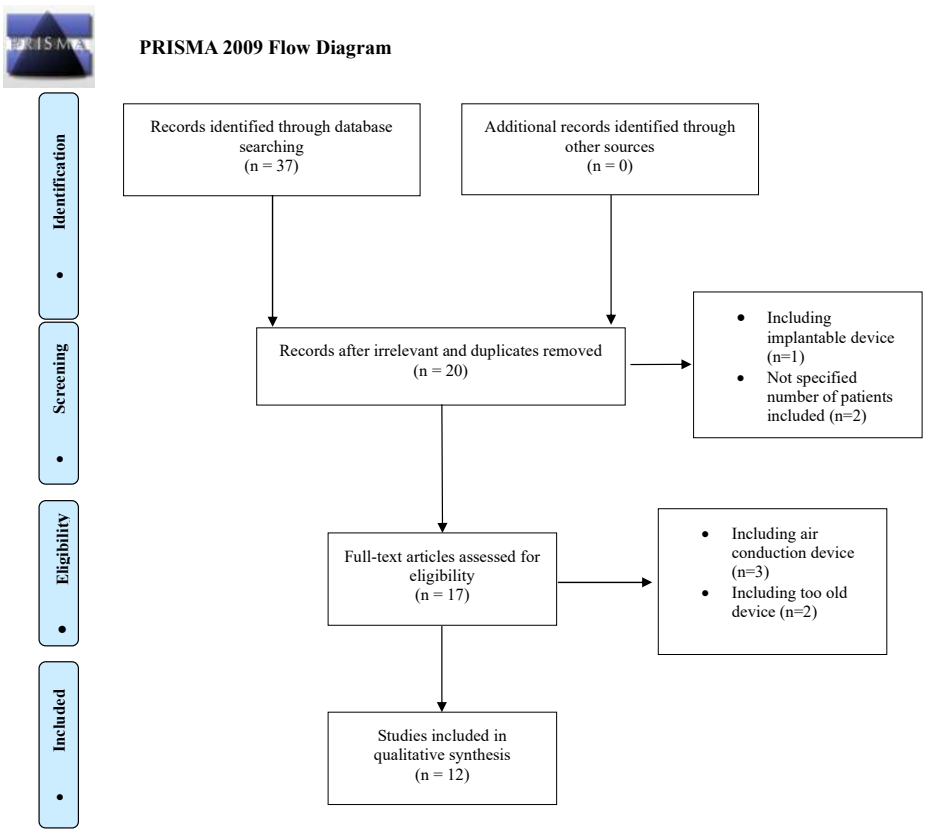

Fig. 1. *Flowchart outlining the paper selection process of the systematic review (based on PRISMA guidelines). PRISMA indicates preferred reporting items for systematic review and meta-analyses.*

Table I. *General characterizes of included studies.*

Authors	Type of study	N. partecipants	Control	Sex (M/F)	Mean age (range)	Type of deafness	Follow-up	Abbreviations
Dahm V et al. 2018	Prospective	12	8 of 12 of the partecipants done additional measurment with Contact Mini	(5/7)	44±30	Chronic otitis media (n=8). Otosclerosis (n=1). Middle ear malformation (n=1). Chronic external otitis (n=1). Persistent traumatic eardrum perforation (n=1).	2 weeks	-
Dahm V et al. 2019	Academic, prospective, randomized cross-over trial	13	-	(3/10)	37.5±25.5	Unilateral CHL (n=10), bilateral CHL (n=3): Canal wall down (n=3), chronic otitis media (n=6), external auditory canal stenosis (n=1), atresia (n=3)	4 weeks	-
Faber H.T. et al. 2012	Retrospective case-control study	30	-	(18/12)	48±29	SSD	from 2 to 73 weeks	SSD = single side deafness
Favoreel A. et al. 2019	Prospective study with repeated-measure design	10	Each subject serves as its own control	(4/6)	10.5±6.5	Uni or bilateral CHL: CHL due to a congenital malformation of the pinna and/or ear canal (n=7), CHL due to a tympanic perforation (n=3), CHL in combination with tympanosclerosis (n=2). Six out of ten subjects had previous experience with a bone-anchored hearing aid.	3 weeks	CHL=CHL
Gawliczek T. et al. 2018	Prospective nonrandomized crossover study	15	-	(9/6)	26.5±7.5	Induced bilateral CHL	1 session	-
Gawliczek T. et al. 2018	Prospective	15	-	(9/6)	26±8	Simulated bilateral CHL	1 session	-
Moteki H. et al 2019	Prospective	9	-	(6/3)	43.5±25.5	Hearing loss due to: bilateral middle ear anomaly (n=1), bilateral aural atresia (n=3), unilateral aural atresia (n=2), and single-sided deafness (n=3)	3 months	-
Neumann et al. 2019	Prospective study with a single-subject, repeated-measure design	11	Each subject serves as its own control	(7/4)	5.2±4.5	CHL: bi- (n=1) and unilateral (n=8) aural atresia, one of the latter combined with a malformed contralateral middle ear, or frequently discharging ears (n=1)	8 weeks	-

Osborne M.S. et al 2019	A prospective, single-subject, repeat measure, cohort study	21	Each subject serves as its own control	(10/11)	9.5±4.5	CHL: unilateral (n=20), bilateral (n=1) and congenital (n=14), acquired (n=7)	From 4 to 12 weeks	CHL=CHL
Skarzynski P.H. et al. 2019	Prospective	10	Each subject serves as its own control	(5/5)	40.5±24.5	The main etiologies for the CHL were cholesteatoma, chronic otitis media, and congenital malformations of the outer or middle ear.	1 session	CHL=CHL
Urík M et al. 2019	Prospective	17	-	(11/6)	12±7	Bilateral CHL (n=5). Unilateral CHL (n=6). Unilateral SHL (n=6).	2 weeks	CHL=CHL SHL=SHL
Weiss R. et al. 2019	Prospective, single-subject, reapeted-measure study	10	-	(6/4)	41.5±20.5	Underwent middle ear surgery with transient hearing loss due to auditory canal tamponade.	3 weeks	-

in the aided condition compared to the unaided condition (7). The next year, Dahm V, with another research group, compared the average daily wearing time of a Contact Mini processor mounted on a softband with ADHEAR. This study involved 13 subjects between 12- and 63-years-old with CHL that were fitted all with both devices. The results show a statistically significant difference concerning the daily usage, while there was no statistically significant audiological difference between the two devices. Comparing the two devices in this study, audiologic assessment of aided sound field thresholds, WRS, and SRT in quiet and in noise showed no statistically significant differences (8).

About the ADHEAR system, also Favoreel A. et al. evaluated the audiological benefit of this device in ten of children (4-17 years old) with CHL during a short-term exposure of three weeks and compared it to a BCD on a softband. The children achieved significant audiological improvement with the ADHEAR immediately after the first attachment, with no acclimatization time, and this remained stable over a time period of three weeks (9). Moreover, Gawliczek et al. studied the audiological benefit of the ADHEAR system in subjects with induced bilateral CHL, to evaluate the additional benefit of bilateral fitting compared with unilateral fitting and to compare the outcomes with BC devices attached to a softband (BAHA 5 sound processor). For the sound field thresholds and the speech understanding in quiet and in noise, no statistically significant differences between the devices or between treatment conditions were found. For the sound localization a statistically significant difference of approximately 7 degrees ($p=0.043$) was observed between ADHEAR and BAHA in the bilateral treatment conditions (3).

Neumann et al. also evaluated the audiological and clinical outcome of the ADHEAR system, comparing it with conventional BCDSs (BAHA 5 sound processor) in a short- and mid-term follow-up in ten children under 10 years old. As a result, this system significantly improved the functional hearing gain and speech perception in quiet and noise in paediatric patients with CHL due to aural atresia or chronic otitis media with discharging ears (2). A similar study was conducted by Osborne et al. assessing the audiological effectiveness of the ADHEAR system when compared with the child's unaided thresholds and those obtained with a BC hearing aid worn on a softband. Twenty-one children aged between 5 and 15 years old with a CHL were enrolled. The results of paired test analysis of the

Table II. *Summary of studies specifically involving the use of non-implantable BCDs.*

Authors	Device	Description of the device	Type of management	Audiometric result	Patient satisfaction	Abbreviation
Dahm V et al. 2018	ADHEAR. Contact Mini.	ADHEAR: attached to the hairless skin behind the ear. It functions by the connection of two components, the audio processor (AP) and the adhesive adapter (AA). The single-use, water resistant AA is placed behind the auricle in the mastoid area and remains there for 3–7 days. The AP is then connected via the snap connector on the AA, and transfers vibrations to the inner ear without applying pressure. CONTACT MINI: digital miniature BC system that does not required surgery. It can be incorporated into a wide range of headpieces and hair bands.	A sound field audiometry. Freiburg monosyllables word test. Oldenburg sentence test. SSQ12. AQoL-8D.	Average aided threshold = 30.8 dB HL (±7.1 SD), unaided threshold = 45.1 dB HL (±7.0 SD) with the adhesive BCD. Freiburg monosyllables word test in the unaided condition: mean WRS = 29% at 65 dB SPL (±25 SD) and 40% at 70 dB SPL (±26 SD). In the aided condition: mean WRS = 59% at 65 dB SPL (±30 SD) and 68% at 70 dB SPL (±27 SD). SRT in quiet = 56.8 dB SPL (±6.1 SD). SRT in quiet aided = 44.5 dB SPL (±6.4 SD). Masking-noise situation: OlSa: SRT = -1.2 dB (±0.9 SD) in the aided condition. SRT = -0.4 dB (2.1 SD) in the unaided condition.	First visit: mean SSQ12 = 4.4(±1.6 SD), mean AQoL-8D = 0.75 (±0.17 SD).After 2 weeks: mean SSQ12 = 6.1 (±2.5 SD), mean AQoL-8D = 0.88 (±0.14 SD).	SSQ = Speech, Spatial, and Qualities of Hearing OlSa = Oldenburg sentence test AQoL = Assessment of Quality of Life SRT = speech recognition threshold. WRS = word recognition score
Dahm V et al. 2019	ADHEAR. Contact Mini.	ADHEAR: attached to the hairless skin behind the ear. It functions by the connection of two components, the audio processor (AP) and the adhesive adapter (AA). The single-use, water resistant AA is placed behind the auricle in the mastoid area and remains there for 3–7 days. The AP is then connected via the snap connector on the AA, and transfers vibrations to the inner ear without applying pressure. CONTACT MINI: digital miniature BC system that does not required surgery. It can be incorporated into a wide range of headpieces and hair bands.	At the first visit: pure-tone thresholds, SSQ12 and AQoL-8D. After 2 weeks wearing the first device: sound field measurements, Freiburg monosyllables word test, and OlSa in quiet and in noise. Tests carried out in aided and unaided conditions. SSQ12 and AQoL-8D. After 2 further weeks with the second device: same tests.	Median average aided thresholds: with adhear = 35dB HL, with BCD = 30 dB HL. Median average functional hearing gain: with adhear = 17 dB, with the control device = 19 dB, Median WRS: unaided = 25.0% at 65 dB SPL and 40.0% at 70 dB SPL, with the device = 47.5% at 65 dB and 52.5% at 70 dB, OlSa: without adhear median SRT in quiet = 54.3 dB S/N . With the BCD median SRT = 41.9 dB. In noise SRT in the unaided condition = 0.4 dB S/N, In noise SRT with adhear = -0.65 dB S/N. In noise SRT in the unaided condition = 0.8dB S/N, In noise SRTwith BCD. = -0.2dB S/N	SSQ 12: statistically significant improvement for the total score as well as for the subscores with both devices compared with the baseline visit T0 (all $p<0.001$). Only for the qualities subscore, the improvement with the adhesive BCD compared with the conventional BCD was statistically significant ($p<0.039$). AQoL-8D: statistically significant improvement with both devices compared with T0 ($p<0.001$ in both cases).	SSQ = Speech, Spatial, and Qualities of Hearing OlSa = Oldenburg sentence test AQoL = Assessment of Quality of Life SRT = speech recognition threshold WRS = word recognition score
Faber H.T. et al. 2012	BAHA Intenso. BAHA Classic. BAHA Divino.	The Baha Intenso: is a BC sound processor and the most powerful of our head worn devices. Baha Divino: offers an advanced elaboration of the digital sound ensuring the best amplification possible. The Baha Divino directional system guarantees an execellent signal to noise ratio in noisy enviroment.	Air and BC threasholds. Questionnaires: APHAB GHABP SSD questionnaire SSQ. After the trial patients were divided into two groups: BCD+ and BCD-	Mean air conduction threshold: BCD+=31.2 dB. BCD- = 16.9 dB. Mean bone-conduction threshold: BCD+ = 22.4 dB. BCD- = 9.7 dB.	Satisfied with the BCD headband: BCD+ = 8 patients (57%), BCD- = 3 (19%). Dissatisfied with the BCD headband but chose a BCD: BCD+ = 4(29%). Conversation in noisy environments: no significant difference between groups. Almost always able to understand a conversation with 1 person in a noisy environment: BCD- = 10 (63%), BCD+ = 2 (14%).	APHAB = Abbreviated Profile of Hearing Aid Benefit GHABP = Glasgow Hearing Aid Benefit Profile SSQ = Speech Spatial Qualities of Hearing scale BCD+ = opt for BC device BCD- = do not opt for BCD

Favoreel A. et al. 2019	ADHEAR. BAHA on softband	ADHEAR: attached to the hairless skin behind the ear. It functions by the connection of two components, the audio processor (AP) and the adhesive adapter (AA). The single-use, water resistant AA is placed behind the auricle in the mastoid area and remains there for 3–7 days. The AP is then connected via the snap connector on the AA, and transfers vibrations to the inner ear without applying pressure. BAHA 5 on softband: the BAHA 5 is a processor of bone-anchored hearing aid attached to an elastic headband	First visit: pure tone air- and BC thresholds, free field audiometry and free field SPIQ tests in the following conditions: unaided, aided with the ADHEAR and aided with the BCHA on a softband. Second visit (3 weeks): free field audiometry and free field SPIQ tests with the ADHEAR	Free field threashold: unaided = 50 dB HL. Mean BIAP: first visit: adhear = 28 dB HL (18.6–37.7), BCHA = 26 dB HL (21.6–31.2), second visit: adhear = 28 dB (20.0–36.5). Speech audiometry in quiet: mean SRT: first visit: adhear = 19 dB (10.3–28.1), BCHA =21 dB (12.6–29.4). second visit: adhear = 47dB SPL (41.9-51.5)	SSQ12: mean unaided = 4.9 (4.1–5.8), adhear = 7.3 (6.7–7.8). Speech understanding in noise and in multiple streams: mean unaided = 4.7 (3.8–5.7), adhear = 7.3 (6.4–8.1). Sound localization: unaided = 4.9 (3.8–6.1), adhear = 7.0 (6.1–7.9). Quality scale: unaided = 5.1 (3.8–6.4), adhear = 7.5 (6.7–8.3).	SPIQ = Speech in Quiet Testing BIAP = Bureau International d'Audiophonologie SRT= speech recognition threshold
Gawliczek T. et al. 2018	ADHEAR. BAHA 5 softband.	ADHEAR: attached to the hairless skin behind the ear. It functions by the connection of two components, the audio processor (AP) and the adhesive adapter (AA). The single-use, water resistant AA is placed behind the auricle in the mastoid area and remains there for 3–7 days. The AP is then connected via the snap connector on the AA, and transfers vibrations to the inner ear without applying pressure. BAHA 5 on softband: the BAHA 5 is a processor of bone-anchored hearing aid attached to an elastic headband	Sound field thresholds, speech understanding in quiet and in multinoise were assessed in unaided, unilateral, and bilateral treatment conditions. Sound localization was evaluated in uni- and bilateral treatment conditions.	Sound field threasholds: unilateral: Adhear = 24.3±5.2dB HL, Baha = 24.1±3.7dB HL, bilateral: Adhear = 22.1±4.4dB HL, Baha = 23.8±3.4dB HL. Speech understanding in quiet: WRS at 50dB unilateral: Adhear = 68%, Baha = 77%, WRS at 50dB bilateral: Adhear = 77%, Baha = 81%, WRS at 65dB unilateral: Adhear = 49%, Baha = 51%, WRS at 65dB bilateral: Adhear = 52%, Baha = 52%. SRT: unilateral: Adhear = 35.9±4.6dB SPL, Baha = 34.2±3.3dB SPL, bilateral: Adhear = 33.2±4.1dB SPL, Baha = 34.4±3.0dB SPL. Speech understanding in noise: differences between Adhear and Baha were not statistically significant. Sound localization: difference of 7 degrees (p=0.043) observed between Adhear and Baha in the bilateral treatment conditions.	-	AP = audio processor AA = adhesive adapter SRT = speech recognition threshold. WRS = word recognition score
Gawliczek T. et al. 2018	Baha SoundArc	Is a flexible titanium bow to be worn behind the head, rather than around the head. Similar to the headband and the softband, a disk supporting the sound processor is attached to the side of the device.	Soundfield thresholds, speech understanding in quiet and in noise, and sound localization were measured in unaided conditions and with 1 or 2 Baha 5 sound processors mounted on either a softband or a SoundArc device.	Sound field threasholds: Softband: unilateral = 24.8dB, bilateral = 25.1dB, SoundArc: unilateral = 23.6dB, bilateral = 24.0dB. SRT in quiet: Softband: unilateral = 21.7dB, bilateral = 21.5dB, SoundArc: unilateral = 19.5dB, bilateral = 20.3dB	-	SRT = speech recognition threshold

Moteki H. et al 2019	ADHEAR	ADHEAR: attached to the hairless skin behind the ear. It functions by the connection of two components, the audio processor (AP) and the adhesive adapter (AA). The single-use, water resistant AA is placed behind the auricle in the mastoid area and remains there for 3–7 days. The AP is then connected via the snap connector on the AA, and transfers vibrations to the inner ear without applying pressure.	Free-field audiometry, speech perception tests in quiet and noise, and sound localization tests were carried out prior and at 1 and 3 months after the start of ADHEAR use. at 60–80 dB. The subjective benefits of the ADHEAR were assessed using the SSQ, administered before applying the ADHEAR device and at 1–3 months after application.	Hearing thresholds and functional gain: CHL subgroup: average pure tone threshold: AC = 69 dBHL, BC = 15 dBHL. sensorineural SSD subgroup: average threshold: AC = 102 dBHL, BC for the healthy ear = 17 dBHL. With ADHEAR: CHL = 36.5 dB, SSD = 45.0 dB Speech perception in noise: S0Nnormal ear condition at SN0: unaided = 52%, aided = 59%, S0Nnormal ear condition at SN: unaided = 19%, aided = 43%. Sound localization: no general tendencies among the variations related to the type of hearing loss could be extracted.	SSQ: mean score: unaided: speech = 7.6, spatial hearing =-8.6, perceptive hearing = 11.0, aided: speech =21.7, spatian hearing = 17.8, perceptive hearing = 18.7. For the sensorineural SSD: unaided: speech = 1.3, spatial hearing =-29.9, perceptive hearing = 17.3, aided: speech =3.7, spatian hearing = -24.6, perceptive hearing = 25.6.	AC = air conduction BC = BC S0Nnormal = speech from the front and noise from the normal or betterhearing side SN0 = speech and noise from the front SN = signal-to-noise ratio
Neumann et al. 2019	Adhear. Baha softband	ADHEAR: attached to the hairless skin behind the ear. It functions by the connection of two components, the audio processor (AP) and the adhesive adapter (AA). The single-use, water resistant AA is placed behind the auricle in the mastoid area and remains there for 3–7 days. The AP is then connected via the snap connector on the AA, and transfers vibrations to the inner ear without applying pressure. The BAHA sound processor (BAHA 4, Contact Mini or BAHA 5) was worn on a BAHA Softband.	At T0: hearing thresholds for air and BC, sound field audiometry, speech in quiet and in noise in the unaided and aided conditions with the ADHEAR and a BCDS. At T1 (8 weeks): audiometric measurements with the ADHEAR, fill in the questionnaire SSQP (and LEAQ for children up to 24 months of age) and the ADHEAR questionnaire.	T0: Sound field threashold: unaided = 67.1 dB HL±13.2, BCDS = 50.7 dB HL±9.8, ADHEAR =38.6 dB HL ± 8.5, p=.016. Mean functional gain: ADHEAR = 35.6 dB ± 15.1, BCDS = 29.9 dB ± 14.6. WRS at 65dB in quiet: unaided = 13.8 ± 16.9%, BCDS = 86.3 ± 9.2%, adhear = 91.3 ± 11.3%. WRS in noise: unaided = 18.8 ± 22.3%, BCDS = 75.0 ± 16.9%, adhear =77.5 ± 14.9%. T1: average threshold: aided = 29.7 ± 8.3 dB HL. Functional gain: adhear = 35.8 ± 15.8 dB. WRS in quiet: unaided = 15.7 ± 17.2%, adhear = 90.0 ± 8.2%. WRS in noise: unaided = 4.0 ± 8.9%, adhear = 82.0 ± 19.2%.	Children below 2 years old (n=4): LEAQ: unaided = 20.0 ± 5.9 points, at T1 = 22.0 ± 2.9 points. The parents of 6 children completed the SSQP: unaided T0=2.9 ± 2.7 points, unaided T1 = 4.4 ± 3.1 points, adhear T1 = 7.3 ± 1.5. rated the ADHEAR system as a very valuable aid.	LEAQ = LittlEARS Auditory Questionnaire SSQP = Speech, Spatial and Qualities of Hearing Scale Questionnaire for parents WRS = word recognition score
Osborne M.S. et al 2019	ADHEAR. Ponto on softband	ADHEAR: attached to the hairless skin behind the ear. It functions by the connection of two components, the audio processor (AP) and the adhesive adapter (AA). The single-use, water resistant AA is placed behind the auricle in the mastoid area and remains there for 3–7 days. The AP is then connected via the snap connector on the AA, and transfers vibrations to the inner ear without applying pressure. Ponto on a softband: the Ponto sound processor is mounted on a softband with ready-mounted connector plates	Sound field threshold measurement performed with warble tones: unaided, softband device, ADHEAR at initial visit (V1) and after a minimum of 4 weeks continual use (W4). Complete a LAS, a GCBI and HARQ.	First visit to confirm CHL. Mean air conductions PTA4(0.5–4kHz) thresholds = 57 dBHL±11, softband = 30 dBHL±6., adhear =27dBHL±6. After 4 weeks: mean PTA4 with adhear = 26dBHL±3.	GCBI after 4 weeks = 33±25, with: emotion 24±27, physical health 20±19, learning 36±33, and vitality 24±26. Mean LAS score increased by 4.5 from 4±1.4 to 8.5±1.4 (p=0.0001)	LAS = 10 cm Linear Analogue Scale GCBI = Glasgow Children's Benefit Inventory Questionnaire HARQ = manufacturer's hearing aid review questionnaire

Skarzynski P.H. et al. 2019	ADHEAR. Baha Attract. Baha 4 on softband	ADHEAR: attached to the hairless skin behind the ear. It functions by the connection of two components, the audio processor (AP) and the adhesive adapter (AA). The single-use, water resistant AA is placed behind the auricle in the mastoid area and remains there for 3–7 days. The AP is then connected via the snap connector on the AA, and transfers vibrations to the inner ear without applying pressure. BAHA 4 on softband: the BAHA 4 is a processor of bone-anchored hearing aid attached to an elastic headband. BAHA Attract: is a passive transcutaneous hearing aid in which the sound processor connects onto a magnet to hold it in place.	Subjects were split into two groups: 5 had previously been implanted with a passive transcutaneous BC hearing aid (Baha Attract), the other 5 were provided with a Baha 4 on a softband. Both were also tested with the ADHEAR. Air and BC thresholds, thresholds in sound field and speech understanding in quiet and noise were determined in the unaided condition, with Baha Attract or Baha 4, and with ADHEAR.	Sound field audiometry: PTA4 of implant group: unaided = 58±6dB HL, Baha A. = 33±6dB HL, Adhear = 32±9dB HL. PTA4 of softband group: unaided = 47±10dB HL, Baha4 = 27±6dB HL, Adhear= 29±6dB HL. Speech understanding in quiet: WRS of implant group: unaided = 7%±16%, Baha A. = 66%±24%, Adhear = 66%±33%. WRS of softband group: Baha4 = 83%±17%, Adhear = 84%±13%. Speech understanding in noise: SRT of implant group: unaided = 2.7±5.5dB SNR, Baha A. = –5.0±1.0 dB SNR, Adhear = –3.4±2.4dB SNR. SRT of softband group: unaided = 0.4±2.5 dB SNR, Baha4 = –4.4±1.3 dB SNR, Adhear = –4.4±2.0 dB SNR.	-	SRT = speech recognition threshold WRS = word recognition score PTA = pure tone average
Urík M et al. 2019	ADHEAR	ADHEAR: attached to the hairless skin behind the ear. It functions by the connection of two components, the audio processor (AP) and the adhesive adapter (AA). The single-use, water resistant AA is placed behind the auricle in the mastoid area and remains there for 3–7 days. The AP is then connected via the snap connector on the AA, and transfers vibrations to the inner ear without applying pressure.	Hearing examined after the device was set, after 2 weeks,without the device. SSQ10. AQoL-6D.	Average value of hearing threshold: average functional gain (SNHL) = 4.54±3.81dB HL, average functional gain (CHL) = 13.3±13.88dB HL. Speech audiometry: average functional gain (SNHL) = 2.17±10.23dB HL, average functional gain (CHL) = 13.82±14.11dB HL. Speech audiometry with bubble noise: average functional gain (SNHL) = 6.33±5.28dB HL, average functional gain (CHL) = 14.91±14.10dB HL.	First visit: SSQ6 (SNHL) = 199.88 (±85.68), SSQ6 (CHL) = 215.67 (±54.45), AQoL-6D (SNHL) = 0.80 (±0.24), AQoL-6D (CHL) = 0.78 (±0.25). After 2 weeks: SSQ6 (SNHL) = 267.99 (±50.39), SSQ6 (CHL) = 261.39 (±73.02), AQoL-6D (SNHL) = 0.90 (±0.11), AQoL-6D (CHL) = 0.87 (±0.24).	SSQ = Speech, Spatial, and Qualities of Hearing AQoL = Assessment of Quality of Life
Weiss R. et al. 2019	ADHEAR	ADHEAR: attached to the hairless skin behind the ear. It functions by the connection of two components, the audio processor (AP) and the adhesive adapter (AA). The single-use, water resistant AA is placed behind the auricle in the mastoid area and remains there for 3–7 days. The AP is then connected via the snap connector on the AA, and transfers vibrations to the inner ear without applying pressure.	Postoperative unaided and aided sound-field thresholds. Speech tests in quiet and noise. SSQ12 and a system-specific quality of life questionnaire.	Day of fitting: PTA 4 = 15±2.9dB HL. After 1 week: PTA 4 = 19±7.4dB HL, WRS = 75±16.2%, SRT50 in quiet = 40±9.9dB SPL, SRT50 in noise = -6.7±2.7dB After 3 weeks: PTA 4 = 7±7dB HL and 15±11.4dB HL, WRS = 75±14.1% and 55±8.2%, SRT50 in quiet = 6±8.4dB SPL and 11±5.1dB SPL, SRT50 in noise = -5.4±1.8dB SPL and -7.5±1.6dB SPL (disintegratind and non disintegrting tamponade)	Before surgery: SSQ = 7.2±1.9. After surgery: SSQ = 5.0 ±2.4. After surgery aided: SSQ = 7.1±1.6. After 3 weeks: SSQ = 7.2±1.8	SSQ = Speech, Spatial, and Qualities of Hearing PTA = pure tone average SRT = speech recognition threshold WRS = word recognition score.

mean sound field hearing threshold showed that softband devices improved mean thresholds by 19 dB HL and the adhesive retained BC system by 26.3 dB HL after 4 weeks of use as compared to unaided tests. The mean improvement compared to softband was 5.6 dB HL at visit 1 and 7.3 dB at visit 2. A non-significant 1.7 dB improvement between visits was found with the adhesive retained BC system probably due to an acclimation effect (10).

Moteki et al. also focused on the use of the ADHEAR system applied to patients with various types of hearing loss. Nine patients aged over 18 years old were enrolled and fitted with the devices for three months. Patients showed variations according to their hearing status: for all six patients with CHL, the audiological results revealed that the adhesive BC hearing device gave adequate hearing gain and improved speech perception in noise, while no improvement was found for patients with single-sided deafness (11).

Another paediatric study was conducted by Urik et al, which evaluated the hearing benefit, advantages and disadvantages, in 17 children (11 of them suffered from CHL and 6 with unilateral SHL), using ADHEAR. The average value of hearing threshold in sound field shows a not statistically significant gain in children with SHL, while in children with CHL it is statistically significant. The same results are found measuring the average value of speech audiometry, while for the average value of speech audiometry with bubble noise both groups of children show a statistically significant gain (12). Skarzynski et al. compared the audiological performance of the ADHEAR system in patients with CHL with a BAHA Attract implant (n=5), and patients with a BC device on a softband (BAHA 4). All the subjects were also tested both with the ADHEAR and in the unaided situation, and all of them had clinically significantly better results with the Baha and ADHEAR compared with the unaided condition (5).

The last study on the ADHEAR system analysed in this review is the one made by Weiss et al. evaluating the audiological benefit and patient satisfaction with ADHEAR in patients who underwent middle ear surgery with transient hearing loss due to auditory canal tamponade in eleven adult. The overall average functional hearing gain, calculated as the mean difference between the unaided and aided sound-field audiometry (with the contralateral ear blocked) improved significantly by 15±2.9 dB HL on the day of fitting and by 19±7.4 dB HL after one week. After 3 weeks, the functional hearing gain was 7±7.0 dB HL for the disintegrating tamponade (n=5) and 15±11.4 dB HL for the non-disintegrating tamponade (n=4) (13).

A different analysis was done by Faber et al. who aimed to determine factors predicting whether patients with SSD choose a BCD for the contralateral routing of sound (CROS) after a regular trial with a BCD on a headband. Thirty patients with SSD did a trial with a BCD headband and, after at least one week, answered to four questionnaires. As a result, 47% chose a BCD after an extended BCD headband trial. Required surgery, wearing a device behind the ear, cosmetic aspects, and visibility of deafness were found as possible factors to refrain from using a BCD (14).

Lastly, Gawliczek et al. tested the audiological benefit of a current BAHA sound processor worn on a SoundArc and compared the audiological benefit with the same sound processor on a softband. In 15 normal hearing volunteers (aged 18 to 34, 6 women, 9 men) a bilateral CHL was simulated for the duration of the tests by blocking both ears with a combination of ear plugs and an additional filling of the remaining volume within the pinna with silicon mould material. The results, found after the analysis of hearing and speech understanding, show a clear improvement with a Baha mounted on either a SoundArc or a softband, compared to the unaided condition. Thus, no statistically significant audiological difference between the use of a softband and a SoundArc was found (15).

Secondary outcomes

Nine of the twelve studies included in this review also evaluated the subjective benefits of the devices they were testing. All of them included in the study the ADHEAR system. These devices proved to be a valid option for children with CHL or unilateral SHL who do not want to undertake the risk of surgery or are not capable of undergoing general anaesthesia. Moreover it could be a valuable alternative for children who only need a BC hearing aid for a

limited period (7, 12). Moteki et al. studied this device on adults and found it to be a good option for patients who could not use conventional hearing aids (11). Furthermore, for patients considering the use of surgically implanted hearing devices, the use of ADHEAR may be a preferable option for preoperative assessment due to its non-invasiveness. High level of patient satisfaction and subjective hearing improvement on adults was also found by Weiss et al. (13).

When compared with conventional BC hearing aid, such as BC mounted on softband or headband, it was found to be a valuable alternative for both children and adults with CHL (3, 9). However, Osborne et al. (10) shows that overall Glasgow Children's Benefit Inventory Questionnaire (GCBI) data indicates that the adhesive retained BC system has a benefit on quality of life with improvements in all but three individuals. There was also a negative feedback reported from a headscarf wearer on the reduction of the quality of sound. Another important result was found by Dahm V. et al. (8), who showed that the median reported wearing time of the adhesive device was 8.1 hours compared to the 4.3 hours of conventional BCD usage. A statistically significant difference was found due to the subjects reporting discomfort or pain while wearing the headband or softband.

DISCUSSION

Poor sound transmission to the inner ear can be treated with non-surgically BCDs integrated in an elastic softband or fixed on a steel-spring headband or glasses. However, there are, many problems related to the use of these devices such as discomfort and poor aesthetics, which keep children and adults from wearing them. Firstly, the major drawback is related to the constant static pressure force on the skin and skull of the wearer (2, 4, 8, 16, 17). Moreover, users often complain about sweating under the band or poor sound quality, as well as stigmatization due to its aesthetic appeal. Further disadvantages include damping of sound transmission due to hair between the contact place and skin and unreliable positioning of the transducer if it slips from its place (10). According to the most recent findings in the scientific literature, there are different types of non-implantable BCDs:

- Headband: consists of a steel spring resembling a diadem, to which a disc with a connector for a processor is attached. Headbands are often used for temporary preoperative trials but occasionally also for permanent use (7, 8, 13-15)
- Softband: elastic bands worn around the head and most frequently used in young children. Since headbands have shown to induce discomfort in children, softbands were introduced (3, 5, 8, 10, 13, 16, 18).
- SoundArc: flexible titanium bow to be worn behind the head. Similar to the headband and the softband, a disk supporting the sound processor is attached to the side of the device. This solution was proposed by Cochlear Inc, as an alternative to softband GalwSpeech. On the market there is also a similar solution proposed by Autel S.r.l, Melodi Flex (15).
- Adhesive device: consists of a BC audio processor retained on the head with an adhesive adapter placed over the mastoid process behind the auricle. The integrated transducer in the audio processor converts sound into mechanical vibrations that are transmitted via the adhesive adapter and relayed through the skin to the mastoid bone, similarly to other skin-drive solutions. Sound is transmitted via BC to the inner ear, providing a hearing impression (2, 3, 5, 7-13).

The most common sound processors on the market are the ones produced by the Cochlear, the Oticon Medical and the BHM. In particular, the Cochlear processors analysed in the studies are the BAHA 4 and BAHA 5 Sound Processor, while produced by the Oticon Medical it was considered the Ponto sound processor, and by the BHM the Contact Mini sound processor. These sound processors can be mounted on the support described (headband, softband, and soundarc), chosen by the patient as he or she preferred (2, 3, 5, 7, 8, 10, 13-15, 18).

All these systems use BC through the skin to increase hearing capabilities, but they have a limitation because of the damping effect of skin and skull. Usually, BCDs apply a lot of pressure on the head, causing discomfort if the device is worn for few hours. To overcome this pressure issue, a new

adhesive device was introduced, such as ADHEAR, produced by MED-EL (2, 3, 5, 7-13). It consists of a BC audio processor retained on the head with an adhesive adapter placed over the mastoid process behind the auricle. The integrated transducer in the audio processor converts sound into mechanical vibrations that are transmitted via the adhesive adapter and relayed through the skin to the mastoid bone, similarly to other skin-drive solutions. Sound is transmitted via BC to the inner ear, providing a hearing impression (2, 3, 5, 7-13).

Another possibility is mounting BC devices in the frame of eyeglasses (19). A receiver, inserted in the final part of the leg of the eyeglasses, transfers the vibrations produced by the sonar waves to the mastoid and then directly to the cochlea and inner ear. On the market now there are the Beta Flex Extend, produced by Autel S.r.l., La Belle Spectacle Hearing Systems of Bruckhoff, AN-Evo1 di BHM-tech, and this solution is proposed also by Amplifon S.p.a. This solution is not analysed in the studies included in this review, but it is important to underline this alternative solution, even if nowadays it is not so common in the clinical routine.

From the audiological point of view, all the studies included show comparable results testing different devices. For example, for what concern the ADHEAR system, when analysed alone compared to the unaided condition, it shows improvement both from the audiological findings and high satisfaction of the patients (11-13). But it was also compared to more traditional devices, such as different sound processor munted on softband. In particular, when compared to BAHA sound processor, Gawliczek and Skarzynski found in adults patients comparable audiological outcomes between the ADHEAR and the BAHA mounted on a softband (3, 5). Same results were found in paediatric patients by Neumann and Favoreel (2, 9). Also other devices on the market were tested compared to ADHEAR, such the Contact Mini sound processor used as a control device by Dahm and her group, and the Oticon Ponto used by Osborne (7, 8, 10).

Non-implantable BCDs seems to be a good choice for patient who cannot or would not undergo surgery, due to their non-invasiveness. It is also a good solution for patient who cannot wear air-conduction devices. Thus, the subjects mostly analysed in the studies are children for whom surgical correction is still a very challenging procedure and adults with a transient HL or preferred a non-invasive solution (20). Patients included suffered from CHL, sensorineural hearing loss (SHL) or single-side deafness (SSD).

Lastly, a big issue that these solutions want to solve is the cosmetic appearances of the hearing aid. This aspect should not be neglected because people are more inclined to wear a device not so visible from the outside (14). Therefore, the hearing aid are as small as possible, often coloured like patient's hair, or masked behind for example headband or softband that can be made of different colour and seen from the outside like a dress accessory.

All the type of hearing aids analysed in this systematic review are largely used in the clinical practice, as an efficacy solution CHL. Considering both the audiological benefits and high satisfaction of patients, non-implantable BCD could be considered a safe and effective solution for patients suffering from conductive hearing loss, sensorineural hearing loss or single-side deafness. Between the different devices described, the adhesive solution is the most common used thanks to the little size and adherence to the skin without applying too much pressure. More studies are required to confirm these promising results and to identify the best BCD, as small and performing as possible.

REFERENCES

1. Magele A, Schoerg P, Stanek B, Gradl B, Sprinzl GM. Active transcutaneous bone conduction hearing implants: Systematic review and meta-analysis. s.l.: PLoS One 2019. doi:10.1371/journal.pone.0221484.
2. Neumann K, Thomas JP, Voelter C, Dazert S. A new adhesive bone conduction hearing system effectively treats conductive hearing loss in children. 2019; 122:117-25.
3. Gawliczek T, Munzinger F, Anschuetz L, Caversaccio M, Kompis M, Wimmer W. Unilateral and Bilateral Audiological Benefit with an Adhesively Attached, Noninvasive Bone Conduction Hearing System 2018; 39(8):1.

4. Mertens G, Gilles A, Bouzegta R, Van de Heyning P. A Prospective Randomized Crossover Study in Single Sided Deafness on the New Non-Invasive Adhesive Bone Conduction Hearing System. 2018; 39(8):940-9.
5. Piotr H. Skarzynski, Anna Ratuszniak, Kamila Osinska, Magdalena Koziel, Bartlomiej Krol, Katarzyna B. Cywka, Henryk Skarzynski. A Comparative Study of a Novel Adhesive Bone Conduction Device and Conventional Treatment Options for Conductive Hearing Loss. 2019; 40(7):858-64.
6. Liberati A, Altman DG, Tetzlaff J, et al. The PRISMA statement for reporting systematic reviews and meta-analyses of studies that evaluate health care interventions: explanation and elaboration. Journal of Clinical Epidemiology 2009; 62/doi.org/10.1136/bmj.b2700
7. Dahm V, Baumgartner WD, Liepins R, Arnoldner C, Riss D. First Results with a New, Pressure-free, Adhesive Bone Conduction Hearing Aid. 2018; 39(6):748-54.
8. Dahm V, Auinger AB, Liepins R, Baumgartner WD, Riss D, Arnoldner C.A Randomized Cross-over Trial Comparing a Pressure-free, Adhesive to a Conventional Bone Conduction Hearing Device 2019 doi: 10.1097/MAO.0000000000002184.
9. Favoreel A, Heuninck E, Mansbach, AL. Audiological benefit and subjective satisfaction of children with the ADHEAR audio processor and adhesive adapter. 2019; 129:109729.
10. Osborne MS, Child-Hymas A, Gill J, Lloyd MS, McDermott AL. First Pediatric Experience with a Novel, Adhesive Adapter Retained, Bone Conduction Hearing Aid System. 2019; 40(9):1199-1207.
11. Moteki H, Kitoh R, Usami SI. The availability of an adhesive bone conduction hearing device: a preliminary report of a single-center experience. 2019 doi.org/10.1080/00016489.2019.1708969.
12. Urík M, Hošnová D, Šlapák I, Jančíková J, Odstrčilík J, Jarkovský J, Baumgartner WD. First experiences with a new adhesive bone conduction hearing device in children. 2019; 126:109614.
13. Weiss R, Loth A, Leinung M, Balster S, Hirth D, Stöver T, Helbig S, Kramer S. A new adhesive bone conduction hearing system as a treatment option for transient hearing loss after middle ear surgery. 2019; 277:751-9.
14. Faber HT, Kievit H, de Wolf MJ, Cremers CW, Snik AF, Hol MK Analysis of factors predicting the success of the bone conduction device headband trial in patients with single-sided deafness. 2012; 138(12):1129-35.
15. Gawliczek T, Wimmer W, Munzinger F, Caversaccio M, Kompis M. Speech Understanding and Sound Localization with a New Non-implantable Wearing Option for Baha. 2018; doi.org/10.1155/2018/5264124.
16. Verhagen CVM, Hol MKS, Coppens-Schellekens W, Snik AFM, Cremers CWRJ. The Baha Softband: A new treatment for young children with bilateral congenital aural atresia. 2008; 72(10):1455-9.
17. Magliulo G, Turchetta R, Iannella G, Valperga di Masino R, de Vincentiis M. Sophono Alpha System and subtotal petrosectomy with external auditory canal blind sac closure. 2014; 272(9):2183-90.
18. Zarowski AJ, Verstraeten N, Somers T, et al. Headbands, testbands and softbands in preoperative testing and application of bone boneanchored. 2011; 71:124-31.
19. LH Mens. Speech understanding in noise with an eyeglass hearing aid: asymmetric fitting and the head shadow benefit of anterior microphones. 2010; 50(1):27-33.
20. Hearing rehabilitation in congenital aural atresia using the bone-anchored hearing aid: audiological and satisfaction results. Fuchsmann C, Tringali S, Disant F, Buiret G, Dubreuil C, Froehlich P, Truy E. 2010. doi.org/10.3109/00016489.2010.499879.

Evaluation of the periodontal healing of the second mandibular molar distal site following insertion of PRF in the third molar post extraction alveolus

P.C. Passarelli[1*], A. Romeo[1*], M.A. Lopez[2], P. De Angelis[1], V. Desantis[1], G.B. Piccirillo[1], R. Papa[1], P. Papi[3], G. Pompa[3], A. Moffa[2], M. Casale[2] and A. D'Addona[1]

[1]Department of Head and Neck, Division of Oral Surgery and Implantology, Institute of Clinical Dentistry, Università Cattolica del Sacro Cuore, Fondazione Policlinico Universitario Gemelli, Rome, Italy; [2]Unit of Otolaryngology, UOS ORL TI, Campus-Biomedico University, Rome, Italy; [3]Department of Oral and Maxillo-facial Sciences, "Sapienza" University of Rome, Rome, Italy

*The first two authors contributed equally to this paper.

The aim of this study was to evaluate the periodontal healing of the distal sites of the mandibular second molars, comparing the extraction therapy of the third molar with and without PRF adjunct into the post-extraction alveolus. The study sample was composed by 40 consecutive patients who underwent extraction of mandibular third molars. Patients were divided in two groups: the last 20 participants who have only been subjected to extraction (spontaneous healing group, SHG) and the first 20 patients who had PRF adjunct (PRF group, PG). Healing was evaluated by analyzing the variations in terms of PPD (Probing Pocket Depth), REC (Recession), CAL (Level of Clinical Attachment), BoP (Bleeding on Probing) and GI (Gingival Index) from Baseline to further follow-ups at 1 month and 3 months. The disto-vestibular (DV) and disto-lingual (DL) PPD values of the second mandibular molar were measured at Baseline and after three months in the two groups. Patients of the PG group showed lower PPD values at 1 month and 3 months postoperatively: DV: 3.6±1.09 - DL: 3.5±1.15 and DV: 2.5±0.83 - DL: 2.6±1.09, respectively. Patients belonging to the SHG also showed lower PPD values, reporting respectively the following DV values after 3 months: 2.7±0.86 - DL: 2.75±0. 85. However, there was no statistically significant difference comparing the results obtained in PG and SHG groups at 1 and 3 months (p>0.05). The insertion of PRF inside the post-extraction alveolus of the mandibular third molar leads to limited improvement in terms of periodontal healing, compared to extraction therapy only.

Periodontal disorders distal to mandibular second molar develop when the third inferior molars in half-inclusion, more frequently in a mesio-inclined or horizontal position, contribute to the formation of a periodontal pocket distal to the second molar. This pathological scenario often results in the need to remove the asymptomatic third mandibular molar. (1-5). Several authors focused their attention on the periodontal healing at the distal root of the second mandibular molar following the extraction of the adjacent third molars (6-8). In a study conducted on 195 patients, Blakey found that 62% of them had a probing pocket depth (PPD) of at least 4 mm on the distal side of the second molar, which resulted in a mean worsening of 2 mm in 33% of cases at a two-year follow-up (9, 10). Subsequently, 77% of patients experienced a further loss of periodontal attachment at the distal side of the adjacent second molar at the 4-year follow-up (1, 2). A study conducted by Petsos et al. on 78 patients, found out

Key words: oral surgery, third molar, extraction, bleeding disorder, platelet-rich fibrin, autologous growth factors

Corresponding Author:
Dr Pier Carmine Passarelli,
Department of Head and Neck, Division of Oral Surgery and Implantology, Institute of Clinical Dentistry, Università Cattolica del Sacro Cuore, Fondazione Policlinico Universitario Gemelli, Rome, Italy
Tel.: 39 0630155278 - Fax: 39 0630154751
email: piercarmine.passarelli@unicatt.it

0393-974X (2020)

that young patients could benefit from mandibular third molar extraction in terms of oral hygiene and periodontal attachment levels, particularly in cases of semi-inclusion (1, 11). More recently, in 2017, Qu et al. (12), confirmed that the presence of a mandibular third molar, even if asymptomatic, represents an important risk factor for the onset of periodontal problems affecting the adjacent molar (1).

Even if prophylactic extraction of mandibular third molars is still controversial and debated in scientific literature (13), this decision should be taken as soon as possible, as this surgical procedure should be ideally performed before the onset of symptoms. Platelet-rich fibrin (PRF) belongs to a new generation of platelet aggregates, allowing for a simplified preparation without biochemical manipulation of blood. PRF has showed even better results compared to collagen membranes, as it induces greater proliferation of periosteal cells, faster wound healing and does not result in pain, dryness, or purulent complications (14). The aim of this study was to evaluate the periodontal healing of the distal sites at the mandibular second molars, comparing the extraction therapy of the third molar with and without PRF adjunct into the post-extraction alveolus.

Experimental section - patient selection

This retrospective study was conducted and implemented at the Agostino Gemelli University Policlinic (Rome, Italy), at the Oral Surgery and Implantology Unit. Due to the retrospective nature of the study, there was no need for approval by the local institution review board. We included consecutive patients who underwent the extraction of mandibular third molars between 2017 and 2019. In particular, we compared the last 20 patients who had the sole extraction (spontaneous healing, SHG, group) with the first 20 patients who had PRF adjunct (PRF, PG, group), that has recently become our post-extraction alveolus routine regimen.

The study sample was composed by 40 patients, 20 males and 20 females, aged between 18 and 55 years. Healing was evaluated by analyzing the variations of several clinical parameters immediately before surgery and at 1 and 3 months postoperatively. Exclusion criteria were: uncontrolled systemic diseases (15), syndromic diseases (16), blood disorders (17, 18), diseases of the immune system (19), patients on dialysis at the time of extraction, absence of the II molar adjacent to the III molar subject to extraction, smokers, allergies or hypersensitivity reactions to antibiotics, anti-inflammatories, use of corticosteroid use in the 12 months prior to extraction.

MATERIALS AND METHODS

PRF preparation

Blood samples (30 mL for each patient) were taken by a competent health professional (doctor or nurse) and collected into 3 disposable dry tubes. Subsequently, the tubes were placed and balanced symmetrically inside the PC-02 centrifuge (Process, Nice, France), as specified in the user manual. The speed was set at 2700 rpm for a total duration of 12 minutes. Centrifugation was performed immediately after blood collection to prevent the activation of fibrinogen into fibrin that would have resulted in a minimal amount of PRF, with low consistency.

With centrifugation, the most superficial layer of blood in the test tube, the supernatant (PPP), became clearly recognizable thanks to its liquid nature, yellow color, and easiness to be separated from the remaining part of the preparation. The PPP was separated with scissors from the lower red layer rich in red blood cells. The PRF, compressed between two sterile gauzes, appeared as a membrane of about 3 to 1.5 cm with a suturable consistency.

Preoperative measurements

Panoramic radiographs of the dental arches, obtained with a digital method (20), showed the position of the mandibular third molar, evaluated in accordance with the Pell and Gregory's (21) and Winter's classifications (22). Both the classification systems take into account three parameters of unequivocal importance: the angle of the included element, its position in relation to the upright branch of the mandible and its depth of inclusion in relation to the occlusal plane of the adjacent teeth. In particular, the Winter classification allows to determine the inclination angle of the third molar in relation to the axis of the second molar.

It is, therefore, possible to distinguish: mesio-inclined elements, which are the most frequent and present a low

degree of difficulty; subsequently, in order of frequency, the elements in horizontal inclusion and the normo-inclined elements; lastly, the disto-inclined elements are statistically the least frequent and, in general, the most challenging to deal with (23). The following clinical measurements were performed during the clinical examination at the level of the second mandibular molar adjacent to the third molar to be removed:

•PPD (Probing Pocket Depth): detected on 6 sites (Disto-Vestibular, Vestibular, Mesio-Vestibular, Mesio-Lingual, Lingual, Disto-Lingual)

•REC: recession

•BoP (Bleeding on Probing) (24): detected on 6 sites (DV, V, MV, ML, L, DL) and measured by a dichotomous index (0: absence of bleeding - 1: presence of bleeding)

•GI (Gingival Index) (25): detected on 4 sites (D, V, M, L) assigning values from 0 to 3:

-0: Normal gingiva;

-1: slight inflammation, slight variation in gingival color with mild edema, absence of BoP;

-2: Moderate inflammation, redness, edema and BoP;

-3: Severe inflammation, redness, edema / ulceration and tendency to spontaneous bleeding.

•Biotype detection (Thin or Thick)

All these measurements were obtained with a 12mm "University of North Carolina" periodontal probe by the same calibrated operator at the time of surgery, one month and 3 months after surgery.

Surgical protocol

The same surgical protocol was applied for all included patients in the two groups. Local anesthesia at the alveolar inferior nerve was first performed with a truncular technique using a 1.8 ml tube of 2% Mepivacaine as anaesthetic and secondly reinforced using plessic technique using 1-2 Mepivacaine tubers with Adrenaline (ratio 1: 100.000). After verifying that the entire area was anaesthetised, a mucoperiosteal trapezoidal flap with the distal discharge was raised. Where necessary, a vestibular osteotomy was performed, using a surgical handpiece and odontotomy, using a turbine equipped with an air / water cooling system with special drills. Immediately after the avulsion of the tooth, a careful alveolar curettage was performed using alveolar spoons of various sizes. At this point, the PRF was inserted into the post-extraction socket in the PG group. The surgical wound was closed using a 3-0 silk suture. All patients kept alternately an ice pack in contact with the skin corresponding to the extraction site for the first hour after surgery. Postoperative medications included:

•Amoxicillin + clavulanic acid 1g twice a day for 6 days, to be started as prophylaxis the night before the surgery;

•Oral Ketorolac 20mg/ml 15 drops immediately after the surgery;

•Betametason I.M. 4 mg/ml (Massetere muscle) immediately after the surgery;

•Chlorhexidine 0.12% mouth rinses twice a day for 7 days.

Statistical analysis

The primary outcomes were the differences in PPD, BoP and GI values at baseline and at 1- and 3-months follow-up in the PG and SHG groups. The second mandibular molar adjacent to the third molar extracted were considered as a single statistical unit. Normal distribution was evaluated with the Shapiro-Wilk test. For within group comparisons, normally distributed data were compared with the repeated measurement ANOVA test, while non-parametric data were compared with the Friedman's test, followed by a pairwise Wilcoxon signed rank test. For between group comparisons, normally distributed data were compared with the Welsch t-test, while non-parametric data were compared with the Kruskal-Wallis test. Normal data were presented as mean± standard deviation. The dichotomous variables, in this case the BoP, were analyzed with the $\chi 2$ test. The significance level was set at $p < 0.05$. Statistical analysis was performed with IBM SPSS software for Mac Os.3.

RESULTS

The baseline disto-vestibular and disto-lingual PPD values were DV: 5.0±2.20 - DL: 5.25±2.36 and DV: 5.15±2.01 - DL: 5.3±2.34, for the PG and the SHG, respectively, without statistically significant differences ($p>0.05$) (Table I).

Patients of the PG group presented lower PPD values at 1 month and 3 months postoperatively: DV: 3.6±1.09 - DL: 3.5±1.15 and DV: 2.5±0.83 - DL: 2.6±1.09, respectively. As a consequence, the 1-month periodontal attachment gain was DV: 1.4 - DL: 1.75 compared to baseline ($p < 0.05$) and the 3 months gain

Table I. *disto-vestibular and disto-lingual PPD values.*

	PPD DV PG	PPD DV SHG	PPD DL PG	PPD DL SHG
Baseline	5.0±2.20	5.15±2.01	5.25±2.36	5.3±2.34
1 month	3.6±1.09		3.5±1.15	
3 months	2.5±0.83	2.7±0.86	2.6±1.09	2.75±0.85
Delta Δ 1 month	1.4		1.75	
Delta Δ 3 months	2.5	2.45	2.65	2.55
P value 1 month	<0.05		<0.05	
P value 3 months	<0.05	<0.05	<0.05	<0.05

PPD DV*=Disto-vestibular periodontal probing depth;* ***PPD DL****=Disto lingual periodontal probing depth;* ***PG****=PRF Group;* ***SHG****=Spontaneous healing group. Data are presented as mean ± standard deviation.*

Table II. *Comparison of the results obtained in PG and SHG groups.*

	BoP DV PG	BoP DV SHG	BoP DL PG	BoP DL SHG
Baseline	0.5±0.52	0.6±0.51	0.5±0.52	0.6±0.51
1 month	0.1±0.31		0.1±0.31	
3 months	0	0	0.1±0.31	0.2±0.42
Delta Δ 1 month	0.4		0.4	
Delta Δ 3 months	0.5	0.6	0.4	0.4
P value 1 month	<0.05		<0.05	
P value 3 months	<0.05	<0.05	<0.05	<0.05

BoP DV*=Disto-vestibular bleeding on probing;* ***BoP DL****=Disto-lingual bleeding on probing;* ***PG****=PRF Group;* ***SHG****=Spontaneous healing group.*

was DV: 2.5 - DL: 2.65 ($p < 0.05$). Patients belonging to the SHG also showed lower values at the periodontal test, reporting respectively the following DV values after 3 months: 2.7±0.86 - DL: 2.75±0.85).

The 3-month gain in terms of decrease in PPD is DV: 2.45 - DL: 2.55 compared to baseline, these changes are statistically significant ($p < 0.05$). Regarding REC, no gingival recession was found in any of the treated patients, both in the PG and SHG groups, neither in the baseline nor at subsequent follow-ups. Finally, we found a statistically significant improvement in GI and BoP at follow-ups in both groups; however, there was no statistically significant difference comparing the results obtained in PG and SHG groups ($p > 0.05$) (Table II).

DISCUSSION

Periodontal disorders affecting the second mandibular molar and secondary to the presence

of the adjacent third molar have been extensively studied in the past (26-28) A study of 100 patients conducted by McFall et al. (29) showed that the second mandibular molar represents one of the most extracted teeth due to periodontal problems and, consequently, a careful analysis of its conditions in the presence of the adjacent third molar is always recommended. Elter (30) et al showed that the presence of the mandibular third molar is associated with a twofold increase in the risk of developing a distal PPD ≥ 5mm to the adjacent second molar.

However, there is still no consensus in the literature and the debate regarding the advantages and disadvantages of extraction to prevent or cure periodontal disorders of the second molar is still ongoing. Many parameters can influence the periodontal healing following the third molar avulsion, such as the type of suture, the extension of the surgical flap and the osteotomy (31, 32). We believe that the use of a standardized surgical protocol, as used in this study, may be of considerable importance to minimize bias. A parameter that may affect the periodontal status of the mandibular second molar is the position of the third molar in relation to the mandible. This was analyzed in our study using the Pell and Gregory's and Winter's classifications. In our series, the categories 2B and normo-inclined are more represented. However, there was no correlation between this finding and the severity of the PPD (33). Therefore, although the position of the third molar to the jaw represents an element of extraordinary importance for surgical strategies, it does not represent an element of predictability with respect to the periodontal status of the adjacent tooth.

PRF has been shown to be very useful in stimulating periodontal healing and bone regeneration thanks to its high levels of growth factors, platelets and cytokines, including PDGF, TGF-β1, IGF and VEGF (34-36). A study by Sammartino et al. (37) showed the histological changes secondary to the use of PRP in preventing periodontal problems at the treated sites in terms of bone maturation. Chang et al. reported that PRF stimulates the proliferation of osteoblasts, periodontal ligament cells and growth factors during a culture period of 3 days (38). Moreover, PRF showed positive healing effects when used for the preservation of post-extraction socket and in sinus lift procedures, also during simultaneous dental implantation (39). According to Hoaglin et al. there is a lower risk of osteomyelitis infections when compared to natural healing, by filling the third molar extraction sockets with PRF (40).

The use of PRF in the post-extractive alveolus has been proved to enhance bone healing and regeneration, to reduce the infection and to preserve the quality and density of the bone (41). Histological analysis was not performed in this study due to the absence of surgical re-entry procedures, which could cause excessive patient discomfort and were not justified from an ethical point of view, since no implant treatment was requested. The results of our study confirmed that the extraction of the mandibular third molar, both with and without the use of PRF, leads to a reduction of PPD values at the distal site of adjacent second molars. Hence, there were no pathological findings in 97.5% of the sites after 3 months (42). A statistically significant reduction in BoP and GI values in both groups was probably caused by an improvement in patients' oral hygiene, a finding that could be related to the better cleaning of the area of the second molar following the extraction of the third molar.

The insertion of PRF inside the post-extraction alveolus of the mandibular third molar leads to limited improvement in terms of periodontal healing, compared to extraction therapy only. Therefore, PRF does not appear clinically relevant for periodontal healing. Further studies with larger sample size are still needed to evaluate the efficacy of PRF in preventing post-operative complications and post-extractive algic symptomatology.

REFERENCES

1. Becker W, Becker BE, Berg LE. Periodontal treatment without maintenance. A retrospective study in 44 patients. J Periodontol 1984; 55(9):505-9. doi:10.1902/jop.1984.55.9.505.
2. Chace R Sr, Low SB. Survival characteristics of periodontally-involved teeth: a 40-year study. J Periodontol 1993; 64(8):701-5. doi:10.1902/jop.1993.64.8.701.

3. Hirschfeld L, Wasserman B. A long-term survey of tooth loss in 600 treated periodontal patients. J Periodontol 1978; 49(5):225-37. doi:10.1902/jop.1978.49.5.225.
4. McFall WT Jr. Tooth loss in 100 treated patients with periodontal disease. A long-term study. J Periodontol 1982; 53(9):539-49. doi:10.1902/jop.1982.53.9.539.
5. Passarelli PC, Lajolo C, Pasquantonio G, et al. Influence of mandibular third molar surgical extraction on the periodontal status of adjacent second molars. J Periodontol. 2019; 90(8):847-55. doi:10.1002/JPER.18-0415.
6. Ash M, Costich E, Hayward J. A study of periodontal hazards of 3rd molars. J Periodontol 1962; 33:209.
7. Kugelberg CF. Periodontal healing two and four years after impacted lower third molar surgery. A comparative retrospective study. Int J Oral Maxillofac Surg 1990; 19(6):341-5. doi:10.1016/s0901-5027(05)80077-3.
8. Kugelberg CF, Ahlström U, Ericson S, Hugoson A, Thilander H. The influence of anatomical, pathophysiological and other factors on periodontal healing after impacted lower third molar surgery. A multiple regression analysis. J Clin Periodontol 1991; 18(1):37-43. doi:10.1111/j.1600-051x.1991.tb01117.x.
9. Blakey GH, Jacks MT, Offenbacher S, et al. Progression of periodontal disease in the second/third molar region in subjects with asymptomatic third molars. J Oral Maxillofac Surg 2006; 64(2):189-193. doi:10.1016/j.joms.2005.10.014.
10. Blakey GH, Golden BA, White RP Jr, Offenbacher S, Phillips C, Haug RH. Changes over time in the periodontal status of young adults with no third molar periodontal pathology at enrollment. J Oral Maxillofac Surg 2009; 67(11):2425-30. doi:10.1016/j.joms.2008.12.064.
11. Petsos H, Korte J, Eickholz P, Hoffmann T, Borchard R. Surgical removal of third molars and periodontal tissues of adjacent second molars. J Clin Periodontol 2016; 43(5):453-60. doi:10.1111/jcpe.12527.
12. Qu HL, Tian BM, Li K, Zhou LN, Li ZB, Chen FM. Effect of Asymptomatic Visible Third Molars on Periodontal Health of Adjacent Second Molars: A Cross-Sectional Study. J Oral Maxillofac Surg 2017; 75(10):2048-57. doi:10.1016/j.joms.2017.04.006
13. Friedman JW. The prophylactic extraction of third molars: a public health hazard. Am J Public Health 2007; 97(9):1554-9. doi:10.2105/AJPH.2006.100271.
14. De Angelis P, De Angelis S, Passarelli PC, Liguori MG, Manicone PF, D'Addona A. Hard and Soft Tissue Evaluation of Different Socket Preservation Procedures Using Leukocyte and Platelet-Rich Fibrin: A Retrospective Clinical and Volumetric Analysis. J Oral Maxillofac Surg 2019; 77(9):1807-15. doi:10.1016/j.joms.2019.05.004
15. Azzolino D, Passarelli PC, De Angelis P, Piccirillo GB, D'Addona A, Cesari M. Poor Oral Health as a Determinant of Malnutrition and Sarcopenia. Nutrients 2019; 11(12):2898. doi:10.3390/nu11122898.
16. Passarelli PC, Pasquantonio G, Manicone PF, et al. Orofacial signs and dental abnormalities in patients with Mulvihill-Smith syndrome: A literature review on this rare progeroid pathology Medicine (Baltimore) 2018; 97(18):e0656. doi:10.1097/MD.0000000000010656.
17. Passarelli PC, De Angelis P, Pasquantonio G, Manicone PF, Verdugo F, D'Addona A. Management of Single Uncomplicated Dental Extractions and Postoperative Bleeding Evaluation in Patients with Factor V Deficiency: A Local Antihemorrhagic Approach. J Oral Maxillofac Surg 2018; 76(11):2280-3. doi:10.1016/j.joms.2018.06.022.
18. Passarelli PC, Pasquantonio G, D'Addona A. Management of Surgical Third Lower Molar Extraction and Postoperative Progress in Patients with Factor VII Deficiency: A Clinical Protocol and Focus on This Rare Pathologic Entity. J Oral Maxillofac Surg 2017; 75(10):2070.e1-2070.e4.
19. Bollero P, Passarelli PC, D'Addona A, et al. Oral management of adult patients undergoing hematopoietic stem cell transplantation. Eur Rev Med Pharmacol Sci 2018; 22(4):876-87. doi:10.26355/eurrev_201802_14365.
20. Saccomanno S, Passarelli PC, Oliva B, Grippaudo C. Comparison between Two Radiological Methods for Assessment of Tooth Root Resorption: An *In Vitro* Study. Biomed Res Int 2018; 2018:5152172. doi:10.1155/2018/5152172.
21. Pell GJ, Gregory BT, Impacted Mandibular third molars: classification and modified techniques for removal. Dent Digest 1933; 39:330-8.

22. Winter GB. Principles of exodontia applied to the impacted third molar. American Medic Books 1926.
23. Chiapasco M. Manuale illustrato di chirurgia orale, 3rd ed. EDRA: Milan, Italy; 171-3.
24. Mühlemann HR, Son S. Gingival sulcus bleeding--a leading symptom in initial gingivitis. Helv Odontol Acta 1971; 15(2):107-13.
25. Löe H. The Gingival Index, the Plaque Index and the Retention Index Systems. J Periodontol 1967; 38(6):610-6. doi:10.1902/jop.1967.38.6.610.
26. Simonpieri A, Schoeffler C, Girard M.O, Diss A, Dohan D. Le Platelet Rich Fibrin – PRF biomatériau de cicatrisation performant. L'Information Dentarie 2005; 87:803.
27. Choukroun J, Simonpiéri A, Schoeffler C, Girard MO, Dohan D. Concentrés plaquettaires : technologies, biologie associée, applications cliniques, analyses histologiques: 4 partie: analyses histologiques. Implantodontie 2004; 13:167-72.
28. Choukroun J, Diss A, Simonpieri A, et al. Platelet-rich fibrin (PRF): a second-generation platelet concentrate. Part V: histologic evaluations of PRF effects on bone allograft maturation in sinus lift. Oral Surg Oral Med Oral Pathol Oral Radiol Endod 2006; 101(3):299-303. doi:10.1016/j.tripleo.2005.07.012.
29. McFall WT Jr. Tooth loss in 100 treated patients with periodontal disease. A long-term study. J Periodontol. 1982; 53(9):539-49. doi:10.1902/jop.1982.53.9.539
30. Elter JR, Cuomo CJ, Offenbacher S, White RP Jr. Third molars associated with periodontal pathology in the Third National Health and Nutrition Examination Survey. J Oral Maxillofac Surg 2004; 62(4):440-5. doi:10.1016/j.joms.2003.12.002.
31. Kugelberg CF, Ahlström U, Ericson S, Hugoson A, Thilander H. The influence of anatomical, pathophysiological and other factors on periodontal healing after impacted lower third molar surgery. A multiple regression analysis. J Clin Periodontol 1991; 18(1):37-43. doi:10.1111/j.1600-.
32. Simonpieri A, Dohan D. Intérêt du PRF pour les réhabilitations bimaxillaires complexes avec greffes osseuses multiples, implantations postextractionelles et mise en charge immédiate. Présentation d'un cas clinique. Implantodontie 2005; 11:1.
33. Dohan DM, Choukroun J, Diss A, et al. Platelet-rich fibrin (PRF): a second-generation platelet concentrate. Part I: technological concepts and evolution. Oral Surg Oral Med Oral Pathol Oral Radiol Endod 2006; 101(3):e37-e44. doi:10.1016/j.tripleo.2005.07.008.
34. Dohan D, Donsimoni J-M, Navarro G, Gaultier F. Platelet concentrates part II: Associated biology. Implantodontie 2003; 12:17-25.
35. Dohan DM, Choukroun J, Diss A, et al. Platelet-rich fibrin (PRF): a second-generation platelet concentrate. Part II: platelet-related biologic features. Oral Surg Oral Med Oral Pathol Oral Radiol Endod 2006; 101(3):e45-e50. doi:10.1016/j.tripleo.2005.07.009.
36. Simonpieri A, Schoeffler C, Girard MO, Diss A, Dohan D. Le Platelet Rich Fibrin – PRF biomatériau de cicatrisation performant. L'Information Dentarie 2005; 87:803.
37. Sammartino G, Tia M, Gentile E, Marenzi G, Claudio PP. Platelet-rich plasma and resorbable membrane for prevention of periodontal defects after deeply impacted lower third molar extraction. J Oral Maxillofac Surg 2009; 67(11):2369-73. doi:10.1016/j.joms.2009.04.093.
38. Chang IC, Tsai CH, Chang YC. Platelet-rich fibrin modulates the expression of extracellular signal-regulated protein kinase and osteoprotegerin in human osteoblasts. J Biomed Mater Res A 2010; 95(1):327-32. doi:10.1002/jbm.a.32839.
39. Jeong SM, Lee CU, Son JS, Oh JH, Fang Y, Choi BH. Simultaneous sinus lift and implantation using platelet-rich fibrin as sole grafting material. J Craniomaxillofac Surg. 2014; 42(6):990-4. doi:10.1016/j.jcms.2014.01.021.
40. Hoaglin DR, Lines GK. Prevention of localized osteitis in mandibular third-molar sites using platelet-rich fibrin. Int J Dent. 2013; 2013:875380. doi:10.1155/2013/875380.
41. Miron RJ, Zucchelli G, Pikos MA, et al. Use of platelet-rich fibrin in regenerative dentistry: a systematic review. Clin Oral Investig 2017; 21(6):1913-27. doi:10.1007/s00784-017-2133-z.
42. Al-Hamed FS, Tawfik MA, Abdelfadil E, Al-Saleh MAQ. Efficacy of Platelet-Rich Fibrin After Mandibular Third Molar Extraction: A Systematic Review and Meta-Analysis. J Oral Maxillofac Surg 2017; 75(6):1124-35. doi:10.1016/j.joms.2017.01.022.

Teaching parotid surgery to ENT residents in the era of new technologies: an ex-vivo ovine model

V. Rinaldi[1], A. Costantino[2,3], A. De Virgilio[2,3], G. Spriano[2,3], R. Alloni[4], A. Moffa[1] and M. Casale[1]

[1]Unit of Otolaryngology, Integrated Therapies in Otolaryngology, Campus Bio-Medico University, Rome, Italy; [2]Otorhinolaryngology Unit, Humanitas Clinical and Research Center IRCCS, Milan, Italy; [3]Department of Biomedical Sciences, Humanitas University, Milan, Italy; [4]Surgery Unit, University Campus Bio-Medico, Rome, Italy

Surgical training has recently assumed a central role in the otolaryngology field, and the necessity to train residents and fellows' skills in a progressive manner has led to an incredible widespread of *ex-vivo* animal models for several surgical procedures. To report our experience with an *ex-vivo* ovine model for parotid gland dissection in a training context. A junior resident (PGY-1) and a post-graduate student with no experience in parotid surgery were guided by a skilled surgeon in the parotid gland dissection for each step of the procedure. Three different adult lamb heads were used for this feasibility study. A specific preparation of the model was performed before the training session. Similarity between the ovine model and the human were recorded. The resident and the post-graduate student were able to carry out a complete parotid gland dissection under supervision. The correct identification of surgical landmarks has led to a proper surgical simulation. The facial nerve dissection was adequately performed, and all branches were isolated. Parotid surgery training on an *ex-vivo* ovine model is useful, easy repeatable, and low cost. The ovine model presented in this study has similarities in size, structure, and tissue consistence to the human parotid, making it an ideal model for residents to simulate parotid surgery.

An adequate training opportunity for surgical residents has a pivotal role also in the otolaryngology field (1). Although the direct clinical experience is surely the most common method to improve surgical skills, some issues are unavoidably encountered. The necessity to train residents and fellows' skills in a progressive manner lead to a delay in the surgical learning curve that should not be underestimated (2).

In the common academic practice, we need to take account of patients' safety and expectations, restrictions of working hours and in particular financial limitations due to healthcare system demands (3). In this context, the possibility to improve knowledge of surgical anatomy and practice of anatomic dissection should be included in all training programs (4). Adequate surgical training leads to reducing the risk for the patient and a faster learning curve. This is true for new surgical techniques as much as the older ones. The most realistic and useful surgical training is surely specimen based. Although the preservation of anatomical structures could not be always provided, the possibility to identify surgical landmarks, and to practice surgical maneuvers represents the main purpose of these training sessions.

Unfortunately, cadaver models are not always available due to cost for institutions and the related ethical problems. On the other hand, animal models are readily available, and no ethical issues are encountered unless live animals are specifically

Key words: Parotid gland; facial nerve; simulation; ex-vivo; animal model

Corresponding Author:
Dr Antonio Moffa,
Unit of Otolaryngology, Integrated Therapies in Otolaryngology, Campus Bio-Medico University, Via Álvaro del Portillo 21, 00128 Roma (RM).
Tel.: 39 06.22.54.11
e-mail address: a.moffa@unicampus.it

0393-974X (2020)

required. Several *ex-vivo* animal models have been described for the otolaryngology training, with promising results in terms of anatomy and tissue consistence reproducibility. In particular, the ovine model was described as a high-fidelity realistic tissue for several procedure in head and neck surgery (5-7). The aim of the present study is to report our experience with an *ex-vivo* ovine model for parotid gland dissection in a training context. We describe similarity with the human according to surgical landmarks, tissue consistence and overall quality of the training session.

MATERIALS AND METHODS

Three different adult lamb heads were used for this feasibility study. No live or euthanized animals were used in this study, and no specific ethic committee approval was required. The lamb head was obtained from farm-raised animals and was purchased in a slater slaughterhouse at a cost of 4$. The head was stored at 4°C for at least 3 days after the animal death as already described in a previous paper (7). A junior resident (PGY-1) and a post-graduate student with no experience in parotid surgery were guided by a skilled surgeon in the parotid gland dissection for each step of the procedure. Moreover, the same procedure was previously performed by the skilled surgeon as a demonstration for the student. A specific preparation of the model was performed before the training session. The external auditory canal was completed exposed prior to the simulation to easily guide the resident during the dissection of the main trunk of the facial nerve (Fig. 1). All the dissection was carried out on an operating table with cold blade surgical instruments. Similarity between the ovine model and the human were recorded by the skilled surgeon. The present study was conducted in the simulation room at the Campus Bio-Medico University (Italy) in July 2019.

RESULTS

The resident and the post-graduate student were able to carry out a complete parotid gland dissection under supervision (see Electronic supplementary material). First, a skin flap was elevated with an L shape incision to visualize the parotid gland (Fig. 2). Then, a superficial parotidectomy was performed. The posterior border of the superficial lobe was separated from the auditory canal and retracted anteriorly. The main trunk of the facial nerve was exposed at the level of his emergency form the stylomastoid foramen between the cartilaginous

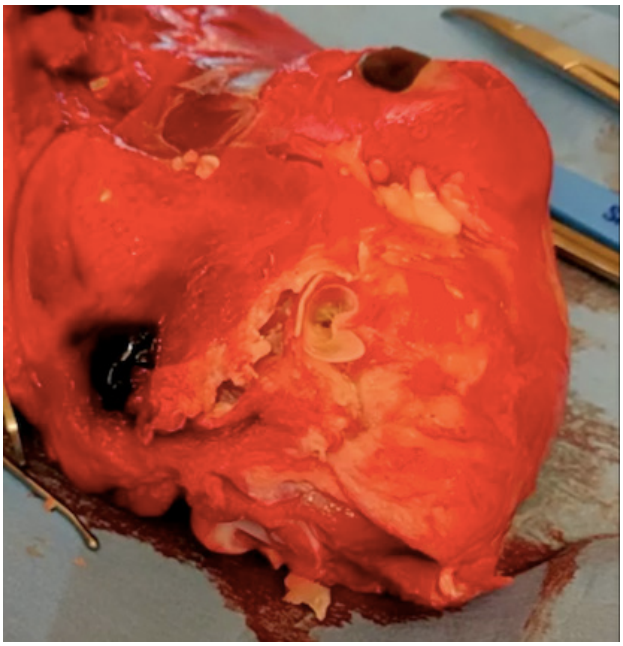

Fig. 1. *The adult lamb head after adequate preparation with the external auditory canal completely exposed.*

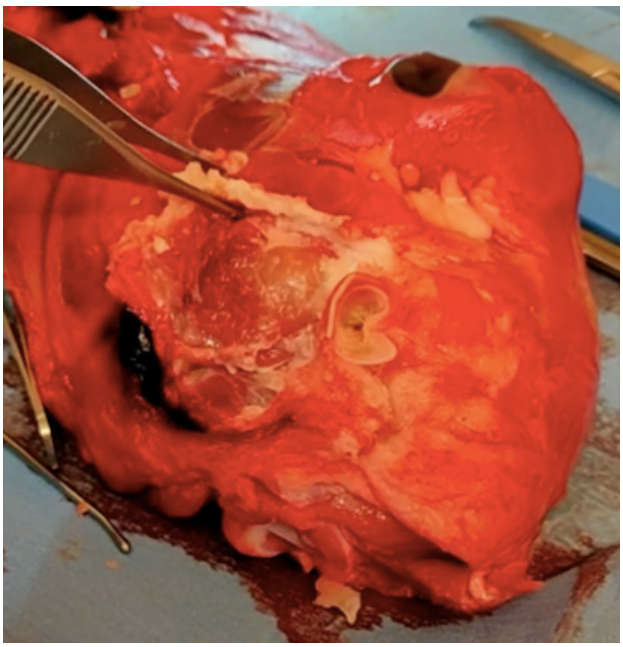

Fig. 2. *Elevation of a skin flap in order to directly visualize the parotid gland.*

portion of the auditory canal, the mastoid process, and the superior border of the posterior belly of the digastric muscle.

After the identification of the main trunk of the facial nerve, the parotid tissue dissection has continued in a plane superficial to the nerve toward the periphery of the gland. A careful dissection of the peripheral branches of the facial nerve was carried out, and the superficial lobe of the gland was elevated (Fig. 3). Finally, a meticulous dissection was conducted to isolate the main and peripheral branches of the nerve from the deep lobe of the parotid gland (Fig. 4).

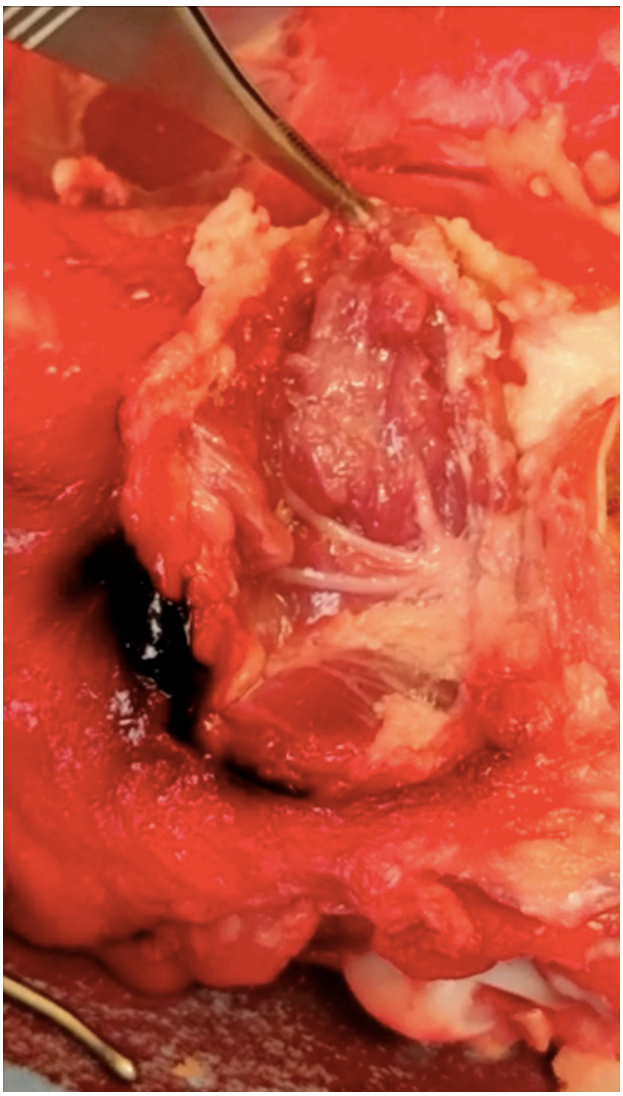

Fig. 3. *Superficial parotidectomy with the facial nerve branches exposed.*

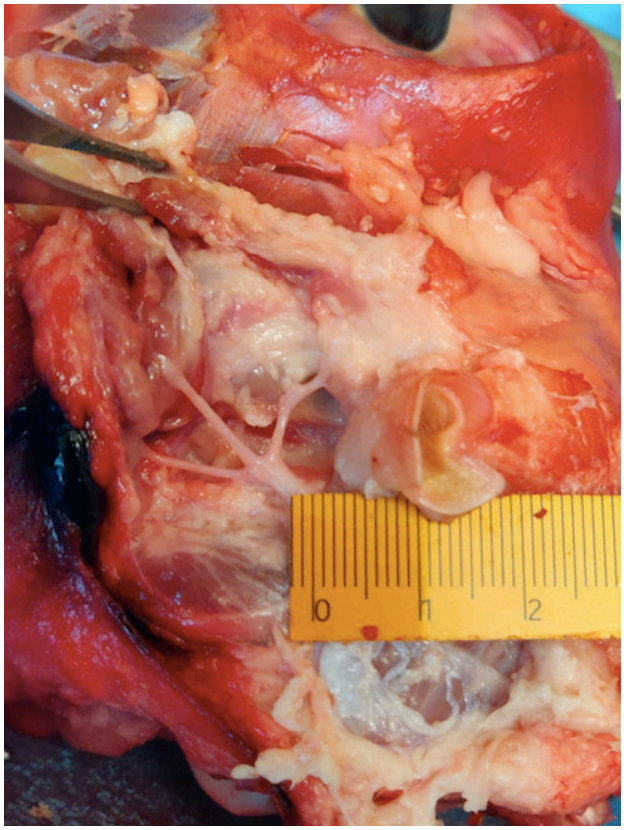

Fig. 4. *Isolation of the main and peripheral branches of the nerve from the deep lobe of the parotid gland. Note the anatomic relationship between the main trunk of the facial nerve and tragal pointer.*

No differences in terms of tissue consistency were found compared to human specimen. The three main branches of the ovine facial nerve (auriculo-palpebral, dorsal buccal, ventral buccal) were recognized and easily isolated during the dissection (5). The anatomical relationship between the main trunk of the facial nerve and the tragal "pointer" represented a realistic surgical landmark for the dissection.

DISCUSSION

The goal of this study was to present our preliminary experience with parotid dissection using an *ex-vivo* ovine model. During the simulation session, the anatomical model has proved to be an adequate alternative to common human cadaver dissection. In our opinion, although some anatomical differences could be identified during the dissection

(8), the possibility to train young residents with this ex-vivo surgical model should be considered as a valid alternative to human specimens.

The purpose of cadaver dissection is both related to the acquisition of surgical skills, and the comprehension of anatomical structures and relationships. Some issues related to *ex-vivo* animal dissection are comparable to human specimen dissection. The tissue consistency is partially impaired, and the possibility to familiarize with some anatomical structures could not be always provided. However, although neck dissection is not always permitted due to the abnormal anatomy determined by tissue breakdown, the parotid gland is adequately maintained. This major salivary gland is almost superficial, and it is rapidly encountered during the dissection.

Moreover, the anatomy of the facial nerve is completely preserved. Although some differences in terms of facial nerve branches are encountered (5), the possibility to understand how the gland dissection should be performed to preserve the nerve is the most important element of this surgical model. In addition, the continuous repetition of surgical steps promotes a rapid learning curve able to properly introduce naïve residents in parotid surgery. The low-cost of *ex-vivo* animal models is indeed a fundamental point of strength for these simulations. The possibility to easily repeat the surgical procedures lead to a rapid acquisition of surgical skills, that could be exploited in real surgery in the operating room. The cost of approximately 4-5$ per specimen makes this model a good alternative to the more expensive and rarely available human cadavers. Further studies are recommended to evaluate the expedite of surgical skills during a tailored training program, and to quantify the corresponding benefit in the common clinical activity during real surgery.

REFERENCES

1. Javia L, Deutsch ES. A systematic review of simulators in otolaryngology. Otolaryngol Head Neck Surg 2012; 147(6):999-1011. doi:10.1177/0194599812462007.
2. Musbahi O, Aydin A, Al Omran Y, Skilbeck CJ, Ahmed K. Current Status of Simulation in Otolaryngology: A Systematic Review. J Surg Educ 2017; 74(2):203-15. doi:10.1016/j.jsurg.2016.09.007.
3. Javid P, Aydın A, Mohanna PN, Dasgupta P, Ahmed K. Current status of simulation and training models in microsurgery: A systematic review. Microsurgery 2019; 39(7):655-68. doi:10.1002/micr.30513.
4. Gardner AK, Scott DJ, Hebert JC, et al. Gearing up for milestones in surgery: Will simulation play a role?. Surgery 2015; 158(5):1421-7. doi:10.1016/j.surg.2015.03.039.
5. Ianacone DC, Gnadt BJ, Isaacson G. Ex vivo ovine model for head and neck surgical simulation. Am J Otolaryngol 2016; 37(3):272-8. doi:10.1016/j.amjoto.2016.01.015.
6. Ghirelli M, Mattioli F, Federici G, et al. Ex Vivo Porcine Larynx Model for Microlaryngoscopy Laryngeal Surgery: Proposal for a Structured Surgical Training. J Voice 2020; 34(4):629-35. doi:10.1016/j.jvoice.2019.02.007.
7. Rinaldi V, Costantino A, Moffa A, Casale M. Ex-vivo surgical model for "Barbed Snore Surgery": a feasibility study. Eur Arch Otorhinolaryngol 2019; 276(12):3539-42. doi:10.1007/s00405-019-05660-w.
8. Niimi Y, Matsumine H, Fukuda S, et al. Surgical anatomy of ovine facial and hypoglossal nerves for facial nerve reconstruction and regeneration research: An experimental study in sheep. Microsurgery 2020; 40(1):51-8. doi:10.1002/micr.30405.

The efficacy of Barbed Sutures for Anterior Pharyngoplasty: technical aspects and preliminary results

V. Rinaldi[1], A. Moffa[1,2], L. Sabatino[1], M. Cassano[2], P.C. Passarelli[3], M. Mantovani[4], L. Pignataro[4] and M. Casale[1]

[1]Integrated Sleep Surgery Team UCBM - Unit of Otolaryngology – Integrated Therapies in Otolaryngology, Campus Bio-Medico University, Rome, Italy; [2]Unit of Otolaryngology, University of Foggia, Foggia, Italy; [3]Department of Head and Neck, Division of Oral Surgery and Implantology, Institute of Clinical Dentistry, Università Cattolica del Sacro Cuore, Fondazione Policlinico Universitario Gemelli, Rome, Italy; [4]Department of Otolaryngology, Department of Clinical Sciences and Community Health, Fondazione I.R.C.C.S. Ca' Granda, Ospedale Maggiore Policlinico, University of Milan, Milan, Italy

After the first experiences with the Barbed Sutures (BS) in sleep surgery, we present the Modular Barbed Anterior Pharyngoplasty (M.B.A.Ph.), a functional tenso-structural reconstruction of the soft palate, as a surgical solution for Obstructive Sleep Apnea (OSA) due to antero-posterior collapse at the drug induced sleep endoscopy (DISE) for snoring and mild-moderate OSA. The action of the BS is sustained over time by means of solid and stable tissue scarring. M.B.A.Ph. avoids palatal fibro-muscular resection and minimize iatrogenic bleeding (bloodless surgery). The technique is described in detail and some preliminary results are presented.

Obstructive Sleep Apnea (OSA) is a growing health concern, affecting nearly one billion people worldwide and characterized by repeated episodes of vibration and collapse of pharyngeal airway during sleep resulting in noise production (snoring), airflow cessations, oxygen desaturations, fragmentation of sleep, daytime sleepiness (1). Palatal surgery is a cornerstone of OSA operative management. The recent evolution of OSA surgery has been focusing on the goal of reducing the excessive collapsibility of the pharyngeal structures thus obtaining the expansion and stabilization of the pharyngeal airspace. The velum and pharynx are the most common site of obstruction in OSA patients and in the last decades, several surgical palatal procedures have been proposed. Pang et al. (2) described the modified cautery assisted palatal stiffening operation (CAPSO) technique done under local anesthesia in patients with snoring and mild OSA.

After the first experiences with the Barbed Sutures (BS) in sleep surgery (3, 4), we are now aiming to present the Modular Barbed Anterior Pharyngoplasty (M.B.A.Ph.), a functional tenso-structural reconstruction of the soft palate, as a surgical solution for OSA due to antero-posterior collapse at the drug induced sleep endoscopy (DISE) for snoring and mild-moderate OSA.

M.B.A.Ph. is one of the modules of an innovative approach to treat retropalatal OSA customizable to the single patient anatomic and DISE features

Key words: modular barbed anterior pharyngoplasty, snoring, obstructive sleep apnea hypopnea syndrome (osahs), modular barbed snoring and osahs surgery and technical update.

Corresponding Author:
Dr Antonio Moffa,
Integrated Sleep Surgery Team UCBM,
Unit of Otolaryngology, Integrated Therapies in Otolaryngology,
Campus Bio-Medico University,
Via Álvaro del Portillo 21, 00128 Roma, Italy
Tel.: 39 06.22.54.11
e-mail: a.moffa@unicampus.it

0393-974X (2020)

and embeddable in a multi-level surgical program: the Modular Barbed Snoring and OSAHS Surgery (M.B.S.O.S.®) (5) .Through the application of specific direction vectors and the use of BS, with the M.B.A.Ph the surgeon is able to lift, shorten, advance and stiffen the soft palate by suspension to specific rigid fibro-osseous holds (posterior nasal spine, palatal aponeurosis, hamuli of the pterygoid processes) in the complete anatomic respect of oropharyngeal fibro-muscular structures. The main landmarks of (M.B.S.O.S.®) are shown in Fig. 1. In our study we evaluated the efficacy and safety of the BS for anterior pharyngoplasty.

MATERIALS AND METHODS

M.B.A.Ph. was performed under general anesthesia in 18 selected subjects presenting with mild to moderate OSA syndrome presenting an antero-posterior collapse at DISE associated with a thick and ptosic uvulopalatal complex. The group was composed of 16 men and 2 women, with mean age of 53.83 (range from 44 to 61) and an average BMI of 27.98 (from 23.3 to 29.3). All the patients were already tonsillectomized. At the end of the 6-month follow-up period, there was a statistically significant reduction in mean post-operative AHI values (18.66±2.6 vs 7.0±4.2 events/hour; p-value = 0.0023) and mean Epworth Sleepiness Scale (ESS) scores (6.8±2.3 vs 2.8±0.7; p-value <0.0027).

Suture technique

M.B.A.Ph. is a routine procedure in our institution with no need for ethical approval. The operation requires general anaesthesia with orotracheal intubation. The patient is placed in supine position and a Boyle-Davis mouth gag is used to expose the orapharynx. Usually a 3.0 PDO bidirectional BS (Stratafix bidirectional BS-Ethicon) iss preferred. The main steps of the procedure are reported in Fig. 2.

1. The end point of osseous palate on the midline (the posterior nasal spine) and the reliefs of pterygoid hamuli.are marked with a dermographic pen on the palatal mucosa.
2. A reduction of the palatal bulk is performed (preferably with low-temperature plasma radiofrequency ablation) by resecting a semilunar

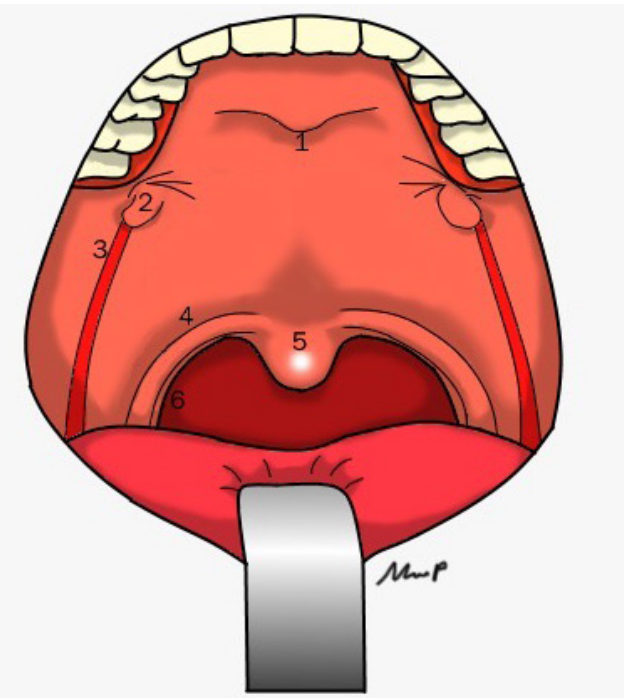

Fig. 1. *The main landmarks of the Modular Barbed Snoring and OSAHS Surgery (M.B.S.O.S.®). **1**): posterior nasal spine; **2**): hamuli of the pterygoid processes; **3**): pterygomandibular raphe; **4**): palatoglossus muscle or the anterior margin of the tonsillar fossa; **5**): uvula; **6**): palatopharyngeus muscle or the posterior margin of the tonsillar fossa.*

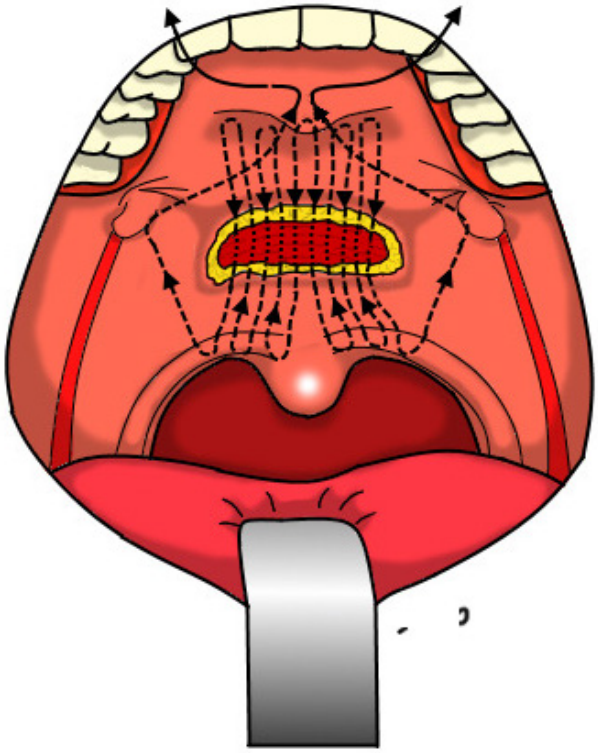

Fig. 2. *The main steps of the Modular Barbed Anterior Pharyngoplasty (MBAPh).*

strip of mucosa and the annexed minor salivary glands, to expose the palatal muscular layer.

3. One of the 2 BS needles is driven from the posterior nasal spine downwards through the muscular layer until it perforates the mucosa adjacent to the ipsilateral base of the uvula.
4. The needle is then reinserted through the same mucosal hole and driven upwards encircling the palatopharyngeal muscle and reemerging upwards at the level of the palatal aponeurosis (lateral to the posterior nasal spine.
5. The point 3) is repeated once to extend laterally the palatal muscular folding.
6. The needle is driven again from the palatal aponeurosis downward to encircle the palatopharyngeal muscle.
7. The needle is driven upwards to reach the ipsilateral pterygoid hamulus.
8. The needle is driven back to the posterior nasal spine.
9. The same maneuvers are repeated secularly on the opposite site using the other half of the BS (steps 1 to 9);
10. Finally, both threads are cut flush to the palatal mucosal covering of the posterior nasal spine.

DISCUSSION

BS is a relatively new device, introduced by John Alcamo in 1964. In recent years, this innovative suture gained popularity as an alternative to conventional materials, since its approval by the US Food and Drug Administration for soft tissue application in 2005. The advantages of BS have given surgeons a new tool for soft tissue suturing[6]. This stitch consists of permanent suture that has directional projections (or barbs) along its entire length, which imparts tensile strength without the need for tying. The stich is passed into the tissue in the opposite direction to the splay of the barb, allowing the suture to pass easily. When a force is applied in the opposite direction, the barb of the sutures grasps the surrounding tissue and secures the tissue in place. Currently three types of BS are commercialy available: The Quill Self–Retaining System (SRS) bidirectional BS (Angiotech, Vancouver, BC, Canada), V-Loc unidirectional BS (Covidien) and Stratafix unidirectional and bidirectional BS (Ethicon)[7]. The main limitation of the BS is its cost. However, the reduction in intraoperative time, reduction in length of hospitalisation and use of fewer stitches compared with standard ones may offset this increased cost (8).

In the MBAPh, at the end of the procedure, the semilunar mucosal gap is completely sealed, and the uvula is anteriorized. The tenso-structural modifications obtained with the procedure generate a muscular folding of the soft palate and suspension to the rigid fibro-osseous holds. The soft palate will result to be lifted, shortened, advanced and especially stiffened with an improved retropalatal space and reduced collapsibility. Surgical time was kept under 40 minutes and the procedure were bloodless. Patients were discharged two days after the operation. The same post-operative instructions (concerning diet, activity, and pain control) as those usually indicated after tonsillectomy are given to patients. Hyaluronan-containing mouthwash after meals are recommended during the first operative week.

All the cases were uneventful with no complication in the postoperative period. Hemorrhagic risk is rare

because of the hemostatic action of the BS. Thread extrusion through the oral and/or pharyngeal mucosa is not frequent (less than 10% of the case) and it is easily managed by cutting off the extruded part: usually it is better to wait the third postoperative weeks when the scarring is able to maintain the desired tensostructural modifications. Asymptomatic and spontaneously healing mucosal granulomas can appear 45-60 days after surgery. The published case series showed that the use of BS in OSA surgery is safe and effective (9). The main advantages of M.B.A.Ph over traditional surgery are:

1) It is a bloodless, safe, quick and repeatable surgery;
2) The stiffening of the soft palate is achieved through muscular folding and suspension to rigid holds and it;
3) It is based on the complete anatomic respect of palatal fibro-muscular structures;
4) BS assures homogeneous tissue tensioning along the full length of the thread, provides excellent tissue grip, avoids the need for knotting, does not alter any muscle function; moreover the action of BS is replaced over time by means of solid and stable tissue scarring.

Tonsil surgery (tonsillectomy or tonsillotomy) can be associated to M.B.A.Ph in case of grade 2 to 4 tonsils. In our experience, postoperative pain and recovery time are limited, especially if low-temperature plasma surgery is used (5).

- Modular Barbed Anterior Pharyngoplasty (M.B.A.Ph.) is a functional tenso-structural reconstruction of the soft palate indicated for mild to moderate OSA cases with an antero-posterior collapse at the DISE.
- The action of the BS is sustained over time by means of solid and stable tissue scarring.
- Our technique avoids palatal fibro-muscular resection and minimize iatrogenic bleeding (bloodless surgery).

ACKNOWLEDGEMENTS

I would like to thank Michelangelo Pierri for the Figures.

REFERENCES

1. Arnaud C, Bochaton T, Pépin JL, Belaidi E. Obstructive sleep apnoea and cardiovascular consequences: Pathophysiological mechanisms. Arch Cardiovasc Dis. doi:10.1016/j.acvd.2020.01.003.
2. Pang KP, Woodson BT. Expansion sphincter pharyngoplasty: a new technique for the treatment of obstructive sleep apnea. Otolaryngol Head Neck Surg 2007; 137(1):110-4. doi:10.1016/j.otohns.2007.03.014.
3. Mantovani M, Minetti A, Torretta S, Pincherle A, Tassone G, Pignataro L. The velo-uvulo-pharyngeal lift or "roman blinds" technique for treatment of snoring: a preliminary report. Acta Otorhinolaryngol Ital 2012; 32(1):48-53.
4. Salamanca F, Costantini F, Mantovani M, et al. Barbed anterior pharyngoplasty: an evolution of anterior palatoplasty. Acta Otorhinolaryngol Ital 2014; 34(6):434-8.
5. Rinaldi V, Costantino A, Moffa A, et al. Postoperative Pain and Wound Healing After Coblation-Assisted Barbed Anterior Pharyngoplasty (CABAPh): An Observational Study. Indian J Otolaryngol Head Neck Surg 2019; 71(S2):1157- 62. doi:10.1007/s12070-018-01577-8.
6. Crosetti E, Caracciolo A, Arrigoni G, Delmastro E, Succo G. Barbed suture in oral cavity reconstruction: preliminary results. Acta Otorhinolaryngol Ital 2019; 39(5):308-15. doi:10.14639/0392-100X-2130.
7. Moya AP. Barbed sutures in body surgery. Aesthet Surg J 2013; 33(3S):57S-71S. doi:10.1177/1090820X13499577.
8. Massoud W, Thanigasalam R, El Hajj A, et al. Does the use of a barbed polyglyconate absorbable suture have an impact on urethral anastomosis time, urethral stenosis rates, and cost effectiveness during robot-assisted radical prostatectomy? Urology 2013; 82:90-4.
9. Moffa A, Rinaldi V, Mantovani M, et al. Different barbed pharyngoplasty techniques for retropalatal collapse in obstructive sleep apnea patients: a systematic review. Sleep Breath 2020; 24(3):1115-27. doi:10.1007/s11325-020-02088-z.

Intraneural electrical stimulation of median nerve: a simulation study on sensory and motor fascicles

M. Stefano, F. Cordella and L. Zollo

Advanced Robotics and Human-Centred Technologies - CREO Lab, Università Campus Bio-Medico di Roma, Rome, Italy

Neuroprostheses can be an innovative solution to improve quality of life of upper limb amputees. In this framework, the recovery of sensory feedback is a property widely requested by amputee subjects. Neural prostheses are based on neural interfaces that allow delivering direct current stimuli to the nerve fibers. The study of the interaction between the nerve and the electrode is fundamental to investigate activation properties in the nerve. Furthermore, the results could provide useful insight into improve the design of the electrodes and to advance and ameliorate tactile sensations, elicited by these interfaces, obtaining tactile feedback more like natural sensations. This work aims at studying, by means of a FEM Neuron computational model, the axon fibers activation by means of neural stimulation provided through the intraneural electrodes DS-file. Three different types of stimulation waveforms (i.e. biphasic charge balanced stimulus with inter-pulse delay, biphasic charge balanced stimulus without inter-pulse delay, biphasic charge unbalanced stimulus with inter-pulse delay), three different nerve fascicles, i.e. two sensory and one motor fascicle, and ten distances from the electrode in the fascicles, are considered. The efficacy of the stimulation expressed as the percentage of activation of the fibers, and the safety, in terms of current intensity and used waveform, are studied in the previously described different conditions and the results are compared. The obtained results show that: i. stimulating a sensory fascicle with implanted active sites can activate a fascicle close to it, but not all the fascicles belonging to the same nerve. In fact, in the nerve considered in this study, a motor fascicle cannot be activated due to the values of the electrical potential which are too low to activate the fibers; ii. the current intensity necessary to activate fibers increases according to the distance from the source of the stimulus; iii. by using a biphasic charge unbalanced stimulus, the threshold to activate the fibers is lower than using the other tested waveforms. It is an important result because the stimulation is efficient and safer since current intensity is lower than the one used for the other two waveforms.

Neuroprostheses are a widely used solution for human nervous system injuries, disorders and disabilities. Thanks to these devices, an improvement of the quality of life of the patients can be reached. Neuroprosthetic devices are used for different kind of disease. For example, Parkinson (1), migraine (2) and other central nervous system diseases can be treated by Deep Brain Stimulation. Furthermore, neuroprosthesis also include retinal implants, to overcome some forms of blindness (3), or in case of spinal cord injuries to provide spinal cord stimulation for motor rehabilitation (4).

Thanks to neuroprosthetics, also upper limb amputees can obtain improvements in their quality of life. In fact, commercially available myoelectric upper limb prostheses allow to decode muscle electrical

Key words: Finite Element Method, Neuroprostheses, Computational model, Intraneural stimulation, ds-file electrode

Corresponding Author:
Dr Mattia Stefano,
c/o Advanced Robotics and Human-Centred Technologies - CREO Lab
Università Campus Bio-Medico di Roma,
Via Alvaro del Portillo 21, 00128 Roma
Tel.: 06 22541 9610 - Fax: 06 22541 9609
e-mail: m.stefano@unicampus.it

0393-974X (2020)

activity, recorded by myoelectric electrodes, and to provide patients with only an efferent control. These devices do not provide afferent information (5, 6), which are instead fundamental to interact with the environment. As reported in literature (5), the lack of sensory feedback is one of the main reasons for the prosthesis use abandonment.

Sensory feedback is a quality widely required by amputees to improve the dexterity and the embodiment of the robotic prosthetic hand (6). Therefore, several solutions for delivering sensations related to tactile feedback were proposed in the field of upper limb neuroprosthetics, such as electrotactile, vibrotactile, direct current stimulation, etc. Among them, the electrical neural stimulation of peripheral nerve is the technique that more than the others allow to restore sensory feedback eliciting sensations like natural ones (7-9). To electrically stimulate the nerves to restore sensory feedback, different interfaces were developed, such as intraneural or cuff electrodes and flat interfaces.

Due to the high invasiveness of the neural solution, it is fundamental to preliminary study the nerve-electrode interaction by means of computational simulations. From the simulation results, optimal stimulation parameters and location of the electrode into the nerve can be derived, to obtain a better fiber recruitment related to the tactile sensation to be provided to the amputees. The study of stimulation parameters and electrode implant properties from a computational framework can be a useful support guide to the experimental tests and can lead to design new generation of electrodes and novel interfaces suitable for restoring sensory feedback.

The study of neuroprosthetic devices and stimulation techniques through a computational framework is a useful method to set stimulation parameters and to study the interaction between nerve tissue and electrode, as demonstrated in recent papers (2, 10, 11). Several works deal with multiscale computational approach to study the nerve-electrode interaction, coupling the results from a Finite Element Model simulation and from computational axon or neuron model. In the study of Shiraz et al. (10), a computational multiscale method was used to study the pudendal nerve stimulation, different kind of stimulators, electrodes and tissues were considered, according to the location of the pudendal nerve. In (12), a similar problem it is considered: different kind of electrodes, Transverse Intrafascicular Multichannel Electrode (TIME) model and Flat Interface Nerve Electrode (FINE) model, are used.

The study treated the selectivity of these kind of electrodes using a fixed stimulus waveform. In this paper, a realistic computational model, using the Finite Element Method (FEM), of the human median nerve and of the ds-FILE intraneural electrode is introduced (13). This type of electrode is different from the electrodes used in (12). Its geometrical properties and active sites shape are different from the ones of the TIME model; furthermore, since it is an intraneural electrode, it has different characteristics with respect to the FINE model. The ds-FILE electrode has been already used in experiments on human amputees (6), making it particularly interesting for future comparison between the results obtained in simulation and the experimental ones.

In this work, fibers activation in sensory and motor fascicles, keeping the location of the electrode fixed, is studied. Focusing on the possible stimulation of a motor fascicle when active sites of the electrode are inside a sensory fascicle is an important issue that, to our knowledge, is still not covered by the literature. Further, to study the fibers activation, ten different distances from the electrode are considered in each fascicle. The three types of waveform used are the safest as reported in literature (14). The goal of this work is to study nerve fibers activation subject to a current stimulus. The stimulus waveform and the current level required to excite a population of nerve fibers in the target nerve are modelled. Potential distribution in two sensory and one motor fascicles was studied. The active sites of the electrode were positioned in a target sensory fascicle, the other sensory fascicle was close to this one (Fig. 1a) and the fascicle related to the motor fibers was at a certain distance from the sensory fascicles, as shown in Fig. 1b. For each fascicle ten different distances from the electrode were tested.

The MRG axon model (15) is used to evaluate the nerve fibers activation and recruitment. On the basis

of the results, conclusions can be drawn on how axon fibers located at different distances from the active sites in a nerve fascicle and in a fascicle close to it are activated, as a function of type of waveform signal and current amplitude.

The paper is structured as follows: in Section II, methods to generate the hybrid model and to investigate stimulus parameters are described, in Section III and IV results and discussion are provided. Section V reports conclusion and future perspectives.

MATERIALS AND METHODS

To obtain a realistic simulation of a human median nerve, a Finite Element Method model is built considering nerve anatomical properties. A current stimulus from the intraneural electrode is delivered to the nerve model and the electric potential distribution into the nerve is studied. After an interpolation of electric potential values on different sections of the axon fiber, the activation of the fibers is studied. Electric potential is used as external potential in an axon model built in Neuron software (16). The activation of the axons is evaluated by the generation of the action potential on the first and last node of Ranvier of the axon fiber. In the next subsections, a detailed description of the Finite Element Method model of the interaction between the electrode and the nerve and a description of the used axon model are provided.

A. Finite element model for nerve and electrode

To obtain a realistic human median nerve model, image data from the histological section of the human median nerve (17) are analyzed (Fig. 2a). The image is segmented using the software imageJ (Fig. 2b), and the obtained geometry is imported in COMSOL Multiphysics v5.3® (COMSOL, Ltd, Cambridge UK) and extruded along the longitudinal axis to build a 3D geometry (Fig. 2c). The nerve model is segmented in three different tissue classes: epineurium, perineurium, endoneurium.

Based on the literature (12), the values of conductivity are set as follows. Anisotropic conductivity tensor is assigned to endoneurium, with longitudinal value of 0.571 S/m and transverse value of 0.0826 S/m. The epineurium and perineurium are assumed isotropic media with a conductivity of 0.0826 S/m and 0.00088 S/m, respectively. The electrical conductivity related to the different tissues are shown in Table I. A homogeneous medium of saline solution simulates the intraoperative environment.

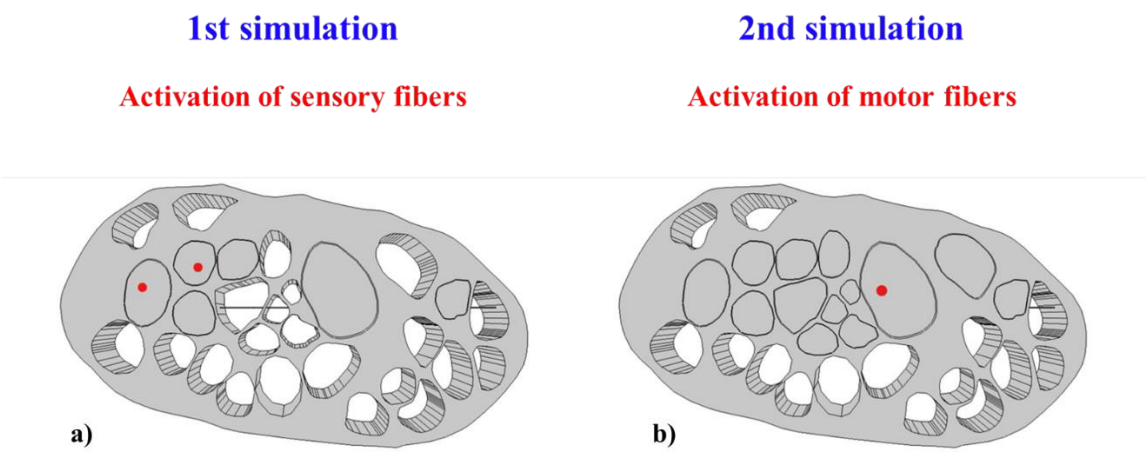

Fig. 1. ***a)****: Nerve fascicle with red spots related to sensory fibers;* ***b)****: nerve fascicle with red spot related to motor fascicle. They are considered to study electric potential distribution on axon fibers along the nerve, for ten distances from the active site.*

At the outer surface of the saline solution (cylinder) a Dirichlet boundary condition is set. A quasi-static approximation of the Maxwell's equations (18) is used as shown in the following equation

$$\nabla\cdot(\sigma\ \nabla V)=0$$

and the differential equations are solved using finite element methods (Fig. 2d). The radius of the external cylinder is set at 38 mm, that is larger than the dimension of the human median nerve (19). Two simulations are performed. From the first simulation, a nerve fascicle with active sites of the electrode implanted into it is considered. The electrical potential distribution into the target fascicle and in a nerve fascicle close to it is studied (Fig.1). These fascicles correspond to sensory fibers according to (17). In this simulation some fascicles far from the target fascicle are excluded from the computing to optimize it.

From the second simulation electric potential distribution into a fascicle, that according to literature could be related to motor fibers, are studied. According to studies of Jabaley (17), the electric potential distribution into the fascicle named Flexor Carpi Radialis is considered. The electrode position is the same of the first simulation Fig. 1. Also, other fascicles are included compared to the previous simulation, to understand how other fascicles affect the potential distribution into the nerve.

The electrode geometry is built in Comsol ® (Fig. 3) and the ds-FILE electrode is modeled as a polymide structure with 20 µm thickness and 360 µm height. Sixteen active sites are considered according to the ds-FILE properties (6). The conductivity of polymide is $6.7\cdot10^{-14}$ S/m and of active sites is $8.9\cdot10^{6}$ S/m. The electrode is placed trasversally at half height of the nerve model. The current amplitude is set to 10 µA, which is an arbitrary level to be scaled at subsequent stages.

Table I. *electrical conductivity related to different tissues.*

Tissue	Conductivity (S/m)	Reference
Endoneurium	0.571	(12)
	0.0826	
Epineurium	0.0826	(12)
Perineurium	0.00088	(12)

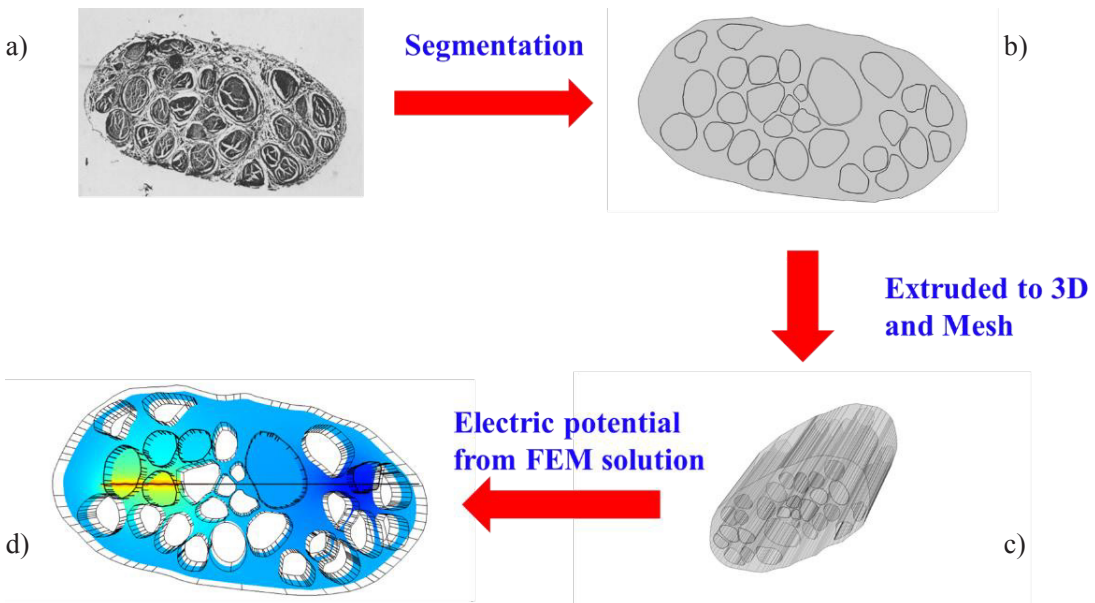

Fig. 2. *Scheme of the Finite Element Method model of the nerve fiber-electrode interaction.*

B. Median nerve axon model

A computational double layer model of myelinated axon is developed. Axons are grouped in fascicle in human median nerve. The axon model is considered to detect activation of nerve fibers with imperfect insulation, McIntyre-Richardson-Grill ion channel mechanisms for nodes of Ranvier (15) are considered. Between two nodes of Ranvier, two myelin, two paranodal and ten internodal sections (10) are considered. Axons diameters follow a two gaussian distribution cited in (20), myelinated nerve fibers fall in two classical groups, the smaller Aδ, and the larger Aα groups of fibers. The two gaussian have mean of 4 and 12 and standard deviation of 1.5 and 1 respectively (12, 20). All the geometrical properties are interpolated on data extracted from the work of McIntyre et al. (15), to obtain 100 axons of different geometrical properties, according to the diameter values extracted from the gaussian distribution.

The first node of Ranvier is randomly placed between 0 and Δx of the arclength of the nerve fiber. Note that Δx is defined as node to node distance for a fiber. Compartments are inserted between two nodes of Ranvier along the fiber and the model is ended by a node (10). This procedure is repeated for 100 fibers in the nerve as studied in (10).

A fiber is considered activated when the action potential propagates it along all the fiber length. The percentage of activation (PA) of fibers, defined as the number of activated fibers out of 100, is calculated. Models are imported in Neuron v7.4 to solve the differential equations using the Backward Euler integration method with 0.005 ms steps. Electrical potential along the nerve is solved in Comsol®,

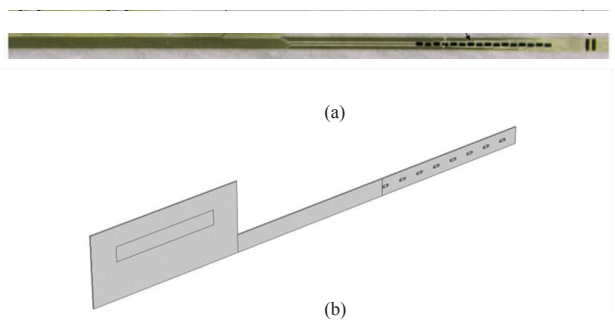

Fig. 3. *ds-FILE electrode (**a**); CAD model of the ds-FILE electrode (**b**).*

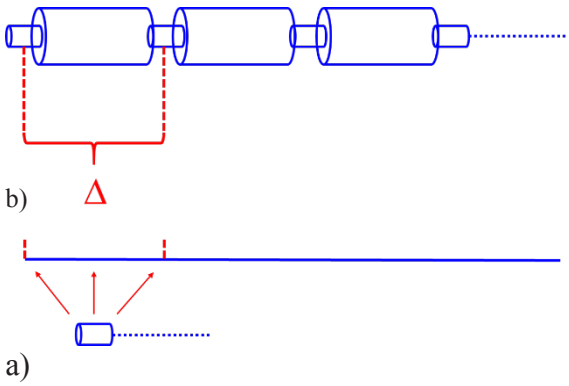

Fig. 4. *Schematic representation of the axon model. (**a**): The axon divided in different compartments: node of Ranvier (small cylinder) and myelin, paranodal and internodal sections (big cylinder). The distance between two nodes of Ranvier is defined as Δ. (**b**): The first node of Ranvier of the axon is randomly placed between 0 and Δ along the arclength of the nerve fiber, represented as the blue solid line.*

interpolated in Matlab ® to assign each electrical potential value to the different sections of axon, and imported as extracellular potential in Neuron on MRG axon model. The extracellular potential variation is performed according to the waveform shown in Fig. 4, 5, 7.

Three stimuli are considered, they are already proven in the literature as safe and effective as reported in (14) in terms of effective action potential initiation, tissue damage and corrosion of electrode materials. The three waveform considered (Fig. 5, 7) are: i) biphasic charge balanced pulses of 80 µs with inter-pulse delay of the same duration, ii) biphasic charge balanced pulses of 80 µs duration without an inter-pulse delay and iii) biphasic charge unbalanced pulses of 80 µs duration with inter-pulse delay of the same duration. Under quasi-static approximation, current values are multiplied to simulate different current amplitude. The percentage of activation of the fibers is measured for the three types of stimuli, the stimulus (i) is the same as described in (6).

RESULTS

In this section data related to the percentage of activation of human median nerve fibers in different fascicles (Fig.1) as the current stimulus

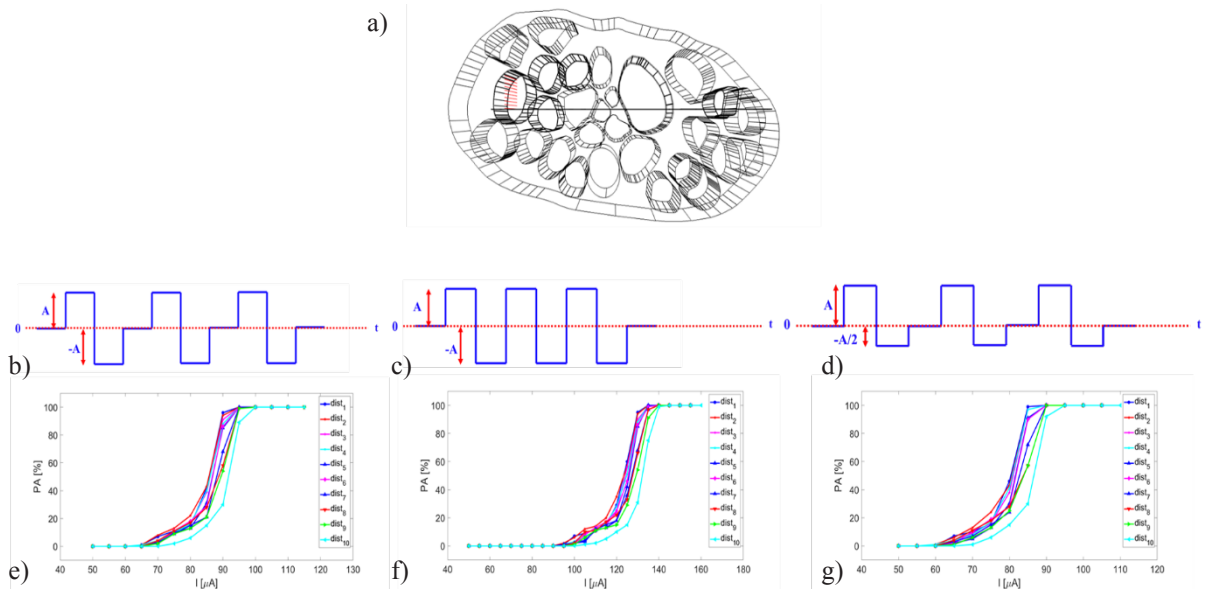

Fig. 5. ***a)****: 3D scheme of the target fascicle as shown in Fig.1: red lines highlight ten distances considered from the electrode in the fascicle. Three different types of stimulus waveform;* ***b)****: biphasic charge balanced stimulus with inter-pulse delay;* ***c)****: biphasic charge balanced stimulus without inter-pulse delay, d) biphasic charge unbalanced stimulus with inter-pulse delay. Time duration of pulses and inter-pulse delay is 80 μs;* ***e, f, g)****: Percentage of activation vs current amplitude, for the corresponding stimulus waveform;* ***b, c, d, respectively)****: for ten different distances from the active site in the same fascicle.*

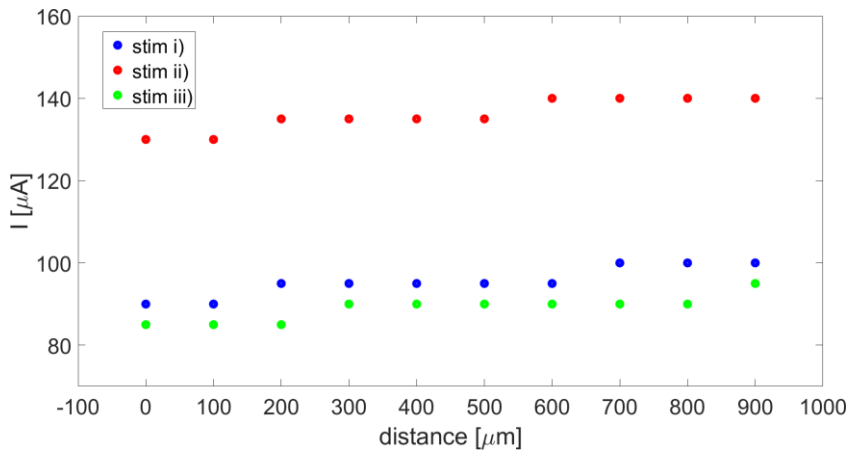

Fig. 6. *Current amplitude to obtain a 95% < PA < 100% vs distance from the active site, for three different stimulus waveform shown in Fig. 5.*

change are reported for the three different types of stimulus waveforms. In Fig. 5e, 5f, 5g the PA versus current intensity obtained using the first type of stimulus waveform is shown. The PA is studied for ten distances from the active site in the first target fascicle shown in Fig. 5a.

The PA versus current intensity is reported in Fig. 5e, 5f, 5g for the three different stimulation waveforms and for ten distances from the active site. Simulation were performed varying the current amplitude of the three different stimulus waveforms. From Fig. 5e, related to the biphasic charge balanced stimulus with inter-pulse delay, it is possible to observe that the current amplitude to activate axon fibers is in the range between 65 to 100 μA for all the distances from the considered active site. From Fig. 5f and Fig. 5g, it

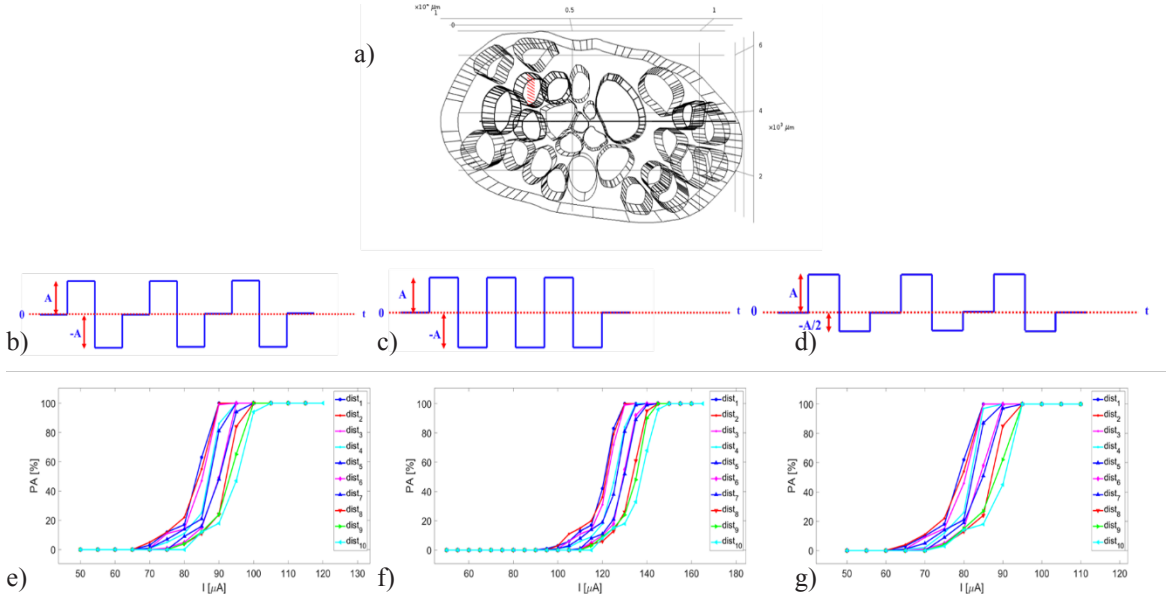

Fig. 7. ***a)****: 3D scheme of the target fascicle as shown in Fig.1: red lines highlight ten distances considered from the electrode in the fascicle. Three different types of stimulus waveform;* ***b)****: biphasic charge balanced stimulus with inter-pulse delay;* ***c)****: biphasic charge balanced stimulus without inter-pulse delay;* ***d)****: biphasic charge unbalanced stimulus with inter-pulse delay. Time duration of pulses and inter-pulse delay is 80 μs;* ***e, f, g)****: Percentage of activation vs current amplitude, for the corresponding stimulus waveform;* ***b, c, d respectively)****: for ten different distances from the active site in the same fascicle.*

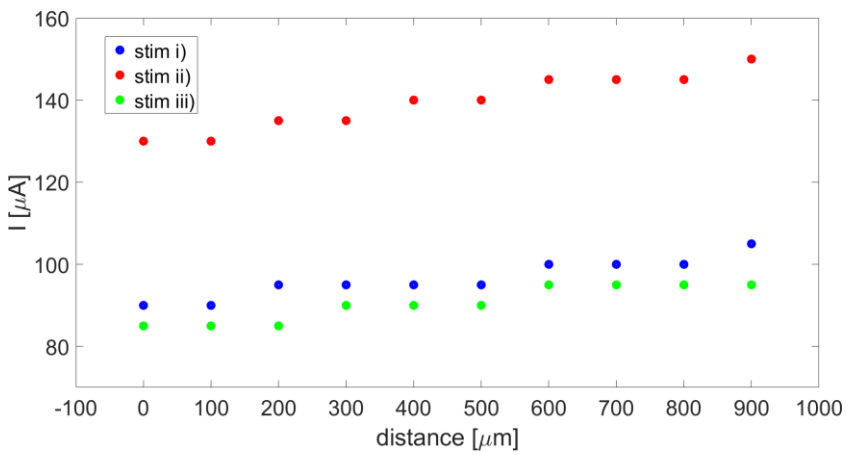

Fig. 8. *Current amplitude to obtain a 95% < PA < 100% vs distance from the active site in the second fascicle, for ten different distances.*

is shown that the current amplitude to activate axon fibers is in the range 95 to 145 μA and 60 to 95 μA, respectively. The corresponding waveform stimuli are the charge balanced stimulus without interpulse delay and the charge unbalanced stimulus.

The current amplitude ranges are found experimentally, starting from an arbitrary current amplitude value of 50 μA. For the PA evaluation three consecutive pulses are considered. Considering the ten distances from the active site from which the electrical potential distribution is evaluated, they are along all the course of the nerve. The first distance is close to the active site, other distances are 100 μm each from the other so the first is around some microns far to the active site and the last is 1 mm from the active site. All the distributions are in a

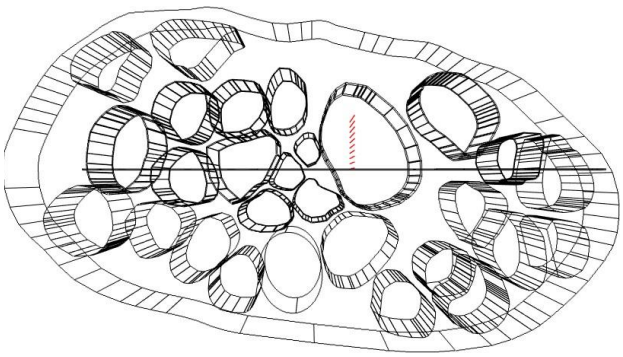

Fig. 9. *3D scheme of the motor fascicle. The red lines highlight ten distances from the electrode.*

nerve fascicle where the active site is implanted in. According to literature, this fascicle could be related to sensory fibers. In Fig. 6, the current amplitude necessary to obtain in the range 95%-100% of activated fibers for three different waveforms as the distance from the active site change is shown.

In Fig. 7e, 7f, 7g the percentage of activation as the current amplitude changes for the different waveforms are considered. The target fascicle considered is the second fascicle shown in Fig. 7a, the first distance considered is the lowest one in Fig.7 a close to the electrode and the other distances are 100 μm apart from each other. For such fascicle, the PA vs current amplitude was analogously studied. Results related to the fibers subjected to the i) stimulus waveform are shown in Fig. 7e, it is possible to note that starting from a current amplitude of 70 μA axon fibers are activated and a PA=100% is reached at 110 μA. Results shown in Fig. 7e, 7f are related to waveform signal ii) and iii). Axon fibers are activated starting from 95 μA and 65 μA and the PA=100% is reached at a current amplitude value of 150 μA and 110 μA, respectively. The minimum current amplitude to obtain a 95%-100% of activation for three different waveforms is shown in Fig. 8.

No plots are shown about the simulation related to axon fibers in motor fascicle shown in Fig. 9. From the simulation, it was found that the current amplitude necessary to activate the axon fibers is one order of magnitude higher than the current amplitude used to activate fibers in the fascicles shown above.

DISCUSSION

Computational FEM-Neuron hybrid models can be useful to design novel neural interfaces in the research field of upper limb prostheses. The same approach can be used to develop new modalities for restoring sensory feedback in upper limb amputees. A computational simulation allows to study electrical potential distribution into nerve fascicles subjected to an electrical current stimulus through an intraneural electrode.

The activation can be studied using an axon model built in Neuron. Knowing the activation properties is an important element to evaluate the efficacy of the neural stimulation. Therefore, the percentage of activation for three different stimulus waveforms by varying the stimulus intensity and the distance between the electrode and the possible location of an axon fiber is studied.

In Fig. 5, 7, it can be observed that the increase of current amplitude lead to an increase of percentage of activation of nerve fibers. They have the same trend for the three type of stimulus waveform and for both the fascicles considered. The current amplitude to activate axon fibers is different according to the signal waveform and the distance from the electrode into the considered fascicle. Regarding the fascicle in Fig. 5a, it is possible to note from Fig. 5e-5g that the current values to reach the 100% of activated fibers is different, in particular it is lower in the case of the third considered stimulus waveform and it is higher for the charge balanced ones. The same trend is observed in Fig. 7e-7g related to the second sensory fascicle.

Note that, observing the percentage of activation related to each waveform, Fig. 5e-5g for the first fascicle and Fig. 7e-7g for the second one, the current amplitude values necessary to activate a given percentage of fibers increase according to the distance considered from the active site. Values are different according to the considered waveform. The minimum values of current to obtain a 95% to 100% of activation, shown in Fig.6 for the first fascicle and in Fig. 8 for the second fascicle, allow to note that when the distance from the active site, i.e. the source of the current, increases, an increase of current is

required to activate a given percentage of axons.

A quantitative analysis has been done, showing that the safest waveform is the third one, because current values are lower than the corresponding ones for the other waveforms while the effectiveness of the stimulation is practically the same. The reason could be related to the sign of the stimulus and its time duration. To activate a neural cell, it is necessary to depolarize the membrane: if the depolarization is above a threshold, an action potential fires.

These results can be useful to know the range of current amplitude that had to be used to activate fibers selectively in a fascicle where the active sites of the electrode are in the inner part of the fascicle or in a fascicle close to it. Results about the motor fascicle percentage of activation as current amplitude varies are not shown, because they are not of interest in this framework. Note that the current amplitude required to activate nerve fibers, for all the waveforms, is one order of magnitude higher than that used to stimulate fibers close to the active site. Therefore, current values sufficient to activate sensory fibers in fascicles like those shown in Fig. 1a, cannot stimulate fibers in fascicles like those in Fig. 1b.

In this work a computational hybrid FEM NEURON model was used to study the electric potential distribution in the human median nerve and the activation of axon fibers into it. Two FEM computational simulations considering two different sensory fascicles and a motor fascicle were performed to investigate how an intraneural electrode fixed in each location in the human median nerve can activate axon fibers of sensory or motor fascicles. In the first simulation, a sensory fascicle with active site in the inner part of it was considered and activation properties in ten different distances from the electrode for three type of waveform stimulus and at different values of current amplitude to obtain an activation percentage above 95% is studied.

In the second simulation, a sensory fascicle close to the one analyzed in the first simulation and a motor fascicle were considered. The activation properties in ten different distances with respect to the inner part of each fascicle for three type of waveform as shown in Results and different values of current amplitude that let to obtain a percentage of activation above 95% are studied. The obtained results demonstrated that related to the sensory fascicles studied, the current amplitude to activate axons increases according to the distance from the electrode and the third stimulus is the safest because compared with the other waveforms the same percentage of activation can be obtained using lower values of current amplitude.

From the second simulation, it was observed that, if a stimulation of a sensory fascicle is performed using the current amplitude values considered in the results, the motor fascicle fiber was not activated, since the electric potential values are lower than the ones needed to activate the fiber. In fact, the needed value should be of one order of magnitude higher. Future work will be devoted to improving the analysis considering other sensory fascicles and considering different kinds of electrodes.

ACKNOWLEDGEMENTS

This paper has received funding from the European Union's Horizon 2020 research and innovation program under grant agreement No 899822, it was supported partly by INAIL prosthetic center with PPR AS 1/3 (CUP: E57B16000160005) project and partly by Fondazione ANIA with the project "Development of bionic upper limb prosthesis characterized by personalized interfaces and sensorial feedback for amputee patients with macro lesion after car accident".

REFERENCES

1. Deep Brain Stimulation for Parkinson's Disease Study Group, Deep-brain stimulation of the subthalamic nucleus or the pars interna of the globus pallidus in Parkinson's disease, New England Journal of Medicine 2001; 345(13):956-63.
2. Salkim E, Shiraz A, and Demosthenous A, Impact of neuroanatomical variations and electrode orientation on stimulus current in a device for migraine: a computational study, Journal of Neural Engineering 2020; 17(1):016006.
3. Humayun M. S, Weiland J. D, Fujii G. Y, et al. Visual perception in a blind subject with a chronic microelectronic retinal prosthesis, Vision research

2003; 43(24): 2573-81.
4. Angeli C. A, Edgerton V. R, Gerasimenko Y. P, Harkema S. J, Altering spinal cord excitability enables voluntary movements after chronic complete paralysis in humans, Brain, 2014; 137(5):1394-1409.
5. Cordella F, Ciancio A. L, Sacchetti R, Davalli A, Cutti A. G, Guglielmelli E, Zollo L, Literature review on needs of upper limb prosthesis users, Frontiers in neuroscience 2016; 10:209.
6. Zollo L, Di Pino G, Ciancio A. L et al. Restoring tactile sensations via neural interfaces for real-time force-and-slippage closed-loop control of bionic hands, Science robotics 2019; 4(27): eaau9924.
7. Raspopovic S, Capogrosso M, Petrini F. M. et al. Restoring natural sensory feedback in real-time bidirectional hand prostheses, Science translational medicine 2014; 6, 222:222ra19.
8. Rossini P. M, Micera S, Benvenuto A. et al. Double nerve intraneural interface implant on a human amputee for robotic hand control, Clinical neurophysiology 2010; 121(5): 777-83.
9. Tan D. W, Schiefer M. A, Keith M. W, Anderson J. R, Tyler J, Tyler D. J, A neural interface provides long-term stable natural touch perception, Science translational medicine 2014; 6:257-257ra138.
10. Shiraz A. N, Craggs M, Leaker B, Demosthenous A. Minimizing stimulus current in a wearable pudendal nerve stimulator using computational models, IEEE Transactions on Neural Systems and Rehabilitation Engineering 2016; 24(4):506-15.
11. Stefano M, Cordella F, Zollo L, The intraneural electrical stimulation of human median nerve: a simulation study, The 29th IEEE International Conference on Robot & Human Interactive Communication 2020; 1-6.
12. Raspopovic S, Petrini F. M, Zelechowski M, Valle G, Framework for the development of neuroprostheses: from basic understanding by sciatic and median nerves models to bionic legs and hands," Proceedings of the IEEE 2016; (105)1: 34-49.
13. Poppendieck W, Muceli S, Dideriksen J, Rocon E, Pons J. L, Farina D, Hoffmann K. P, A new generation of double-sided intramuscular electrodes for multi-channel recording and stimulation, 37th Annual International Conference of the IEEE Engineering in Medicine and Biology Society (EMBC) 2015; 7135-8.
14. Merrill D. R, Bikson M, Jefferys J. G, Electrical stimulation of excitable tissue: design of efficacious and safe protocols, Journal of neuroscience methods 2005; 141, 2:171-98.
15. McIntyre C. C, Richardson A. G, Grill W. M, Modeling the excitability of mammalian nerve fibers: influence of afterpotentials on the recovery cycle, Journal of neurophysiology 2002; 87(2):995-1006.
16. Hines M. L, Carnevale N. T, The neuron simulation environment, Neural computation 1997; 9(6):1179-1209.
17. Jabaley M. E, Wallace W. H, Heckler F. R, Internal topography of major nerves of the forearm and hand: a current view, The Journal of hand surgery 1980; 5(1): 1-18.
18. Bossetti C. A, Birdno M. J, Grill W. M, Analysis of the quasi-static approximation for calculating potentials generated by neural stimulation, Journal of neural engineering, 2007; 5(1):44-53.
19. Brill N. A, Tyler D. J, Quantification of human upper extremity nerves and fascicular anatomy, Muscle & nerve 2017; 56(3):463-71.
20. 20. Vallbo A. B, Johansson R. S, Properties of cutaneous mechanoreceptors in the human hand related to touch sensation," Human Neurobiology 1984; 3(1):3-14.

New methods and tools to assess nutritive sucking in new-borns: effect of different feeding bottles on nutritive performance

F. Taffoni[1], V. Focaroli[2,3], A. M. Visco[4], F. Noce[5] and R. Lubrano[4,6]

[1]Advanced Robotics and Human-Centred Technologies - CREO Lab, Università Campus Bio-Medico di Roma, Rome, Italy; [2]Istituto di Scienze e Tecnologie della Cognizione (ISTC), CNR, Rome, Italy; [3]Laboratory of Developmental Neuroscience, Università Campus Bio-Medico di Roma, Rome, Italy; [4]Complex Operative Unit of Pediatric and Neonatology, ASL Latina, 04100 Latina, Italy; [5]Università degli Studi Roma Tre, Rome, Italy; [6]Università degli Studi di Roma La Sapienza, Italy.

Nutritive sucking is a fundamental process assuring the primary infant nourishment in the first months of life. When feeding is impaired for pathological conditions, the growth of the infant may be delayed with a cascade effect on the overall development. While literature studied nutritive sucking development in infants with feeding problems, like in severe premature babies or with low weight at birth, few works assesses to what extent different feeding bottles may influence feeding performance of healthy new-borns. This work proposes a method for functional characterization of feeding bottles based on the most promising and reliable indices used to quantitatively assess feeding skills in clinical applications. Thirty healthy new-borns have been fed with two different bottles instrumented with a device for feeding monitoring. Their impact on feeding performance is objectively assessed and discussed. The approach presented here, even if preliminary, paves the way to a new method for functional characterization of feeding bottles. Further studies may allow to confirm our analyses with a higher number of bottles and infants.

The Nutritive Sucking (NS) is a highly organized process (1) that guarantees the primary source of nourishment in the first six months of infant life (2). Ultrasound techniques have been exploited to study *in-vivo* mechanisms of NS as well as to compare the anatomy of nipples and the morphology of artificial teats (3, 4). During NS, the lips are sealed around the nipple, the jaw and tongue drop down and away from the palate, enlarging the oral cavity and creating negative intraoral sucking pressure (IP) while the tongue is used to compress the nipple against the hard palate, thus generating a positive expression pressure (EP) (5). Such combined action allows extracting milk from the breast and it is the result of a long process, beginning during the first quarter of gestational life (10-11 weeks), when the brain development is coupled with the development of anatomic structures such as lips, jaw, cheeks, tongue, palate, pharynx and larynx. Oral and gag reflexes appear around 12 to 16 weeks, sucking at 24 weeks, while the concurrent presence of sucking and swallowing by 28 weeks, although not fully coordinated until about 32 to 34 weeks (see (6) for a review).

When the developmental sequence presented above is modified (as in extreme premature birth) it is quite common to observe feeding problems. In a recent pilot study, Tamilia and colleagues (7) showed a correlation between neuroimaging-demonstrated microstructural brain abnormalities and variations

Key words: nutritive sucking, technology-aided assessment, feeding performance

Corresponding Author:
Dr Fabrizio Taffoni,
c/o Advanced Robotics and Human-Centred Technologies,
CREO Lab, Università Campus Bio-Medico di Roma,
Via Alvaro del Portillo 21, 00128 Roma
Tel.: 39 06 22541 9464 - Fax: 39 06 22541 9609
e-mail: f.taffoni@unicampus.it

0393-974X (2020)

in NS patterns of extreme premature infants. Lau and colleagues (8) studied NS in preterm babies bottle-fed, and found a progressive development of the IP both in terms of rhythm and intensity, and in terms of coordination with the EP. Medoff Cooper and colleagues compared IP in preterm and full-term infants and found differences in sucking behaviors as a function of gestational age at birth as well as the interaction of maturation and experience (9). In (10), authors characterized differences in maturation of feeding between healthy preterm and full-term infants exploiting objective features derived from IP and EP respectively. Pineda and colleagues (11) proposed the use of a standardized feeding assessment tool to identify differences in oral feeding performance, along with differences in specific types of feeding-related behaviors, among full-term infants compared with preterm infants at term equivalent age.

Analysis has been carried out addressing the impact of different bottles of sucking performance on healthy infants. This is a very important topic since craniofacial growth and development is influenced by functional stimuli such as sucking, chewing, swallowing and breathing (12). The main studies available in literature (13-16) are focused on functional characterization of nipples. The bulk of research looks at sucking pattern and milk flow: the more rapid milk flow from soft artificial nipples with large holes results in more frequent swallowing, less frequent opportunities for breathing, and significantly increased interruption in ventilation (17).

To the best of our knowledge, no studies have yet analyzed the effect of different feeding bottles on NS in healthy newborns. This research aims to address this lack and proposes the measure of the most promising and reliable indices used to quantitatively assess feeding skills in clinical applications (see (18) for a review), in order to identify how different features of feeding bottles can influence NS and can promote feeding performance in healthy newborns.

Since this preliminary work aims to present the feasibility of the approach, only two bottle

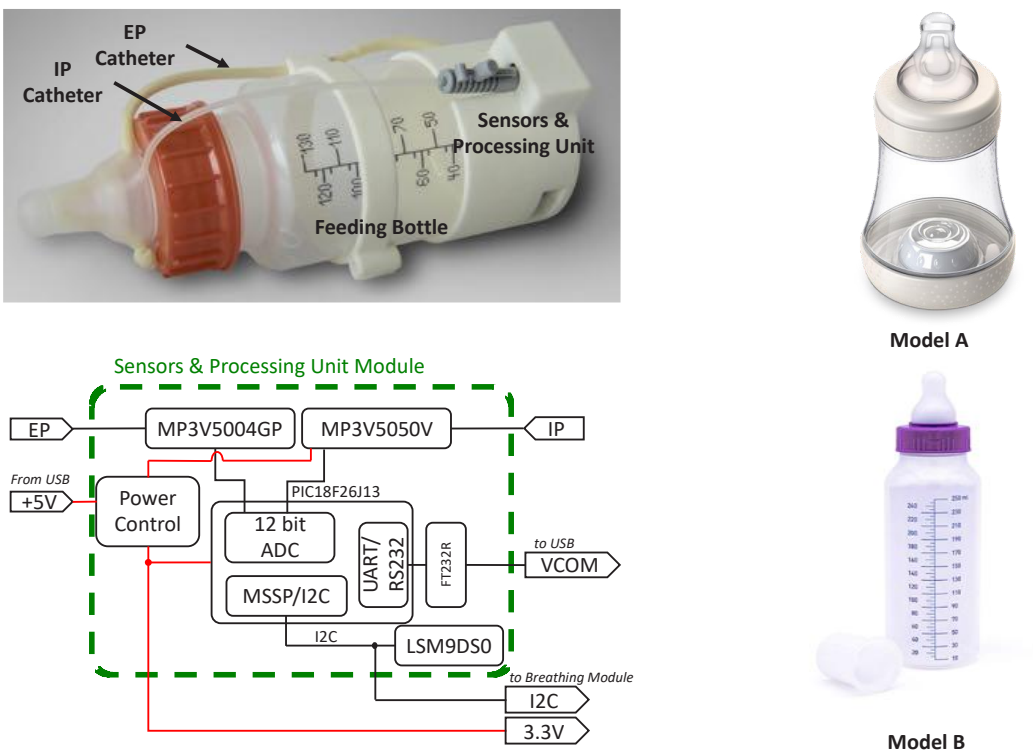

Fig. 1. *On the left, the FAM system: top) example of mounting on a sample bottle; bottom functional diagram of the Sensors and processing unit module. More details are available in 20 On the right the two bottles compared in this study.*

Table I. *Newborns enrolled in the study.*

Enrolment code	Weight [g]	Gestational Age		Sex
		Weeks	Days	
001	3490	37	2	M
002	2865	40	0	F
003	4320	38	4	M
004	2020	39	0	F
005	3300	37	6	F
006	2900	38	4	F
007	3100	38	0	M
008	3190	38	3	F
009	3290	38	6	M
010	3030	39	6	F
011	3170	39	5	F
012	2110	37	4	M
013	4390	41	4	F
014	2750	36	4	F
015	3370	40	2	M
016	2350	37	2	F
017	2200	37	3	F
018	2190	37	4	M
019	2170	36	0	M
020	3860	40	2	M
021	3300	39	3	F
022	2950	41	1	M
023	3130	40	4	M
024	3460	40	3	F
025	3250	38	0	F
026	2740	38	4	M
027	3450	40	0	M
028	2920	38	2	M
029	2080	36	1	M
030	2300	39	2	F

models have been compared. The materials and methods section presents the tool used to measure sucking pressure exerted by infants during feeding, the feature considered for the analysis, the data analysis performed, and the experimental procedure. The result section describes the main differences observed in the population when fed with the two different feeding bottles. Finally, the discussion and conclusion section provide the interpretation of results and show how to exploit quantitative and objective parameters to assess the overall performance of the feeding task in healthy infants.

MATERIALS AND METHODS

System for objective assessment of nutritive sucking

The work aims to present a method for functional comparison of feeding bottles in healthy newborns capable of autonomous bottle feeding, for this reason the analysis presented is based on the measure of the only IP, one of the main variables considered in literature (9, 19). Indeed, according to the seminal work of Lau and colleagues (8), a well-defined and rhythmic IP is characteristic of full-term healthy newborns, and its attainment, represents the last developmental stage of NS in premature babies.

IP pressure has been measured using the Feeding Assessment Monitor (FAM), an instrumented module developed by the authors to assess the autonomous feeding readiness in preterm infants, see Fig. 1. The module can be easily mounted at the base of the bottle using mounting flanges. It is provided with two pressure sensors to measure IP, EP and can be also expanded to measure breathing frequency (20). In this study, the FAM has been configured to measure the only IP with a sample frequency of 200Hz. An uncompressible air-filled catheter for gavage (PVC feeding tube, Teleßex Medical, 2E040205; internal diameter: 1 mm, external diameter 1.7 mm, length: 200 mm) has been used to connect the IP sensor (a MP3V5050V, by Freescale Semiconductor) with the mouth: the catheter enters the feeding teat through an incision at its base and it is threaded out at the tip, protruding about 2 mm in the oral cavity as in (10).

Two bottles have been compared: Model A is provided with a silicone membrane to allow bottle ventilation and avoid the establishment of a negative pressure inside the bottle during NS. It is equipped with a teat whose shape

is modelled to fit with intraoral cavity of a newborn thus promoting his/her latching-on. Model B is a disposable feeding bottle equipped with a standard teat with a conventional symmetric geometry and not provided with a valve for bottle ventilation. The raw pressure data are stored in the text file for later off-line feature extraction and off-line analysis (see Data Analysis section).

Participants

The study has been carried out in the Complex Operative Unit of Paediatric and Neonatology of Ospedale Civile Santa Maria Goretti in Latina (Italy), as part of the daily clinical routine. Parents of the newborns signed a written informed consent describing the purpose of the study (1). Thirty newborns (15 males) not breastfed were recruited by the medical team in their first month of life. Infants were all born between the 36th and 40th weeks of gestational age (mean 38th week and 5 days) and capable of autonomous bottle feeding. Table I reports the descriptive statistics of the sample enrolled in the study, in terms of weight, gestational age and sex.

Procedure

Each baby enrolled in the study was fed with the two bottles in the same day. Both models were instrumented with the FAM device just before the feeding session and filled with the quantity of milk requested from the dietary necessities of the infant. A nurse or a parent was asked to feed the baby while a second person, trained in the use of the FAM, takes care of data acquisition (Fig. 2).

Fig. 2. *Experimental setup.*

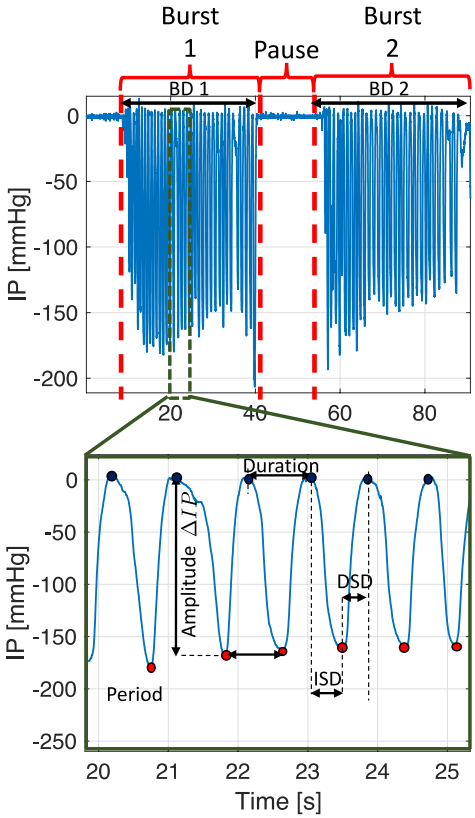

Fig. 3. *Automated segmentation of IP. The software marks each suck as a local minimum (red circle) between two local maxima (blue circle). Sucking events are grouped in the same burst if the pause between two consecutive sucks is lower than 2 s. In figure, the main variables analized are reported. Additional details on segmentation are available in (11).*

Fig. 3 reports an example of data segmentation and the extraction of the main features for burst and single suck assessment. The normality of the features has been tested with the Kolmogorov-Smirnov test (k-test) and the inter-subject comparison performed with a two-sample t-test or with the Wilcoxon rank sum test, depending on the distribution type (normal vs non-normal distribution respectively). Automated segmentation of IP. The software marks each suck as a local minimum (red circle) between two local maxima (blue circle). Sucking events are grouped in the same burst if the pause between two consecutive sucks is lower than 2 s. In figure, the main variables analyzed are reported. Additional details on segmentation are available.

The bottle presentation order was randomized from infant to infant, to avoid any presentation bias. IP data recorded from FAM were stored in a text file saved as "subjectEnrolmentCode_feedingSession.txt". A Case

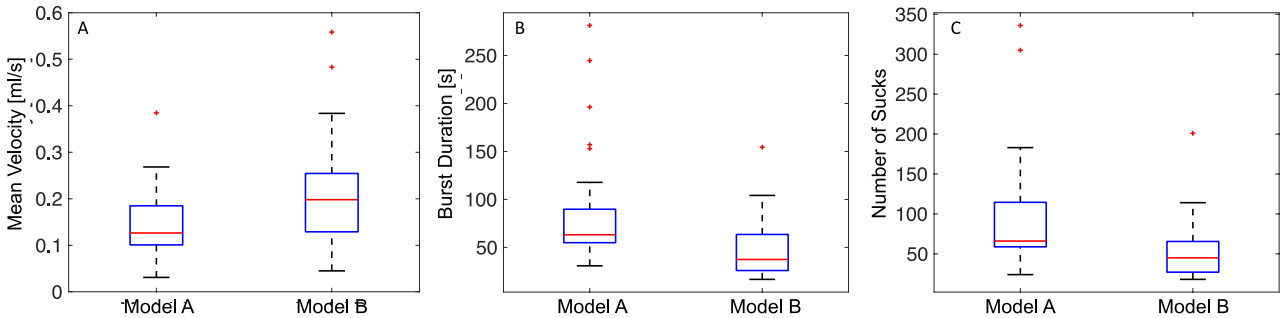

Fig. 4. ***A)****: Mean sucking velocity;* ***B)****: overall duration of the bursts started during the first minute of feeding;* ***C)****: Overall number of sucking events for the bursts taken in consideration.*

Repot Form (CRF) was filled reporting the quantity of milk effectively delivered, the duration of the feeding session, and the occurrence of any feeding problem reported from medical staff, like frequent interruptions for burping or regurgitations. All data gathered were processed to extract features of performance by blind coders.

Data Analysis

The analysis of feeding sessions was carried out taking into consideration both the information reported on the CRFs and the quantitative data about IP measured with FAM. Regarding these ones, it was necessary to extract features describing performance. NS is organized in sequences of sucks called bursts. Each burst is isolated from another by a period of inactivity (i.e. a pause) lasting at least 2 seconds (18). IP data were reviewed to identify all the bursts started in the first minute of feeding thus standardizing the analysis across different feeding sessions. IP segmentation was carried out according to (10): each suck was identified as a negative peak in the IP trace, and a burst as a sequence of sucks closer than 2 seconds each other. Quantitative features about timing, amplitude, and regularity of suction were extracted from the bursts selected as well as from the single suck event to perform a microstructural sucking analysis as reported in (9). In details, the microstructure of a single sucking event was assessed in terms of:

- Sigle Suck Duration (mean, maximum, initial and final) is the duration of a single suck, expressed in seconds.
- Sucking Amplitude (mean, maximum, initial and final) – it expresses the depressurization peak (in mmHg) inside the oral cavity for each suck. Initial and final amplitudes were measured as the average depressurization peaks registered from the first and the last five sucking events, respectively. This criterion was adopted for all variables which have initial and final measures.
- Coefficient of Variation of Duration (COV_D) – it expresses the variability of the duration of single sucks.
- Increasing Sucking Duration (ISD – mean, minimum, maximum, initial and final). The IP pressure is characterized by an increasing phase (IS), when the depressurization inside the mouth of the baby increases, and a decreasing phase (DS), when pressure inside the mouth returns to its original level. During IS phase, the tongue moves forward arching the nipple, while the mandible goes down to extent the oral cavity and get milk. In the DS, the mandible, and the tongue throwback to the initial position, with time constant depending on mechanical feature of the anatomical structures involved, nipple included. The ISD represents the duration of the IS phase, expressed in seconds.
- Increasing Sucking Slope (ISS mean, initial and final) expresses the ΔIP/ISD ratio or, in other terms, the mean velocity of depressurization measured for the single suck.
- Smoothness: this feature quantifies the regularity of movement. According to (21) the first derivative of the IP signal (i.e. the speed of variation of the IP) has been calculated and the local maxima of the trace obtained have been counted. This value, with the negative sign, is called smoothness referred to the speed profile (σ_pk): the lower this value, the lower the regularity of the sucking.

Bursts were assessed according to the following indices:

- Burst Duration (BD) – it concerns the overall duration (in seconds) of the bursts started in the first minute.

- Number of sucks – is the number of sucks measured in the bursts started in the first minutes.
- Number of pauses – is the number of pauses recorded in the first minute.
- Coefficient of Variation of Amplitude (COV_A) – it expresses the variability of sucking pressure in a single burst. It is defined as follows: $cov_A = \frac{\sigma_A}{\overline{IP}}$, where σ_A represents the standard deviation of the amplitude, and $\overline{IP}$, its mean in the sequence of bursts;

RESULTS

One participant refused Model B, for this reason he was excluded from the analysis. The remaining 29 subjects (14 males) have a mean gestational age of 38 weeks and 6 days. The analysis of data reported on the CRF showed a significative difference in the mean velocity of feeding, lower with Model A than Model B (mdn: 0.127 vs. 0.198 ml/s, z=-2.1461, p=0.03, Fig. 4A). No significative differences were observed in the effective amount of milk extracted from the bottle.

Overall, 4403 versus 2812 sucking events were recorded from the bursts started in the first minute, respectively with Model A and Model B. Burst duration was higher with model A (mdn: 63.17 vs. 37.45 s, z=3.4524, p<<0.01, Fig. 4B): coherently a higher number of sucking events was registered with Model A (mdn: 66 vs. 45, z=3.1736, p=0.0015, Fig. 4C).

The amplitude of sucking reached by newborns was lower with Model A than with Model B (mdn: -133,14 vs. -114.34 mmHg, z= -2.4260, p=0.015, Fig. 5A): In both models, the amplitude of sucking was significantly higher at the end of the burst: for Model A it was -83.11 vs -49.28 (z: -2.7370, p=0.0062, Fig. 5B): for Model B it was: -69.21 vs. -42.71 mmHg (z:-3.4524 e p<<0.01, Fig. 5C): No differences of amplitude were observed between models in the initial and final phases of the burst.

Regarding the microstructural analysis of the sucking events, no differences were observed in terms of instability or ISS, while a significantly longer ISD was observed for Model A respect to Model B (mdn: 0.464 vs. 0.439 s, z=2.0528, p=0.0401). Because the CRF, 10 out of the 29 infants analyzed reported annotations of frequent interruptions for burping

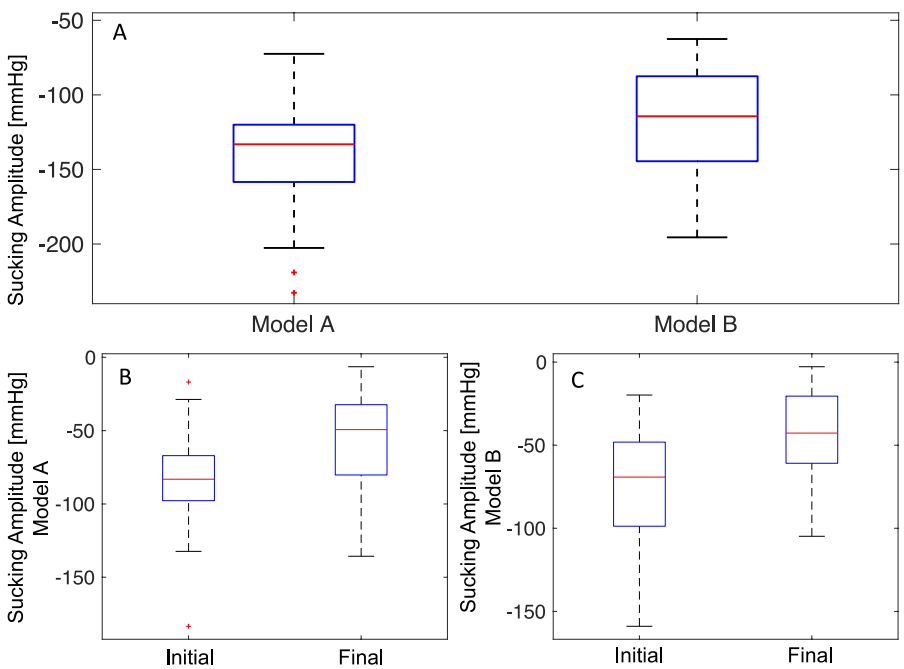

Fig. 5. ***A)****: Maximum Sucking Amplitude;* ***B-C*** *comparison between initial and final sucking amplitude registered with Model A and Model B respectively.*

or regurgitations, these babies were reconsidered for a separated cross-over analysis to identify any difference in the performance registered with the two feeding bottle models. Even in this subgroup, the mean sucking velocity was higher with Model B than model A (mdn: 0.1106 vs. 0.2034 s, z=-2.0788, p=0.0376, Fig. 6). The higher duration of the bursts measured with model A is confirmed and incremented (mdn: 58.93 vs. 30.81 s, z=2.9103, p<<0.01, Fig. 6B). Coherently, the number of sucking events increased, and it was significantly higher with Model A (65 vs. 33, z=2.6487, p=0.0081, Fig. 6.C).

The amplitude of sucking showed a statistical trend both for the mean and the minimum IP (i.e. the maximum depressurization level). In details, mean IP was -66.85 vs. -48.78 mmHg respectively for Model A and B (z=-1.9276, p=0.0539, Fig. 7.A). This trend is due to a significant change in the mean IP registered with model B in the subgroup: the IP increases from -61.93 mmHg, measured in the overall group, up to -48.78 mmHg. On the contrary, the mean pressure measured for Model A in the subgroup (-66.85 mmHg) remains very close to the one measured for the overall sample (-71.23 mmHg). The maximum depressurization level reached -144.83 vs. -117.93 mmHg (model A vs Model B, z=-1.9486, p=0.0518). Looking at any differences between the beginning and the end of the burst, no significant differences were observed with Model A, while it was registered a significant increasing in depressurization level when infant were fed with Model B: -69.44 vs. -25.26 mmHg respectively at the beginning and at the end of the burst (z: -2.4568, p = 0.0140, Fig. 7.B). Even in this subgroup, infants fed with Model A showed an ISD longer than the one registered with model B (mdn ISD: 0.483 vs. 0.449 s, z=2.1544, p=0.03, Fig. 7.C). No differences were observed in terms of instability or ISS.

DISCUSSION

This work aims at introducing a method to compare different feeding bottles in infants capable of autonomous feeding. While many studies analyze feeding skills in preterm newborns with feeding difficulties, few works address this topic in healthy infants. Generally, those studies investigate only the flux of the teats without considering the overall performance of the feeding task. This is an important aspect because, beyond to promote a proper nutrition, it provides functional stimuli useful for craniofacial growth and development. For this reason, it is important to identify the characteristics of the bottle that better promote sucking.

This preliminary study compares two bottles, one provided with a ventilation valve at the base and with a slow flux teat with anatomical shape (Model A), one disposable model without any ventilation valve and with a classical slow flux teat with radial symmetry (Model B). The analysis of data shows how, for the same quantity of milk, infants fed with Model A have a slower suction characterized by longer bursts with a higher number of sucking events. A similar result is also observed in the subgroup of

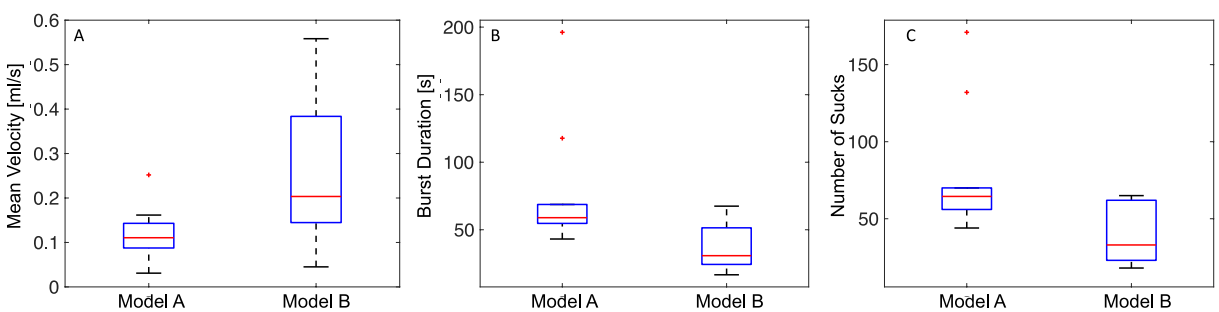

Fig. 6. *Data of subjects with annotation of feeding problems. **A**): Mean sucking velocity; **B**): overall duration of the bursts started during the first minute of feeding; **C**): Overall number of sucking events for the bursts taken in consideration.*

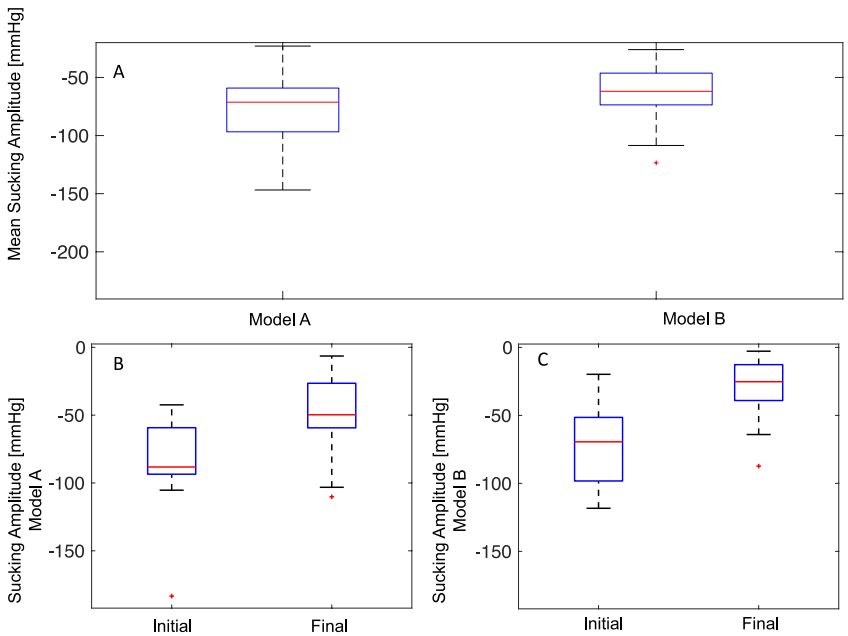

Fig. 7. *Data of subjects with annotation of feeding problems. **A**): Mean sucking velocity; **B**): overall duration of the bursts started during the first minute of feeding; **C**): Overall number of sucking events for the bursts taken in consideration.*

ten babies with the annotation of feeding problems in the CRF. This first finding seems to suggest a lower flux with Model A than Model B. This interpretation is further confirmed by findings about the ISD. The increasing of suction is obtained thanks to the active contraction of muscles involved in the process. Longer duration of increasing sucking phase without a significant difference in the mean IP would confirm a lower flux from Model A. Coherently with this interpretation, the data show longer ISD for Model A, both in the overall sample and in the subgroup of infants with annotation of problems. Regarding sucking amplitude, data on the overall sample do not show any difference in terms of mean IP, while it is observed a higher depressurization with Model A.

Looking at depressurization level in the subgroup with annotations of problems, it is observed a trend in the IP both for the mean values and for the maximum depressurization level. In details, higher depressurizations were observed with Model A. These findings may suggest a worst latching with Model B as well as differences in the milk flux. Results concerning the subgroup with annotations of problems seem to suggest the former interpretation: poor latching-on can cause air ingestion which reduce the depressurization inside the mouth and cause burping or regurgitations.

Regarding fatigue, it is useful to consider the differences observed in sucking amplitude between the beginning and the end of the bursts started in the first minute, when the effect of fatigue should be more evident. Babies show a significant reduction in the IP amplitude with both models: at the end of the bursts the module of IP was lower of about 40% with respect to the one measured at the beginning. This reduction is physiological and due to sucking activity, but what is interesting to note is the temporal scale in which it takes place. The overall duration of the bursts measured with Model A is 69% higher than the burst duration measured with model B (mdn: 63.17 vs. 37.45 s). More interesting, in the 10 babies with annotations of burping or regurgitation, we found a significant difference in the IP amplitude measured at the beginning and at the end of the burst only for model B.

This finding, and in particular the absence of a significant difference in the IP amplitude measured at the beginning and at the end of the bursts for Model

A in the subgroup with annotation of problems, may suggest an effect of the silicone membrane at the base of Model A. This membrane, allowing air passage into the feeding bottle, avoids the creation of a negative pressure inside the bottle that may hinder the milk extraction. This effect is more evident and confirmed in children with problems of regurgitation and/or burping, as the ones considered in the subgroup.

Looking at any irregularity, we considered the smoothness that we measured in terms of number of peaks in the IP velocity, and the coefficients of variation for IP amplitude and duration. These features do not present any significant differences both in the overall group and in the subgroup with annotation of difficulties. These findings can be explained with the consideration that regularity deficits are usually observed in infants not ready for autonomous oral feeding, typically in preterm children, younger than 36 weeks of gestation. In this study, we only considered older infants with a mature feeding, thus, we do not have a chance to observe differences due to the readiness to autonomous oral feeding. The only possibility was to observe a change in the pattern of suction due to the model of the feeding bottle, but this was not the case.

In conclusion, the proposed method allowed to assess the overall performance of the feeding task in healthy infants, using two different models of feeding bottle. The analysis of quantitative data and of the annotations reported in the CRF show how Model A promotes longer bursts with higher number of sucking events. This pattern is a characteristic of breastfeeding and allows a longer stimulation of craniofacial structures, thus promoting their development. Moreover, we measured a better latching-on confirmed by the analysis of data in the subgroup with annotation of problems during feeding.

Finally, the microstructural analysis of feeding suggests a reduced fatigue effect with model A. The approach presented here, even if preliminary, paves the way to a new method for functional characterization of feeding bottles, to identify quantitative and objective parameters to compare their functions on-field. Further studies may allow to confirm our analyses with a higher number of bottles and infants.

ACKNOWLEDGEMENTS

This work was partially supported by Artsana S.p.A in agreement with the Italian legislation on sponsorship for non-profit research (D.M. 17/12/2004).

REFERENCES

1. Goldfield EC, Richardson MJ, Lee KG, S Margetts. Coordination of sucking, swallowing, and breathing and oxygen saturation during early infant breast-feeding and bottle-feeding. Pediatr Res 2006; 60(4): 450-455.
2. World Health Organization. Global strategy for infant and young child feeding. Geneva: WHO Publications 2002.
3. Weber F, Woolridge MW, Baum JD. An ultrasonographic study of the organization of sucking and swallowing by newborn infants. Dev Med Child Neurol 1986; 28:19-24.
4. Nowak AJ, Smith WL, Erenberg A. Imaging evaluation of artificial nipples during bottle feeding. Arch Pediatr Adolesc Med 1994, 48:40-42
5. Woolridge MW. The 'anatomy' of infant sucking. Midwifery 1986; 2 (4):164-71.
6. Pinelli J, Symington AJ. Nonnutritive sucking for promoting physiologic stability and nutrition in preterm infants. Cochrane Database of Systematic Reviews 2005.
7. Tamilia E, Parker MS, Rocchi M, Taffoni F, Hansen A, Grant PE, Papadelis C. Nutritive sucking abnormalities and brain microstructural abnormalities in infants with established brain injury: a pilot study. J Perinatol 2019; 39(11): 1498-1508.
8. Lau C, Alagugurusamy R, Schanler RJ, Smith EO, Shulman RJ. Characterization of the developmental stages of sucking in preterm infants during bottle feeding. Acta Paediatr 2000; 89(7): 846-52.
9. Medoff-Cooper B, Mcgrath JM, Shults J. Feeding patterns of full-term and preterm infants at forty weeks postconceptional age. J Dev Behav Pediatr 2002; 23(4): 231-6.
10. Tamilia E, Formica D, Scaini A, Taffoni F. An

automated system for the analysis of newborns' oral-motor behavior. IEEE Trans. Neural Syst. Rehabilitation Eng 2015; 24(12):1294-1303.
11. Pineda R, Prince D, Reynolds J, Grabil M, Smith J. Preterm infant feeding performance at term equivalent age differs from that of full-term infants. J Perinatol 2020; 40 (4): 646-54.
12. Chen X, Xia B, Ge L. Effects of breast-feeding duration, bottle-feeding duration and non-nutritive sucking habits on the occlusal characteristics of primary dentition; BMC Pediatr 2015; 15(1): 46.
13. Fadavi S, Punwani IC, Vidyasagar D. Mechanics and energetics of nutritive sucking: a functional comparison of commercially available nipples. J Pediatr 1997; 130:740-5.
14. Mathew O. Nipple units for newborn infants: a functional comparison. Pediatr 1988; 81:688-91.
15. Mathew O, Belan M, Thopil CK. Sucking patterns of neonates during bottle feeding: comparison of different nipple units. Am J Perinatol 1992; 9:265-9.
16. Jackman KT. Go with the flow: choosing a feeding system for infants in the neonatal intensive care unit and beyond based on flow performance. Newborn Infant Nurs Rev 2013; 13(1):31-4.
17. Walker M. Breastfeeding management for the clinician: using the evidence 2013.
18. Tamilia E, Taffoni F, Formica D, Ricci L, Schena E, Keller F, Guglielmelli E. Technological solutions and main indices for the assessment of newborns' nutritive sucking: a review. Sensors 2014; 14(1):634-58
19. Scherman A, Wiedrick J, Lang WC, et al. Quantification of nutritive sucking among preterm and full-term infants. Res rep neonatol 2018; 8:53.
20. Taffoni F, Tamilia E, Giorgino M, et al. A novel system to study the coordination of sucking and breathing in newborns during bottle feeding. IEEE Sens J 2016; 16(23):8589-96.
21. Tamilia E, Delafield J, Fiore S, Taffoni F. An automatized system for the assessment of nutritive sucking behavior in infants: a preliminary analysis on term neonates. In 36th Conf Proc IEEE Eng Med Biol Soc 2014; 5752-5.

Gait training with Achilles ankle exoskeleton in chronic incomplete spinal cord injury subjects

F. Tamburella[1], N.L. Tagliamonte[2], M. Masciullo[1], I. Pisotta[1], M. Arquilla[1], E.H.F. van Asseldonk[3], H. van der Kooij[3], A.R. Wu[4], F. Dzeladini[5], A.J. Ijspeert[5] and M. Molinari[1]

[1]Spinal Rehabilitation Laboratory (SPIRE Lab) and Laboratory of Robotic Neurorehabilitation (NeuroRobot Lab), Neurorehabilitation 1 Department, IRCCS Fondazione Santa Lucia (FSL), Rome, Italy; [2]Advanced Robotics and Human-Centered Technologies Research Unit, Università Campus Bio-Medico di Roma, Rome Italy; [3]Department of Biomechanical Engineering, University of Twente, Enschede, The Netherlands; [4]Department of Mechanical and Materials Engineering, Queen's University, Kingston, Canada; [5]BioRobotics Laboratory, School of Engineering, Institute of Bioengineering, École Polytechnique Fédérale de Lausanne, Lausanne, Switzerland

Powered exoskeletons (EXOs) have emerged as potential devices for Spinal Cord Injury (SCI) to support the intervention of physical therapists during therapy (rehabilitation EXOs) as well as to assist lower limb motion during the daily life (assistive EXOs). Although the ankle is considered a key joint for gait restoration after SCI, very few ankle exoskeletons were developed and tested in incomplete SCI (iSCI) population. Among those, the Achilles ankle exoskeleton is the only one embedding a Controller inspired by the neuromuscular system (NeuroMuscular Controller, NMC). In a previous study we demonstrated that a period dedicated to train iSCI subjects in using the Achilles EXO as an assistive aid, improved robot-aided walking speed and surprisingly also generated a positive trend in free walking speed on long and short distances thus suggesting a possible unexpected rehabilitation effect. To further investigate this result, a case-control longitudinal study was conducted in the present work. The aim of this study was to test the hypothesis that Achilles-aided training could improve performance of free walking of chronic iSCI people more than conventional intensity-matched gait rehabilitation. Before and after conventional and robot-aided rehabilitation a number of variables were analyzed, including spatiotemporal parameters, joint kinematics, ground reaction forces, muscle force, spasticity and its related symptoms, balance and personal experience about the training. Results showed that only the NMC-controlled Achilles training allowed participants to significantly walk faster, with a longer step length and a reduced gait cycle time. A slight force and spasticity improvements were also experienced. In terms of subjects' personal experience, Achilles training was perceived more interesting and less physically demanding than conventional rehabilitation.

According to recent estimates, the number of people living with a Spinal Cord Injury (SCI) is increasing year by year, not only due to the increased frequency of spinal lesions but also to the improvements in life expectancy of SCI subjects (1). Recovery of locomotor ability is of high priority for SCI subjects, independently from the severity of the pathology, the time after injury and the age at the time of injury, and it is a realistic objective for subjects with incomplete SCI (iSCI) lesions (2). The finding that cats, completely spinalized

Key words: robot-aided gait rehabilitation, spinal cord injury, ankle exoskeleton, neuromuscular controller

Corresponding Author:
Dr Federica Tamburella,
Senior Researcher Physical Therapist,
PhD Biomedical Science and Engineering,
SPIRE Lab and NeuroRobot Lab,
Neurorehabilitation 1 Department and Spinal Center,
IRCCS Fondazione S. Lucia, Via Ardeatina 306, 00179 Rome Italy
Tel.: +39 06 51 50 16 78
e-mail: f.tamburella@hsantalucia.it

0393-974X (2020)

at the thoracic level, could be trained to step again on a moving treadmill belt (3, 4) fueled a strong interest in rehabilitation following SCI.

From several animal models and different rehabilitation approaches, a clearer picture is emerging regarding how to train the spinal cord to regain functions, especially locomotion. Literature data demonstrated that gait recovery can be achieved by exploiting plasticity of neuronal centers and by the re-activation of parts of a sensory motor system that are still intact, especially by using task-specific stimulus and by favoring the recruitment of both spinal circuitries and spared supraspinal connections (5). It has been showed that muscular strength, balance capabilities, spasticity, and age are the major factors determining walking recovery (6). Moreover, the ankle is considered a key joint, for gait restoration after SCI (7, 8) since it plays an important role in the mechanics and energetics of walking (9) and the feedback from its afferents is critical for the neural control of walking (10-12). Because of its importance, providing assistance at the ankle joint during gait may be important in iSCI subjects, who exhibit abnormal ankle kinematics and propulsion (9).

In the last decade, powered exoskeletons (EXOs) have emerged as potential devices for SCI recovery, to support the intervention of Physical Therapists (PhTs) in a rehabilitation context (rehabilitation devices) as well as to assist lower limbs in case of paralysis or muscles weakness during daily life (assistive devices) (13). Rehabilitation EXOs can enhance gait recovery by delivering weight-bearing and physical support to movements (single or multiple joints), as well as repetitive, symmetric and intense locomotor training, that may facilitate neuroplasticity in a dose-dependent manner (10), as shown in the animal models (14-17).

In both rehabilitation or assistive contexts, the development of control algorithms capable of adapting EXOs behavior and physical assistance to the ever-changing needs of patients is a crucial challenge (1). Literature data showed that interaction controllers are a key aspect to increase EXOs effectiveness in adaptively supporting gait as well as in promoting and improving the users experience by enhancing motivation and acceptability (18). In fact, end-users only accept a device if it matches their own purposes (19), and they quickly discard devices that do not fulfil their personal expectations, even if they were prescribed by healthcare professionals (19).

Among several commercial devices and research prototypes developed over the last two decades (20-23) only a few EXOs were specifically devised for the ankle joint. Moreover, different control strategies have been used. The EXO in (24), based on pneumatic actuators, is activated by a proportional myoelectrical controller and allows a reduction of muscular activity while still maintaining the unaltered joint torque. The EXO in (25) provides assistance through pneumatic muscles emulating soleus muscle behaviour, and increases walking speed reducing metabolic cost, particularly in elderly individuals. Other ankle prototypes are based on series elastic actuation and model-based control, such as the device reported in (26), or on artificial pneumatic actuation and muscle stiffness control, such as the system for elderly people described in (27). The Achilles ankle exoskeleton, developed for people with iSCI (28), includes series elastic actuators to generate positive plantar flexion, with limited mass and high power density, and has the potential to reduce the metabolic cost of walking (29). Achilles is controlled by means of a novel Neuromuscular Controller (NMC), which is based on a musculoskeletal model with virtual Hill-type muscles activated by stance/swing reflexes (30). The model can recreate human behavior at a variety of speeds and can generate near-physiological gait from the interaction of body dynamics, reflex loops, and virtual muscles with the environment. Hence, the controller does not need any predefined motion patterns or any dedicated commands from the users. The NMC-controlled Achilles is hence peculiar due to its versatility and high compliance to users' natural walking and to its capability of intrinsically adapting robotic assistance to the specific residual functional abilities of users (13). To the best of our knowledge, the Achilles (13) and the pneumatic ankle EXO described in (9) were the only systems specifically tested in iSCI subjects during overground walking.

In our previous study (13), the NMC-controlled Achilles was tested as an assistive device in a group

of 4 chronic iSCI participants. We demonstrated that 5 sessions, dedicated to train subjects in using the exoskeleton as an assistive aid, were sufficient to improve robot-aided walking speed. Surprisingly, this training also generated a positive trend in free walking speed on long and short distances thus suggesting a possible unexpected rehabilitation effect.

The objective of the present paper is to test the hypothesis that Achilles-aided training can improve the performance of free walking of chronic iSCI people more than conventional gait rehabilitation. To this aim, the presumed Achilles-related positive rehabilitation outcomes found in in 4 chronic iSCI subjects (EXP), were compared to the results of a standard rehabilitation therapy purposely administered to a homogenous group of 4 chronic iSCI participants (CTRL) with a case-control longitudinal study (13).

MATERIALS AND METHODS

The study was conducted at the Fondazione Santa Lucia (FSL) in Rome. The protocol was written according to the Helsinki declaration and approved by Independent FSL Ethical Committee (Prot. CE/PROG. 509). The written informed consent was obtained from all participants according to the FSL ethical procedures.

Enrolled participants

Eight iSCI participants were recruited from January to November 2017. Before enrolment, all participants underwent a preliminary assessment performed by a medical doctor and a Physical Therapist (PhD).

Inclusion criteria were: i): age: 18-75; ii): traumatic/ non-traumatic iSCI, chronic phase (at least 3 months after injury) incomplete motor lesion (AIS C or D at enrolment) at cervical, thoracic or lumbar level; iii): ability to ambulate overground (with aids if necessary); iv): evidence of preserved cognitive functions (Mini-Mental State Examination score >26) (13).

Exclusion criteria were: i): any clinical condition contraindicating gait; ii): untreatable chronic pain; iii): severe spasticity (Ashworth scale score > 3); iv): severe reduction in lower limb joint Range Of Motion (ROM) higher than 20 deg; v): any skin problem inhibiting robot usage; vi) major depression or psychosis.

Participants' neurological status was measured at the enrollment by means of the American Spinal Injury Association (ASIA) scale and of the ASIA Impairment Scale (AIS) (31). Mean time between SCI and enrolment was 18.3±13.5 months for EXP group and 21.6±11.1 months for CTRL group. Gait abilities were also assessed by means of the Walking Index for Spinal Cord Injury (WISCI) (32). Epidemiological, clinical and neurological data are reported in Table I. Furthermore, participants were screened by means of the Centre for Epidemiologic Studies Depression Scale (CES-D) (33). In the followings EXP and CTRL subjects will be labeled as E1, E2, E3, E4 and C1, C2, C3, C4, respectively.

Table I: *Epidemiological, clinical and neurological data of all participants.*

	E1	**E2**	**E3**	**E4**	**C1**	**C2**	**C3**	**C4**
Age	58	69	47	42	57	67	48	40
Gender	M	M	M	M	F	F	M	M
AIS level	D	D	D	D	D	D	D	D
SCI level	C7	T10	L4	T11	C6	T10	T5	C7
Aetiology	Traumatic	Traumatic	Ischemic	Traumatic	Traumatic	Traumatic	Ischemic	Ischemic
WISCI level	20	16	16	16	20	16	16	16

Achilles-aided gait training for EXP participants

- Achilles Exoskeleton and NeuroMuscular Controller: Achilles ankle exoskeleton was developed to assist plantar/dorsiflexion during walking. The system is connected to the user lower leg and foot through carbon fiber shells. The foot shells are inserted within standard shoes and include sensorized insoles to detect gait phases (Fig. 1) (28).

Achilles is composed by a compliant actuators (linear motor and leaf spring) able to accurately control the delivered torque based on a low-level torque control loop (whose feedback signal is the torque estimated starting from the measurement of two encoders and from the knowledge of the spring stiffness and of the kinematic structure). The high-level abovementioned NMC is implemented on top of the low-level torque control loop.

The NMC (34) is based on a reflex-based neuro-mechanical simulation of walking developed by H. Geyer (30). The full sagittal plane controller consists of seven Hill-type muscle units per leg, i.e. hip flexor, gluteus, hamstring, vastus, gastrocnemius, tibialis anterior, and soleus. It uses joint angles and gait phases information as inputs to calculate joint torques to be delivered by the EXO. Joint angles yield virtual muscle length, velocity, and force sensory information, which are used to activate the virtual muscles through reflex loops. The forces generated by these muscles are then used to produce lower limb joint torques. Different reflex loops are employed depending on the gait phases: stance reflexes support body weight while swing reflexes allow for leg swing.

Due to the controller modularity, Achilles includes only the ankle module and thus only the soleus and tibialis anterior muscles (the biarticular gastrocnemius was excluded to avoid control issues due to the missing knee). During the stance phase, the soleus muscle is driven by positive force feedback to increase tension while negative force feedback decreases the tension on the tibialis anterior. During swing and throughout the gait cycle, a positive length feedback on the tibialis anterior prevents overextension.

The NMC was demonstrated to produce human-like joint kinematics and joint torques, for both healthy and SCI subjects (34, 35), without the need for tuning its biomechanical or reflex parameters. The nominal torque output of the controller corresponds to the contribution of the muscles required for a simulated human (mass: 80 kg; height: 1.8 m) to walk at 1.3 m/s. A gain (between 0 and 1) multiplying the nominal torque was used to scale the level of assistance starting from 100%. Setting the gain to zero put Achilles in zero-torque mode, a condition in which the robot only follows the user's motion without providing any assistance. This mode is particularly useful to record

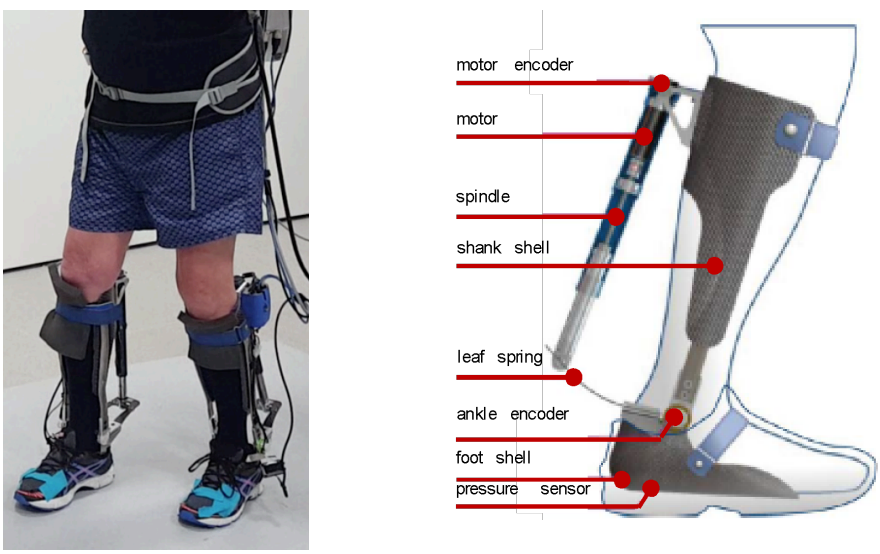

Fig. 1. *Achilles ankle exoskeleton;* ***a****): Picture of the system worn by a participant;* ***b****): Sketch of the components.*

ankle joint angles during assessment sessions.

- Gait Training: EXP group underwent 10 sessions of 40-minute gait training 3 times per week with the main goal of improving comfortable gait speed wearing the Achilles (13). Each gait training session was composed by few minutes of preparation, followed by standing balance exercises, and by a specific walking training (Fig. 2). Preparation phase was devoted to a familiarization with the Achilles device, by performing ankle (dorsal/plantar flexion) or knee movements (flexion/extension), followed by specific balance training and body weight shift exercises propaedeutic for stance/swing management. This initial balance training was expected to have positive effects on subsequent gait performance of iSCI participants, and it was performed with both eyes open and closed, to properly train the somato-sensory system (36). The last part of the session was devoted to train Achilles-aided walking with progressive increase in gait speed over flat and sloped paths.

In a preliminary initial session, Achilles assistance level was customized based on the specific features of each participant (13). This setting was maintained unchanged along the training sessions. The results of the customization process turned out to be consistent with the clinical status of each participant, evaluated through the force assessment procedure detailed below. Indeed, a higher level of assistance was set for the most affected ankle.

Conventional gait training for CTRL participants

The training of the CTRL group was similar to the one of the EXP group, with the exception of the use of Achilles (Fig. 2). The timeline and the exercises were almost the same and were performed by the same PhT. During the preparation phase, the PhT performed active-assisted ankle and knee movements. For the balance and body weight shift exercises, similarly to the EXP group, the PhT guided participants' movements with girdle contacts. For the last part of the session, to train gait with progressive increase in gait speed, the PhT guided the participants mainly through verbal instructions and corrections.

Assessment methods

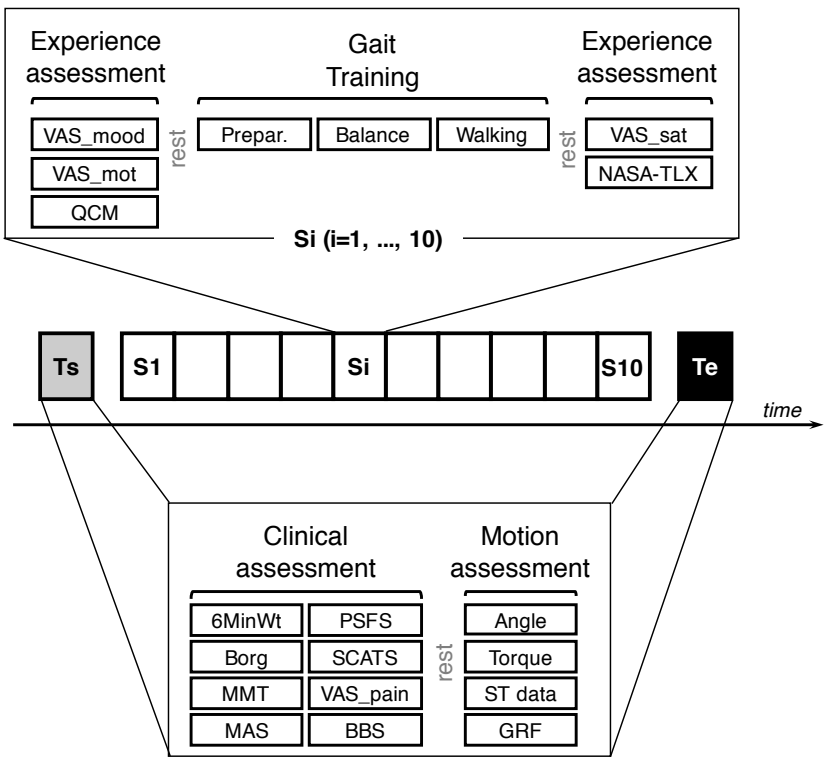

Fig. 2. *Overview of the protocol. Ts and Te indicates the assessment moments. Si (i=1, ..., 10) indicate the training sessions. The same protocol was adopted for EXP and CTRL group.*

Before the start of the training (Ts) and after the end of the training (Te), EXP and CTRL participants were assessed in free walking conditions by considering the following outcome measures (Fig. 2):

- Motion outcome measures: Spatio-Temporal (ST) parameters (speed, step length and width, gait cycle time and stance phase percentage) and Ground Reaction Forces (GRFs) were assessed by using four force plates (P6000, BTS Bioengineering) both for the EXP and CTRL groups. The raw data of the three components of the GRF vector, Antero Posterior (AP), Medio Lateral (ML), Vertical (V), were normalized with respect to the participants' body weight and low-pass filtered by using a zero-lag second order Butterworth filter with a cut-off frequency of 5 Hz. For the EXP group, ankle kinematic pattern was measured by means of Achilles encoders during robot-aided walking in zero torque mode. For the CTRL group, ankle kinematic pattern was measured by means of an optoelectronic motion capture system (Flex13, Optitrack, Natural Point). Markers data were imported in the OpenSim biomechanical software to calculate inverse kinematics based on a scaled subject-specific virtual model of the participant. Ankle angle and GRFs were time-normalized and segmented into Gait Cycles (GCs), by considering, for each leg, a heel strike for the beginning of the cycle and the subsequent heel strike for its end. Heel strike events were identified based on insole detection for the EXP group and based on force plates data for the CTRL group. Data of 5 GCs were extracted and averaged for each assessment moment (Ts and Te).

- Clinical outcome measures: 6-minute gait speed, fatigue, muscle force, spasticity, spasticity related symptoms and dynamic balance were considered. A 6-minute walking test (6MinWT) (37) was used to measure the distance walked over that time span and to analyze walking endurance with and without Achilles for the EXP group, and only in free walking condition for CTRL group. Specifically, the test was explained and it was performed on a rectangular indoor track of 50 m. Borg Scale was linked to the 6MinWT to assess fatigue perception (38, 39). Manual Muscle Test (MMT) of the Medical Research Council was used to assess bilaterally muscle force of hip, knee and ankle joints by considering a score that ranges from 0 (no movement) to 5 (ability to complete whole range of motion against maximum resistance) (40). The 5-points Modified Ashworth Scale (MAS) (7) was used to evaluate spasticity, the Penn modified Spasm Frequency Scale (PSFS) (7) was used for spasms assessments and Spinal Cord Assessment Tool for Spastic Reflexes (SCATS) (7) for clonus assessments. PSFS score ranges from 0 (no spasm) to 4 (spasms occurring more than 10 times per hour), while SCATS includes 3 subscales respectively for clonus, flexor and extensor spasms assessment ranging from 0 (no spasm) to 3 (severe spasm). For pain perception, Visual Analogue Scale (41) was employed (VAS_Pain) based on a 10 cm line, with 0 representing "no pain" and 10 representing "the worst pain you can imagine". Fourteen tasks on the 56-point Berg Balance Scale (BBS) (7) were selected to evaluate dynamic balance.

- User experience outcome measures: to evaluate the dedication and engagement, the acceptability, and the commitment to the standard rehabilitation training, versus Achilles-aided training, the mood, motivation, satisfaction and workload were measured for both groups. Motivation and mood were assessed before each training session, while satisfaction about the training and perceived workload were measured immediately after. Since motivation is a complex construct, defined as the level of commitment to a task, it was evaluated by using an adapted version of the Questionnaire for Current Motivation (QCM) (39), a 18-statement scale based on 4 subscales: Mastery Confidence, Incompetence/Fear-To-Fail, Challenge, Interest, rated on a Likert scale from 1 to 7 (42, 43). Furthermore, VAS motivation (VAS_Mot) (from 1 "Not motivated at all", to 10 "Completely motivated") and mood (VAS_Mood) (from 1 "Bad mood", to 10 "Good mood"), have been used to test the positive/negative participants' attitude towards the training. VAS was also used for the assessment of the satisfaction (VAS_Sat) defined as "freedom from discomfort and satisfaction with the training" (41). The perceived workload was assessed by using the National Aeronautics and Space Administration Task Load Index (NASA-TLX) (44) composed by 6 subscales: Mental Demand, Physical Demand, Time Pressure, Perceived Performance, Frustration and Effort (13).

Statistical analysis

Statistical tests were performed by using the software Statistical Package for the Social Science (SPSS - Chicago, IL). Differences between EXP and CTRL data at Ts and Te were tested with the Independent T-test for

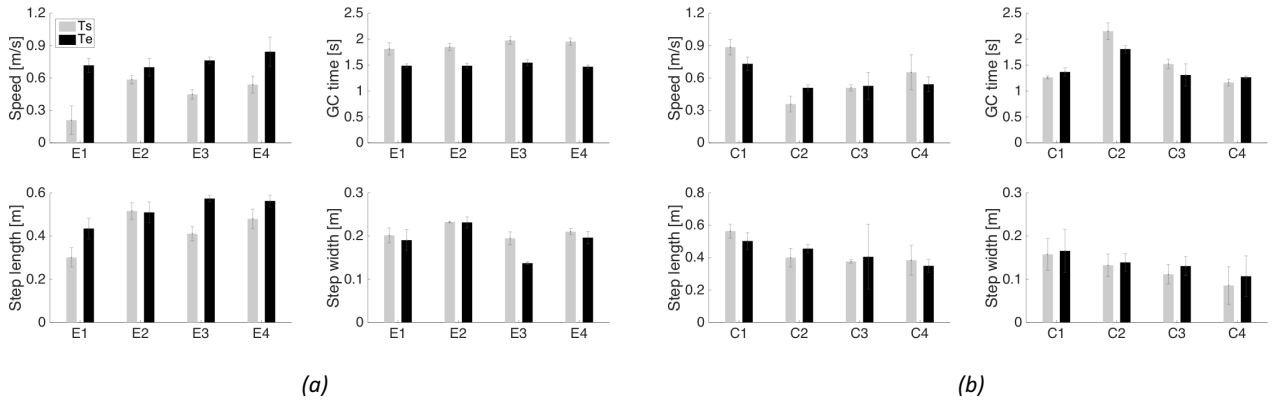

Fig. 3. *Walking speed, step length, step width and GC time for the EXP group (a) and for the CTRL group; **b**): collected during motion assessments at Ts and Te.*

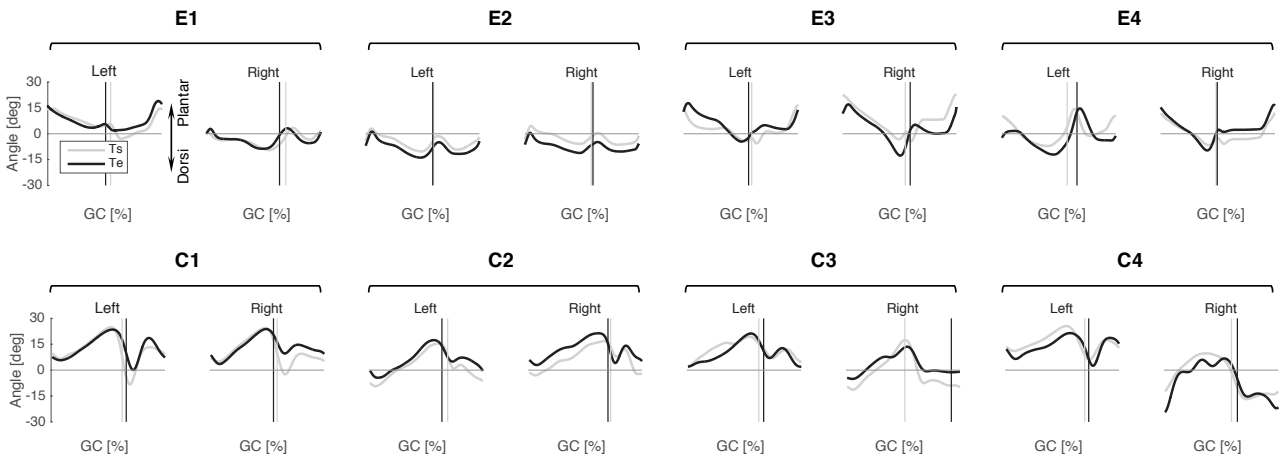

Fig. 4. *Ankle angles for all participants, collected during the motion assessments at Ts and Te. Data are displayed separately for left and right limbs.*

parametric variables and with the Mann-Whitney test for non-parametric variables. For EXP and CTRL groups Ts versus Te comparisons were performed by means of the Paired-T test for parametric variables (ST data, 6MinWT, Borg, MMT, MAS, SFS, SCATS, VAS_Pain) and by means of the Wilcoxon test for non-parametric variables . For Experience assessment, Mann Whitney analysis was used to compare EXP versus CTRL data at Ts and Te, while Wilcoxon test was selected to compare Ts versus Te data for EXP and CTRL groups. Statistical significance was considered for $p<0.05$.

RESULTS

No one withdrew from the study and the outcome measures were obtained for all iSCI participants. Both at Ts and Te, no statistical differences were found for any analyzed variables in the comparison between EXP and CTRL data ($p>0.05$). Comparing Ts versus Te data, a statistically significant improvement was obtained only in the EXP group for the ST parameters, as detailed below.

A Motion outcome measures

Significant improvements in ST parameters at Te were found only for the EXP group (Fig. 3). All EXP participants significantly improved gait speed at Te in comparison to Ts ($p = 0.009$). Only 2 out of 4 participants of the CTRL group, namely C2 and C3, improved gait speed but without any statistical significance. A similar trend was observed for GC time, which was significantly reduced at Te

for EXP group (p = 0.022). On the contrary only 2 CTRL participants showed an improvement in this parameter at Te, even if not statistically significant. Step length data showed a significant increase in all EXP participants (p = 0.022), while only minor not significant changes were present in the CTRL group. For the EXP group step width decreased at Te, even if the difference with respect to Ts was not statistically significant. No evident differences between Ts and Te were observed for CTRL participants.

Data on ankle angles are reported in Fig. 4 for each EXP and CTRL participant. The stance percentage is also reported. For EXP participants, NMC-controlled Achilles did not force the ankle joints towards predefined trajectories as evident by looking at the heterogeneity of ankle kinematics. E1 showed a more pathological pattern at left ankle in comparison to the right one, and no substantial modifications were obtained after Achilles-aided training. For E2 and E3 the training allowed both ankles, and the right one, to partially recover dorsiflexion at Te. A similar trend of recovery was evidenced for E4 left ankle.

The right ankle of C1 had a reduced ROM in comparison to the contralateral one. On the contrary, no clear differences between left and right ankles

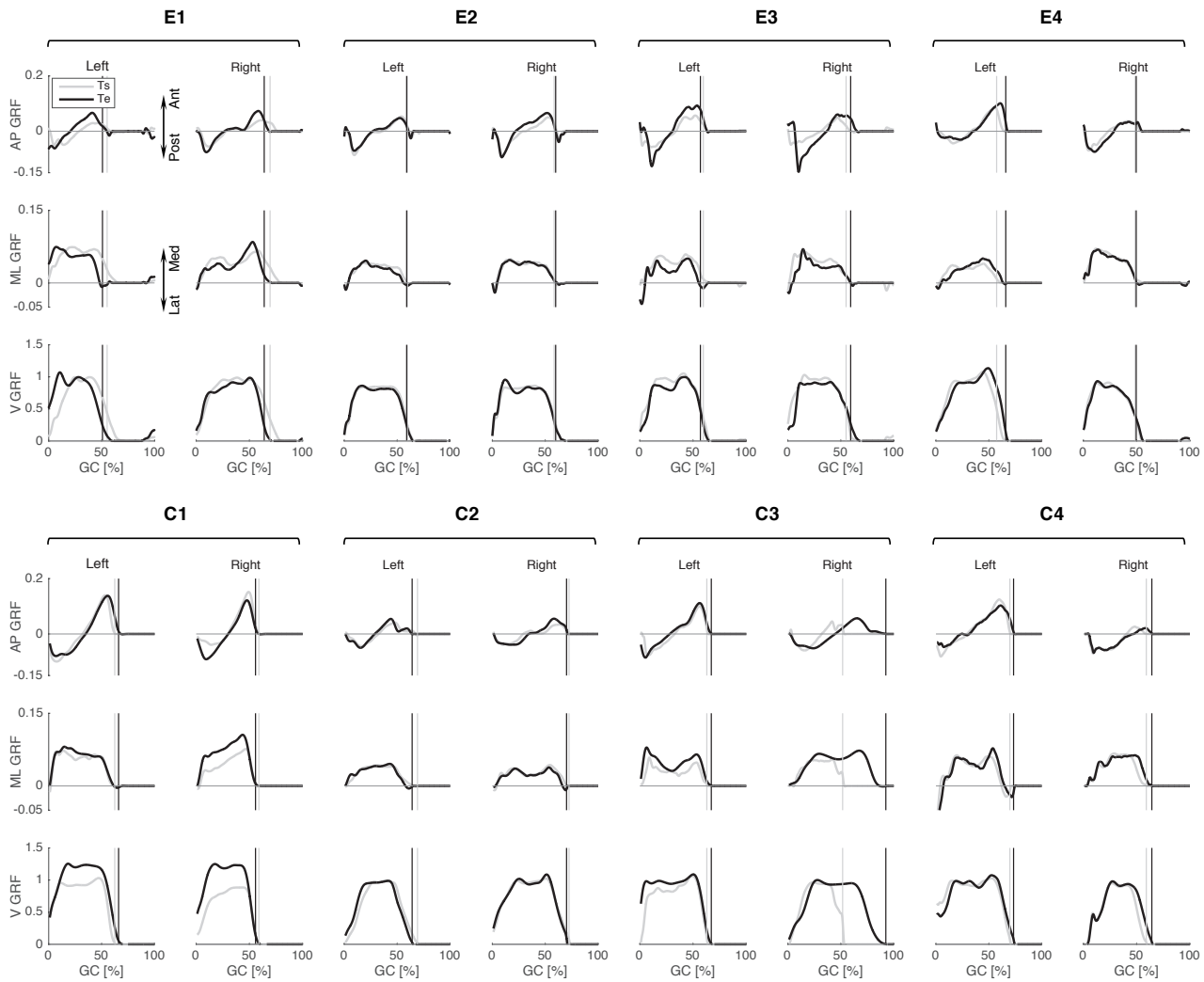

Fig. 5. *Antero-posterior (AP), medio-lateral (ML) and Vertical (V) GRFs for all EXP and CTRL participants, collected during the motion assessments at Ts and Te. Data are displayed separately for left and right limbs.*

were pointed out for C2. Both C1 and C2, after conventional gait training, showed an increase of plantarflexion, during the swing phase. A similar result was observed for the right ankle of C3, that after the training was more dorsiflexed than the contralateral one. C4 kinematic data clearly denoted that the right ankle is the most affected joint. For C4 no specific gait training effects were found for both ankles. Furthermore, for all participants no substantial variations in stance phase duration were observed after Achilles-aided or conventional gait trainings.

GRFs data are reported in Fig. 5 for each EXP and CTRL participant. Few right/left asymmetries were found for some participants, but very minor changes were found by comparing Ts and Te for both groups. Some irregularities in the patterns with respect to physiological normative data (13) were possibly due to some instabilities due to the walking limitations of the patients. It is worth noticing that the presence of Achilles (in zero-torque mode) did not alter GRFs data of EXP participants with respect to free walking (13).

Clinical outcome measures

- 6MinWT gait endurance: EXP participants were unable to complete 6MinWT test without the support of the Achilles. 3 out of 4 EXP participants chose not to perform the 6MinWT after verbal explanation of the trial because they considered it too physically demanding for their clinical condition, while E1 started the test and stopped after 186 s. On the other hand, 6MinWT was easily completed, without any rest, in the Achilles-aided condition by all the EXP participants already at Ts. At Te Achilles-aided training significantly improved 6MinWT path length for the EXP participants ($p = 0.047$) and particularly for E3. This improvement was associated with a reduction of the perceived fatigue, as assessed by the Borg Scale, which was particularly evident for E1, E3 and E4. As regards CTRL group, improvements in free walking 6MinWT performance and Borg Scale data were present only for C3 and C4, while for C1 and C2 no variations at Te with respect to Ts were pointed out (Fig. 6).

Besides the effects on gait endurance and fatigue, the training also slightly, not significantly, improved dynamic balance for EXP and CTRL participants as indicated by BBS data (EXP:BBS score was 34.75±8.61 at Ts and 38.25±6.49 at Te; CTRL:BBS score was 35.00±2.16 at Ts and 38.75±2.98 at Te).

Force, spasticity and spasticity related symptoms

Despite the reduced sample size (8 subjects) and the similarities among participants (in terms of SCI lesion level, AIS and WISCI scores, as well as in the overall good functional and clinical status), the EXP and CTRL participants were heterogeneous in terms of muscle force, spasticity and spasticity related symptoms (Fig. 7). Even if no statistically significant modifications were highlighted for any clinical data in the comparison between Ts and Te, some slight differences for CTRL and EXP participants were experienced after the training.

For the EXP group, no MMT variations were found for two participants (E1, E2) while for E3 1-point improvement was found for the knee scores of flexor muscles at both sides (at Te MMT= 4 for the left knee and MMT= 4 for the right knee). For

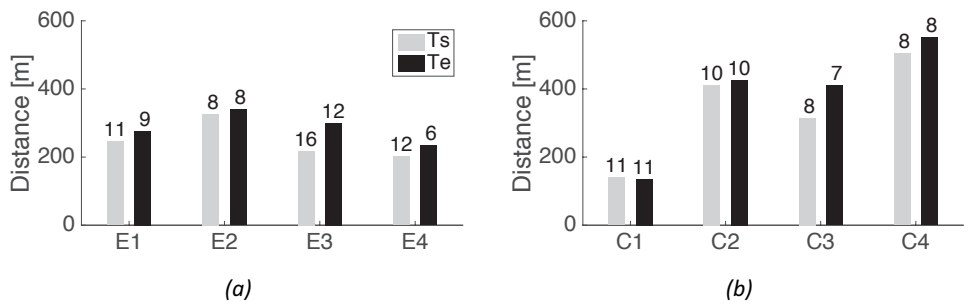

Fig. 6. *Traveled distance for the EXP group in the Achilles-aided condition (**a**): and for the CTRL group in the free walking condition (**b**): collected during the 6MinWT at Ts and Te. Borg Scale scores are shown on the top of the bars.*

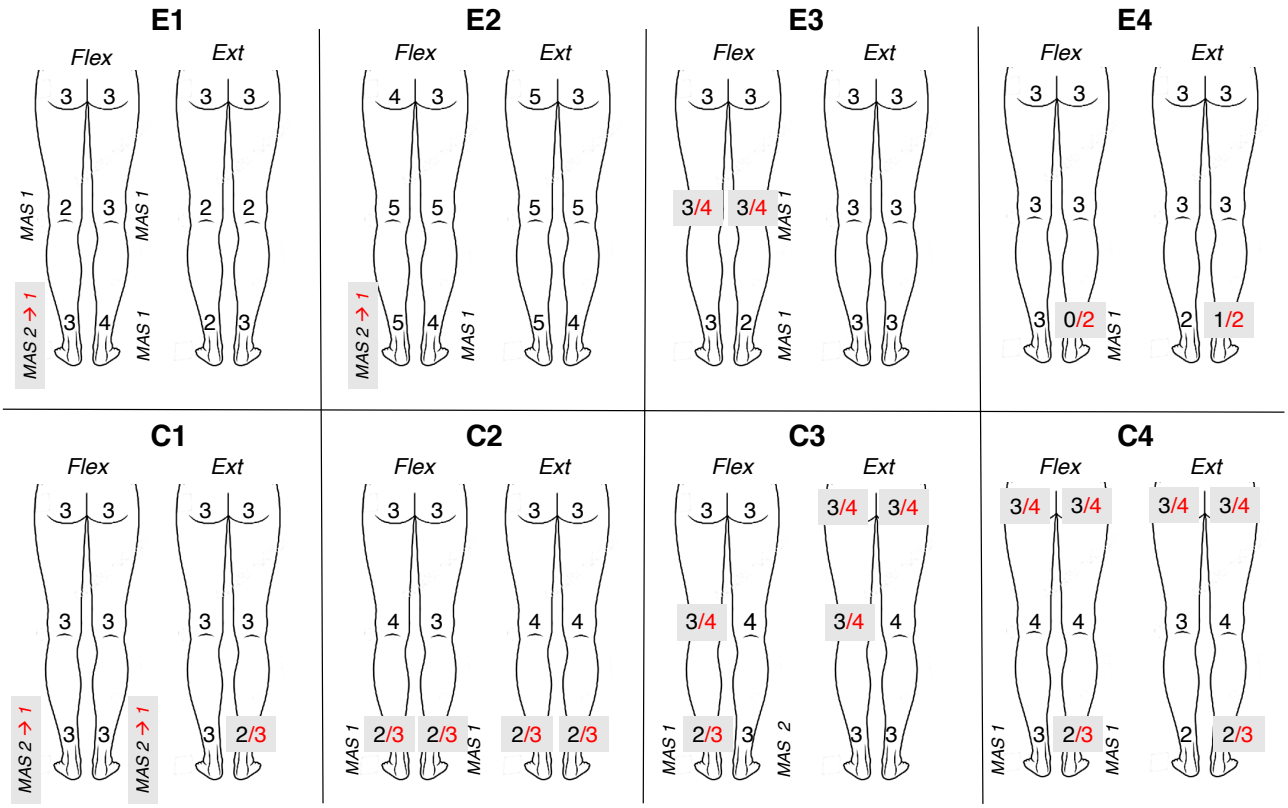

Fig. 7. *Data of force (MMT) and spasticity (MAS) for flexor (Flex) and extensor (Ext) muscles for hip, knee and ankle. MMT scores are included in legs silhouette, MAS scores are on leg sides. Black data refer to Ts assessment. Red MMT and MAS data inside grey boxes highlight changes at Te with respect to Ts.*

E4, MMT scores suggested a force enhancement at the right ankle flexor (Te: MMT=2) and extensor (Te: MMT=2). Spasticity and spasticity related symptoms indicated a general low degree of spasticity, clonus, and spasm at Ts. In detail, E1 presented a very low level of spasticity (MAS=1) at right and left knee, as well as at right ankle. At the left ankle, a slightly higher level of spasticity was denoted (MAS=2) and mild clonus and mild flexors spasm were present as well for E1 at left ankle. For E2 spasticity was detected at right (MAS=1) and, particularly, at left (MAS=2) ankle. E3 presented a low spasticity level at the right knee and ankle (MAS=1). E4 had a low degree of spasticity only at the right ankle, associated with mild clonus and flexor spasms, similarly to E1. No significant modifications were reported for Te evaluations, except for the reduced left ankle spasticity for E1 and E2 at MAS (1-point decrease). Pain symptoms were present in all the EXP participants except for E3. Achilles training positively reduced pain symptoms for all EXP participants (Ts: 4.25±2.60, Te: 2.25±2.50) (Fig. 7).

For the CTRL, group C1 improved the ankle extensor force for the right leg by only one point (Te: MMT=3), C2 improved by one point in the muscle force of both ankles for flexor and extensor muscles, thus reaching at Te a MMT score of 3. In contrast, the force improvements were present not only at ankle joints for C3 and C4. C3 flexor muscle force improved for left knee (Te MMT= 4) and left ankle (Te MMT= 3), while extensor muscles force improved for both hips (Te MMT= 4) and for left knee (Te MMT= 4). For C4, hip forces improved for flexor and extensor muscles bilaterally (Te MMT= 4), as well as for the right ankle (Te MMT= 3). MAS data showed that at Ts a slight (MAS=1) or a marked increase of muscle tone (MAS=2) was present at the ankle right and left flexor muscles for all CTRL participants, associated

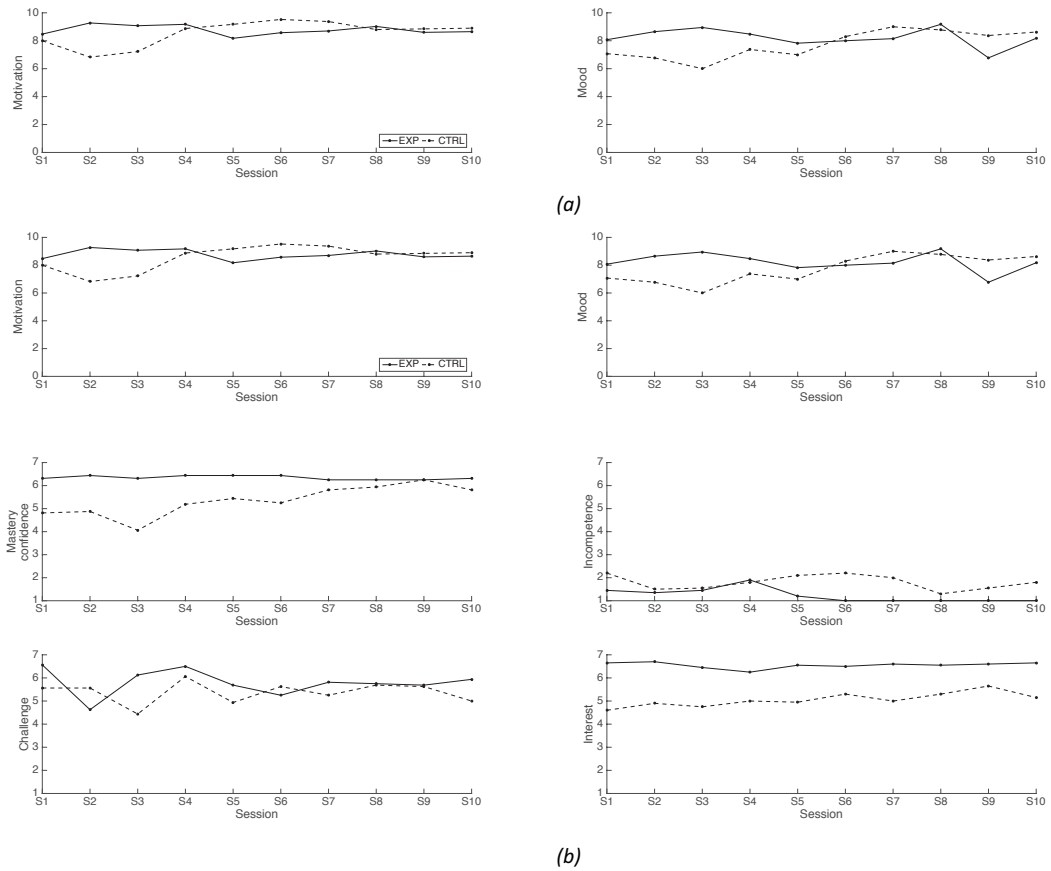

Fig. 8. *Experience data collected before each training session. a) VAS Motivation and VAS Mood results: b)QCM subscale results.*

with mild flexor spasms for almost all participants (C2, C3, C4). Only for C2 and C4 a low clonus was present. At Te no substantial modifications in spasticity and spasticity related symptom were pointed out with the only exception of a minor bilateral reduction of ankle spasticity for C1 (Ts MAS=2, Te MAS=1). Pain symptoms were present in all CTRL participants, and conventional gait training obtained a minor reduction of pain with respect to robot-aided training, as indicated by VAS_pain mean data (Ts: 2.75±3.77, Te: 1.50±3.00) (Fig. 7).

User experience outcome measures

Statistical analysis revealed no significant differences in user experience outcome measures in the comparison between the two groups (CTRL vs EXP data) at Ts and at Te, as well as in the comparison between Ts and Te for CTRL and EXP groups. VAS mood and motivation results (Fig. 8a) showed very low variability among training sessions and between groups: both groups presented good motivation towards training and rated mood as good for all training sessions.

The daily evaluation scores of the QCM questionnaire factors showed differences in two of the subscales, i.e. Mastery confidence and Interest. EXP group rated both Mastery Confidence and Interest, higher than CTRL group: only at S8 CTRL participants started rating the level of Mastery similarly to EXP participants. The subscale Incompetence and Challenge did not show clear differences between groups (Fig. 8b).

Regarding the experience data collected after each training session, satisfaction was maintained very high along training sessions for all the participants with a minor lower rating for the CTRL group at the beginning (Fig. 9a). Each dimension of the NASA-TLX workload was considered independently (Fig.

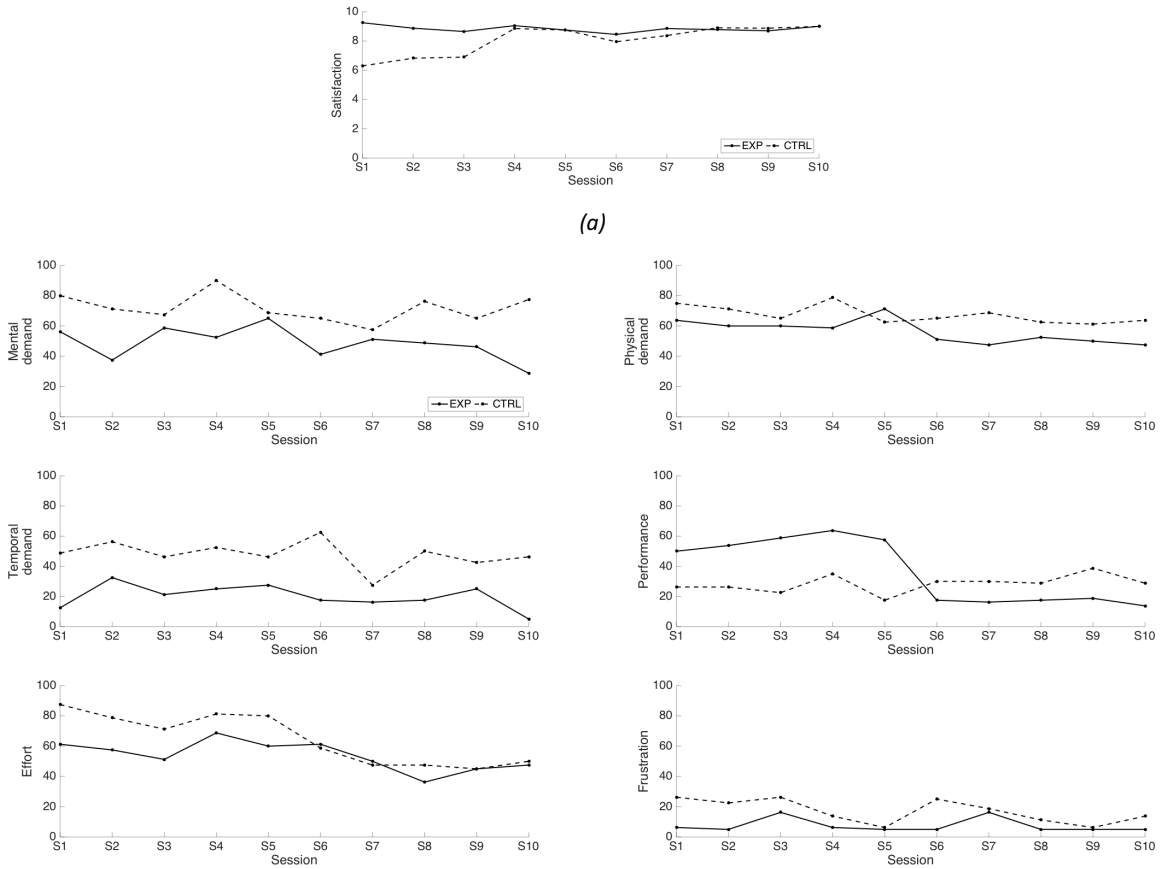

Fig. 9. *Experience data collected after each training session;* ***a****): VAS Satisfaction results;* ***b****): NASA-TLX sub scores results.*

9b). Mental demand was slightly higher in the CTRL group, even if similar trends were found for both groups. Physical demand was rated similarly with a slightly decreasing trend for both groups. Along the sessions, the CTRL participants rated the Temporal demand higher than EXP participants. In the Performance subscale EXP group showed a decreasing trend at Te in comparison to Ts, while the CTRL group rated the perceived Performance lower but stable along the sessions. Both groups showed a similar Effort evaluation, initially higher between S1 and S5 and then lower between S6 and S10. Frustration was very low for both groups (Fig. 9b).

DISCUSSION

There is increasing interest in the use of robotic training devices in walking rehabilitation of iSCI individuals. These devices provide promising opportunities to increase the intensity of training and the effectiveness of rehabilitation programs and to reduce PhTs' physical demands (1, 9). Nowadays EXO-aided rehabilitation has not yet demonstrated clear advantages over conventional gait training approaches, in terms of feasibility, safety and efficacy in chronic iSCI population (45, 46).

Nowadays the only EXO with the NMC embedded, tested as an assistive device for SCI population, is the NMC-controlled Achilles, even if ankle plays an important role in the mechanics and neural control of walking (9). Even if no positive rehabilitation effects were expected from an assistive device, some gait improvements were obtained after a short NMC-controlled Achilles training period in chronic iSCI participants, in terms of increase of walking speed on short and long distances (13, 29).

Those promising results were compared in the present work to the outcomes of a conventional intensity-matched conventional gait rehabilitation, purposely administered to a group of chronic iSCI participants selected based on a case-control paradigm.

We enrolled additional 4 clinically homogenous chronic iSCI participants as CTRL group, to test the hypothesis that Achilles-aided training could improve walking performance in chronic iSCI people, more than conventional gait rehabilitation. In comparing the effects of conventional and robotic gait rehabilitation, the focus was on possible improvements in terms of gait speed. Anyhow we also assessed additional multiple parameters on motion, clinical features and subjective experience.

EXP and CTRL ST and clinical data were comparable at Ts ($p>0.05$). Despite no statistical significance was obtained for CTRL group data in the comparison between Ts and Te, EXP participants significantly improved gait speed, gait cycle time and step length after 10 training sessions with the NMC-controlled Achilles. Furthermore, Achilles-aided training significantly improved 6MinWT results associated with a trend of reduction of the perceived fatigue assessed by means of the Borg Scale. Only minor not significant positive trend of 6MinWT variations were observed in CTRL participants data, but not for all of them. These data confirmed that Achilles-NMC training allows to increase speed, better manage long distances, and to reduce walking effort more than a conventional gait training in chronic iSCI participants. It must be stressed that iSCI participants were in a chronic stage, in which further recovery rarely occurs, especially more than one year after the lesion (47). As already declared in (13), kinematic data demonstrated the NMC-controlled Achilles capability to provide motor assistance in chronic iSCI subjects, by automatically and intuitively adapting to intended motion in line with participants' clinical features without the need of any prescribed motion pattern.

While in our previous work (13) clinical assessment was planned only to safely monitor clinical conditions during the training, in this study it was used to compare Achilles-aided and conventional gait trainings. Despite the short-term training and the chronic condition of participants, the observed variations highlighted some trends of improvement for both EXP and CTRL groups (see Fig. 7), even if not statistically significant. MMT score improved in E3 and E4 at knees and ankles respectively, and ankle MAS improved in E1 and E2. For CTRL group muscle force of different joints improved for all subjects: C1 and C2 improved ankle force, while C3 and C4 showed greater hip and knee force. These data were associated to a spasticity reduction only for C1.

Moreover, for both groups a similar reduction in the pain perception was found. We can speculate that conventional gait training enhances muscle force improvement in more districts than Achilles training, i.e. not only at the ankle or at the ankle proximal joint (i.e. knee) but also at the hip. The effects on spasticity are almost similar for both types of gait training. The combination of motion (Fig. 3) and clinical data (Fig. 7) showed that at Te EXP participants were able to walk significantly faster, with a longer step and a reduced GC time with slight force and spasticity trends of improvement. On the contrary, the conventional gait rehabilitation did not allow CTRL participants to significantly walk faster or with longer step, but a trend of muscle force improvements for all the lower limb joints was observed.

The assessment of user experience showed that both groups had a positive tendency in approaching the conventional and Achilles-aided gait training, with minor differences in some of the evaluated variables (Fig. 8). All participants were motivated, in a good mood and showed very low frustration, thus demonstrating that all of them had positive feeling towards the training (Fig. 8a). All participants relied on therapy, either robotic or conventional, to improve their own residual deficit after SCI and perceived the training as challenging and interesting. The EXP group showed more interest than the CTRL group at the QCM subscale (Fig. 8b). This result was reasonably not surprising.

Unexpectedly, the EXP group showed a high level of Mastery confidence in dealing with Achilles from the beginning (S1), while the CTRL group reached the same level of Mastery confidence only close to the end of the training (starting from S8). Moreover, the evaluation of the Effort subscale (Fig. 9b) decreased

in the middle of the training for EXP and CTRL groups. This results can be explained by considering that both trainings required strong self-commitment, also in terms of physical effort, but moving towards the end of the training and acquiring self-confidence and mastery, both groups reduced the commitment, with an impact on the physical effort (see Fig. 9b, Physical demand subscale). Perceived performance was higher for the EXP group at the beginning of the training and then declined at S6, while it was stable, even if lower, for the CTRL group.

We speculate that Achilles EXO gives to the users the feeling of higher control on gait ability. This was also explained by the high level of mastery already starting at S1, and possibly to the easier and faster improvements, due to the higher speed and longer step, that apparently are perceived as indicators of greater autonomy. This perception let the EXP participants feel more independent only initially, given the drop in the perceived performance evaluation at S6.

The slight difference in the evaluation of Physical demand (Fig. 9b), lower for EXP group, could be due to the perceived physical assistance provided by the Achilles. It is possible that EXP group during gait felt the constant assistance delivered by the NMC controller by means of the Achilles, while the CTRL group only received verbal assistance by the PhT. The observation that the CTRL group had to focus the attentional resources more on the indications of the PhT might explain the higher Mental demand rate and the higher Temporal pressure. CTRL participants were more focused on the accurate walking execution than the EXP group, perceiving more pressure on the gait training performance. Furthermore, considering muscle force improvements in more than one joint after conventional gait rehabilitation (Fig. 7), we might suppose that the higher recruitment of hip and knee muscles could have influenced Mental and Temporal demands.

In conclusion, the NMC-controlled Achilles addresses the main challenges in EXO clinical applications since it provides physical assistance based on users' residual functional abilities while still preserving natural and not stereotyped gait patterns, as indicated by the heterogeneity of ankle joint kinematics and by gait differences among participants (13). Moreover, the results of the present case-control preliminary study suggested that 10 training sessions with the NMC-controlled Achilles, under a PhT's supervision, increase chronic iSCI gait performance in terms of speed and step length more than conventional gait rehabilitation and enhance subjects' experience and engagement during gait rehabilitation.

Only Achilles training allowed participants to significantly walk faster, with a longer step and a reduced GC time, associated with slight force improvement and spasticity reduction. Moreover, we found that Achilles training was perceived more interesting and less physically demanding than conventional gait rehabilitation.

Limitations

The sample size of the iSCI participants (N = 8) was relatively small thus reducing the statistical relevance of the study. Nevertheless, some statistical differences were obtained for the EXP group and, as suggested by Friston (48), significant results based on small samples may indicate a larger treatment effect than the equivalent results with a large sample. Furthermore, follow-up measurements, to ensure that the obtained functional gait gains were retained over time were missed and should be added in future investigations to confirm these preliminary findings. Despite these limitations, our results are encouraging in supporting the idea that improving gait with Achilles ankle exoskeleton in chronic iSCI patients is feasible and safe when performed in a supervised and controlled environment. Although the optimal dose and protocol of training remain not specifically defined, robotic training is a promising method and appears to be a particularly powerful potential way to promote functional recovery.

ACKNOWLEDGEMENTS

Authors thank all the participants involved in this study. Financial support was provided by the FP7 EU research program, project no. ICT-2013-10-611626 (SYMBITRON - Symbiotic Man-Machine Interactions in Wearable Exoskeletons to Enhance Mobility for Paraplegics). Partial financial support

was provided also by Italian Ministry of Health (Ricerca Corrente) and by the European sub-project EXPERIENCE, funded by the FSTP-1 cascade funding program of the H2020 EUROBENCH project (ICT-2017-1-779963).

FT, NLT, M Masciullo, MA and IP contributed to the conception and design of the work and to data interpretation. FT, IP and MA contributed to the perform robotic trainings. FT and M Masciullo contributed to the recruitment of participants, to the execution of conventional rehabilitation trainings and to clinical assessments. FT, NLT, IP and MA worked on assessments, data collection and elaboration. FT worked on the statistical analysis. FT, NLT, M Masciullo and IP wrote the manuscript and EHFVA, HVDK, ARW, FD, AJI and M Molinari revised it.

REFERENCES

1. Tamburella F, M.M., Pisotta I, Tagliamonte NL, Molinari M. Lower Limb Wearable Systems for Mobility and Rehabilitation Challenges: Clinical Focus in Wearable Robotics: Challenges and Trends. Biosystems & Biorobotics. Springer 2017.
2. Ditunno P.L, et al. Cross-cultural differences in preference for recovery of mobility among spinal cord injury rehabilitation professionals. Spinal Cord 2006; 44(9):567-75.
3. Barbeau, H. and S. Rossignol, Recovery of locomotion after chronic spinalization in the adult cat. Brain Res 1987; 412(1):84-95.
4. Fawcett J.W. and Curt A, Damage control in the nervous system: rehabilitation in a plastic environment. Nat Med 2009; 15(7):735-6.
5. Tamburella F, Molinari M, Scivoletto G. Approach to Gait and Balance Rehabilitation in Spinal Cord Injury, ed. H.V. Sandrini G., Saltuari L., Smania N., Pedrocchi A. (eds). Vol. 19. January 2018, Advanced Technologies for the Rehabilitation of Gait and Balance Disorders. Biosystems & Biorobotics: Springer, Cham
6. Scivoletto G, et al. Clinical factors that affect walking level and performance in chronic spinal cord lesion patients. Spine 2008; 33(3):259-64.
7. Tamburella F, Scivoletto G, Molinari M, Somatosensory inputs by application of KinesioTaping: effects on spasticity, balance, and gait in chronic spinal cord injury. Front Hum Neurosci 2014; 8:367.
8. Arazpour M, et al, The influence of ankle joint mobility when using an orthosis on stability in patients with spinal cord injury: a pilot study. Spinal Cord 2013; 51(10):750-4.
9. Sawicki G.S, Domingo A, Ferris D.P, The effects of powered ankle-foot orthoses on joint kinematics and muscle activation during walking in individuals with incomplete spinal cord injury. J Neuroeng Rehabil 2006; 3:3.
10. Donelan J.M, Pearson K.G, Contribution of sensory feedback to ongoing ankle extensor activity during the stance phase of walking. Can J Physiol Pharmacol 2004; 82(8-9):589-98.
11. Capaday C, The special nature of human walking and its neural control. Trends Neurosci, 2002; 25(7):370-6.
12. Nielsen J.B, Sensorimotor integration at spinal level as a basis for muscle coordination during voluntary movement in humans. J Appl Physiol (1985) 2004; 96(5):1961-7.
13. Tamburella F, et al. Neuromuscular Controller Embedded in a Powered Ankle Exoskeleton: Effects on Gait, Clinical Features and Subjective Perspective of Incomplete Spinal Cord Injured Subjects. IEEE Trans Neural Syst Rehabil Eng 2020; 28(5):1157-67.
14. See P.A. de Leon R.D. Robotic loading during treadmill training enhances locomotor recovery in rats spinally transected as neonates. J Neurophysiol 2013; 110(3):760-7.
15. de Leon, R.D, See P.A, Chow C.H, Differential effects of low versus high amounts of weight supported treadmill training in spinally transected rats. J Neurotrauma 2011; 28(6):1021-33.
16. Macias M, et al. Exercise-induced motor improvement after complete spinal cord transection and its relation to expression of brain-derived neurotrophic factor and presynaptic markers. BMC Neurosci 2009; 10:144.
17. Petruska J.C, et al. Changes in motoneuron properties and synaptic inputs related to step training after spinal cord transection in rats. J Neurosci 2007; 27(16):4460-71.
18. Rossini P.M. and G. Dal Forno. Integrated technology for evaluation of brain function and neural plasticity. Phys Med Rehabil Clin N Am 2004; 15(1):263-306.

19. Shah S.G, I Robinson, AlShawi S, Developing medical device technologies from users' perspectives: a theoretical framework for involving users in the development process. Int J Technol Assess Health Care 2009; 25(4):514-21.
20. Yana T, C.M, Maria Oddo C, Vitiello N. Review of assistive strategies in powered lower-limborthoses and exoskeletons. Robotics and Autonomous Systems 2015; 64:120-36.
21. Mekki M, et al. Robotic Rehabilitation and Spinal Cord Injury: a Narrative Review. Neurotherapeutics 2018; 15(3):604-17.
22. Dijkers M.P, et al. Systematic Reviews of Clinical Benefits of Exoskeleton Use for Gait and Mobility in Neurologic Disorders: A Tertiary Study. Arch Phys Med Rehabil 2019.
23. Gorgey A.S. Robotic exoskeletons: The current pros and cons. World J Orthop 2018; 9(9):112-9.
24. Kao P.C, Lewis C.L, Ferris D.P. Invariant ankle moment patterns when walking with and without a robotic ankle exoskeleton. J Biomech 2010; 43(2):203-9.
25. Norris J.A, Kevin P, Granata A, Melanie R, et al. Effect of augmented plantarflexion power on preferred walking speed and economy in young and older adults. Gait Posture 2007; 25(4):620-7.
26. K.Kim J.J.K, Kang S.R, Jeong G.Y, Kwon T.K, Analysis of the assistance characteristics for the plantarflexion torque in elderly adults wearing the powered ankle exoskeleton, in International Conference onControl Automation and Systems (ICCAS), IEEE, Editor 2010; 576-9.
27. A. Polinkovsky, R.J.B., N.I. Kern, R.D. Quinn, An ankle foot orthosis with insertion point eccentricity control, in Intelligent Robots andS ystems, IROS., IEEE/RSJ International Conference 2012; 1603-8.
28. van Dijk W, Meijneke C, van der Kooij H. Evaluation of the Achilles Ankle Exoskeleton. IEEE Trans Neural Syst Rehabil Eng 2017; 25(2):151-60.
29. meijneke C.v.D W, van der Kooij H, Achilles: An autonomous lightweight ankle exoskeleton to provide push-off power, in 5th IEEE RAS/EMBS International Conference on Biomedical Robotics and Biomechatronics, IEEE: Sao Paulo, Brazil 2014.
30. Geyer H. Herr H. A muscle-reflex model that encodes principles of legged mechanics produces human walking dynamics and muscle activities. IEEE Trans Neural Syst Rehabil Eng 2010; 18(3):263-73.
31. Association, A.S.I. International Standard for Neurological Classification of Spinal Cord Injury (rev). Chicago American Spinal Injury Association 2000; 1-23.
32. Ditunno, P. and J.D. Jr, Walking index for spinal cord injury (WISCI II): scale revision. Spinal Cord 2001; 39:654-6.
33. Dozeman E, et al. The center for epidemiological studies depression scale (CES-D) is an adequate screening instrument for depressive and anxiety disorders in a very old population living in residential homes. Int J Geriatr Psychiatry 2011; 26(3):239-46.
34. Dzeladini F, Wu A.R, Renjewski D, Arami A, et al. Effects of a neuromuscular controller on a powered ankle exoskeleton during human walking. in 2016 6th IEEE International Conference on Biomedical Robotics and Biomechatronics (BioRob) 2016.
35. Wu A.R, Florin Dzeladini, Tycho J H Brug, et al. An Adaptive Neuromuscular Controller for Assistive Lower-Limb Exoskeletons: A Preliminary Study on Subjects with Spinal Cord Injury. Front Neurorobot 2017; 11:30.
36. Tamburella F, Scivoletto G, Molinari M, Balance training improves static stability and gait in chronic incomplete spinal cord injury subjects: a pilot study. Eur. J. Phys. Rehabil. Med 2013; 49(3):353-64.
37. Poole-Wilson, P.A, The 6-minute walk. A simple test with clinical application. Eur. Heart J 2000; 21(7):507-8.
38. Laboratories, A.T.S.C.o.P.S.f.C.P.F. ATS statement: guidelines for the six-minute walk test. Am J Respir Crit Care Med 2002; 166(1):111-7.
39. Lewis J.E, Nash M.S, Hamm L.F, Martins S.C, Groah S.L. The relationship between perceived exertion and physiologic indicators of stress during graded arm exercise in persons with spinal cord injuries. Arch Phys Med Rehabil 2007. 88(9):1205-11.
40. Wright W, Muscle training in the treatment of infantile paralysis. Boston Med Surg J 1912.
41. Heller G.Z, Manuguerra M, Chow R, How to analyze the Visual Analogue Scale: Myths, truths and clinical relevance. Scand J Pain 2016; 13:67-75.
42. Colombo, R, Pisano F, Mazzone A, et al. Design strategies to improve patient motivation during robot-aided rehabilitation. J Neuroeng Rehabil 2007; 4:3.

43. Morone G, et al. Proof of principle of a brain-computer interface approach to support poststroke arm rehabilitation in hospitalized patients: design, acceptability, and usability. Arch Phys Med Rehabil 2015; 96(3S):S71-8.
44. Galy E, J. Paxion, C. Berthelon, Measuring mental workload with the NASA-TLX needs to examine each dimension rather than relying on the global score: an example with driving. Ergonomics 2018; 61(4):517-27.
45. Yozbatiran N, Berliner J, K O'Malley M, et al. Robotic training and clinical assessment of upper extremity movements after spinal cord injury: a single case report. J Rehabil Med 2012; 44(2):186-8.
46. Siedziewski L, Schaaf R.C, Mount J, Use of robotics in spinal cord injury: a case report. Am J Occup Ther 2012; 66(1):51-8.
47. Tefertiller C, Pharo B, Evans N, Winchester P. Efficacy of rehabilitation robotics for walking training in neurological disorders: a review. J. Rehabil. Res. Dev 2011; 48(4):387-416.
48. Friston, K, Ten ironic rules for non-statistical reviewers. Neuroimage 2012; 61(4):1300-10.

Effectiveness of a sensor-based technology in upper limb motor recovery in post-acute stroke neurorehabilitation: a randomized controlled trial

M. Tramontano[1], G. Morone[1*], A. Palomba[2], S. De Angelis[1], A. Mercuro[1], C. Caltagirone[1] and M.G. Grasso[1]

[1]Fondazione Santa Lucia IRCCS, Rome, Italy; [2]Multidisciplinary Department of Medicine for Surgery and Orthodontics, University of Campania Luigi Vanvitelli, Naples, Italy

Sensor-based technological therapy devices could be a possible neurorehabilitation strategy for motor rehabilitation in patients with stroke during the post-acute hospitalization, especially for treating upper extremities function limitations. The audio-visual feedback devices are characterized by interactive therapy games that allow training the movement of shoulders, elbows, and wrist, measuring the strength and the active range of motion of upper limb, registering data in an electronic database to quantitatively monitoring measures and therapy progress. This study aimed to investigate the effects of sensor-based motor rehabilitation in add-on to the conventional neurorehabilitation for improving the upper limb functions in patients with subacute stroke. Thirty-seven patients were enrolled in the study and randomly assigned to the experimental group and the control group. The training consisting of twelve sessions of upper limb training compared with twelve sessions of upper limb sensory-motor training, without robotic support. Both rehabilitation programs were performed for 40 minutes three times a week, for 4 weeks, in addition to conventional therapy. All patients were evaluated at the baseline (T0) and after 4 weeks of training (T1). The within-subject analysis showed a statistically significant improvement in both groups in all clinical scales. The analysis of effectiveness revealed that, compared with baseline (T0), the improvement percentage in the Modified Barthel Index was greater in the experimental group than the control group. The use of a sensor-based training with audio-video-feedback could be a useful complementary strategy for improving upper limb motor functions in patients with stroke during post-acute neurorehabilitation

Stroke is a major cause of disability worldwide and the second cause of death (1). Its global burden is growing, because of lower mortality and higher incidence (1). Upper limb motor impairment is the most frequent stroke consequence (2). Stroke rehabilitation plays a key role in reducing motor impairment and disability (3). It can include a wide variety of therapeutic options, but their efficacy on motor functions is still unclear (4). Upper limb rehabilitation of stroke patients represents one of the main aims of rehabilitative process for its functional and social participation implications. Functional recovery after stroke is driven by affected harm use in a task-oriented manner, leading to axonal sprouting and novel neuronal connections (5). It is known that task-oriented exercises are effective in improving upper limb functions (6). While intensity and task-oriented characteristics of the training are clearly important, the engagement, motivation, the involvement of adequate neural infrastructure provide increased resource to allow the recovery process (7).

Technological devices can help the therapist in this kind of training, providing enriched and top down (8) therapy over a longer period, indeed they

Key Words: sensor-based motor rehabilitation, subacute stroke, Stroke rehabilitation, upper limb sensory-motor training

Corresponding Author:
Dr Giovanni Morone,
Santa Lucia Foundation,
IRCCS, Via ardeatina 306, 00179, Rome Italy
Tel.: 3906 51501077
e-mail: g.morone@hsantalucia.it.

0393-974X (2020)

DISCLOSURE: ALL AUTHORS REPORT NO CONFLICTS OF INTEREST RELEVANT TO THIS ARTICLE.

are often integrated in clinical practice for stroke patients (9). Moreover, they can help understanding individual needs (giving quantitative measures of impairment) and optimizing learning strategies, by adapting rehabilitation "as needed" (10). Despite their use in stroke rehabilitation, there is still an evidence gap regarding optimal treatment dose and frequency, and characteristics of patients that could benefit from this treatment in terms of severity, latency from stroke event and type of robot. These details are important to guide clinicians to improve therapeutic decision making and define technology application field in upper limb neurorehabilitation.

The PABLO® Upper Extremity is a sensor-based device product by Tyromotion for upper limb unilateral and bilateral training (12, 13). It allows interactive therapy games with audio-visual feedback, training upper limb movements at the three joints (shoulder, elbow and wrist) and measuring the strength of hand functions and the active range of motions of the upper extremity. Three sensors allow to detect movement accelerations in the three dimensions of the space and one sensor detect the hand's strength applied during the movements. These quantitative measures may be used to monitor individual data and therapy progress. PABLO®-Tyromotion is considered a neurocognitive task-oriented approach of rehabilitation and required an active participation of patients.

Based on these considerations, our hypothesis is that an audio-visual feedback and hand training performed with a sensor-based technology (PABLO®-Tyromotion) in addition to the conventional neurorehabilitation, may increase the effect of conventional therapy in upper limbs functions of patients with stroke. For that purpose, the study aim was to evaluate the effects of a sensor-based technology on the upper limbs motor recovery in patients with stroke during post-acute neurorehabilitation.

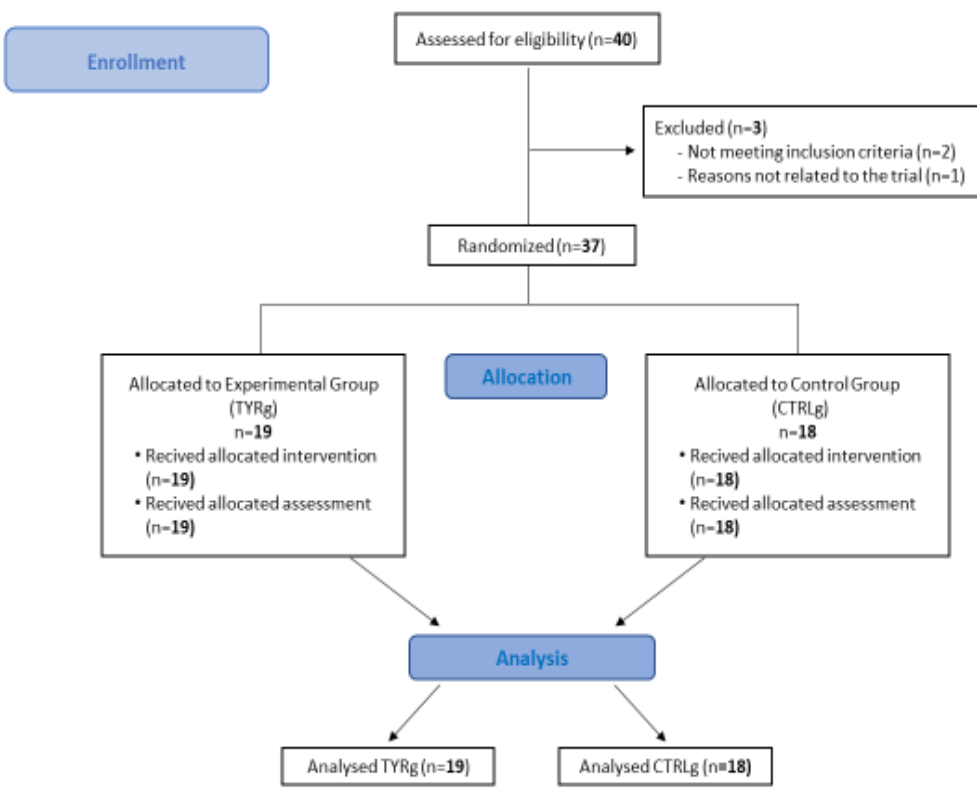

Fig. 1. *Flow Chart.* ***TYRg****= Experimental Group;* ***CTRLg****= Control Group.*

MATERIAL AND METHODS

Trial design

This was a two-arm single-blind randomized controlled trial (Fig 1). The guidelines for Good Clinical Practice, and the Consolidated Standards of Reporting Trials (CONSORT), were followed. The trial was approved by the Local Ethics Committee with the number CE/PROG.631. All participants gave their written informed consent for the participation in the study. A researcher who was not involved in the intervention sessions assessed the patients' eligibility to participate, based on the inclusion and exclusion criteria. Participants were randomly assigned to one of two groups: experimental (TYRg) or control group (CTRLg).

Participants

Thirty-seven patients (27 males, mean age 58.46 years) with a diagnosis of stroke in sub-acute phase (<6 months after stroke) were recruited and enrolled on the basis of consecutive sampling from January 2018 to February 2020 at the Fondazione Santa Lucia (FSL), Institute for Research and Health Care.

Inclusion criteria were as follows: hemiplegia/hemiparesis in the subacute phase caused by a first-ever stroke, lesions that were confirmed by computed tomography or magnetic resonance imaging, and age between 25 and 80 years, with Mini-Mental State Examination (MMSE) ≥ 24 (14) and Medical Research Council (MRC) scale (15, 16) ranging from 1 to 4. Exclusion criteria were: Modified Ashworth Scale (MAS) (17) >3 at the upper limb; cognitive deficits affecting the ability to understand task instructions (MMSE <24) (14); MRC scale (15, 16) with score 0 or 5; presence of clinically evaluated severe comorbidities; pregnancy; subjects with artificial pacemaker; subjects involved in other studies. Demographic characteristics of the sample are reported in Table I.

Interventions - The experimental group's intervention

TYRg performed twelve sessions of upper limb training with PABLO®-Tyromotion. For each session, the

Table I. *Demographic characteristics at baseline*.

	TYRg (n=19)	CTRLg (n=18)	p value
Age (years)* ±SD	56.8 ± 9.2	60.2 ± 14.9	0.438
Sex n (%)#			0.463
Male	15 (78.95)	12 (66.67)	
Female	4 (21.05)	6 (33.33)	
Disease subtype n (%)#			1.000
Ischemic	10 (52.63)	9 (50.00)	
Hemorrhagic	9 (47.37)	9 (50.00)	
Time since stroke (months)* ±SD	4.79±0.79	4.89±0.66	0.684
MRC	64.7±21.5	73.3±15.1	0.265
MBI	75.5±24.1	72.0±29.3	0.831

Mean ± standard deviation. ***TYRg=*** *Experimental Group;* ***CTRLg=*** *Control Group;* ***MRC=****Medical Research Council Scale for muscle strength, upper limbs, ranging from 0 (most affected) to 110 (least affected);* ***MBI=*** *Modified Barthel Index, ranging from 0 (most affected) to 100 (least affected); #: Chi-square test; *: t-Student test*.

training consisted in interactive-games based on virtual reality which allowed a task-oriented approach and a neurocognitive feedback. The proposed exercises required precision tasks and one-dimensional and bidimensional reaction, allowing to train the attention, the strength control and movement control, the coordination, and the movement precision. All the proposed tasks required the full collaboration and motivation of the patient. The interactive games were chosen from those proposed by the Tyromotion PABLO® System (13).

Control group's intervention

CTRLg performed twelve session of upper limb sensory-motor training, without robotic support. Subjects performed specific exercises that aimed to recovery global upper limb functions, to control hand grasp and to improve hand's fine movements. Both groups performed the training three times a week for 4 weeks. Each session lasted 40 minutes and was performed in addition to the conventional neurorehabilitation (18-20). Both trainings were carried out by physiotherapists with experience in neurorehabilitation.

Outcomes

At enrolment, clinical and demographic data were collected. A blinded examiner assessed primary and secondary outcomes. All patients were evaluated at baseline (T0) and after 4 weeks of training (T1). The primary outcome were the changes in functionality of the upper limb measured in 9 Hole Peg Test (9HPT) (21), at 1 month. Secondary outcome measure was the Modified Barthel Index (MBI) (22). Moreover, the measurement of exerted force for pinch, lateral grip, three-point grip and interdigital grip was performed using the evaluation system of the Tyromotion PABLO® device. All clinical scale scores were collected by a researcher not aware of the allocation group and not involved in the intervention sessions.

Sample size

The sample size complied with the minimum number of participants recommended by a power analysis performed on preliminary data (α=0.05; β=0.8; ES=0.5) for nonparametric between group comparisons (23). This sample-size estimation procedure recommends that at least 15 patients be included in each group (24).

Blinding

A researcher, not involved in the intervention sessions, carried out the randomization. Block randomization was performed with a computer-generated randomization list using a block size. Allocation concealment was ensured by using an automatic random number generator (www.random.org). The researcher responsible for the randomization process, deposited the list in a secure web-based storage.

Statistical Analysis

All the statistical analyses were carried out with the IBM SPSSS Statistic Software version 23, IBM Corp. Armonk, NY, U.S.A. Data were reported in terms of means and standard deviations. The paired T-test and the Wilcoxon signed ranks test were used for the within-subjects comparison for both groups at times T0-T1. The Mann-Whitney U-test and the unpaired t-test was used to compare data between groups at T0 and T1. The

Table II. *Results of within subject analysis and of the percentages of effectiveness.*

	TYRg				CTRLg			
	T0 mean ± SD	T1 mean ± SD	p-value (T1-T0)	Increase T1vsT0 (%) ± SD	T0 mean ± SD	T1 mean ± SD	p-value (T1-T0)	Increase T1vsT0 (%) ± SD
9-HPT	294.5±220.6	166.9±132.7	0.000*	NA	229.6±232.5	196.1±199.9	0.016*	NA
MBI	75.5±24.1	92.2±9.0	0.000*	73.3±20.9	72.00±29.3	83.39±21.8	0.001*	60.0±27.8

Mean ± standard deviation; ***TYRg*** *= experimental group;* ***CTRLg*** *= Control Group;* ***9-HPT****=9 Hole Peg Test;* ***MBI****=Modified Barthel Index;* ***NA****= not applicable; The Effectiveness is the percentage of improvement and was calculated as follow: [(T1 score – T0 score / maximal score-T0 score) X 100] *= significant for p<0,05 within subjects' analysis.*

significance was considered for $p<0.05$. The descriptive analysis was performed using [(T1 score – T0 score / maximal score-T0 score) X 100] (25) to calculate the percentages of effectiveness in the two groups.

RESULTS

Thirty-seven patients met the inclusion criteria and were enrolled in the study. None of the enrolled subjects left the study before the end. The statistical analysis was performed using the data of thirty-seven subjects (TYRg=19, CTRLg=18). There were no significant between-group differences in demographics and clinical data in outcome measures at baseline (T0).

Both groups showed a statistically significant improvement along time in the within subjects' analysis, in 9HPT and MBI; no significant differences were found in the between-group analysis. The analysis of effectiveness revealed that, compared with baseline (T0), the improvement percentage in the MBI was greater in the TYRg than the CTRLg (Table II).

Regarding the MRC scores, both groups show a significant improvement for the within group analysis, in all the assessed items (Table III). Significant differences in the between-subjects' analysis were found for the elbow extension, forearm supination and forearm pronation MRC scores in the TYRg with respect to the CTRLg (Table IV).

Table III. *MRC scale Scores.*

	TYRg			CTRLg		
	T0 mean ± SD	T1 mean ± SD	p-value (T1-T0)	T0 mean ± SD	T1 mean ± SD	p-value (T1-T0)
Shoulder Flex	2.9±1.0	3.7±1.0	0.001*	3.4±0.8	3.8±1.1	0.035*
Shoulder Ext	3.1±1.0	4.1±0.9	0.000*	3.4±0.8	3.8±1.1	0.035*
Shoulder Abd	3.1±0.9	3.9±1.1	0.000*	3.2±1.0	3.6±1.1	0.005*
Shoulder Add	3.6±1.0	4.4±0.9	0.001*	3.6±0.9	4.1±0.9	0.005*
Shoulder Lat.Rot	2.9±0.9	3.7±0.8	0.000*	2.9±0.9	3.4±1.1	0.007*
Shoulder Med.Rot	3.3±0.9	4.1±0.8	0.001*	3.3±0.8	3.9±0.8	0.002*
Elbow Flex	3.4±0.8	4.5±0.8	0.000*	3.6±0.8	4.0±1.0	0.005*
Elbow Ext	3.6±1.1	4.5±0.9	0.001*	3.4±0.9	3.8±1.0	0.008*
Forearm Sup	3.2±0.9	4.3±0.9	0.000*	3.1±0.8	3.6±1.0	0.005*
Forearm Pron	3.3±1.0	4.4±0.8	0.000*	3.6±1.0	3.2±0.8	0.014*
Wrist Flex	2.8±1.2	3.7±1.0	0.001*	3.3±0.8	3.7±1.0	0.008*
Wrist Ext	2.8±1.2	3.7±1.1	0.001*	3.3±0.8	3.6±0.9	0.025*
Metacarpophalangeal joints Flex	2.8±1.3	3.8±1.1	0.000*	3.3±0.8	4.0±1.0	0.001+
Metacarpophalangeal joints Ext	2.8±1.2	3.7±1.2	0.000*	3.3±1.0	3.6±1.0	0.0014*
Interphalangeal joints Flex	2.6±1.4	3.7±1.2	0.000*	3.3±0.9	3.9±1.1	0.002*
Fingers Abd	2.4±1.3	3.3±1.1	0.000*	3.2±0.9	3.4±0.9	0.046*
Fingers Add	2.5±1.3	3.7±1.0	0.000*	3.4±0.8	3.8±1.0	0.008*
Metacarpophalangeal and Interphalangeal joints of Thumb Flex	2.7±1.3	3.8±1.0	0.000*	3.6±0.7	4.1±0.8	0.002*
Metacarpophalangeal and Interphalangeal joints of Thumb Ext	2.7±1.2	3.7±1.1	0.001*	3.4±0.7	3.7±1.0	0.025*
Thumb Abd	2.7±1.1	3.7±1.1	0.001*	3.5±0.7	3.9±0.8	0.008*
Thumb Add	2.9±1.3	4.1±1.1	0.000*	3.6±0.7	4.1±0.9	0.003*
Opposition of Thumb and Little finger	2.6±1.3	3.5±1.2	0.000*	3.1±0.9	3.6±1.0	0.002*

Mean ± standard deviation. ***TYRg****= Experimental Group;* ***CTRLg****= Control Group;* ***Abd****=abduction;* ***Add****=adduction;* ***Ext****=extension;* ***Flex****=flexion;* ***Pron****=pronation;* ***Sup****=supination;* ***Lat****=lateral;* ***Med****=medial;* ***Rot****=rotation; *= significant for p<0,05 within subjects' analysis.*

Table IV. *MRC statistically significant values for the between-group analysis.*

	TYRg		CTRLg			
	T0 mean ± SD	T1 mean ± SD	T0 mean ± SD	T1 mean ± SD	p-value (T0-T0)	p-value (T1-T1)
Elbow Ext	3.6±1.1	4.5±0.9	3.4±0.9	3.8±1.0	0.392	0.028*
Forearm Sup	3.2±0.9	4.3±0.9	3.1±0.8	3.6±1.0	0.558	0.036*
Forearm Pron	3.3±1.0	4.4±0.8	3.6±1.0	3.2±0.8	0.745	0.013*

Mean ± standard deviation. ***TYRg****= Experimental Group;* ***CTRLg****= Control Group;* ***Ext****=extension;* ***Flex****=flexion;* ***Pron****=pronation;* ***Sup****=supination; *= significant for p<0.05 in the between subjects' analysis.*

Table V. *PABLO®-Tyromotion scores.*

	TYRg			CTRLg		
	T0 mean ± SD	T1 mean ± SD	p-value (T1-T0)	T0 mean ± SD	T1 mean ± SD	p-value (T1-T0)
Hand grip-extension force	7.1±6.2	9.6±7.8	0.01*	7.3±6.0	9.1±7.4	0.20
Precision pinch thumb-forefinger	2.0±1.5	2.7±1.5	0.00*	2.4±1.7	1.8±1.7	0.06
Precision pinch thumb-middle finger	1.9±1.6	2.6±1.3	0.01*	2.1±1.5	2.5±1.3	0.03*
Precision pinch thumb-ring finger	1.5±1.3	2.0±0.8	0.01*	1.5±1.0	2.1±1.1	0.00*
Precision pinch thumb-Little finger	1.1±1.3	1.3±0.6	0.20	1.2±0.9	1.5±1.1	0.15
Lateral pinch thumb- forefinger	3.0±1.9	3.7±1.6	0.00*	3.7±2.2	3.8±2.0	0.07
Interdigital pinch forefinger-middle finger	1.0±1.0	1.8±1.2	0.00*	1.7±1.5	1.6±1.1	0.60
Interdigital pinch middle finger - ring finger	1.0±1.2	1.8±1.3	0.00*	1.2±1.2	1.4±1.2	0.07
Interdigital pinch ring finger - Little finger	0.8±1.2	1.3±1.2	0.00*	1.0±1.0	1.4±1.5	0.04*
Pinch thumb- forefinger- middle finger	1.9±1.1	3.1±1.2	0.00*	2.6±1.6	3.1±1.6	0.15
Shoulder Abd/Add	127.2±53.1	140.6±50.2	0.41	131.9±52.3	141.6±51.6	0.17
Shoulder Flex/Ext	154.8±46.7	177.9±47.9	0.00*	151.8±45.2	160.0±45.2	0.16
Elbow Flex/Ext	154.2±51.7	165.6±49.1	0.03*	162.9±42.4	158.6±46.6	0.67
Forearm Sup/Pron	102.4±48.6	130.4±40.2	0.01*	107.3±35.3	127.0±42.6	0.04*
Wrist Flex/Ext	105.2±32.1	124.8±33.5	0.00*	105.6±30.0	108.1±36.6	0.71

Mean ± standard deviation. ***TYRg****= Experimental Group;* ***CTRL****=Control Group.* ***Ext****=extension;* ***Flex****=flexion;* ***Pron****=pronation;* ***Sup****=supination;* ***Abd****=abduction;* ***Add****=adduction; *=significant for p<0.05 in the within subjects' analysis.*

The PABLO®-Tyromotion scores show a statistically significant improvement in 13 out of the 15 evaluated districts for TYRg and 4 out of the 15 for CTRLg, considering the within subjects' analysis (Table V); no significant differences were found in the between subjects' analysis. No side effects were reported.

DISCUSSION

The aim of this study was to evaluate the effects of a sensor-based training performed with PABLO®-Tyromotion on the upper limb motor recovery in patients with stroke during post-acute neurorehabilitation. Both groups showed significant improvements in terms of arm motor recruitment and functional recovery. However, the percentage of functional improvement in MBI was greater for TYRg than CTRLg, while between groups differences were not significant.

Consistently, Tyromotion instrumental scores improved more in TYRg than CTRLg, in functions directly involved in exercises. We can hypotize that these results are related to the strength of PABLO®-Tyromotion training, as the possibility to gain a stronger and lasting intrinsic motivation (26) and the visual feedback allowing greater awareness of upper limb abilities and improvements over time. Moreover, this sensor-based motor rehabilitation provides intensive and motivating task-oriented training (27) and might increase cognitive network involvement as for example attentional and executive resources (28, 29). It is noteworthy that most of the researches published in literature on the technological devices for upper limb regards robot or electromechanical assisted machines introduced more than 20 years ago (30) while sensor based technology has been only recently introduced with few research studies most of which regards chronic subjects.

Tiemmermans and colleagues are finding feasible and usable sensor-based task-oriented training, in a small sample of chronic stroke patients, treated for eight weeks (31). The same research group compared sensor-supported versus robot-supported task-oriented arm training for highly functional chronic stroke patients, highlighting possible best treatment option with sensor-based training in this specific stroke population (32). Our results are in accordance with previous studies regarding upper limb sensor-based training in subjects with stroke. A recent review stated that robot and sensor assisted training ensures high-quality therapy to the largest possible patient group with lower health care costs (12). In addition, sensor-based technology might be a good option to measure training parameters as frequency, intensity, amount, and dose and as an outcome to quantify in a lab and in the real world for improvement ability (33).

The present study has some limitation. Firstly, the small study sample included different types of stroke (i.e. haemorrhagic and ischemic, right and left hemiparesis), resulting in a heterogonous group. Second, although the patients have shown themselves available and pleasantly satisfied with the training with PABLO®- Tyromotion, we did not use any validated scale to measure enjoyment and intrinsic motivation (34). In addition, future instrumental assessments (35, 36) of muscles' activity, and training parameters as frequency and intensity may be considered. In conclusion the use of a sensor-based training with audio-video-feedback could be a useful complementary strategy for improving upper limb motor functions in patients with stroke during post-acute neurorehabilitation. Future studies on larger populations are needed to better understand the clinical value of the achieved results.

ACKNOWLEDGEMENT

The study was partially supported by the Italian Ministry of Health (Ricerca Corrente).

REFERENCES

1. Katan M, Luft A. Global Burden of Stroke. Semin Neurol 2018; 38(2):208-11.
2. Raghavan P. Upper Limb Motor Impairment After Stroke. Phys Med Rehabil Clin N Am 2015; 26:599-610.
3. Pollock A, Farmer SE, Brady MC, et al. Interventions for improving upper limb function after stroke. Cochrane Database Syst Rev 2014; 2014:CD010820.
4. Veerbeek JM, van Wegen E, van Peppen R, van der Wees PJ, Hendriks E, Rietberg M, Kwakkel G. What

is the evidence for physical therapy poststroke? A systematic review and meta-analysis. PLoS One 2014; 9:e87987.
5. Overman JJ, Clarkson AN, Wanner IB, et al. A role for ephrin-A5 in axonal sprouting, recovery, and activity-dependent plasticity after stroke. Proc Natl Acad Sci U S A 2012; 109:E2230-E2239.
6. French B, Thomas LH, Coupe J, et al. Repetitive task training for improving functional ability after stroke. Cochrane Database Syst Rev 2016; 11:CD006073.
7. Winstein C, Varghese R. Been there, done that, so what is next for arm and hand rehabilitation in stroke? Neurorehabilitation 2018; 43:3-18.
8. Morone G, Spitoni GF, De Bartolo D, et al. Rehabilitative devices for a top-down approach. Expert Rev Med Devices 2019; 16:187-95.
9. Klamroth-Marganska V. Stroke Rehabilitation: Therapy Robots and Assistive Devices. Adv Exp Med Biol 2018; 1065:579-87.
10. Squeri V, Basteris A, Sanguineti V. Adaptive regulation of assistance 'as needed' in robot-assisted motor skill learning and neurorehabilitation. IEEE Int Conf Rehabil Robot 2011; 2011:5975375.
11. Rodgers H, Bosomworth H, Krebs HI, et al. Robot assisted training for the upper limb after stroke (RATULS): a multicentre randomised controlled trial. Lancet 2019; 394:51-62.
12. Jakob I, Kollreider A, Germanotta M, Benetti F, Cruciani A, Padua L, Aprile I. Robotic and Sensor Technology for Upper Limb Rehabilitation. PMR 2018; 10:S189-S197.
13. Tramontano M, Morone G, De Angelis S, Casagrande Conti L, Galeoto G, Grasso MG. Sensor-based technology for upper limb rehabilitation in patients with multiple sclerosis: A randomized controlled trial. Restor Neurol Neurosci 2020 (in press).
14. Folstein MF, Folstein SE, McHugh PR. "Mini-mental state". A practical method for grading the cognitive state of patients for the clinician. J Psychiatr Res 1975; 12:189-98.
15. Florence JM, Pandya S, King WM, et al. Intrarater reliability of manual muscle test (Medical Research Council scale) grades in Duchenne's muscular dystrophy. Phys Ther 1992; 72:115-26.
16. Paternostro-Sluga T, Grim-Stieger M, Posch M, et al. Reliability and validity of the Medical Research Council (MRC) scale and a modified scale for testing muscle strength in patients with radial palsy. J Rehabil Med 2008; 40:665-71.
17. Ansari NN, Naghdi S, Arab TK, Jalaie S. The interrater and intrarater reliability of the Modified Ashworth Scale in the assessment of muscle spasticity: limb and muscle group effect. NeuroRehabilitation 2008; 23:231-237.
18. Tramontano M, Bergamini E, Iosa M, Belluscio V, Vannozzi G, Morone G. Vestibular rehabilitation training in patients with subacute stroke: A preliminary randomized controlled trial. NeuroRehabilitation 2018; 43:247-254.
19. Tramontano M, Dell'Uomo D, Cinnera AM, et al. Visual-spatial training in patients with sub-acute stroke without neglect: a randomized, single-blind controlled trial. Funct Neurol 2019; 34:7-13.
20. Morone G, Tramontano M, Iosa M, et al. The efficacy of balance training with video game-based therapy in subacute stroke patients: a randomized controlled trial. Biomed Res Int 2014; 2014:580861.
21. Chen HM, Chen CC, Hsueh IP, Huang SL, Hsieh CL. Test-retest reproducibility and smallest real difference of 5 hand function tests in patients with stroke. Neurorehabil Neural Repair 2009; 23:435-40.
22. Shah S, Vanclay F, Cooper B. Improving the sensitivity of the Barthel Index for stroke rehabilitation. J Clin Epidemiol 1989; 42:703-9.
23. Cohen J. Statistical power analysis for the behavioral sciences. Revised edition. New York: Academic Press 1977.
24. Lum PS, Burgar CG, Shor PC, Majmundar M, Van der Loos M. Robot-assisted movement training compared with conventional therapy techniques for the rehabilitation of upper-limb motor function after stroke. Arch Phys Med Rehabil 2002; 83:952-9.
25. Shah S, Vanclay F, Cooper B. Efficiency. effectiveness. and duration of stroke. Stroke 1990; 21:241-6.
26. Vansteenkiste M, Lens W, Deci E L. Intrinsic versus Extrinsic Goal-Contents in Self-Determination Theory: Another Look at the Quality of Academic Motivation. Educational Psychologist 2006; 41:19-31.
27. Li C, Rusák Z, Horváth I, Ji L. Influence of complementing a robotic upper limb rehabilitation system with video games on the engagement of the participants: a study focusing on muscle activities. International journal of rehabilitation

research 2014. Internationale Zeitschrift fur Rehabilitationsforschung. Revue internationale de recherches de readaptation 2014; 37:334–342.
28. Green CS, Bavelier D. Learning, attentional control, and action video games. Curr Biol 2012; 22(6):R197-R206.
29. Iosa M, Ghanbari Ghooshchy S, Morone G, et al. Visuomotor Integration for Coupled Hand Movements in Healthy Subjects and Patients with Stroke. Front Bioeng Biotechnol 2020; 8:591.
30. Morone G, Cocchi I, Paolucci S, Iosa M. Robot-assisted therapy for arm recovery for stroke patients: state of the art and clinical implication. Expert review of medical devices 2020; 17:223-233.
31. Timmermans AA, Seelen HA, Geers RP, et al. Sensor-based arm skill training in chronic stroke patients: results on treatment outcome, patient motivation, and system usability. IEEE Trans Neural Syst Rehabil Eng 2010; 18(3):284-92.
32. Timmermans AA, Lemmens RJ, Geers RP, Smeets RJ, Seelen HA. A comparison of treatment effects after sensor- and robot-based task-oriented arm training in highly functional stroke patients. Conf Proc IEEE Eng Med Biol Soc 2011; 2011:3507-10.
33. Schwarz A, Bhagubai MMC, Wolterink G, Held JPO, Luft AR, Veltink PH. Assessment of Upper Limb Movement Impairments after Stroke Using Wearable Inertial Sensing. Sensors (Basel) 2020; 20(17):E4770.
34. van der Kooij K, van Dijsseldonk R, van Veen M, Steenbrink F, de Weerd C, Overvliet KE. Gamification as a Sustainable Source of Enjoyment During Balance and Gait Exercises. Front Psychol 2019; 10:294. doi:10.3389/fpsyg.2019.00294.
35. Bergamini E, Iosa M, Belluscio V, Morone G, Tramontano M, Vannozzi G. Multi-sensor assessment of dynamic balance during gait in patients with subacute stroke. J Biomech 2017; 61:208-15.
36. Belluscio V, Bergamini E, Iosa M, Tramontano M, Morone G, Vannozzi G. The iFST: An instrumented version of the Fukuda Stepping Test for balance assessment. Gait Posture 2018; 60:203-8.

Clinical and functional outcomes of cad/cam mandibular reconstruction with free fibular flap comparing traditional versus micro-invasive intraoral surgical approaches

A.R. Bolzoni[1,2], A Pollice[2], M Nuti[2], A. Baj[1,2], D.S. Rossi[2] and G.A. Beltramini[2]

[1]Department of Biomedical, Surgical and Dental Sciences, Università degli Studi di Milano, Milan, Italy; [2]Maxillo-Facial and Dental Unit, Fondazione Ca' Granda IRCCS Ospedale Maggiore Policlinico Milan, Italy

The surgical incision plays a pivotal role in any surgical procedure. A good surgical approach should allow optimal visualization, respect the anatomy and ensure the best aesthetic outcome possible, especially when the lesions involve the face. In this retrospective study, carried out from June 2014 to April 2018, different types of surgical approaches to perform mandibular reconstruction were compared. Twenty-one patients who underwent mandibular reconstruction with free fibular flap (FFFs) using CAD-CAM technology and Virtual Surgical Planning (VSP) were included in the study, regardless the condition, the timing of reconstruction (primary vs secondary), the number of fibular segments or the type and size of the mandibular defect. The patients were treated for mandibular defects secondary to benign or low-grade oncological lesions and different non-oncological conditions. However, patients requiring neck dissection were excluded from the study. Patients were divided into two groups according to the type of surgical approach used: 7 patients received a traditional transcervical approach together with an intraoral approach, while 14 patients were operated through an intraoral approach combined with different microinvasive approaches, including the sub-mandibular, the retro-mandibular and the pre-auricular approaches. Different factors were statistically compared: characteristics of the harvested fibula, surgical timing, days of hospitalization, as well as complication, functional and aesthetic outcomes. According to this study, no statistically significant differences were observed between the two groups in any of the features considered. These results support the hypothesis that the combination of different microinvasive approaches and the traditional approach are superimposable, and they can be safely exchanged when the underlying defects allow it.

The mandibular reconstruction continues to be a challenge for the maxillofacial surgeon. The mandible represents the bearing platform of the lower teeth and the site of insertion of the masticatory muscles as well as the extrinsic tongue muscles, therefore it has a crucial role for mastication, deglutition, and phonation. Moreover, the mandible is a major aesthetic landmark of the face: it defines the cosmetic contour of the lower third of the face and contributes to the overall facial harmony. The surgeon has to deal with the complexity of this region, in terms of functions and aesthetic and he has to guarantee a successful surgical demolition to eradicate the illness (1, 2). Therefore, an accurate planning and a multidisciplinary approach are required to optimise the functional and cosmetic outcomes.

There are many indications for a mandibular reconstruction, ranging from congenital abnormalities to traumatic injuries and inflammatory diseases, such as osteoradionecrosis or osteomyelitis,

Key words: cad/cam mandibular reconstruction, intraoral surgical approaches, surgical incision

Corresponding Author:
Dr Alessandro Remigio Bolzoni,
Department of Biomedical, Surgical and Dental Sciences,
Università degli Studi di Milano, Milan, Italy
Tel.: +393343390423 - Fax: +390255032842
e-mail: alessandro.bolzoni1@unimi.it

0393-974X (2020)

as well as malignant and benign tumours' ablative surgery, that require necessary radicality. Indeed, the age of the patients who need a good reconstruction in terms of functional and aesthetic outcomes is increasing overtime (3). Even though the complete demolition of the lesion is still a predominant aspect of the head and neck surgery, many efforts have been made to guarantee a total recovery of the mandible's function and aesthetic. The goals of the mandibular reconstruction are: to restore the bone and its internal and external soft tissue envelopes, to re-establish the form of the lower third of the face and to provide a support for dental rehabilitation (4-8). An excellent recovery of the oral function and of the facial width, height and projection would allow the patient to resume normal family and social lives, thereby improving his quality of life as well as the survival rate (9, 10).

Many mandibular reconstruction procedures have been attempted and reported; however, the outcomes have considerably changed with the introduction of the free vascularized bone flaps (11). The free osteocutaneous fibular flap (FOFF), first introduced by Taylor et al. (12), has become the state-of-the-art to reconstruct the mandible. The free fibula flap provides a considerable length of bone, that allows multiple osteotomies and extensive remodelling, and a large skin paddle that is adequate for the small soft tissue defects. Moreover, it reduces the donor site morbidities (13-17).

Moreover, the introduction of the CAD-CAM technology and the Virtual Surgical Planning (VSP) has strongly contributed to a global improvement of the mandibular reconstruction. This technique has replaced the free-hand method in multiple centres, and it is becoming the gold standard to achieve a successful bone reconstruction (18, 19). The CAD-CAM technology allows for a detailed pre-operative three-dimensional (3D) virtual surgical planning, to be obtained, that is translated into custom patient-specific plates and surgical cuttings guides that allow an accurate and symmetric bone reconstruction (20). The advantages of this technique have been well documented in the literature (21-23). This technology confers reproducible and accurate results, it decreases the surgical timing, it improves the bone-to-bone contact as well as the facial symmetry and the functional outcomes (24).

Contrary to the free-hand method, the CAD-CAM technology introduced the possibility of performing the mandibular resection and reconstruction through a transoral approach, reserving a submandibular incision for the microvascular reconstruction. Even though the choice of the surgical approach is mainly guided by the site and the extent of the defect, the prospect to perform only a transoral incision is highly promising in terms of cosmetic and functional outcomes and it reduces the complications related to the transcervical approach (25).

The purpose of this study is to compare traditional versus micro-invasive surgical approaches used in CAD-CAM mandibular reconstruction with free fibular flap, in terms of clinical and functional outcomes, such as the oromandibular functions, facial symmetry and post-operative complications.

MATERIALS AND METHODS

Twenty-one patients were included in this retrospective study, carried out in the Maxillofacial Unit of Fondazione IRCCS Cà Granda Ospedale Maggiore Policlinico of Milan between June 2014 and April 2018. All the patients underwent mandibular reconstruction with free fibular flap (FFFs) using CAD-CAM technology and Virtual Surgical Planning (VSP). The traditional transcervical approach was compared with different microinvasive approaches.

The patients were divided into two groups according to the surgical approach used. The first group, specifically the "traditional approach" group, included all those patients who underwent a mandibular reconstruction by means of a laterocervical approach together with an intraoral approach. The transcervical approach consisted of an "apron" incision, from mastoid to mentum. In this way the mandible and the cervical regions were exposed from the symphyseal and submental regions superiorly, to the thyroid cartilage inferiorly, and to the lateral surfaces of the mandible, including the condyles (26). The incision was carefully selected to avoid complications such as wound dehiscence, skin flap necrosis or exposure of the carotid artery consequent to neck dissection. The intraoral approach consisted of a single incision through the vestibule of the oral cavity. This technique allows

safe access to the full external surface of the mandible. However, being limited to the lower border of the mandible, the mandibular angle, and parts of the ramus, it is well known in literature to be more appropriate in case of anterior mandibular defects (14).

The second group, namely the "microinvasive approach" group, consisted of the patients who had a mandibular reconstruction through an intraoral approach, described above, combined with different transfacial approach, other than the laterocervical one. These were the submandibular, the retromandibular and the pre-auricular approaches. The submandibular (or Ridson) approach, initially described by Ridson (27) and later modified by Meyer, is known to be the most useful approach to expose the mandibular ramus and posterior body region. It was performed as a single incision 1.5 to 2 cm below the inferior border of the mandible at the site of the defect. In the retromandibular approach, the incision was placed below the lobe of the ear and it continued inferiorly, 3 to 3.5 cm behind the posterior border of the mandible, to expose the ramus and to reach the area of the condyle (28). The preauricular approach, that represents the standard approach to the TMJ and its components, was performed as a single incision following the natural crease of the tragus. When a greater access was required, the Al -Kayat and Bramley modification with temporal extension was used.

The inclusion criteria were as follows patients requiring mandibular reconstruction with FFFs and availability of preoperative and postoperative high-resolution CT scans of the maxillofacial skeleton. All the patients who underwent mandibular reconstruction with FFFs using CAD-CAM technology were considered, regardless the timing of the reconstruction (primary vs secondary reconstruction), the number of fibular segments or type and the size of the mandibular defect. The patients were treated for mandibular defects secondary to benign (or low grade) oncological and different non-oncological conditions. The patients with malignant oncological lesions that inevitably required neck dissection and lymphadenectomy were excluded from the study.

The clinical condition of the patients was evaluated, with particular care to the comorbidities and past medical history. All the oncological patients underwent tumour staging. The mandibular defects were classified according to the Urken's (29) classification in all patients. CT scans were performed to determine the entity of resection and to accomplish the reconstructive planning. CT angiography of the lower limb was performed in occurrence with the CT scans for the VSP to assess the viability of the vasculature of the donor site. Finally, a post-operative CT scan of the maxillofacial district was performed within one month from the surgical procedure.

Differences in terms of follow-up, characteristics of the fibula segments, surgical timing and days of hospitalization were analysed. Donor-site and recipient-site complications, functional outcomes in terms of speech and oral competence, as well as aesthetic outcomes were recorded in both groups.

The statistical analysis was performed through QuickCalcs-GraphPad software®, SPSS software® and MEDCALC® software. Comparison between the two groups was made using a Student's T test and Chi-squared test. A P-value <0.05 was considered as significant.

RESULTS

Twenty-one patients were included in the study. Two groups were formed: 14 patients operated on according to the microinvasive intraoral approaches and 7 patients who received the transcervical approach. The surgical procedures were all performed by the same surgical teams. The "microinvasive intraoral approach" group included 6 men and 8 women, with a mean age of 43.4 (range: 26 to 67). The "traditional approach" group included 4 men and 3 women, with a mean age of 43 (range: 16 to 67). Mean length of the follow-up was 26 months and it ranged from 6 to 51 months. Difference in follow-up between the two groups was not statistically significant (P=0.3619). No total flap failures were observed. The three patients diagnosed with malignant tumours of the mandible did not show signs of local recurrence during the follow-up.

The patients were treated for mandibular defects secondary to benign oncological and to different non-oncological conditions. The "intraoral approach" group included three patients with low grade malignant lesions, who did not require the neck dissection. In the "intraoral approach" group all the patients underwent a primary mandibular reconstruction, while in the "traditional approach" group there were 5 out of 7 patients who received

Table I. *Clinical features of the twenty -one patients included in the study. Highlighted rules represent the patients who underwent a secondary reconstruction*.

Patient	Sex	Age	Etiology	Type of mandibular defect (Urken's classification)	Type of surgical approach
1	F	53	Malignant mesenchymal tumour	B dx	IO + SMm
2	F	61	Low grade mucoepidermoid carcinoma	R-B	IO + SMm
3	M	60	Low grade mucoepidermoid carcinoma	B-R	IO + SMm
4	F	46	Ameloblastoma	B-R	IO + SMm
5	M	18	Odontogenic fibromyxoma	R-B	IO + SMm
6	F	38	Keratocyst odontogenic tumor	B dx	IO + SMm
7	F	32	Keratocyst odontogenic tumor	B-R	IO + SMm
8	F	55	Ossifying fibroma relapse	B sx	IO + SMm
9	F	58	Ameloblastoma relapse	S-B	IO + SMm
10*	F	37	Ameloblastoma	R-B	IO + LC
11	F	38	Keratocystic odontogenic tumour	B-R-C	IO+PA+SMe
12*	F	55	Pseudoarthrosis	S-B	IO + LC
13	M	23	Keratocystic odontogenic tumour	R-B	IO+PA+SMm
14*	M	65	Fracture secondary to	B sx	IO + LC
			osteoradionecrosis		
15*	F	29	Pseudoarthrosis	B dx	IO + LC
16*	M	32	FFFs flap necrosis following ameloblastoma resection	C-R-B	IO + LC
17	M	31	Chronic sclerosing osteomyelitis	C-R-B	IO+PA+SMm
18*	M	67	Pseudoarthrosis (following SCC resection and RT)	B-S	IO + LC
19*	M	16	Odontogenic fibromyxoma	B-S-B	IO + LC
20	M	26	Keratocystic odontogenic tumour	C-R-B	IO+PA+SMm
21	M	29	Keratocystic odontogenic tumour	B-R	IO+RM+SMm

a secondary reconstruction. The main indication for the second reconstruction was pseudoarthrosis, followed by osteoradionecrosis resulting in mandibular fracture. In only one patient the indication was failure of the primary reconstruction due to flap necrosis. The patients who received a secondary reconstruction are highlighted in the table below (see Table 1). The mandibular defects were classified according to the Urken's classification in both groups. The patients' characteristics, the etiology of the lesion, the Urkens's classification of the defect and the type of approach used are listed in the table below (Table I).

The characteristics of the harvested fibula, including the number of bone segments as well as the length of the mandibular defects, are illustrated in the table below (Table II).

The mean length of the defect in the "intraoral approach" group, 8.5 cm (range: 5 to 15.5 cm), was higher compared to that of the "traditional approach" group, corresponding to 7.9 cm (range: 3.5 to 15.5 cm). However, the difference in the length of the defect was not statistically significant (P=0.7354). The mean quantity of the harvested fibula was similar in the two groups: 11 cm (range: 3.5 to 17 cm) in the "intraoral approach" group and 9.79 cm (range: 3.5 to 13.5 cm) in the "traditional group". This difference was not statistically significant (P=0.5359). The mean number of fibular segments was almost equivalent in the two groups: 2.64 in the "intraoral approach" group and 2.57 in the "traditional approach" with no statistically significant difference between the two (P=0.8788). There was neither a statistically significant difference between the mean number of osteotomies carried out in the two groups (P=0.8860). In the "intraoral approach" group double-barrelling was performed in 5 out of 14, while it was carried out only in 1 out of 7 patients who underwent a traditional approach reconstruction.

The surgical timing and the days of hospitalization were also evaluated in the two groups. Regarding the surgical timing, no statistically significant difference was observed (P=0.2659). Neither the difference in days of hospitalization between the two groups was statistically significant (P=0.1872). In fact, the hospitalization lasted on average 15.14 days (range: 11 to 20 days) in the "traditional approach" group and 13.5 days (range: 12 to 17 days) in the

"microinvasive approach" group. Surgical timing and the days of hospitalizations of each patient are showed in the table below (Table III).

Regarding post-operative complications, in the "microinvasive approach" group, the total proportion of complications was 50%, only 0.7% of the patients had donor-site complications, while 42.8% had recipient site complications. The "traditional approach" group showed a donor-site complications rate of 1.4 % and a recipient-site complications rate of 28.5 %, with a total proportion of complications equal to 42.8 %. The differences in total proportion of complications (P=0.7612), along with that of the donor (P=0.8780) and the recipient site (P=0.5346) were not statistically significant. All the complications and their distributions are listed in the following table (Table V).

Specifically, considering the donor site complications, among the "traditional approach" patients, there was one case of partial venous stasis of the skin paddle that was treated with leech therapy. In the "microinvasive approach" group, one patient showed a deficit of the 1st and 2nd toes in plantar flexion.

In relation to the recipient site complications, there was one case of submandibular dehiscence that was left to heal by secondary intention in the "traditional approach" group. The dehiscence observed in the "microinvasive approach" group was further complicated by the reconstruction plate exposition and therefore it required surgical revision. The post-operative haemorrhage observed

Table II. *Characteristics of the harvested flap and its corresponding mandibular defect in the two groups.*

Patient	Type of defect	Length of defect(cm)	The quantity of harvested bone (cm)	No. of fibular segments	No. of osteotomies	Double-barreling	Surgical approach
1	B dx	5	15	2	4	YES	*Microinvasive*
2	R-B	6	15	2	4	YES	*Microinvasive*
3	B-R	3.5	8	1	3	NO	*Microinvasive*
4	B-R	9	22	4	8	YES	*Microinvasive*
5	R-B	10	24	5	10	YES	*Microinvasive*
6	B dx	7	20.5	3	6	YES	*Microinvasive*
7	B-R	6	19.5	3	6	YES	*Microinvasive*
8	B sx	6	16	3	6	YES	*Microinvasive*
9	S-B	5.5	17.5	5	10	YES	*Microinvasive*
10	R-B	8	15	2	4	NO	*Traditional*
11	B-R-C	13	23	2	4	NO	*Microinvasive*
12	S-B	6	21.5	4	8	YES	*Traditional*
13	R-B	11.5	22	4	8	YES	*Microinvasive*
14	B sx	7	15.5	2	4	NO	*Traditional*
15	B dx	3.5	9.5	1	2	NO	*Traditional*
16	C-R-B	10.5	18.5	3	6	NO	*Traditional*
17	C-R-B	12.5	25	3	6	YES	*Microinvasive*
18	B-S	5	12.5	2	3	NO	*Traditional*
19	B-S-B	15.5	23	4	8	NO	*Traditional*
20	C-R-B	10	16.5	2	4	NO	*Microinvasive*
21	B-R	9	15.5	2	4	NO	*Microinvasive*
MEAN		8.75	12.19	2.88	5.92		

Table III. *Surgical timings and days of hospitalization of the "microinvasive approach" group.*

Patient	Surgical timing (min)	Days of hospitalization
1	670'	16
2	480'	13
3	410'	14
4	470'	12
5	480'	17
6	485'	13
7	465'	15
8	465'	12
9	445'	13
11	360'	12
13	400'	13
17	570'	12
20	375'	12
21	480	15
MEAN	**468.21**	**13.5**

Table IV. *Surgical timings and days of hospitalization of the "traditional approach" group.*

Patient	Surgical timing (min)	Days of hospitalization
10	570'	11
12	580'	16
14	420'	13
15	670'	17
16	390'	11
18	485'	20
19	480'	18
MEAN	**513.57**	**15.14**

in the "microinvasive approach" group was caused by a leakage of the micro-anastomosis and it was surgically treated. Only in the "traditional approach" group was there a case of cutaneous fistula, while in the "microinvasive approach" group a single case of malocclusion (crossbite) was observed. Other complications included one case of sialocele and one case of stupor of the marginal mandibular nerve in the "microinvasive approach" group.

Finally, a clinical evaluation of the speech, oral competence and aesthetics was carried out by the surgeon during the follow-up period. Considering the severity of the primary lesion and the resulting deformity of the mandible, the functional and aesthetic outcomes were highly satisfactory in both groups.

DISCUSSION

A good selection of the patient (30) and a well-planned surgical incision is one of the most crucial steps in any surgical procedure. The choice of the surgical approach is mainly dictated by the site and the extent of the defect, especially when a requirement of oncological radicality is present. The right placement of the incision not only allows optimal visualization, but substantially contributes to the final aesthetic and functional outcomes. In maxillofacial surgery, many attempts have been made to reduce scarring of the face by skin incisions in areas where scars cannot be easily seen. The microinvasive intraoral surgical approach, as well as allowing for more hidden

Table V. *Distribution of donor-site and recipient-site complications in the two groups.*

Donor site complications	**"Micronivasive approach" patients (%)**	**"Traditional approach" patients (%)**
Partial skin graft loss	-	1(1.4)%
Total skin graft loss	-	-
Motor deficit	1(0.7%)	-
Recipient site complications		
Infection	-	-
Wound dehiscence	1(0.7%)	1(1.4%)
Haemorrhage	-	1(1.4%)
Venous stasis	-	-
Malocclusion	1(0.7%)	-
Reconstruction plate exposition	1(0.7%)	-
Cutaneous fistula	1(0.7%)	1(1.4%)
Sensitive deficit	-	-
Partial flap loss	-	-
Total flap loss	-	-
Need for surgical revision	2(1.4%)	-
Other	2 (1.4%) (*stupor of the marginal mandibular nerve, sialocele*)	-

scars that contribute to an excellent aesthetic result, also reduces the rate of complications related to the transcervical approach, such as scar contracture at the level of the neck, seromas or cutaneous fistulae.

In this study the traditional approaches and the microinvasive intraoral approach in use for the CAD-CAM mandibular reconstruction with the FFFs were compared. Different factors should be considered. The microinvasive approaches coupled with the submandibular approach remain limited to benign or low-grade oncological lesions, where the neck dissection is not necessarily required. However, according to this study the microinvasive approaches can reach the same mandibular exposure of the traditional approach. As matter of fact, the difference in length of the defect between the two groups was not statistically significant (P=0.7354). The two methods are also equivalent in terms of surgical timing (P=0.2659) and days of hospitalization (P=0.1572). Nevertheless, one must consider that the intraoral approach could potentially reduce the days of hospitalization since no surgical drainage is required and the number of possible postoperative complications is lower than in the transcervical approach. However, the difference in post-operative complications between the two groups was not statistically significant, neither in terms of the donor-site nor of the recipient-site complications.

In terms of functional and aesthetic outcomes, both approaches resulted highly satisfactory, even though the microinvasive approach obviously reduced the extent of the resulting scar. Moreover, oncological patients diagnosed with low grade lesions who underwent an intraoral approach together with submandibular microvascular reconstruction, did not show recurrences at the last follow-up. This study showed that it was possible to obtain a lesser visible scar without impairing the accuracy of the reconstruction and that the two methods can be safely interchanged when the underlying defects allows it. However, further studies are needed to truly evaluate the difference between the two techniques and to provide an algorithm to safely choose between the two methods.

First, the sample should be increased. Second, factors more related to the wound healing itself, rather than to the entire procedure, should be investigated. In terms of outcomes, the appearance and characteristics of the scar could be further analysed to evaluate the presence of retractile bands, scar contracture or hypertrophy. The functional impairments such as, difficult to raise the chin or latero-deviation of the head could be included. The patients' satisfaction pertinent to the scar should be recorded. Finally, considering the available data, the possible indications for the different types of approaches could be based on the location of the surgical defect. Moreover, recent studies proposed an intraoral-approach only procedure, where the submandibular incision to perform the microvascular anastomosis was not required (31). This kind of technique might be also investigated in the future.

The reconstruction of the mandibular defects requires an elaborate approach: the mandible has an important role in speech, oral continence, airway management, deglutition and mastication. Although restoring critical mandibular functions is the primary concern of the reconstructive procedure, basic plastic surgery principles should be applied to achieve good aesthetic outcomes. As a matter of fact, the mandible represents a major component of the facial harmony, intermingling form and function in a delicate balance. For aesthetic outcomes, not only the resultant bony reconstruction, but also skin thickness, colour, texture and soft tissue integrity will contribute to restore the anatomic contour and to achieve aesthetically pleasing results.

The major aesthetic units involved in mandibular reconstruction are the lips, the chin and the neck, the surgeon should consider how a defect relates to them and plan the incision in a way to minimize and to obscure the scars. This study demonstrated that the microinvasive intraoral approach can be safely used when the extent of the lesion allows it. The microinvasive intraoral approach ensures a smaller scar, reduces the number as well as the severity of complications and improves the aesthetic outcomes. As a matter of fact, scarring is not only a cosmetic concern, but it can really affect the patients' quality of life.

REFERENCES

1. Baj A, Bolzoni A, Torretta S, Pignataro L. Arterial microanastomoses on the reverse flow of the internal carotid artery reverse flow: an extreme solution

in free-flap revascularisation. How we do it. Acta Otorhinolaryngol Ital 2014; 34(5):368-71.
2. Baj A, Fusco N, Bolzoni A, Carioli D, Mazzucato C. A novel integrated platform for the identification of surgical margins in oral squamous cell carcinoma: results from a prospective single-institution series. BMC Cancer 2019; 19(1):467.
3. Segna E, Bolzoni AR, Giannì AB, Baj A, Beltramini GA. Impact of reconstructive microsurgery on patients with cancer of the head and neck: a prospective study of quality of life, particularly in older patients. Br J Oral Maxillofac Surg 2018; 56(9):830-4.
4. Trignano E, Fallico N, Faenza M, Rubino C, Chen HC. Free fibular flap with periosteal excess for mandibular reconstruction Microsurgery 2013; 33(7):527-33.
5. Baj A, Bolzoni A, Russillo A, Lauritano D. Cone-morse implant connection system significantly reduces bacterial leakage between implant and abutment: An in vitro study J. Biol. Regul. Homeost. Agents 2017; 31(2S1):203-8.
6. Bolzoni A, D'orto O, Laganà F, Avvantaggiato P, Candotto V, Survival and success rate of spiral implants inserted mandible J. Biol. Regul. Homeost. Agents 2020; 34(1S2):7-11.
7. Beltramini G, Rossi D, Bolzoni A, Piva A, Laganà F, Implants outcome inserted in different sites J. Biol. Regul. Homeost. Agents 2020; 34(1S2):13-17.
8. Baj A, Beltramini GA, Bolzoni A, et al. Bacterial colonization of the implant-abutment interface of conical connection with an internal octagon: an in vitro study using real-time PCR. J Biol Regul Homeost Agents 2017; 31(2 Suppl 1):163-168. PMID: 28691468.
9. Misch CE, Qu Z, Bidez MW, Mechanical properties of trabecular bone in the human mandible: Implications for dental implant treatment planning and surgical placement, J. Oral Maxillofac. Surg 1999; 57(6):700-6. doi: 10.1016/S0278-2391(99)90437-8.
10. Candotto V, Scapoli L, Gaudio R, Giannì AB, Bolzoni A et al. Gabapentin affects the expression of inflammatory mediators on healthy gingival cells, Int. J. Immunopathol. Pharmacol 2019. doi: 10.1177/2058738419827765.
11. Ferreira JJ, Zagalo CM, Oliveira ML, Correia AM, Reis AR. Mandible reconstruction: History, state of the art and persistent problems. Prosthetics and Orthotics International 2015; 39(3):182-9. doi: 10.1177/0309364613520032.
12. Ian Taylor G, Miller GDH, Ham FJ, The free vascularized bone graft: A clinical extension of microvascular techniques, Plast. Reconstr. Surg 1975; 55(5):533-44. doi: 10.1097/00006534-197505000-00002.
13. Baj A, Beltramini GA, Demarchi M, Giannì AB, Extended-pedicle peroneal artery perforator flap in intraoral reconstruction, Acta Otorhinolaryngol. Ital 2013; 33(4):282-5.
14. A Baj, Bellocchio G, Marelli S, Goglio L, Formillo P, Giannì AB. Reconstruction of the anterior floor of the mouth using a peroneal perforator free flap. A case report Acta Otorhinolaryngol. Italy 2010; 30(1):47-51.
15. Baj A, Lovecchio N, Bolzoni A, Mapelli A, Giannì AB, Sforza C. Stair ascent and descent in assessing donor-site morbidity following osteocutaneous free fibula transfer: A preliminary study. J. Oral Maxillofac. Surg 2015. doi: 10.1016/j.joms.2014.07.043.
16. Di Giuli R. Zago M, Beltramini GA, et al. Donor-Site Morbidity After Osteocutaneous Free Fibula Transfer: Longitudinal Analysis of Gait Performance. J. Oral Maxillofac. Surg 2015; 73(1):184-93. doi: 10.1016/j.joms.2018.10.016 LK.
17. Baserga C, Massarelli O, Bolzoni AR, Rossi DS, Beltramini GA, Baj A, Giannì AB. Fibula free flap pedicle ossification: Experience of two centres and a review of the literature. J Craniomaxillofac Surg 2018; 46(9):1674-8. doi: 10.1016/j.jcms.2018.06.019. Epub 2018 Jul 5. PMID: 30075903.
18. T De Maesschalck , D S Courvoisier , P Scolozzi . Computer-assisted versus traditional freehand technique in fibular free flap mandibular reconstruction: a morphological comparative study, Eur. Arch. Oto-Rhino-Laryngology 2017; 274(1):517-526. doi: 10.1007/s00405-016-4246-4.
19. Ferri A, Varazzani A, Bolzoni AR, Della Monica M et al. A multicenter survey on computer-aided design and computer-aided manufacturing mandibular reconstruction from Italian community. Microsurgery 2019;39(7):673-4. doi: 10.1002/micr.30505.
20. A R Bolzoni, A Baj, AH. Sweed, AB. Giannì, EF. Montrasio, GA. Beltramini. Role of axial split osteotomy of free fibula flap in mandibular reconstruction and dental rehabilitation. Plast.

Reconstr. Surg. - Glob. Open 2020; 8(1):e2546. doi:10.1097/GOX.0000000000002546.

21. A. Bolzoni, A. Mapelli, A. Baj, F. V. Sidequersky, A. B. Giannì, and C. Sforza, Evaluation of three-dimensional mandibular movements after reconstruction with free fibula flap, Acta Otorhinolaryngol. Ital 2015; 35(6):371-8. doi: 10.14639/0392-100X-504.
22. F. Goker, A. Baj, A. R. Bolzoni, C. Maiorana, A. B. Giannì, and M. Del Fabbro, Dental implant-based oral rehabilitation in patients reconstructed with free fibula flaps: Clinical study with a follow-up 3 to 6 years, Clin. Implant Dent. Relat. Res 2020, doi: 10.1111/cid.12928.
23. F. Goker, A.Baj, AR Bolzoni, C, Maiorana et al. Effectiveness of dental implants placed into microvascular free flaps, Oral Dis 2020; 31. doi: 10.1111/odi.13451.
24. A. H. Sweed, A. R. Bolzoni, A. Kadubiec, G. A. Beltramini, A. Cherchi, and A. Baj, Factors influencing CAD/CAM accuracy in fibula free flap mandibular reconstruction, Acta Otorhinolaryngol. Ital 2020; 40(2):138-43. doi: 10.14639/0392-100X-N0400.
25. A. R. Bolzoni, E. Segna, G. A. Beltramini, A. H. Sweed, A. B. Giannì, and A. Baj, Computer-Aided Design and Computer-Aided Manufacturing Versus Conventional Free Fibula Flap Reconstruction in Benign Mandibular Lesions: An Italian Cost Analysis, J. Oral Maxillofac. Surg 2020; 78(6):1035. E1-1035. e6. doi: 10.1016/j.joms.2019.03.003.
26. L. E. Landa, B. F. Tartan, A. Aguz, C. A. Skouteris, C. Gordon, and G. C. Sotereanos, The transcervical incision for use in oral and maxillofacial surgical procedures, J. Oral Maxillofac. Surg 2003; 61 (3):343-6. doi: 10.1053/joms.2003.50035.
27. F. Risdon, D.D.S, F.R.C.S. Ankylosis of the Temporomaxillary Joint**Read at the Seventieth Midwinter Clinic of the Chicago Dental Society. J. Am. Dent. Assoc 1934; 1933-7. doi:10.14219/jada.archive.1934.0286.
28. N. Patel and R. Cronyn, The periangular approach to the posterior mandible: A novel approach and technique, J. Craniofac. Surg 2018; 29(8):e824-e826, doi: 10.1097/SCS.0000000000004946.
29. M. L. Urken, H. Weinberg, C. Vickery, D. Buchbinder, W. Lawson, and H. F. Biller, Oromandibular Reconstruction Using Microvascular Composite Free Flaps: Report of 71 Cases and a New Classification Scheme for Bony, Soft-Tissue, and Neurologic Defects, Arch. Otolaryngol. Neck Surg 1991; 117(7):733-44. doi: 10.1001/archotol.1991.01870190045010.
30. Segna E, Bolzoni AR, Baserga C, Baj A. Free flap loss caused by heparin- induced thrombocytopenia and thrombosis (HITT): a case report and literature review. Acta Otorhinolaryngol Italy 2016; 36(6):527-33.
31. E. Nkenke, A. Agaimy, C. Von Wilmowsky, and S. Eitner, Mandibular reconstruction using intraoral microvascular anastomosis following removal of an ameloblastoma, J. Oral Maxillofac. Surg 2013; 71(11):1983-92. doi: 10.1016/j.joms.2013.03.027.

Evaluation of factors influencing accuracy of virtual surgical planning in orthognatic surgery

G. Soncini[1], A. Bolzoni[1,2], C. Baserga[1,2], F. Cullati[1], D. S. Rossi[1], A. B. Giannì[1,2]

[1]*Maxillo-Facial and Dental Unit, Fondazione Ca' Granda IRCCS Ospedale Maggiore Policlinico Milan, Italy;* [2]*Department of Biomedical, Surgical and Dental Sciences, Università degli Studi di Milano, Milan, Italy*

Three-dimensional virtual surgical planning has become routine practice in orthognatic and reconstructive surgery for the possibility to realize presurgical evaluation of intraoperative bones movements, the prediction of postoperative results and the high level of accuracy. Thanks to surface superimposition between 3D planned and 3D postoperative model of maxillo-facial skeleton, a medium discrepancy less than 1 mm was found in scientific literature, considering 15 different points of maxillofacial skeleton. In our study we decided to evaluate different factors that could invalidate that result in the same cohort of patients, such as sex, kind of dentofacial deformity, asymmetry, type of surgical approach and entity of maxillo-mandibular movements (more or less than 1 mm). We found out no significant differences among groups. We can state that virtual surgical planning and 3D surgical splints are a valid means of diagnosis, treatment and predictivity regardless factors that could influence post-operative results. In conclusion, virtual surgical planning and 3D surgical splints facilitated diagnosis, treatment planning and accuracy regardless of sex, dentofacial deformity class, surgery techniques, entity of advancement and asymmetry.

The two-jaw orthognatic surgery, Le Fort I osteotomy of the upper jaw, combined with sagittal splint ramus osteotomy (SSRO) and eventually genioplasty, is an efficient procedure to correct dento-maxillofacial deformities (1, 2). The success of two-jaw surgery relies on surgical technique and accurate surgical planning (3, 4). Conventional planning is carried out on the basis of X-ray cephalometric analysis, face bow transfer and mock surgery on plaster cast dental models mounted in a semi-adjustable articulator that leads to the production of an intermediate and final occlusal splint. Hitherto, this has been the gold standard for treatment planning and it is generally satisfactory but it has a number of limitations; in fact it's a time-consuming process, it requires a long learning curve and experience and it has a high risk of inaccuracy. This may lead to errors during the treatment plan (5-7). Furthermore, conventional planning consists of a bidimensional study of the dentofacial deformities while, in the most cases, these pathologies affect both three-dimensional planes (8, 9).

Virtual surgical planning, thanks to the CBCT scans, offers new possibilities of surgical solution and aesthetic results like demonstrated from a lot of studies about reconstructive surgery (10). Also virtual surgical planning aids to obtain a comprehensive 3D evaluation of dental arches and the surrounding hard and soft tissue structures, to simulate different surgical plans and predict the corresponding results, as well as to facilitate the transfer of the virtual surgical plan to actual outcome using 3D printed splints (11, 12). This has led to a change in the patient's evaluation, from the bidimensional to the

Key words: orthognatic surgery, three-dimensional virtual surgery, maxillofacial surgery, dento-maxillofacial deformities

Corresponding Author:
Dr Alessandro Remigio Bolzoni,
Department of Biomedical, Surgical and Dental Sciences,
Università degli Studi di Milano, Milan, Italy
Tel.: +393343390423
Fax: +390255032842
e-mail: alessandro.bolzoni1@unimi.it

0393-974X (2020)

three dimensional one to improve the diagnostic and therapeutic outcomes (13-17).

In fact, with surface superimposition between 3D planned and 3D postoperative model of maxillo-facial skeleton, a medium discrepancy less than 1 mm was found in scientific literature, considering 15 different points of maxillofacial skeleton. To date, several reports have been produced in literature and they seem to be agreed in stating accuracy superiority of virtual 3D surgical planning, in particular for hard tissues (18, 19); however, in clinical practice, virtual surgical planning has not yet replaced the conventional one, as it was expected before. The purpose of this study is to corroborate the accuracy of virtual surgical planning thanks to the using of specific software (Geomagic study Platform); moreover, we want to demonstrate that, among all possible factors, as others author perform for reconstructive surgery, (20) which one could affect accuracy of VSP.

Table I. *Clinical features of the twenty -one patients included in the study. Highlighted rules represent the patients who underwent a secondary reconstruction*.

Patient	Sex	Skeletal class	Asimmetry (Y/N)	Type of surgery	Maxillary advancement (mm)	Mandibular advancement (mm)	Mean discrepancy (mm) (Zavattero et al 2019)
1	f	3	N	Maxillary first	6	0	0.5
2	f	3	Y	Mandibular first	4	8	0.8
3	m	2	N	Mandibular first	4	15	1.34
4	m	3	N	Maxillary first	15	0	0.4
5	f	3	N	Maxillary first	12	0	0.34
6	m	3	Y	Maxillary first	2	0	0.5
7	m	2	N	Mandibular first	2.8	13.8	0.6
8	m	3	N	Maxillary first	5	4	0.6
9	f	3	N	Maxillary first	2	0	0.8
10	f	3	N	Maxillary first	0	3.6	1.7
11	f	3	N	Maxillary first	1	7.4	0.4
12	f	3	Y	Maxillary first	2	1.5	0.3
13	m	3	N	Maxillary first	4	0.9	0.9
14	f	2	N	Maxillary first	3	8.3	1.7
15	m	3	N	Maxillary first	8.8	0	1.6
16	m	2	N	Maxillary first	0.5	16	0.7
17	f	2	N	Mandibular first	2	15	1.7

MATERIALS AND METHODS

Seventeen consecutive patients were included in this observational multicentre retrospective study at IRCCS Policlinico of Milan and Le Molinette hospital of Turin from December 1, 2014 to June 30, 2016. All patients presented dentofacial deformities that required two-jaw orthognathic surgery with eventually upper jaw segmentation and/or genioplasty. All patients have been studied with a presurgical CBCT scans and 3D photos, later loaded onto ProPlan CMF software to create a 3D reconstruction.

Then we used this kind of reconstruction on a web conference between surgeons and biomedical engineers to perform virtual surgical osteotomies and a somewhat reliable soft tissue prediction. For every patients both jaws were moved; the upper jaw was set forward in all cases except for one, with an average of 4 mm, while the lower jaw was set forward in 11 patients with an average of 8 mm and set back in the others with an average of 3.75 mm. The virtual plan was then transferred to the operating room by using 3D printed surgical splints. After 4 months from surgery a new CBCT scans and 3D photos were taken to compare the planned with the real postoperative results. Thanks to Geomagic study Platform software an accuracy evaluation was made.

An industrial CAD/CAM software (Geomagic Study Platform) allowed us to make a surface superimposition between the 3D planned model and the 3D postoperative one of maxillo-facial skeleton taking as a reference 11 different areas of the skeleton. Once obtained the superimposition, the software created a color-coded mask that visually expressed the entity of the overlap between the two 3D reconstructions; in our study we decided to use 1 mm of minimum difference between the two superimpositions. In this way, it was also possible to identify the quantity of the discrepancies in the superimposition of the two models, by selecting different points. For discrepancies greater than 1 mm, color-coded was associated to red.

Where surgeons decided to do a procedure that was not planned (for example, a non-planned genioplasty) the colour code mask assigned the grey area, that meant out of threshold. We divided patients in two different groups (Table I) considering parameters such as sex, dentofacial deformity, presence of any presurgical asymmetry, kind of surgical technique (mandible or maxilla first) and amount of maxillomandibular movements (more or less than 10 mm) and we obtained medium discrepancy value for each groups. Using a t-student statistical model (with $p<0.05$) we compared statistical significance.

RESULTS

Accuracy evaluations were made considering 11 different points of maxillo-facial skeleton (pogonion, menton, right and left mandibular angle, right and left mandibular branch, right and left mandibular condyle, 1.1 tooth border, 1.6 and 2.6 cusp) with the color-coded mask method; we assessed the superficial discrepancies between the planned and the real 3D maxillo-facial reconstructions. We established the minimum discrepancies at 1 mm; before the work of Zavattero et al. (1) different studies on this subject established the minimum difference at 2 mm (21).

We can observe from the results that we gained, for each patients, a medium discrepancies inferior to the one considered statistically significant by the previous literature (2 mm); for four patients medium discrepancies were between 1.5 mm to 2, while for 1 case it was between from 1 to 1.4 mm. Furthermore, we can observe that the major of the discrepancies were localized in the mandibular area, at menton and pogonion (6.7 mm).

Once these data were obtained, we decided to compare five different parameters among patients and to evaluate if there was a significative difference in accuracy with t student test. We compared the average accuracy of 9 females with the one of 8 males (Table II) and obtained a medium value of 0.91 mm vs 0.83 mm (difference 9%) ($p=0.7$), for dentofacial type we had a higher discrepancy for the second class (1.208 vs 0.736) but it was not statistically significant ($p=0.08$), with a percentage difference of 39% (Table III). We then compared surgery technique with medium accuracy in mandible first vs maxilla first group (Table IV. 1.11 vs 0.8) ($p=0.3$) the amount of mandible and maxilla advancement, considering 1 as a cut off value (Table V. 0.85 vs 0.89) ($p=0.8$) and finally the presence of maxilla and/or mandible

Table II. *Medium discrepancy value according to sex.*

Sex	M	F
	1.34	0.5
	0.4	0.8
	0.5	0.34
	0.6	0.8
	0.6	1.7
	0.9	0.4
	1.6	0.3
	0.7	1.7
	-	1.7
Mean	0.83	0.91
P > 0.05 (0.7) not significant		

asymmetry; three patients had asymmetry with a medium discrepancy in accuracy of 0.53 while the others had no asymmetry with a medium difference of 0.95 (Table VI).

DISCUSSION

3D imaging is becoming more and more important in orthognatic surgery , with the possibility of using specific software that allows us to do surgical planning and simulation; this software also helps us to identify the type and the entity of facial deformities in order to improve diagnosis, treatment and, finally, patient's outcome. The aim of this study is to evaluate the effective accuracy of virtual surgical planning by using a specific software (Geomagic Study Platform) that allows the superimposition of planned and final 3D maxillo-facial reconstruction for each patient and to evaluate the most common parameters that could affect the success of VSP. The result's analysis was carried out by the creation of color-coded masks obtained after the superimposition of the two 3D reconstructions; in this way it was possible to identify both visually and quantitatively the entity of discrepancies in some specific area. The use of a semiautomatic technique for the superimposition and a statistic minimum difference of 1 mm, made our evaluation more refined and accurate in comparison to the other previous studies that established this limit at 2 mm. Nevertheless, our results confirmed what was already known in literature; just in 4 patients the medium difference was between 1.5 mm and 2 mm, and for 1 it was between 1.4 and 1mm.

A systematic review (22) was collected from different scientific database (428 studies), from 2000 to 2013, with our same purpose; after the establishment of different exclusion and inclusion criteria (at least 5 patients, conventional orthogantic surgery and accuracy evaluated by comparison of 3D surgical plan with 3D actual surgical outcome) only 7 studies could be considered. These 7 clinical trials were carried out from 2006 to 2013; 4 of theme used our same software for 3D virtual planning (Materialise Leuven, Belgium) while the other 3

Table III. *Medium discrepancy value according to pre-surgery dentofacial class.*

	1.34	0.5
	0.6	0.8
	1.7	0.4
	0.7	0.34
	1.7	0.5
	-	0.6
	-	0.8
	-	1.7
	-	0.4
	-	0.3
	-	0.9
	-	1.6
Mean	1.21	0.74
P > 0.05 (0.08) not significant		

used different independent programming systems. For 6 studies 3D virtual planning resulted in CAD/CAM surgical splints, while the rest resulted in an intraoperative navigation system.

Accuracy evaluation was carried out in 3 different modalities; hence, results were not easily comparable:

1) Intraclass correlation coefficient (ICC) (23) between the conventional reference point makes it possible to compare the current study with the previous ones regarding precision and accuracy, but it reduces the numerical data to arbitrary categorical data, thereby reducing the amount of information presented. So, it makes the data easier to evaluate but more difficult to assess regarding reproducibility between different study groups
1) Linear and angular difference between reference points in the maxillo-facial segments (24); three reference points per segment are selected on planning and postoperative model, and the segments are then put back together. The mean differences between the reference points are recorded as both linear and angular difference in all three dimensions. The reduction of reference points to the lowest possible reference, makes it feasible to evaluate both linear and angular differences. The disadvantage is the increased risk of error, since the reference points are placed manually, and with fewer reference points, the possibility and severity of errors increase. Previous investigations have shown the accuracy of registration to improve by registering complete areas and surfaces instead of single points, because areas and surfaces are better represented in CT data (25).
2) Percentage of the geometric surface correlation between the two models (21); this method consists

Table IV. *Medium discrepancy difference according to surgical technique.*

Surgery sequency	Maxillary first	Mandibular first
	0.5	0.8
	0.4	1.34
	0.34	0.6
	0.5	1.7
	0.6	
	0.8	
	1.7	
	0.4	
	0.3	
	0.9	
	1.7	
	1.6	
	0.7	
Mean	0.8	1.11
P >0.05 (0.3) not significant		

of an automated comparison of the virtual plan and the actual outcome. Since this method is automated the data are objective and less prone to errors than the manually selected reference points. The accuracy of CBCT voxel-based registrations of skull structures is known to be about half the voxel size of the largest data value, which is about 0.2 mm on average, depending on CBCT scanner (26). A disadvantage of the surface best-fit model is the position of the osteotomy. If the actual osteotomy is displaced from the virtual planned, the surface fit will decrease despite correct position of the segment. To overcome this bias, we decided to use semiautomatic superimposition algorithms in which the operator decided manually 11 different points that were not affected by change during surgery procedure.

The success criterion, proposed by several authors (21, 22), is a difference of maximum 2 mm between the virtual planned surgery and the surgical outcome. Less than 2 mm is thought to be clinically insignificant in conventional lateral cephalometric analysis (27). With our results we have shown what was already known in literature, despite of the using of a more accurate and refine criterion success.

Concerning patients related factors it could be concluded that no difference can be found, as it was reported by Liebregts et al. (28) even if other previous study (29) showed significative difference in particular among, age and advancement entity. They found that soft tissue response was less accurate in elderly people, probably because of different soft tissue elasticity, less fat and different muscular tone. Anyway, this comparison was made considering only soft tissue reconstruction that is, by definition, less accurate than the skeletal one. Surely virtual 3D planning offers several important advantages over conventional treatment planning:

1) Better visualization of dental arch and bony skeleton that improves diagnostic and treatment potentiality, in comparison to the traditional cephalometria (4, 5, 30) ; also soft tissue's visualization improves but its accuracy in predictability is still insufficient, in particular

Table V. *Discrepancy according to mandibular/maxillary movements.*

Mandibular r maxillary movement < or > 10 mm	> 10 mm	<10mm
	0.34	1.7
	0.4	0.4
	0.7	0.5
	1.7	0.8
	0.6	0.3
	1.34	1.7
		0.8
		0.9
		0.6
		0.5
		1.6
Mean	0.85	0.89
P >0.05 (0.3) not significant		

in chin and labial area; anyway, the possibility to visualize both soft and hard tissue allows to obtain an overview of final outcome

1) Possibility to easily simulate surgery movements of segmented bones in three dimension and to evaluate the relationships between maxillo-facial skeleton with skull
2) Treatment plans can be stored online and save the space normally taken up by materials used in conventional planning; furthermore it can be easily visualized and conferred with colleagues, both referring orthodontists and oral maxillofacial surgeons, anywhere in the world via internet (4, 31)
3) Different studies have shown a reduction of the whole time required for the preparation of virtual surgical planning in comparison to the traditional one (5.10 h vs 7.45 h) (32)
4) 3D virtual planning offers an excellent communication tool to teach contemporary treatment of maxillofacial deformities to residents in orthodontist and oral maxillofacial surgery (4, 31)
5) Finally, virtual planning may reduce the overall cost of care due to decrease in operating time, blood loss, complications and need for reoperative surgery (5, 30, 33)

The main limitation of 3D virtual surgical planning is the increase in radiation exposure due to the need for a 3D CBCT scan pre and postoperatively. Although CBCT scans significantly reduce the radiation exposure compared to multislice CT scans, they still increase the exposure compared to conventional panoramic and cephalometric imaging (4, 34). Anyway, we believe that, considering the low dose range associated with our protocol, the therapeutical benefit overcomes the potential

Table VI. *Medium discrepancy according to the presence of asymmetry or not.*

Asimmetry	Yes	No
	0.8	0.5
	0.5	1.34
	0.3	0.4
		0.34
		0.6
		0.6
		0.8
		1.7
		0.4
		0.9
		1.7
		1.6
		0.7
		1.7
Mean	0.53	0.95
P > 0.05 (0.2) not significant		

increased risk associated with CBCT scans. Other limitations could be represented by costs and the delivery of dental casts model that must be sent to the CAD/CAM centre at least four days before web conference planning.

3D virtual planning is an accurate a reproducible method for the treatment of dentofacial deformities; it could be easily translated into common practice and it could be applied in all kind of patients, independently by sex, kind of deformity and kind of surgery. Anyway, there are still some gaps such as predictability of soft tissue's outcomes (41). Other improvements could be derived from new imaging techniques that could enhance anatomic details, in particular for soft tissue; indeed the preference for multislice CT over CBCT presents disadvantages in terms of image quality, supine position during the test and greater radiation doses, while advantages include better identification of soft tissue details and less image distortion where metallic elements are present.

Additional studies are desired for a more complete validation of reproducibility and accuracy of 3D virtual surgical planning. Moreover, there are several different software for virtual surgical planning, but only few of them was used in literature, so it could be interesting make a comparison between most of them in terms of accuracy.

REFERENCES

1. Zavattero E, Michele R, Giovanni G, et al. Evaluation of the accuracy of virtual planning in orthognatic surgery: a morphometric study. J. Craniofacial Surg. 2019; 30(4):1214-20.
2. Islam S, Uwadiae N, Orniston IW. Orthognatic surgery in the management of obstructive sleep apnoea: experience from maxillofacial surgery unit in the United Kindom. Br J Oral Maxillofac Surg 2014;52:496-500.
3. Kor HS, Yang HJ, Hwang SJ. Relapse of skeletal class III with anterior open bite after bimaxillary orthognatic surgery depending on maxillary posterior impaction and mandibular counterclockwise rotation. J Craniomaxillofac Surg. 2014; 42:e230-e238.
4. Swennen GR, Mollemans W, Schutyser F. Three-dimensional treatment planning of orthognatic surgery in the era of virtual imaging. J Oral Maxillofac Surg 2009; 67:2080-92.
5. Baker SB, Goldstein JA, Seruya M. Outcomes in computer-assisted surgical simulation for orthognatic surgery. J Craniofac Surg 2012; 23:509-13.
6. Plooij JM, Maal TJ, Haers P. Digital three-dimensional image fusion processes for planning and evaluating orthodontics and orthognatic surgery. A systematic review. Int J Oralm Maxillofac Surg 2011; 40:341-52.
7. Baek SH, Cho IS, Chang YI, Kim MJ. Skeletodental factors affecting chin point deviation in female patients with Class III malocclusion and facial asymmetry: a three-dimensional analysis using computed tomography. Oral Surg Oral Med Oral Pathol Oral Radiol Endod 2007; 104:628-39.
8. Schwartz HC. Efficient surgical management of mandibular asymmetry. J Oral Maxillofac Surg 2011; 69:645-54.
9. Adolphs N, Liu W, Keeve E. RapidSplint: virtual splint generation for orthognatic surgery – results of a pilot series. Comput Aided Surg 2014; 19:20-28.
10. Bolzoni AR, Baj A, Sweed AH, Giannì AB, Montrasio EF, Beltramini GA. Role of Axial Split Osteotomy of Free Fibula Flap in Mandibular Reconstruction and Dental Rehabilitation. Plast Reconstr Surg Glob Open 2020; 20;8(1):e2546.
11. Uribe F, Janakiraman N, Shajer D. Three-dimensional cone-beam computed tomography–based virtual treatment planning and fabrication of a surgical splint for asymmetric patients: surgery first approach. Am J Orthod Dentofacial Orthop 2013; 144:748-58.
12. Cheong YW, Lo LJ. Facial asymmetry: etiology, evaluation, and management. Chang Gung Med J 2011; 34:341-51.
13. Chabanas M, Chouly F, Boutault F,Payan Y, et al. Evaluating soft tissue simulation in maxillofacial surgery using preoperative and postoperative CT scan. Int Prod of CAES 2004; 419-24.
14. Ferri A, Varazzani A, Bolzoni AR, et al A multicenter survey on computer-aided design and computer-aided manufacturing mandibular reconstruction from Italian community. Microsurgery 2019; 39(7):673-4. doi: 10.1002/micr.30505.
15. Bolzoni A, Mapelli A, Baj A, Sidequersky FV, Giannì AB, Sforza C. Evaluation of three-dimensional mandibular movements after reconstruction with

free fibula flap. Acta Otorhinolaryngol Ital 2015; 35(6):371-8. doi: 10.14639/0392-100X-504.
16. Baj A, Lovecchio N, Bolzoni A, Mapelli A, Giannì AB, Sforza C. Stair ascent and descent in assessing donor-site morbidity following osteocutaneous free fibula transfer: a preliminary study. J Oral Maxillofac Surg 2015; 73(1):184-93.
17. Di Giuli R, Zago M, Beltramini GA, et al. Donor-Site Morbidity After Osteocutaneous Free Fibula Transfer: Longitudinal Analysis of Gait Performance. J Oral Maxillofac Surg 2019; 77(3):648-57.
18. Kaipatur NR, Flores-Mir C. Accuracy of computer programs in presenting orthognatic surgery soft tissue response. J Oral Maxillofac Surg 2009; 67:751-9.
19. Marchetti C, Bianchi A, Muyldermans L, Di Martino M. Validation of new soft tissue software in orthognatic surgery planning. Int J of Oral Maxillofac Surg 2011; 40:26-32.
20. Bolzoni AH, Kadubiec A, Beltramini GA, Cherchi A, Baj A. Factors influencing CAD/CAM accuracy in fibula free flap mandibular reconstruction. Sweed. Acta Otorhinolaryngol Ital 2020; 40(2):138-43. doi: 10.14639/0392-100X-N0400.
21. Marchetti C, Bianchi A, Bassi M, Gori R, Lamberti C, Sarti A. Mathematical modeling and numerical simulation in maxillo-facial virtual surgery (VISU). J Craniofac Surg 2006; 17:661-7.
22. Mazzoni S, Badiali G, Lancellotti L, Babbi L, Bianchi A, Marchetti C. Simulation-guided navigation: a new approach to improve intraoperative three-dimensional reproducibility during orthognathic surgery. J Craniofac Surg 2010; 21:1698-705.
23. Stockbro K, Agaard E. Virtual planning in orthognatic surgery. Int. J. Oral Maxillofac. Surg. 2014; 43: 957-65.
24. Zinser MJ, Mischkowski RA, Sailer HF, Zoller JE. Computer-assisted orthognathic surgery: feasibility study using multiple CAD/CAM surgical splints. Oral Surg Oral Med Oral Pathol Oral Radiol 2012; 113:673-87.
25. Gliddon MJ, Xia JJ, Gateno J, et al. The accuracy of cephalometric tracing superimposition. J Oral Maxillofac Surg 2006; 64(2):194-202.
26. Swennen GR, Mollemans W, De Clercq C, et al. A cone beam computed tomography triple scan procedure to obtain a three-dimensional augmented virtual skull model appropriate for orthognatic surgery planning. J Craniofac Surg 2009; 20:297-307.
27. Donatsky O, Hillerup S, Bjørn-Jørgensen J, Jacobsen PU. Computerized cephalometric orthognathic surgical simulation, prediction and postoperative evaluation of precision. Int J Oral Maxillofac Surg 1992; 21:199-203.
28. Liebrgrets J, Xi T, Timmermans M. Accuracy of soft tissue simulation in bimaxillary osteotomies. Journal of craniomaxillofacial surgery 2015; 43:329-35.
29. Xia JJ, Shevchenko L, Gateno J, et al. Outcome study of computer-aided surgical simulation in the treatment of patients with craniomaxillofacial deformities. J Oral Maxillofac Surg 2011; 69:2014-24.
30. Schendel SA, Jacobson R. Three-dimensional imaging and computer simulation for office-based surgery. J Oral Maxillofac Surg 2009; 67:2107-14.
31. Gateno J, Xia J, Teichgraeber JF, et al. A new technique for the creation of a computerized composite skull model. J Oral Maxillofac Surg 2003; 61:222.
32. Wrozsek MK, Peacock A. Comparison of time required for traditional versus virtual orthognatic surgery treatment planning. International Journal of Oral Maxillo-Facial Surgery 2016; 45: 1065-9.
33. Bolzoni AR, Segna E, Beltramini GA, Sweed AH, Giannì AB, Baj A. Computer-Aided Design and Computer-Aided Manufacturing Versus Conventional Free Fibula Flap Reconstruction in Benign Mandibular Lesions: An Italian Cost Analysis. J Oral Maxillofac Surg 2020; 78(6):1035.e1-1035.e6. doi: 10.1016/j.joms.2019.03.003.
34. Zinser MJ, Sailer HF A paradigm shift in orthognatic surgery? A comparison of navigation computer-aided-designed/computer-aided-manufactured splints, and classic intermaxillary splints to surgical transfer of virtual orthognatic planning, American association of Oral Maxillofacial Surgeons 2013; 71:2151.

Epidemiology of odontogenic sinusitis: an old, underestimated disease, even today. A narrative literature review

M.C. Nurchis[1], D. Pascucci[2], M.A. Lopez[3], A. Moffa[3], P.C. Passarelli[4], F. Bressi[5], M. Casale[3] and G. Damiani[1,2]

[1]Fondazione Policlinico Universitario A. Gemelli IRCCS, Rome, Italy; [2]Università Cattolica del Sacro Cuore, Rome, Italy; [3]Unit of Otolaryngology – Integrated Therapies in Otolaryngology, Campus Bio-Medico University, Rome, Italy; [4]Department of Head and Neck, Division of Oral Surgery and Implantology, Institute of Clinical Dentistry, Catholic University of the Sacred Heart, Gemelli University Polyclinic Foundation, Rome, Italy; [5]Department of Physical and Rehabilitation Medicine, Campus Bio-Medico University, Rome, Italy

Odontogenic sinusitis is an inflammatory condition of the paranasal sinuses resulting from dental pathology. The aim of this study is to provide an overview of the current literature on the dimensions of the phenomenon, quality of life, economic considerations, and approaches to odontogenic sinusitis. A narrative review was conducted following the methodology proposed by Green et al. (2006). There appears to have been an increase in the incidence over the last decade. Nowadays, evidence in the literature reports that 10-12% up to 40% of all sinusitis cases are associated with odontogenic infections. The iatrogenia was by far the leading cause of odontogenic sinusitis (55.97%) while the first and second molars were the most affected teeth with an incidence of 35.6% and 22%. If not properly diagnosed and treated, these infections may lead to a rapid spread, giving rise to potentially life-threatening complications with a significant general health-related Quality of Life detriment. The proper management of patients in a pre-implant logical setting leads to substantial savings, ranging from €38 million to €152 million, for the Italian National Health Service. Odontogenic sinusitis management should involve shared decision-making between the otolaryngologist, dental provider, and patient, where the benefits and risks of dental treatment and endoscopic sinus surgery are discussed.

Odontogenic Sinusitis (OS) is an inflammatory condition of the paranasal sinuses resulting from dental pathology including, mainly, prior iatrogenic causes, infections of maxillary dentition, and odontogenic cysts (1). There appears to have been an increase in the incidence of OS over the last decade (2) which may reflect a decrease in the access to dental care (3). Burnmam et al. reported a 62% increase in the number of patients requiring admission in 2008 for spreading odontogenic infections, compared with 2003-2005 admissions (4).

Additionally, Thomas et al. (2008) reported a doubling of the number of admissions, and bed days, due to dental abscesses requiring drainage, comparing 1998-1999 and 2005-2006 (5). The OS bacteriology is distinctly different from non OS cases. Odontogenic sinus infections are generally polymicrobial with predominantly anaerobic organisms present in cultures, commonly including Peptostreptococcus, Prevotella, and Fusobacterium (1). Anaerobic bacteria are responsible for infectious inflammation in 66.7% of OS cases and correlation between bacteria present

Key words: odontogenic sinusitis; quality of life; multidisciplinary approach; economic impact

Corresponding Author:
Dr Antonio Moffa,
Unit of Otolaryngology, Integrated Therapies in Otolaryngology, Campus Bio-Medico University, Via Álvaro del Portillo 21, 00128 Roma (RM), Italy
Tel.: 39 06.22.54.11
e-mail: a.moffa@unicampus.it

0393-974X (2020)

in pathological teeth and the ones found in infected sinus has been described (6).

The main symptoms related to OS are facial pain; toothache; nasal pain; nasal discharge; postnasal drip; nasal obstruction; discomfort of the face and gums and bad odor. However, symptoms may vary, and many cases can even be asymptomatic (7). Radiologic imaging can provide useful adjunct information in the diagnosis of sinusitis and particularly whether an odontogenic source may be responsible for the infection (8).

Dental radiographs have been shown to have an estimated sensitivity of 60% for caries and approximately 85% for periodontal disease, leaving a high false negative rate (9). CT is the gold standard in the diagnosis of maxillary sinus disease due to its high resolution and ability to discern bone and soft tissue (7). However, if not properly diagnosed and treated, these infections may lead to a rapid spread, giving rise to potentially life-threatening complications with a significant general health-related QOL detriment that is comparable to that previously described for severe chronic diseases such as heart disease, diabetes, and COPD (10).

This disease differs in its pathophysiology, microbiology, diagnostics, and management from sinusitis of other causes, although clinical symptoms are not conspicuous. Which is exactly why appropriate diagnosis and management of pathology of the maxillary sinus of odontogenic origin commonly require the expertise of multiple medical and dental specialists (11). The aim of this work is to provide an overview of the current literature on the dimensions of the phenomenon, quality of life, economic considerations, and approaches to OS.

MATERIALS AND METHODS

A narrative review of studies describing the dimensions of the phenomenon, quality of life, economic considerations, and approaches to OS was conducted following the methodology proposed by Green et al. (2006) (12). The major scientific databases were queried to identify primary articles between January 1950 and August 2020 including, as key terms, odontogenic sinusitis, quality of life, incidence, multidisciplinary approach, and economic impact. The inclusion criteria for relevant articles were the following: original, primary, and secondary studies focusing on the OS epidemiological dimensions, Quality of Life, economic considerations, and the OS approaches. The exclusion criteria were the following: age of participants (i.e. <18), in English only, letters to the editor, conference abstracts, commentaries, and grey literature.

Epidemiology – dimensions of the phenomenon

Over 60 million Europeans, of which 3 million in Italy, and 45 million Americans are affected by Rhinosinusitis (RS) (13). Considering the American (i.e. 327.540.066) (14), European (i.e. 747.713.322) (15), and Italian (i.e. 60.359.546) (16) population, the prevalence of RS amounts to 14%, 8%, and 5% respectively. Nowadays, evidence in the literature reports that 10-12% up to 40% of all sinusitis cases are associated with odontogenic infections (17-21).

Given the high heterogeneity among the frequencies of odontogenic infections correlated to RS reported in the scientific literature, two scenarios, based on the lower (i.e. 10%) and upper (i.e. 40%) frequency of OS associated with RS were considered. According to the first scenario (i.e. 10% frequency), the prevalence of OS on the total population accounts for 1.4% or 4.5 million people, 0.8% or 6 million people, and 0.45% or 271 thousand people in the United States of America, Europe and Italy, respectively. Considering the second scenario (i.e. 40% frequency), the prevalence of OS on the total population amounts to 5.6% or 18 million people, 3.2% or 23 million people, and 1.8% or 1 million people in the United States of America, Europe and Italy, respectively.

As described by Arias-Irimia et al. OS is most common among 40 years old with a female predominance. The mean age increases to 60 years old if OS is associated with implantology procedures. This study further examined the etiological agents of OS. The iatrogenia was by far the leading cause of disease (55.97%) followed by other etiologies as periodontitis (40.38%) and odontogenic cysts (6.66%).

Among the iatrogenic causes, oroantral fistulas accounted for 47.56%, the extrusion of endodontic obturation materials represented the 22.27%, nonspecific foreign bodies amounted to 19.72%, apicectomy equaled to 5.33%, the maxillary sinus floor augmentation pre-implantology surgery represented the 4.17%, and the poorly positioned dental implants accounted to 0.92% of all cases

included under a iatrogenic cause (17). A recent systematic review examining the OS etiology and teeth involved found that the first and second molars were the most affected teeth with an incidence of 35.6% and 22% followed by the third molar (17.4%), the second premolar (14.4%), and the first premolar (7.2%). The canina (3%) and the second ncisive (0.4%) remain scarce and occasional (22).

Quality of Life

A recent study focused on determining whether there is a difference in the impact of sinonasal symptomatology on general health-related quality of life (QOL) in odontogenic chronic (C) RS compared to non-odontogenic CRS. The severity of sinonasal symptomatology and CRS-specific QOL detriment was measured using the 22-item Sinonasal Outcomes Test (SNOT-22) and general health-related QOL was measured using the health utility index from the 5-item EuroQol QOL survey (EQ-5D HUV). Odontogenic CRS had a major impact on individuals, and they were significantly associated with a decrease in the EQ-5D HUV scale (p=0.008). As a result, sinonasal symptoms have a greater impact on general QOL in odontogenic CRS compared to non-odontogenic ones (23).

Implantological procedures and odontogenic sinusitis: economic considerations

Evidence in the literature reported that 1.5 million dental implants are placed annually in Italy (24). A recent systematic review showed that around 5% of sinusitis of odontogenic origin is caused by dental implants (17). In Italy, the number of OS is 271.600 and 1.086.480 considering the 10% and 40% scenario, respectively.

Given that, the OS number caused by implantological procedures, calculated by multiplying the number of OS in Italy by the percentage of OS caused by implantological procedures, is 13.580 and 54.324, considering the 10% and 40% scenario, respectively. From the National Health System perspective, the tariff related to the treatment of implantological complications amounts to € 2.798 for each patient (25).

As a result, guaranteeing the proper management of patients in a pre-implantological setting leads to a potential saving of around € 38 million and €152 million for the National Health System, considering the 10% and 40% scenario, respectively.

Multidisciplinary approach to odontogenic sinusitis

Concomitant management of the dental origin and the associated sinusitis will ensure complete resolution of the infection and may prevent recurrence and complications. A combination of medical and surgical approaches is generally required for the treatment of OS. The removal of a foreign tooth root from the sinus, or the treatment of an infected tooth by extraction or root canal therapy, was required to eliminate the source of infection (26). Thus far, previous studies have confirmed the necessity of a multidisciplinary approach in the OS management.

Trimarchi et al. (2019) reviewed several case series of odontogenic infections from January 2008 to December 2018 and found that multidisciplinary agreement of otorhinolaryngologist and dental surgeon is a crucial step in proper diagnosis and treatment of odontogenic infections (26). Even Craig et al. (2020), in a recent evidence-based review, highlighted that OS management should involve shared decision making between the otolaryngologist, dental provider, and patient, where the benefits and risks of dental treatment and endoscopic sinus surgery are discussed (27).

OS is an underdiagnosed phenomenon with pathophysiologic mechanisms, microbiology, and treatments differing from those seen in RS. Given the multidimensional aspects of OS and their complications, a multidisciplinary approach to OS is necessary as their impact on the clinical practice and on the Italian National Health Service is assuming increasingly important dimensions. Failure to identify odontogenic sources of sinusitis results in persistence of symptoms and failed medical and surgical interventions with a consequence detriment of quality of life and significant economic impacts.

To guarantee an effective multidisciplinary approach, it is essential to establish a link between interprofessional education and interprofessional collaboration (28) involving dental providers and otorhinolaryngologist. These collaborative forms should be supported by investments of several public and/or private stakeholders to sustain this modern successful OS treatment.

REFERENCES

1. Little RE, Long CM, Loehrl TA, Poetker DM. Odontogenic sinusitis: A review of the current literature. Laryngoscope investigative otolaryngology 2018; 3(2):110-4.

2. Hoskison E, Daniel M, Rowson JE, Jones NS. Evidence of an increase in the incidence of odontogenic sinusitis over the last decade in the UK. The Journal of laryngology and otology 2012; 126(1):43.
3. Istituto Nazionale di Statistica (ISTAT). Il Ricorso alle Cure Odontoiatriche e la Salute dei Denti in Italia. Available from: https://www.istat.it/it/files//2015/07/salute_dei_denti_DEFINITIVA.pdf.
4. Burnham R, Bhandari R, Bridle C. Changes in admission rates for spreading odontogenic infection resulting from changes in government policy about the dental schedule and remunerations. British Journal of Oral and Maxillofacial Surgery 2011; 49(1):26-8.
5. Thomas SJ, Atkinson C, Hughes C, Revington P, Ness AR. Is there an epidemic of admissions for surgical treatment of dental abscesses in the UK? BMJ 2008; 336:1219-20
6. Kondrashev PA, Lodochkina OE, Opryshko ON. Microbiological spectrum of causative agents of rhinogenic and odontogenic chronic sinusitis and mucociliary activity of mucosal epithelium in the nasal cavity. Vestn Otorinolaringol 2010; 4: 45-7.
7. Vidal F, Coutinho TM, Carvalho Ferreira DD, Souza RC, Gonçalves LS. Odontogenic sinusitis: a comprehensive review. Acta Odontologica Scandinavica 2017; 75(8):623-33.
8. Patel NA, Ferguson BJ. Odontogenic sinusitis: an ancient but under-appreciated cause of maxillary sinusitis. Current opinion in otolaryngology & head and neck surgery 2012; 20(1):24-8.
9. Douglass CW, Valachovic RW, Wijensinha A, et al. Clinical efficacy of dental radiography in the detection of dental caries and periodontal diseases. Oral Surg Oral Med Oral Pathol 1986; 62:330-9.
10. Gaudin RA, Hoehle LP, Smeets R, Heiland M, Caradonna DS, Gray ST, Sedaghat AR. Impact of odontogenic chronic rhinosinusitis on general health-related quality of life. European Archives of Oto-Rhino-Laryngology 2018; 275(6):1477-82.
11. Shanti RM, Alawi F, Lee SM, Henderson AJ, Sangal NR, Adappa ND. Multidisciplinary approaches to odontogenic lesions. Current Opinion in Otolaryngology & Head and Neck Surgery 2020; 28(1):36-45.
12. Green BN, Johnson CD, Adams A. Writing narrative literature reviews for peer-reviewed journals: secrets of the trade. Journal of chiropractic medicine 2006; 5(3):101-17.
13. Italica AO. Acta Otorhinolaryngologica Italica. Acta Otorhinolaryngologica Italica 2013; 3(2):13-55.
14. United States Census Bureau. U.S. and World Population Clock. Available from: https://www.census.gov/popclock/ (Accessed 31 August 2020).
15. Worldometer. Population of Europe 2020. Available from: https://www.worldometers.info/world-population/europe-population/ (Accessed 28 August 2020).
16. Istituto Nazionale di Statistica (ISTAT). Available from: http://dati.istat.it (Accessed 28 August 2020).
17. Arias-Irimia O, Barona-Dorado C, Santos-Marino JA, Martinez-Rodriguez N, Martinez-Gonzalez JM. Meta- analysis of the etiology of odontogenic maxillary sinusitis. Med Oral Patol Oral Cir Bucal 2010; 15: e70-3.
18. Lee KC, Lee SJ. Clinical features and treatments of odontogenic sinusitis. Yonsei Med J 2010; 51:932-7.
19. Brook I. Sinusitis of odontogenic origin. Otolaryngol Head Neck Surg 2006; 135:349-55.
20. Martensson G. Dental sinusitis. Dtsch zahnarztl Z 1952; 7:1417-27.
21. Troeltzsch M, Pache C, Troeltzsch M, Kaeppler G, Ehrenfeld M, Otto S, Probst F. Etiology and clinical characteristics of symptomatic unilateral maxillary sinusitis: A review of 174 cases. Journal of Cranio-Maxillofacial Surgery 2015; 43(8):1522-9.
22. Lechien JR, Filleul O, Costa de Araujo P, Hsieh JW, Chantrain G, Saussez S. Chronic maxillary rhinosinusitis of dental origin: a systematic review of 674 patient cases. International journal of otolaryngology 2014; 2014:9.
23. Gaudin RA, Hoehle LP, Smeets R, Heiland M, Caradonna DS, Gray ST, Sedaghat AR. Impact of odontogenic chronic rhinosinusitis on general health-related quality of life. European Archives of Oto-Rhino-Laryngology 2018; 275(6):1477-82.
24. Saibene AM, Pipolo GC, Lozza P, Borloni R, Felisati G, Chiapasco MF. Dalle sinusiti odontogene alle complicanze nasosinusali di patologia o trattamento odontoiatrico: un importante cambio di prospettiva. Il Dentista Moderno 2014.
25. Classificazione Diagnosis Related Groups versione 24 - Tariffe in vigore nel Lazio dal 11 luglio 2013 (DCA n.310/2013).
26. Trimarchi M, Vinciguerra A, Galli A, Capparè P, Vinci R, Bussi M. Management of upper odontogenic

infections and the role of multidisciplinary treatment. Journal of Osseointegration 2019; 11(4):548-52.
27. Craig JR, Tataryn RW, Aghaloo TL, Pokorny AT, Gray ST, Mattos JL, Poetker DM. Management of odontogenic sinusitis: multidisciplinary consensus statement. In International Forum of Allergy & Rhinology 2020; 10:901-12.
28. Institute of Medicine (IOM). Measuring the impact of interprofessional education on collaborative practice and patient outcomes. Washington, DC: The National Academies Press 2015. https://doi.org/10.17226/21726.

Time course of the upper limb motor recovery in subacute stroke patients undergoing conventional or robotic rehabilitation. A preliminary report

M. Germanotta[1], A. Cruciani[1], C. Galli[1], D. Cattaneo[2], A. Spedicato[2] and I. Aprile[1]

[1]IRCCS Fondazione Don Carlo Gnocchi, ONLUS, Florence, Italy;
[2]IRCCS Fondazione Don Carlo Gnocchi, ONLUS, Milan, Italy

Upper limb recovery is a complex process and a strong challenge in the rehabilitation of patients after stroke. Several studies have been conducted to compare the efficacy of conventional and robotic rehabilitation to restore the upper limb motor impairment following a stroke. However, the evolution of the upper limb motor ability during an intervention, as well as the time point when the patient stops improving (the so call plateau), are rarely measured, and never compared between the two approaches. These latter aspects are very important considering the need for an optimization of the economic resources. In this study, the time course of the upper limb motor recovery of 24 subacute stroke patients undergoing a 30-session robotic or conventional treatment was analyzed through the upper extremity portion of the Fugl-Meyer Assessment scale (FMA-UE). The FMA-UE was administered before the treatment, and after 10, 20, and 30 rehabilitation sessions. Statistical analysis showed that, according to the FMA-UE, the time course in the two groups was similar: patients did not change between the baseline and the 10-session assessment, while they improved between 10 and 20 sessions, and between 20 and 30 sessions, with most of the gain observed between 10 and 20 sessions. This result suggests that 30-session robotic or conventional rehabilitation programs induce a similar curve trend in the upper limb motor recovery of patients with subacute stroke, with an important increase in the middle of the program and without reaching a clear plateau in the analyzed time interval.

Stroke is one of the most common causes of disability (1), the second-largest contributor after ischemic heart disease globally and in developing countries, and the third cause in developed countries (after ischemic heart disease and lower back and neck pain), with significant regional variation in disease burden across both developed and low- to middle-income countries (2).

Upper limb (i.e., arm, hand, and/or finger) motor impairments are often persistent and disabling (3). After 6 months from stroke, the upper limb functional recovery is complete in only 12% of patients (4); therefore, most stroke survivors show upper limb motor deficit, with a negative impact on their level of activities (5-7) and participation (8, 9). The observed upper limb impairments after stroke comprise paresis, abnormal muscle tone, decreased somatosensation, and coordination (10), worsening their abilities in performing activities of daily living (ADL) (11).

Therefore, improving upper limb function is an essential element of rehabilitation after stroke to maximize recovery (11), especially in the first 6 months since the onset of stroke because the motor and ADL recovery of stroke survivors declines afterward (12). Many techniques that aim to rehabilitate arm function after stroke have been proposed (13). In the

Key words: rehabilitation; stroke; robotics; upper extremity; Fugl-Meyer assessment

Corresponding Author:
Marco Germanotta, PhD,
IRCCS Fondazione Don Carlo Gnocchi,
Adress: Via di Scandicci, 269,
50143 Florence, Italy
e-mail: mgermanotta@dongnocchi.it

0393-974X (2020)

last decades, robotics made a substantial contribution to the field of upper limb rehabilitation after stroke. In fact, a considerable effort has been devoted to developing rehabilitation robots, aimed at supporting recovery from sensorimotor deficits, experienced by individuals after central nervous system damage, with a focus on stroke. Thanks to technological advancements and cost reduction, these devices today are being increasingly employed in clinical practice. Rehabilitation robots can provide tailored therapies that fulfil the main principles of neurorehabilitation, i.e., repetition, high intensity, and task specificity, in a complex and enriched environment, reducing, at the same time, the physical burden on therapists.

According to the abovementioned principles, robotic rehabilitation aims to promote neuroplasticity and, therefore, neurophysiological recovery, inducing functional or structural plasticity in brain networks, controlling both motor and cognitive functions (14). A recent meta-analysis (15) has shown that robotic therapy is likely to improve ADL, motor function, and strength of the upper limb after stroke. However, recent studies on large samples, involving 770 (16) and 224 (17) patients, failed to demonstrate the superiority of a robotic treatment over traditional approaches, in terms of recovery of upper limb motor functions. Based on current literature, a recent meta-analysis affirmed that the outcomes of robotic-assisted arm training are comparable with conventional therapy (18).

Usually, the different rehabilitation approaches are compared in terms of the change of a selected outcome (a clinical scale, or a kinematic /kinetic metrics) before and after the intervention. However, upper limb recovery is a complex process, and the evolution of the motor ability during an intervention, as well as the time point when the patient stops improving (the so-called plateau), are rarely measured (19).

Lee et al (20) examined the time-course changes in neurologic impairments and recovery in functional impairments at the initial rehabilitation baseline, 1, 2 and 4 weeks after a conventional rehabilitation treatment, and 3, 4, 5 and 6 months after stroke in 20 patients, using well-established clinical scales. Other studies addressed this topic (21-24) in patients undergoing a robotic intervention, through the help of the robotic devices themselves; in fact, thanks to the build-in sensing technology, the provided kinematic and kinetic data, are processed to obtain quantitative parameters. These indices are useful for tracking patient progress during robot-assisted rehabilitation and to design patient-tailored rehabilitation protocols; however, the relationship between robotic and clinical assessment is not completely understood. Moreover, as robotic assessments are often similar to the trained movement, it is not known if the time course, as measured by kinematic parameters, resembles the real-time course of recovery, as measured by a clinical assessment that evaluates a wider interval of function, such as the Fugl-Meyer Assessment scale. To the best of our knowledge however, there are no studies that investigated if conventional and robotic approaches differently influence the trend in the upper limb motor recovery during a rehabilitation intervention. In the light of this, the study aims to compare the time course of the upper limb motor recovery in patients undergoing conventional or robotic rehabilitation, using a well-established measure of upper limb motor impairment in stroke.

MATERIALS AND METHODS

Patients

As part of a larger clinical multicenter controlled trial (registered at clinicaltrials.gov, NCT02879279), we studied a subsample of 24 patients affected by subacute stroke, enrolled in inpatients rehabilitation facilities of Fondazione Don Carlo Gnocchi. Written informed consent was obtained from all participants before the study.

Inclusion criteria were as follows: diagnosis of stroke (ischemic or hemorrhagic) clinically and instrumentally defined by CT or MRI; time since stroke between 2 weeks and 6 months; age between 40 and 85 years; and cognitive and language abilities sufficient to understand the experiments and follow instructions. Exclusion criteria were: a previous ischemic or hemorrhagic stroke; behavioural or cognitive disorders that prevented the use of technology; ankylosis of the upper/lower limbs; severe visual acuity deficiency; upper extremity Fugl–Meyer score >58; inability to sign informed consent.

Ethics

The study was conducted under the International

Guidelines for Good Clinical Practice and the Declaration of Helsinki and it was approved by the local ethics board (FDG_6.4.2016_Prot.N.8/2016CE_FDG/FC/SA).

Treatment

In the main trial, the enrolled patients were randomly assigned to two treatment groups: the conventional treatment group (CG) or the robotic treatment group (RG). More information about the trial is available elsewhere (17). In this study, data from 13 patients in the CG and 11 in the RG were analyzed.

In both groups, each patient performed 30 rehabilitation sessions (five per week, for 6 weeks), lasting 45 min each, focused on the recovery of the upper limbs. In the CG, patients performed exercises for hand, arm, and shoulder oriented to sensor-motor re-programming, inhibition of the hypertonus, functional improvement, and task-oriented exercises. In the RG, patients' upper limbs were treated by using the following devices (25): (a) a robotic device that allows passive, active, and active-assistive planar movements of the shoulder and elbow joints (Motore, Humanware, Pisa, Italy) (26); (b) a robotic device that allows passive, active and active-assistive finger flexion and extension movements (Amadeo, Tyromotion, Graz, Austria) (27); (c) a sensor-based device that allows three-dimensional movements of the shoulder, elbow, and wrist joint, both unimanual and bimanual, without mechanical support (Pablo, Tyromotion, Graz, Austria); (d) an electromechanical system with an arm weight support that allows three-dimensional, unimanual and bimanual, movements of the shoulder joint (Diego, Tyromotion, Graz, Austria) the devices are reported in Fig. 1.

The proposed exercises consisted of specific settings in which the patients were asked to actively participate in using motor and cognitive strategies to correctly perform the exercise. Sounds and colours help to focus the patients' attention on the exercise and to stimulate their response. Furthermore, all patients underwent a global conventional rehabilitative protocol of 6 sessions per week, each lasting 45 min, focused on postural changes, re-education, and recovery of gait and balance.

Evaluation

Patients were evaluated at baseline and after 10, 20, and 30 rehabilitation sessions using the upper extremity motor section of the Fugl-Meyer Assessment (FMA–UE) 28. The FMA evaluates recovery in post-stroke hemiplegic patients and it is one of the most widely used quantitative measures of motor impairment (29). It is characterized by high inter-rater reliability (30, 31) and validity (32). This measure includes five domains (motor function, sensory function, balance, joint range of motion, joint pain) to assess synergistic and voluntary movement after stroke. In this study, we considered the motor domain.

The motor domains of the Fugl-Meyer Assessment of Upper Extremity (FMA-UE) rely on direct observation of the motor performance at each item using a 3-point ordinal scale (0 cannot perform, 1 performs partially, and 2 performs fully). FMA-UE includes four motor subscales: Upper Extremity (0–36 points), Wrist (0–10 points), Hand (0–14 points), Coordination/Speed (0–6 points). The total maximum score indicating a good function is 66 points.

Statistical analysis

Baseline characteristics were compared in the two groups (conventional and robotic group), by using the Mann–Whitney U test or the chi-squared test as appropriate. To compare the time course of each rehabilitation treatment, a mixed ANOVA test was used, with time (4 levels: baseline, after 10, after 20, and after 30 sessions) as within-subject factor, and group (2 levels: conventional and robotic) as between-subject factor, followed by post-hoc tests with Bonferroni correction, if necessary.

Moreover, the effect size of the change between two subsequent evaluations was computed by using the Cohen's d, interpreted as follows: 0.20 means a small difference, 0.50 a medium difference, while a value around or above 0.80 means a large difference (33). For each test, a p-value lower than 0.05 was deemed significant. Statistical analysis was performed by using the IBM SPSS package, version 25 (Armonk, NY, USA).

RESULTS

The demographic and clinical characteristics of the enrolled sample are reported in Table I. Patients in the two groups were comparable in terms of sex, age, time elapsed since the acute event, affected side, number of patients with language deficits or hemispatial neglect, and upper limb impairment, as measured by the FMA-UE at the enrollment.

Table I. *Baseline characteristics of the sample (N=24).*

Variables		Conventional group (N=13)	Robotic Group (N=11)	P
Sex	*Women*	6 (46.2%)	3 (27.3.3%)	0.423
	Men	7 (53.8%)	8 (72.7%)	
Age		67.0 (13.5)	69.8 (9.4)	0.691
Time since stroke		83.6 (48.2)	74.9 (46.2)	0.569
Index stroke type	*Ischemic*	6 (46.2%)	8 (72.7%)	0.240
	Hemorragic	7 (53.8%)	3 (27.3%)	
Affected side	*Right*	6 (46.2%)	3 (27.3.3%)	0.423
	Left	7 (53.8%)	8 (72.7%)	
Patients with language impairment		2 (15.4%)	1 (9.1%)	>0.999
Patients with neglect syndrome		1 (7.7%)	1 (9.1%)	>0.999
Baseline FMA-UE		26.0 (16.3)	22.5 (12.4)	0.733

*Data are mean (**SD**) or absolute numbers (%). P values refer to the Mann-Whitney U test, or the Fisher Exact test, as appropriate.*

The time course of recovery in the two groups is depicted in Fig. 2. According to the statistical analysis, the interaction factor *timeXgroup* was not statistically significant (F=420, p=0.671), meaning a similar trend in the two groups. The main effect *time* was significant (F=28,029, p<0.001), meaning a significant change of the FMA-UE over time.

Fig. 1. *Robotic and sensor-based devices used to treat the upper limb of patients assigned to the robotic group: (**A**) Amadeo (Tyromotion); (**B**) Motore (Humanware); (**C**) Diego (Tyromotion); and (**D**) Pablo (Tyromotion).*

The post-hoc analysis showed that the first 10 sessions did not significantly change the motor impairment (p>0.999), while a significant improvement was detected from 10 to 20 sessions (p<0.001), and from 20 to 30 sessions (p=0.023).

As reported in Table II, the magnitude of the improvement was higher when comparing the FMA-UE scores after 10 and after 20 sessions, while lower values were detected comparing the outcome at 20 and 30 sessions. Specifically, the effect size was high for both groups from 10 to 20 sessions, while it was still high for the robotic group and moderate for the conventional group in the last assessment (between 20 and 30 sessions).

DISCUSSION

In this study, we analyzed the time course of the upper limb motor recovery in two groups of patients with stroke undergoing a conventional or a robotic approach.

Two main results emerged from this study that can be summarized as follows: first, the time course of motor recovery was similar in the two groups;

Table II. *Mean difference with standard deviations (SD) and effect size (Cohen's d) across the different time points for the two groups, separately.*

	Conventional Group		Robotic Group	
	Mean Difference (SD)	**Effect Size**	**Mean Difference (SD)**	**Effect Size**
Between baseline and 10 sessions	-1.0 (7.3)	-0.136	1.0 (7.0)	0.143
Between 10 to 20 sessions	7.7 (5.7)	1.358	5.1 (2.0)	2.581
Between 20 and 30 sessions	2.5 (6.4)	0.394	4.5 (3.6)	1.257

second, the central sessions (from 10 to 20) seem the most effective in improving upper limb motor performance when compared to the first (from 1 to 10), when patients did not improve, and the last (from 20 to 30) sessions, where the FMA-UE still shows a decrease of the upper limb motor impairment.

The first result supports the equivalence of conventional and robotic rehabilitation in the recovery of upper limb motor performance after stroke, not only in terms of the outcome (16, 18, 34) but also in terms of the curve trend. With respect to the second result, we can speculate that, in the first phase of the intervention, for the anatomical and functional complexity of the upper limb, patients need of an adequate period of motor-sensory stimulation, produced by the rehabilitation exercises (robotic or conventional), to learn new motor programs troughs neuroplasticity process transforming into active a movement previously carried out passively. This can be an extensive process that requires time to be accomplished; on the contrary, concerning the reduced improvement in the third phase, two possible explanations can be proposed: considering the time elapsed since the acute event, it is possible that patients are approaching a plateau in their possibility to recover from the injury, or it can be also possible that in the final phase of the rehabilitation intervention, a different approach, more specific and tailored, should be proposed to patients to maximize their gains. In this perspective, it could be of interest to verify, in a future study, if two separate interventions (a conventional intervention followed by a robotic intervention, or vice versa) could provide a similar magnitude of the improvement also after 30 sessions.

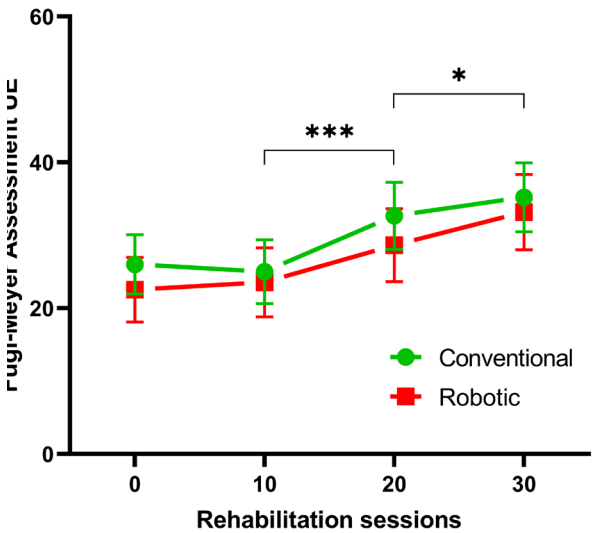

Fig. 2. *Mean values with standard errors of the upper extremity portion of the Fugl-Meyer Assessment (FMA-UE) during the 30-session rehabilitation interventions (conventional and robotic, separately). The mixed ANOVA test showed that the main effect time was significant, while the interaction factor timeXgroup was not significant. The Bonferroni-corrected p-values, referring to the post-hoc tests comparing each timepoint with the subsequent one, are reported.*

Overall, it is particularly important to highlight that a plateau is not evident during the analyzed 30-session intervention, meaning that longer rehabilitation periods could be more beneficial to reduce the upper limb motor impairment determined by the stroke. This result is in accordance with Lee et al (20) that, assessing weekly the neurologic and

the functional impairment in a cohort of stroke patients at several time points (at initial rehabilitation baseline, 1, 2, and 4 weeks after rehabilitation treatment, and 3, 4, 5, and 6 months after stroke), found a statistically significant improvement at every assessment, when compared to the previous one. This indicates that upper limb recovery had not yet plateaued in the investigated period (nearly between 3 and 6 months after the acute event). In fact, according to the authors, upper limb recovery after stroke is a slower process, if compared to the lower limb recovery, that generally reaches a plateau around three months after the acute events (35).

In comparison to Lee, at al (20), we did not observe a statistically significant improvement after 10 rehabilitation sessions. This difference could be explained with the different time elapsed from the acute event in the two studies (about 15 days in the study of Lee et al, and about 80 days in our study).

It is well known that spontaneous recovery plays a major role in functional improvements measured within the first month poststroke (36), while the recovery in the subacute phase is strongly linked to the influence of rehabilitation, with slower improvements that progressively level off after 6 months poststroke (35).

Our results showed a different trend when compared to those obtained using robot-based metrics to assess motor recovery. Mazzoleni et al. (21) studied 25 subacute stroke subjects undergoing a 30-session rehabilitation session with a planar robotic device. The considered kinematic parameters show statistically significant improvements after 10 sessions of robotic treatment; subsequently, a plateau was observed. Similar results were found in a subsequent study by the same group on 12 subacute and 12 chronic stroke patients (22). Duret et al. (23) investigated the time course of motor recovery in 25 stroke survivors over 16 sessions of robot-assisted shoulder/elbow training using a planar device combined with standard therapy, by measuring three robotic parameters (*stiffness*, *slottime*, *robotic power*) every four sessions. Their results showed that the *slottime* significantly decreased after eight sessions, while the *stiffness* decreased after 12 sessions; on the contrary, the *robotic power* did not significantly change during the investigated intervention. Goffredo et al. (24) analyzed data coming from 68 subacute stroke patients who conducted 20 daily sessions of upper limb rehabilitation using the same planar robotic device as in the study of Duret et al. (23) previously described. Specifically, Goffredo et al. (24) analyzed several kinematic parameters provided by the device during each session that showed significant intersession differences during the first 5/10 sessions, while no further significant variations occurred afterward.

The discrepancy between the lack of improvement in the first phase of the rehabilitation intervention in our sample, and the improvements detected by the above-mentioned study, could be related to the different outcome measures: in fact, it is possible that, in the first phase of the intervention, patients mainly acquire the trained task (i.e., the planar reaching movement), and therefore, the related robotic metrics improve. On the contrary, as said before, it is possible that the translation from the trained task to different tasks, as those evaluated through the FMA-UE, need longer times to be obtained.

Regarding the last phases, when our sample continued to improve, while the sample in the abovementioned studies did not, the different outcome measure, also to the differences in the provided intervention could be also related. The kinematic parameters may reach a plateau, or the planar intervention is no longer able to be beneficial for the motor recovery: in fact, it is worth to note that we selected a set of robotic and sensor-based devices to provide a more comprehensive intervention that targets all the upper limb, from the shoulder to the fingers, as in a conventional approach.

Possible limitations of our study are the small sample size and the relatively short time of observation. Future studies, with large samples and a long-term follow-up focusing on the evaluation of the time course of motor recovery in patients undergoing an upper limb rehabilitation intervention are needed to identify the optimum duration and combination of approaches to maximize the recovery.

REFERENCES

1. Gorelick PB. The global burden of stroke: persistent and disabling. Lancet Neurol. 2019; 18(5):417-418.

doi:10.1016/S1474-4422(19)30030-4.
2. Katan M, Luft A. Global Burden of Stroke. Semin Neurol. 2018; 38(2):208-211. doi:10.1055/s-0038-1649503.
3. Lai SM, Studenski S, Duncan PW, Perera S. Persisting consequences of stroke measured by the stroke impact scale. Stroke. 2002. doi:10.1161/01.STR.0000019289.15440.F2.
4. Kwakkel G, Kollen BJ, van der Grond J, Prevo AJH. Probability of regaining dexterity in the flaccid upper limb: impact of severity of paresis and time since onset in acute stroke. Stroke. 2003; 34(9):2181-2186.
5. Gowland C. Recovery of motor function following stroke: Profile and predictors. Physiother Canada. 1982; 34(2):77-84. doi:10.3138/ptc.34.2.077.
6. Kwakkel G, Wagenaar RC, Kollen BJ, Lankhorst GJ. Predicting disability in stroke--a critical review of the literature. Age Ageing. 1996; 25(6):479-489.
7. Feys HM, De Weerdt WJ, Selz BE, et al. Effect of a therapeutic intervention for the hemiplegic upper limb in the acute phase after stroke: a single-blind, randomized, controlled multicenter trial. Stroke. 1998; 29(4):785-792.
8. Broeks JG, Lankhorst GJ, Rumping K, Prevo AJ. The long-term outcome of arm function after stroke: results of a follow-up study. Disabil Rehabil. 1999; 21(8):357-364.
9. World Health Organization. International Classification of Functioning, Disability and Health. Geneva, Switzerland; 2001.
10. Hussain N, Murphy MA, Sunnerhagen KS. Upper limb kinematics in stroke and healthy controls using target-to-target task in virtual reality. Front Neurol. 2018. doi:10.3389/fneur.2018.00300.
11. Pollock A, Farmer SE, Brady MC, et al. Interventions for improving upper limb function after stroke. Cochrane Database Syst Rev. 2014; 2014(11):CD010820. doi:10.1002/14651858.CD010820.pub2.
12. Kwakkel G, Kollen BJ. Predicting activities after stroke: What is clinically relevant? Int J Stroke. 2013; 8(1):25-32. doi:10.1111/j.1747-4949.2012.00967.x
13. Pollock A, Farmer SE, Brady MC, et al. Interventions for improving upper limb function after stroke. Cochrane Database Syst Rev. 2013; 2013(11). doi:10.1002/14651858.CD010820.
14. Turner DL, Ramos-Murguialday A, Birbaumer N, Hoffmann U, Luft A. Neurophysiology of robot-mediated training and therapy: A perspective for future use in clinical populations. Front Neurol. 2013; doi:10.3389/fneur.2013.00184.
15. Mehrholz J, Pohl M, Platz T, Kugler J, Elsner B. Electromechanical and robot-assisted arm training for improving activities of daily living, arm function, and arm muscle strength after stroke. Cochrane Database Syst Rev. 2018; 9:CD006876. doi:10.1002/14651858.CD006876.pub5.
16. Rodgers H, Bosomworth H, Krebs HI, et al. Robot assisted training for the upper limb after stroke (RATULS): a multicentre randomised controlled trial. Lancet. 2019; 394(10192):51-62. doi:10.1016/S0140-6736(19)31055-4.
17. Aprile I, Germanotta M, Cruciani A, et al. Upper Limb Robotic Rehabilitation after Stroke: A Multicenter, Randomized Clinical Trial. J Neurol Phys Ther. 2020; 44(1):3-14. doi:10.1097/NPT.0000000000000295.
18. Mehrholz J, Pollock A, Pohl M, Kugler J, Elsner B. Systematic review with network meta-analysis of randomized controlled trials of robotic-assisted arm training for improving activities of daily living and upper limb function after stroke. J Neuroeng Rehabil. 2020; 17(1):1-14.
19. Page SJ, Gater DR, Bach-Y-Rita P. Reconsidering the motor recovery plateau in stroke rehabilitation. Arch Phys Med Rehabil. 2004; doi:10.1016/j.apmr.2003.12.031.
20. Lee KB, Lim SH, Kim KH, et al. Six-month functional recovery of stroke patients: a multi-time-point study. Int J Rehabil Res. 2015; 38(2):173-180. doi:10.1097/MRR.0000000000000108.
21. Mazzoleni S, Carrozza MC, Sale P, Franceschini M, Posteraro F, Tiboni M. Effects of upper limb robot-assisted therapy on motor recovery of subacute stroke patients: a kinematic approach. In: 2013 IEEE 13th International Conference on Rehabilitation Robotics (ICORR). IEEE; 2013:1-5.
22. Mazzoleni S, Buono L, Dario P, Posteraro F. Upper limb robot-assisted therapy in subacute and chronic stroke patients: preliminary results on initial exposure based on kinematic measures. In: 5th IEEE RAS/EMBS International Conference on Biomedical Robotics and Biomechatronics. IEEE;

2014:265-269.
23. Duret C, Courtial O, Grosmaire AG, Hutin E. Use of a robotic device for the rehabilitation of severe upper limb paresis in subacute stroke: Exploration of patient/robot interactions and the motor recovery process. Biomed Res Int. 2015; doi:10.1155/2015/482389.
24. Goffredo M, Mazzoleni S, Gison A, et al. Kinematic Parameters for Tracking Patient Progress during Upper Limb Robot-Assisted Rehabilitation: An Observational Study on Subacute Stroke Subjects. Appl Bionics Biomech. 2019; doi:10.1155/2019/4251089.
25. Aprile, Cruciani, Germanotta, et al. Upper Limb Robotics in Rehabilitation: An Approach to Select the Devices, Based on Rehabilitation Aims, and Their Evaluation in a Feasibility Study. Appl Sci. 2019; 9(18):3920. doi:10.3390/app9183920.
26. Germanotta M, Cruciani A, Pecchioli C, et al. Reliability, validity and discriminant ability of the instrumental indices provided by a novel planar robotic device for upper limb rehabilitation. J Neuroeng Rehabil. 2018; in press(1):39. doi:10.1186/s12984-018-0385-8.
27. Germanotta M, Gower V, Papadopoulou D, et al. Reliability, validity and discriminant ability of a robotic device for finger training in patients with subacute stroke. J Neuroeng Rehabil. 2020; 17(1):1-10.
28. Fugl-Meyer AR, Jääskö L, Leyman I, Olsson S, Steglind S. The post-stroke hemiplegic patient. 1. a method for evaluation of physical performance. Scand J Rehabil Med. 1975 ;7(1):13-31.
29. Gladstone DJ, Danells CJ, Black SE. The Fugl-Meyer Assessment of Motor Recovery after Stroke: A Critical Review of Its Measurement Properties. Neurorehabil Neural Repair. 2002; doi:10.1177/154596802401105171
30. Duncan PW, Propst M, Nelson SG. Reliability of the Fugl-Meyer assessment of sensorimotor recovery following cerebrovascular accident. Phys Ther. 1983; 63(10):1606-1610.
31. Sanford J, Moreland J, Swanson LR, Stratford PW, Gowland C. Reliability of the Fugl-Meyer assessment for testing motor performance in patients following stroke. Phys Ther. 1993 ;73(7):447-454.
32. De Weerdt WJG, Harrison MA. Measuring recovery of arm-hand function in stroke patients: A comparison of the Brunnstrom-Fugl-Meyer test and the Action Research Arm test. Physiother Canada. 1985; 37(2):65-70. doi:10.3138/ptc.37.2.065
33. Cohen J. Statistical power analysis for the behavioral sciences (revised ed.). 1977.
34. Padua L, Imbimbo I, Aprile I, et al. Cognitive reserve as a useful variable to address robotic or conventional upper limb rehabilitation treatment after stroke: a multicentre study of the Fondazione Don Carlo Gnocchi. Eur J Neurol. 2020; 27(2):392-398. doi:10.1111/ene.14090.
35. Jørgensen HS, Nakayama H, Raaschou HO, Vive-Larsen J, Støier M, Olsen TS. Outcome and time course of recovery in stroke. Part II: Time course of recovery. The copenhagen stroke study. Arch Phys Med Rehabil. 1995; doi:10.1016/S0003-9993(95)80568-0.
36. Krakauer JW. Motor learning: Its relevance to stroke recovery and neurorehabilitation. Curr Opin Neurol. 2006; doi:10.1097/01.wco.0000200544.29915.cc.